Synthesis and evaluation of bioluminescent probes as tools for anticancer drug discovery

Thesis presented for the degree of

Master of Science

by

Maryam Fredericks

Supervisor

Assoc. Prof. Anwar Jardine

Department of Chemistry

University of Cape Town

July 2025

Declaration

I, Maryam Fredericks, declare that "Synthesis and evaluation of bioluminescent probes as tools for anticancer drug discovery" is my own work and to the best of my knowledge has never been reported or submitted for any degree or examination in any university. All sources of information used are cited, acknowledged, and completely referenced at the end of each chapter.

Maryam Fredericks

July 2025

Dedication

To my beloved parents, Mommy and Daddy, I could not have done any of this without your endless love, encouragement, and sacrifices. Every effort in this journey is dedicated to you.

Acknowledgements

فَلِلَّهِ ٱلْحَمْدُ رَبِّ ٱلسَّمَٰوَٰتِ وَرَبِّ ٱلْأَرْضِ رَبِّ ٱلْعَٰلَمِينَ

"So all praise is for Allah—Lord of the heavens and Lord of the earth, Lord of all worlds." [45:36]

To my supervisor, Assoc Prof Anwar Jardine, Prof – you have a heart of gold. I could not have completed this project with anyone else. Thank you for your unwavering patience and guidance throughout this journey.

To Dr Marwaan Rylands, thank you for your invaluable input into my research and for keeping an eye on my chemistry (and me at times).

To my beloved siblings Mr Muhammad Fredericks and Miss Faatimah Fredericks, thank you for all your love, encouragement, and support.

To Dr Stephen de Doncker (UCT NMR unit) and Assoc Prof Edith Antunes (UWC NMR unit), thank you for your assistance with my NMR analyses. Ms Amina Sayed and Mr Evans Matunda of H3D, for granting me access to the LCMS machine and microwave reactor. Dr Lateef Nashed for his assistance in my fluorescence studies and Dr Saif Khan for his assistance in my bioluminescence studies and cell viability assays. Ms Joanne Polzin and Ms Laa-iqa Rylands, thank you for providing me with a creative outlet when I was taking a break from my numerous failed reactions.

To my work bestie and comrade, Miss Thaakirah Phillips - thank you for your love, friendship, and all the coffee runs that carried us through!

To Dr Doaa Ali and all the past and present members of the Jardine research group who I have had the pleasure of working with over the years, the research has always been grueling, but thanks to you the vibes were immaculate. Mr William Chu, Mr Ayabukwa Zambodla and all the members of Lab 7A – thank you for all the chemistry advice, the laughs and for lending me your chemicals when I needed them.

To my friends Miss Rukayah Jacobs and Mrs Aamiena Breda, thank you for always checking up on me and encouraging me throughout this journey.

To all my aunts, uncles, cousins and extended family, thank you for all your love, prayers and support.

I would also like to express my gratitude to the UCT PGFO for the financial assistance throughout my postgraduate studies.

Abstract

Luciferins are a class of small, light-emitting molecules that produce visible light through an oxidation reaction catalysed by luciferase enzymes. This bioluminescent system, when combined with CCD camera technologies, has enabled groundbreaking advances in measuring mammalian gene expression, protein–protein interactions, biochemical labelling, and small molecule dynamics. Among the luciferins, D-luciferin—originally isolated from the American firefly *Photinus pyralis*—is the most extensively studied. Synthetic analogues of D-luciferin have become increasingly important due to their incorporation into a wide range of commercially available assay kits, where they serve as sensitive reporters in both in vitro and in vivo applications. This thesis focuses on the development of improved synthetic methods for D-thioluciferin, C6-substituted analogues, and aza-derivatives of D-luciferin, the latter enabling the design of novel caged bioluminescent probes for advanced molecular imaging.

Abbreviations and Symbols

δ	Chemical shift
ADMET	absorption, distribution, metabolism, excretion, and toxicity
Ar	Aromatic
ATP	Adenosine triphosphate
β-lac	β-lactamase
BLI	bioluminescent imaging
Bluco	β-lactam and D-luciferin conjugate
BRET	bioluminescence resonance energy transfer
br s	broad singlet
$CDCl_3$	deuterated chloroform
CD_3OD	deuterated methanol
Cis	cisplatin
d	doublet
dd	doublet of doublets
DBU	1,8-Diazobicyclo[5.4.0]undec-7-ene
DCM	dichloromethane
DMF	dimethylformamide
DMSO	dimethylsulfoxide
eq	equivalent
FIGs	fluorescence image guided surgery
fLuc	firefly luciferase
GLuc	Gaussia luciferase
FT-IR	Fourier Transform Infrared

HOMO	highest occupied molecular orbital
HPLC	High Pressure Liquid Chromatography
Hz	Hertz
ICT	intramolecular charge transfer
IR	Infrared
J	coupling constant
LCMS	Liquid Chromatography Mass Spectrometry
Lit.	literature
LUMO	lowest unoccupied molecular orbital
Lux	bacterial luciferase
M	Molar
m	multiplet
N_2	nitrogen gas
NIR	near infrared
NLO	non-linear absorption
NMR	Nuclear Magnetic Resonance
OpLuc	Oplophorus luciferase
PBM	photobiomodulation
PDT	photodynamic therapy
ppm	parts per million
PTT	photothermal therapy
R_f	retention factor
RLuc	Renilla luciferase
RQY	relative quantum yield

rt	room temperature
s	singlet
S_NAr	nucleophilic aromatic substitution
TBAB	tetrabutylammonium bromide
THF	tetrahydrofuran
TLC	thin layer chromatography
TPA	two photon absorption

List of Figures

List of Tables

List of Schemes

Contents

Chapter 1 : Introduction

1.1 Bioluminescence

1.1.1 Bioluminescence technology

Light-based technologies have greatly advanced healthcare innovation by enabling precise, non-invasive diagnostic and therapeutic methods.[1-3] Insights into the structure, composition and functional features of tissues, their abnormalities and disease progression have been facilitated by modern medical imaging systems through light–tissue interactions.[3-5] Importantly, light can also serve as a therapeutic agent through heat generation or triggering photochemical and biological reactions.[3] Techniques like photobiomodulation (PBM),[6, 7] photothermal therapy (PTT)[8] and photodynamic therapy (PDT)[9] rely on light to treat conditions ranging from cancer[10, 11] to tissue regeneration in dental stem cells[12] and cranial bones.[13] However, these approaches face a major limitation: the shallow penetration of external light sources into deep tissues, which restricts their effectiveness in certain clinical applications. Various strategies have been employed to address this limitation such as the use of deep tissue penetrating near-infrared (NIR) light,[14] implantation of miniaturised light sources[15] and light-delivering materials such as optic fibres[16] and waveguides.[17] However, a common challenge among these strategies is their invasive light delivery.

To overcome this, researchers have turned to bioluminescence**,** a remarkable naturally occurring phenomenon in which living organisms emit visible light through an internal chemical reaction. It is found across a wide range of species, including marine organisms, bacteria and insects.[18-22] This form of chemiluminescence, arises from the oxidation of luciferin, which is catalysed by the activity of the luciferase enzyme found in bioluminescent organisms.[18, 23] Unlike external light, bioluminescent light originates from within tissues, eliminating the need for invasive devices or deep light delivery methods. This makes bioluminescence particularly promising for theranostic use, where simultaneous diagnosis and therapy are essential. Notably, over 40 types of bioluminescent systems exist in nature, with several already adapted for medical purposes.[24-26]

With progress in protein engineering and delivery technologies, bioluminescence has expanded into various applications such as bioimaging, biosensing and PDT.[3] Additionally, techniques

like bioluminescence resonance energy transfer (BRET) allow for improved light emission and functional versatility.[27, 28]

Bioluminescent imaging (BLI) has significantly advanced the fundamental understanding of in vivo biology and greatly enhanced the utility of small animal models in laboratory research due to its reliable, sensitive, convenient and non-invasive technique. Given that BLI enables the visualisation of various biological phenomena, it has been widely applied to monitor cells and biomolecular processes in living organisms.[29] These applications include pathogen detection,[30] monitoring of protein–protein interactions,[31] studies on ADMET (absorption, distribution, metabolism, excretion, and toxicity)[32] and - importantly to this project - tumour growth tracking[33] and analysis of responses to therapy patterns of gene regulation.[34]

1.1.2 Bioluminescence-based systems: Luciferins and luciferases

Although more than 30 distinct bioluminescent systems exist in nature,[21] only nine luciferins have been structurally elucidated and characterised to date (Figure **1.1**).[29] Among these, the coelenterazine, bacterial, and firefly luciferase systems are particularly noteworthy due to their widespread use and biological significance.

Coelenterazine-based systems are found in marine organisms and used by luciferases such as *Renilla* (RLuc), *Gaussia* (GLuc), and *Oplophorus* (OpLuc).[26] These systems do not require ATP, making them advantageous in ATP-deficient environments. However, they are more prone to spontaneous oxidation, which can lead to background interference.[35] Moreover, coelenterazine has low solubility in water, which limits its suitability for some applications compared to D-luciferin. Its bioluminescence typically presents as a flash rather than a sustained glow, with specific characteristics varying by luciferase type.[3, 36]

The bacterial luciferase (Lux) system operates differently compared to the coelenterazine system. It is genetically encoded in the *luxCDABEG* operon and is self-sufficient, producing all necessary substrates internally.[37, 38] This eliminates the need for external luciferin, enabling continuous bioluminescence with light being emitted around 490 nm. Ideally, these factors would make the Lux system useful in theranostic applications however, introducing this system into eukaryotic cells requires significant optimisation due to differences in cellular environments.[3]

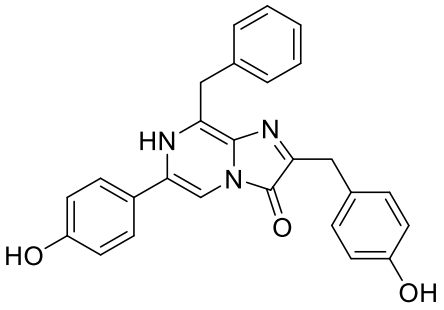

Coelenterazine
Inoune, 1976

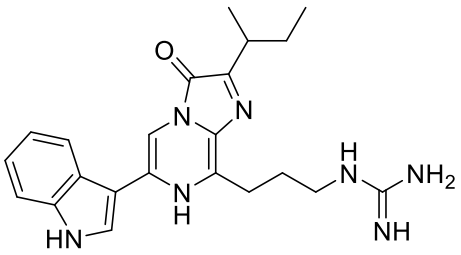

***Cypridina* luciferin**
Shimomura, 1957

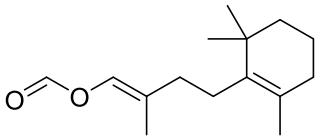

***Latia* luciferin**
Shimomura, 1968

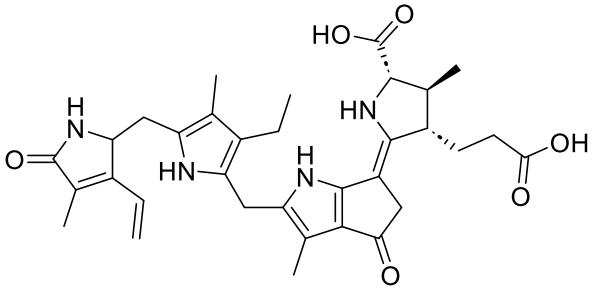

X = H Dinoflagelate luciferin
X = OH Krill luciferin
Nakamuru, 1989

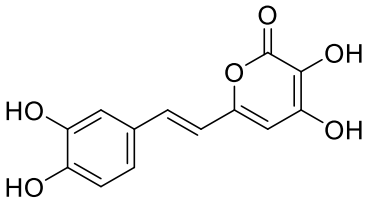

Fungal luciferin
Purtov and Yampolsky, 2015

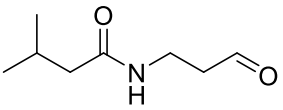

Diplocardia luciferin
Ohtsuka, 1976

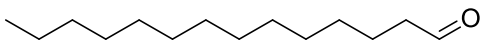

Bacterial luciferin
Cormier, 1963

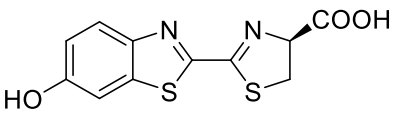

D-luciferin
McElroy, 1957

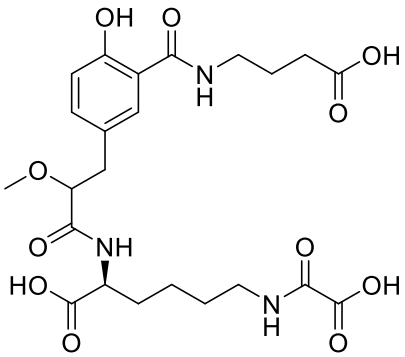

Fridericia heliota luciferin
Petushkov and Yampolsky, 2014

Figure 1.1. Structures of the nine known luciferins. [29]

Finally, one of the most well-known examples of insect bioluminescence is that of the North American firefly (*Photinus pyralis*).[21] Among the various bioluminescent systems, the firefly luciferin–luciferase reaction is the most extensively studied, with research spanning over 50 years. In this system, two essential components are involved: D-luciferin, the light-emitting molecule, and firefly luciferase (fLuc), the enzyme that catalyses the oxidation of luciferin. This oxidation results in the formation of an excited-state molecule called oxyluciferin, which releases light as it returns to its ground state. It requires ATP, Mg^{2+}, and oxygen to function, emitting light at approximately 560 nm (Scheme **1.1**). While ATP dependence may seem like a drawback, it reduces background noise, making the signal clearer. The system also benefits from a high quantum yield (~40%), good water solubility, and low toxicity, making it highly suitable for biological applications.[29]

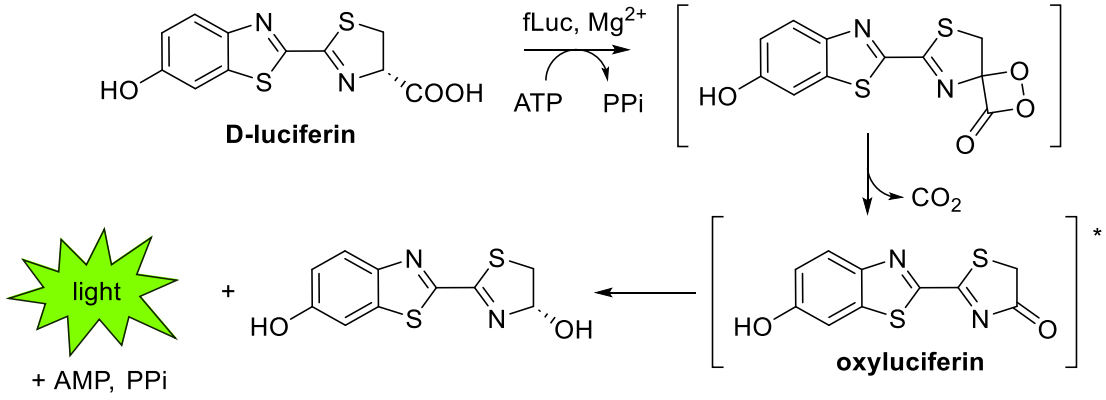

Scheme 1.1. Condensed mechanism of the D-luciferin bioluminescence reaction.

1.1.3 Theranostic applications of bioluminescent probes

Various luciferase–luciferin systems are used in theranostic applications, each with unique characteristics such as light emission wavelength, reaction kinetics, and environmental requirements. Although all luciferases catalyse light-producing reactions, their specific substrates and optimal conditions vary. This makes it essential to carefully select the most appropriate system for a given application. The utility of bioluminescent probes will be discussed according to three principal areas: bioimaging, biosensing and photodynamic therapy (PDT).

(i) Bioimaging

BLI is extensively utilised for non-invasive, real-time monitoring of biological processes. Initially employed to track luciferase-expressing tumour cells, advancements in luciferase-luciferin systems have enabled deeper tissue imaging,[39-44] higher brightness,[42, 44, 45] improved sensitivity[39, 46, 47] and various other factors. Innovations such as the development of red- and near-infrared-emitting luciferins (e.g., AkaLumine-HCl) have facilitated effective visualisation of deep-seated tumours.[43] Furthermore, the integration of luciferin-regenerating enzymes (LRE) with luciferases has enhanced signal stability and duration.[48] Beyond cell tracking, bioluminescence is now applied to monitor physiological parameters, exemplifying the expansion of BLI from structural imaging to functional diagnostics.[47]

Bioimaging has also been employed to assess various enzyme activities, with a notable example being the β-lactamase (β-lac) assay. β-lac is an enzyme expressed by bacteria that hydrolyses β-lactam antibiotics, such as penicillin and cephalosporins.[49] Yao *et al*. developed Bluco, the first β-lactam and D-luciferin conjugate, which serves as a bioluminogenic substrate for evaluating TEM-1 β-lac activity.[50] Bluco is specifically activated by β-lac, which cleaves the β-lactam ring to release free D-luciferin. This liberated D-luciferin is subsequently oxidised by luciferase, producing light and enabling the visualisation of β-lac activity (Scheme **1.2**). This innovative probe allows for the imaging of β-lactamase-expressing, antibiotic-resistant bacteria in vivo.

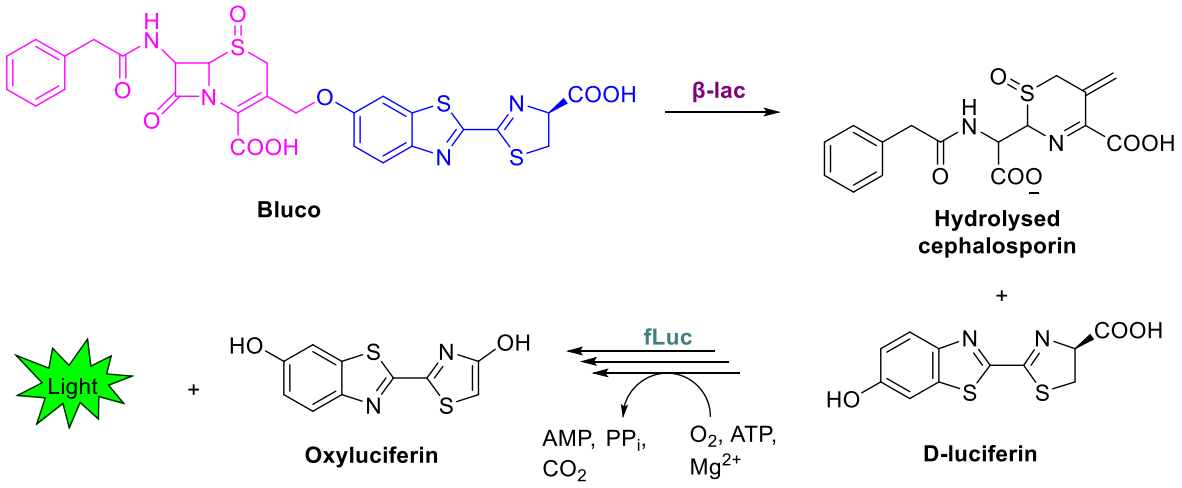

Scheme 1.2. Proposed two-step mechanism for the detection of β-lac.

(ii) Biosensing

Bioluminescent biosensors provide superior sensitivity and specificity compared to fluorescence-based systems due to their resistance to background noise and photobleaching.[51] These biosensors leverage mechanisms such as BRET or analyte-responsive luciferins. Their applications range from detecting antibodies and small molecules to metal ions like mercury[52, 53] and zinc.[54, 55] Additionally, biosensors capable of detecting mechanical forces like a BRET-based molecular tension sensor have been developed by Aird *et al*. for monitoring vinculin dynamics.[56] This example further highlights the expanding utility of bioluminescent systems in mechanobiology.

(iii) Photodynamic Therapy

Bioluminescence-driven photodynamic therapy (BL-PDT) addresses the limitations of traditional PDT by providing an internal light source capable of activating photosensitisers in deep tissues. Although inherently less intense than external light sources, coupling luciferases to photosensitisers via BRET enhances therapeutic efficacy.[57-62] Strategies include direct chemical conjugation,[57-60] fusion proteins,[61, 62] and nanoparticle-mediated delivery.[63-65] A representative example of this is presented by the work of Yan *et al*., in which a luciferase-photosensitiser (chlorin e6, Ce6) conjugate encapsulated in liposomes demonstrated effective tumour ablation in murine models.[58] Gene delivery of luciferase-phototoxic protein constructs[66] and the use of bioluminescent bacteria further extend the potential of BL-PDT in achieving spatially targeted and immune-responsive cancer therapy.[67]

1.1.4 Luciferin analogues with bathochromic shifts

The application of bioluminescence for studying living systems imposes specific constraints on the chemical structures and physicochemical properties of the luciferins used. A major limitation in in vivo BLI is the low stability of natural luciferins in solution, particularly upon exposure to air. Additionally, optimal tissue penetration of light, especially in tumours, occurs within the red and NIR regions. Unfortunately, most naturally occurring luciferins emit light at shorter wavelengths. To address these challenges, various research groups have focused on developing more stable luciferin analogues with red-shifted emission profiles suitable for deep tissue imaging. As a result, a plethora of luciferin derivatives as luminogenic substrates have been developed by various research groups. Figure **1.2** contains a subset of the structurally

modified luciferin analogues synthesised to date, which have exhibited bathochromic shifts (red shifts) relative to D-luciferin.

While D-luciferin has a maximum emission wavelength of 557 nm with natural luciferase, White *et al*. reported that the 6-amino analogue **1.11a** exhibited an emission maximum of 594 nm.[68] It was also demonstrated that mono and di-substituted analogues of alkylaminoluciferin **1.12a–d**[69, 70] and cyclic aminoluciferins **1.13a** and **b**[42] possessed emission maxima ≥ 600 nm. To further expand the range of red-shifted analogues, Conley *et al*. made use of an electron donating amino group and polarisable selenium atom to synthesise **1.14** which exhibited an emission maxima at 600 nm.[71] Interestingly, this compound possessed a characteristic light emission, easily distinguishable from the yellow-green light of D-luciferin and the orange light from aminoluciferin **1.11a**.

Compound **1.16** was found to have an emission maximum similar to that of D-luciferin, however in the presence of click beetle green (CBG) luciferase this maximum increased to 624 nm.[72] On the other hand, compound **1.18a** was also bioluminescent (608 nm) but required a higher pH for stable light emission.[73] In 2013, Iwano *et al*. replaced the benzothiazole moiety of D-luciferin with benzene, styrene or a longer conjugated pi-bond olefinic system, resulting in compounds **1.21-1.24**.[74, 75] This increased conjugated pi-system stimulated the formation of chromophores with long-wavelength absorption ranging from 640 – 675 nm. Like Iwano and colleagues, Jathoul *et al.* also introduced a double bond to achieve a bathochromic shift when synthesising compound **1.25**.[76] However, they preserved the benzothiazole and thiazole rings.

As a result, Jathoul *et al*. successfully synthesised a dual-colour, far-red to NIR emitting analogue of beetle luciferin, infra-luciferin **1.25**. This analogue shifted the emission spectrum of native fLuc into the NIR region (λ_{max} = 706 nm), while maintaining high brightness, thereby improving its suitability for bioluminescence imaging.[76] Finally, the most recent analogue of D-luciferin **1.26**, reported by Steinhardt *et al*., possesses an alkyl group in the benzothiazole ring. This compound was also found to emit a red shift maximum (610 nm) and was subsequently evaluated in HEK293 cells.[77]

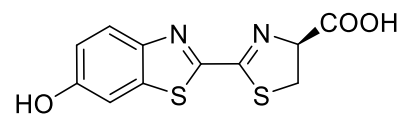

D-luciferin

λ_{em} = 557 nm

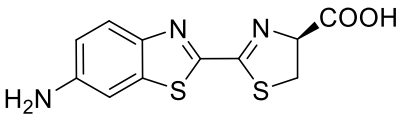

1.11 a

λ_{em} = 594 nm

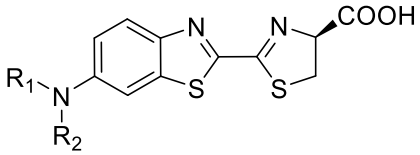

1.12 a R_1 = Me R_2 = H

b R_1 = Me R_2 = Me

c R_1 = Et R_2 = H

d R_1 = Et R_2 = Et

λ_{em} ≥ 600 nm

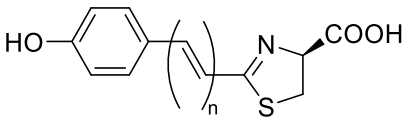

1.21 c n = 2

λ_{em} = 640 - 675 nm

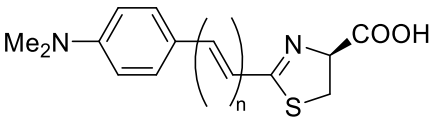

1.22 c n = 2

λ_{em} = 640 - 675 nm

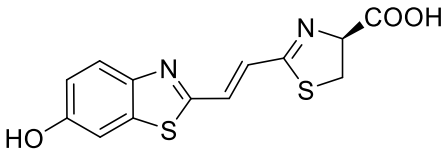

1.25

λ_{em} = 706 nm

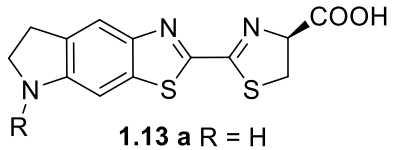

1.13 a R = H

b R = Me

λ_{em} ≥ 600 nm

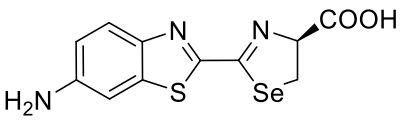

1.14

λ_{em} = 600 nm

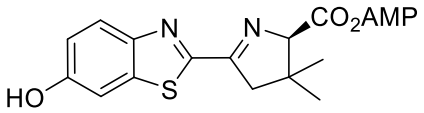

1.16

λ_{em} = 624 nm

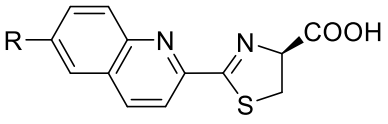

1.18 a R = OH

c R = NHMe

d R = NMe_2

λ_{em} = 608 nm

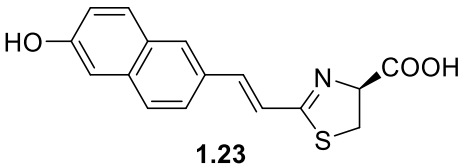

1.23

λ_{em} = 640 - 675 nm

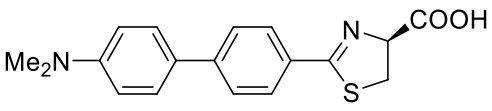

1.24

λ_{em} = 640 - 675 nm

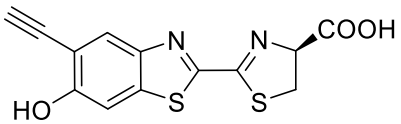

1.26

λ_{em} = 610 nm

Figure 1.2. A subset of structurally modified D-luciferin analogues containing bathochromic shifts.[29]

Despite significant progress achieved by the aforementioned research groups, none of the synthesised analogues exhibited enhanced bioluminescent output in luciferase-catalysed reactions compared to D-luciferin under conditions of excess luciferin and ATP. In the case of aminoluciferins, it has been hypothesised that the diminished light emission may result from inhibition of the bioluminescent reaction by oxidation products of luciferin.[70, 78] For analogues bearing substituted benzothiazole moieties (compounds **1.18-1.24**), the reduced efficacy has been likely attributed to a decreased rate of adenylate intermediate formation and/or increased susceptibility to non-enzymatic oxidation.[74, 79, 80] In both scenarios, the overall light output may also be limited by inherently low quantum yields of the excited states. Thus, D-luciferin remains the most effective substrate for in vitro bioluminescent assays, particularly when substrate availability is not a limiting factor.

1.2 Synthetic strategies towards D-luciferin and its analogues

1.2.1 General synthetic strategies towards D-luciferin

As discussed in the previous sections, D-luciferin and its derivative, D-aminoluciferin, are key bioluminescent compounds widely used in imaging applications.[68, 81-83] Their synthesis typically involves the formation of the thiazoline-thiazole core and functionalization of the benzothiazole system.[84, 85] The classical synthesis described by White *et al.* in 1963 has been used to synthesise D-luciferin and related compounds from *p*-anisidine (Scheme **1.3**).[86] A facile condensation reaction between D-cysteine and 2-cyano-6-hydroxybenzothiazole **2.9** forms the thiazoline-thiazole system through a 1,2-aminothiol click reaction[87] to produce D-luciferin, in an overall yield of 9%. Slightly improved synthetic pathways incorporating the synthesis of the 6-methoxybenzothiazole-2-carboxyamide intermediate have been attempted resulting in an overall yield of 39%, as described by Seto *et al*.[88] However, it was not until 2012 that there was a significant breakthrough in the synthesis of D-luciferin.

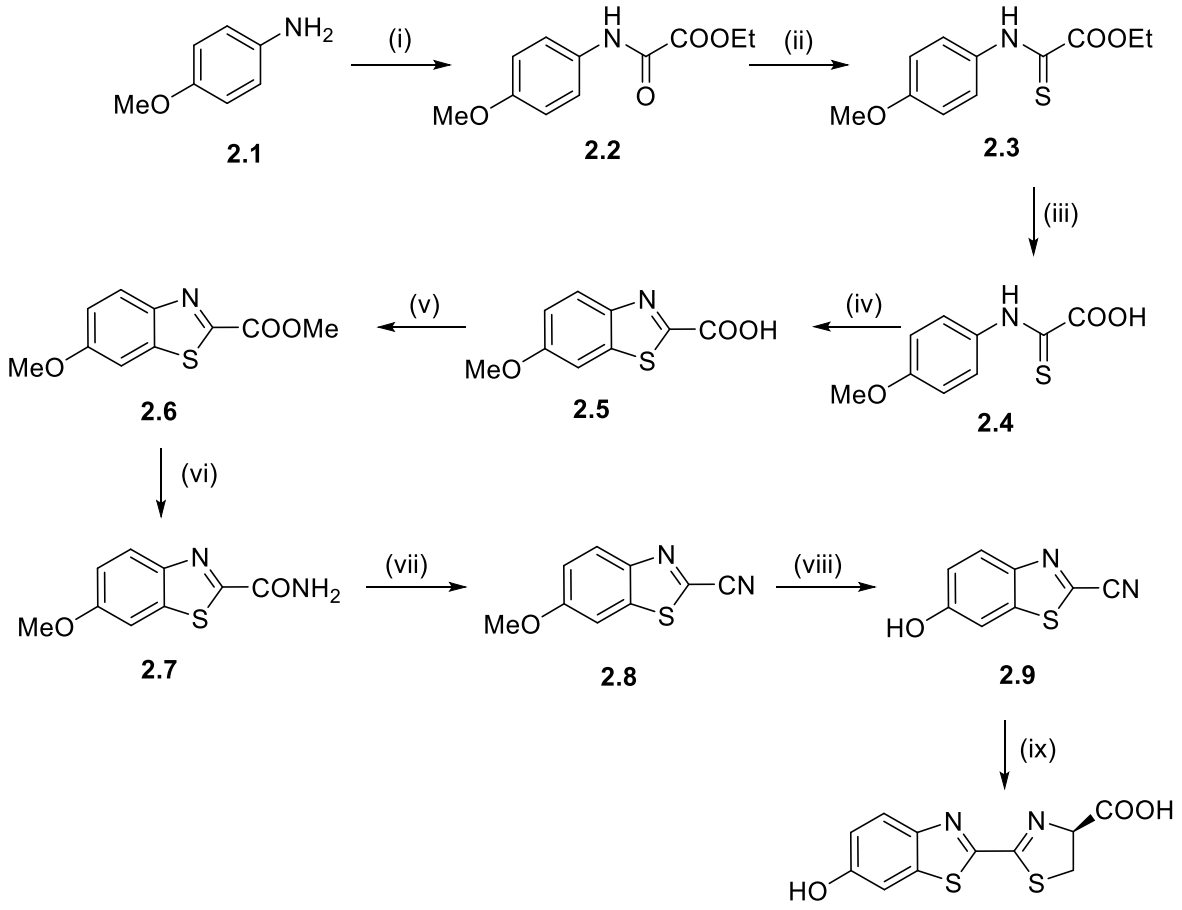

Scheme 1.3. Synthesis of D-luciferin from p-anisidine **2.1**.[85, 86] Reagents and conditions: (i) ethyl oxalate, 180 °C, 5 min, (58%) (ii) P_2S_5, reflux, 40 min, (iii) NaOH, 0 °C then HCl, (iv) $K_3Fe(CN)_6$/ OH^-, <10 °C, 15 min, (76% crude, no isolation in steps ii – iv), (v) CH_2N_2, 0 °C, 15 min, (40%), (vi) anhydrous NH_3/MeOH, heat, 30 min, (100%). (vii) $POCl_3$, reflux, 15 min, (56%), (viii) PyHCl, 200 °C, 1 h, (62%) (ix) D-cysteine (in situ from D-cystine/liquid NH_3/Na, rt, 10 min) and **2.9** in H_2O/MeOH, rt, 0.5 h (94%).

In the method described by McCutcheon and coworkers, *p*-anisidine **2.1** was treated with Appel's salt **1** to provide the expected dithiazole adduct **2.10**. Of note, Nyoni *et al.* demonstrated that DBU could also be utilised as a thiophilic base to extrude sulphur.[89] Therefore, reacting dithiazole **2.10** with DBU produced cyanothioformamide **2.11**. Subsequent palladium and copper-mediated cyclisation produced the key 6-methoxy-2-cyanobenzothiazole **2.8**. The methyl protecting group was then removed from **2.8** to produce 6-hydroxy-2-cyanobenzothiazole **2.9** followed by condensation with D-cysteine to yield D-luciferin (Scheme **1.4**). Overall, this route is four steps shorter than the sequence employed by White *et al.*[86] and produced the key intermediate **2.8** in a markedly better yield of 61%, with an overall yield of 42%.[90]

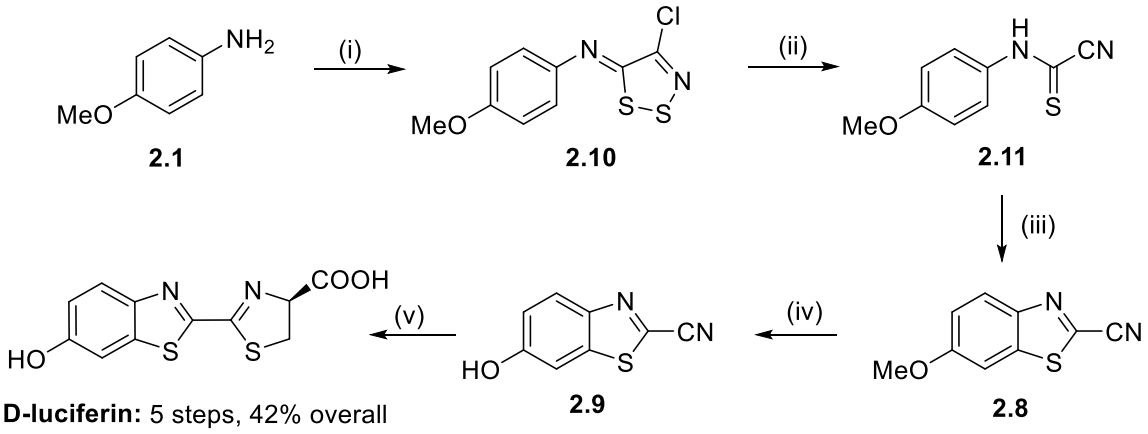

Scheme 1.4. McCutcheon *et al.* synthesis of D-luciferin from *p*-anisidine **2.1**.[90] Reagents and conditions: (i) Appel's salt **1**, DCM, pyridine (2 eq), rt, 3 h, (99%), (ii) DBU (3 eq), DCM, 0 °C-rt, 30 min, (97%), (iii) $PdCl_2$ (10 mol %), CuI (50 mol %), TBAB (2 eq), DMF:DMSO (1:1), 120 °C, 2 h, (87%), (iv) PyHCl (10 eq), neat, 190 °C, 1 h, (61%), (v) D-cysteine, K_2CO_3, H_2O:MeOH, rt, 20 min (86%).

Despite their initial success, in 2015 McCutcheon *et al*. attempted to address the limitations in their original synthetic route by abandoning the use of large volumes of solvent. They were able to replace DBU with a more tractable nucleophile, thiosulphate ($S_2O_3^{2-}$) to access **2.11**. Additionally, they found that this reaction could occur in a single pot following condensation of Appel's salt **1** and **2.1**. This condensed route improved the overall yield of D-luciferin (60%) by eliminating one synthetic step, along with two chromatographic separations (Scheme **1.5**).[91]

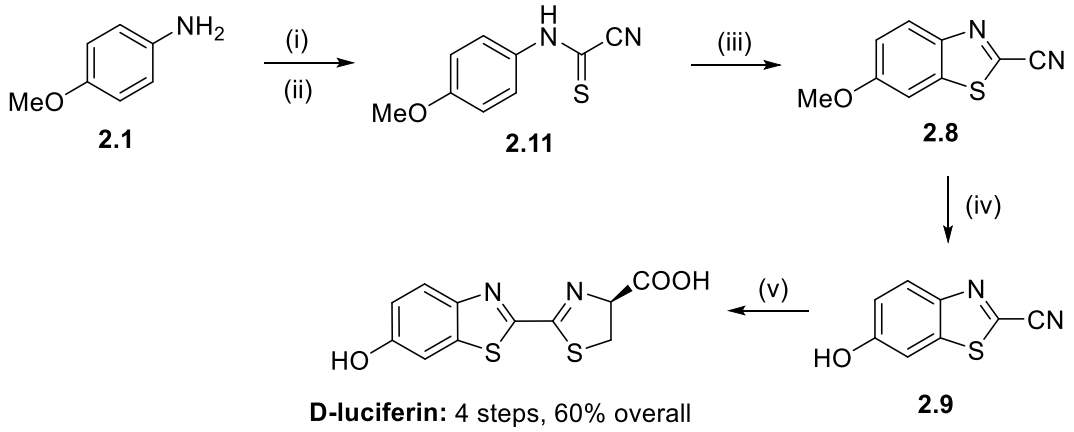

Scheme 1.5. One pot condensation synthesis of D-luciferin employed by McCutcheon *et al*.[91] Reagents and conditions: (i) **1**, DCM, pyridine (2 eq), rt, 3 h, (ii) $Na_2S_2O_3$ (3 eq), H_2O, rt, 3 h (86%), (iii) $PdCl_2$ (10 mol %), CuI (50 mol %), TBAB (2 eq), DMF:DMSO (1:1), 120 °C, 2 h, (87%), (iv) pyr·HCl (10 eq), sulfolane, 180 °C, 1 h, (93%), (v) D-cysteine, K_2CO_3, H_2O:MeOH, rt, 20 min (86%).

However, the work of McCutcheon *et al.* was still not complete. The authors also recognised that the formation of cyanobenzothiazole **2.8** in their original synthesis (step 3, Scheme **1.3**)

was not optimal as it required the use of expensive metal reagents, non-ideal solvents, excess TBAB, and dilute conditions. Based on work from Rakitin,[92] the authors reasoned that **2.8** could be obtained directly from dithiazole **2.10** through thermolysis. In a single pot, under conditions of high temperatures and subsequent treatment with pyr·HCl, **2.8** (20%) as well as **2.9** (61%) were isolated (Scheme **1.6**, **A**). Rather excitingly, the authors also found that the cyclisation/deprotection sequence could be coupled with the formation of imine **2.10** (as in Scheme **1.4**). When condensing **2.1** with Appel's salt **1**, followed by rigorous heating in sulfolane and pyr·HCl treatment, **2.8** and **2.9** were isolated in yields of 21% and 51% respectively. This improved, streamlined synthesis that requires only two steps is the shortest synthesis of D-luciferin from simple anilines to date (Scheme **1.6**, **B**).

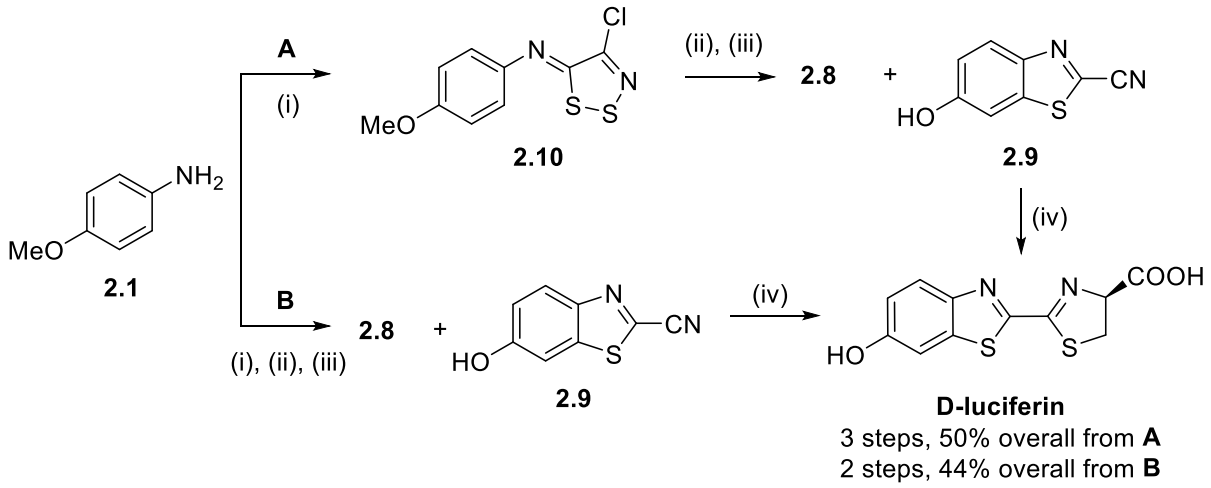

Scheme 1.6. Condensed synthesis of D-luciferin via Appel's salt **1** condensation and thermolysis.[91] Reagents and conditions **(A):** (i) **1**, DCM, pyridine (2 eq), rt, 3 h, (96%), (ii) Sulfolane, 180 °C, 20 min, (iii) pyr·HCl (10 eq), 180 °C, 1 h, **2.8** (20%) and **2.9** (61%). **(B):** (i) **1**, sulfolane, 40 °C, 3 h, (ii) 180 °C, 20 min, (iii) pyrHCl (10 eq), 180 °C, 1 h, **2.8** (21%) and **2.9** (51%), (iv) D-cysteine, K_2CO_3, H_2O:MeOH, rt, 20 min (86%).

1.2.2 General synthetic strategies towards D-aminoluciferin

The synthesis of D-aminoluciferin follows a similar pathway but incorporates an amino functional group instead of the hydroxyl at the 6-position of the benzothiazole ring. The typical synthetic route also published by McCutcheon *et al.*[91] starts with *p*-nitroaniline which was condensed with **1** followed by treatment with sodium thiosulfate to produce the 6-hydroxy-2-cyanobenzothiazole **2.13**. Palladium and copper mediated cyclisation produced benzothiazole **2.14**, followed by reduction of the nitro group and subsequent D-cysteine condensation to produce the desired D-aminoluciferin with an overall yield of 51% (Scheme **1.7**, **A**). The authors were able to further improve their synthetic route by installing a thiol group ortho to the nitro group in the starting material *p*-nitroaniline, thus enabling facile access to D-

aminoluciferin in three steps with an overall yield of 54% (Scheme **1.7**, **B**). Notably, the authors also reported this as the shortest and highest yielding synthesis of D-aminoluciferin to date.

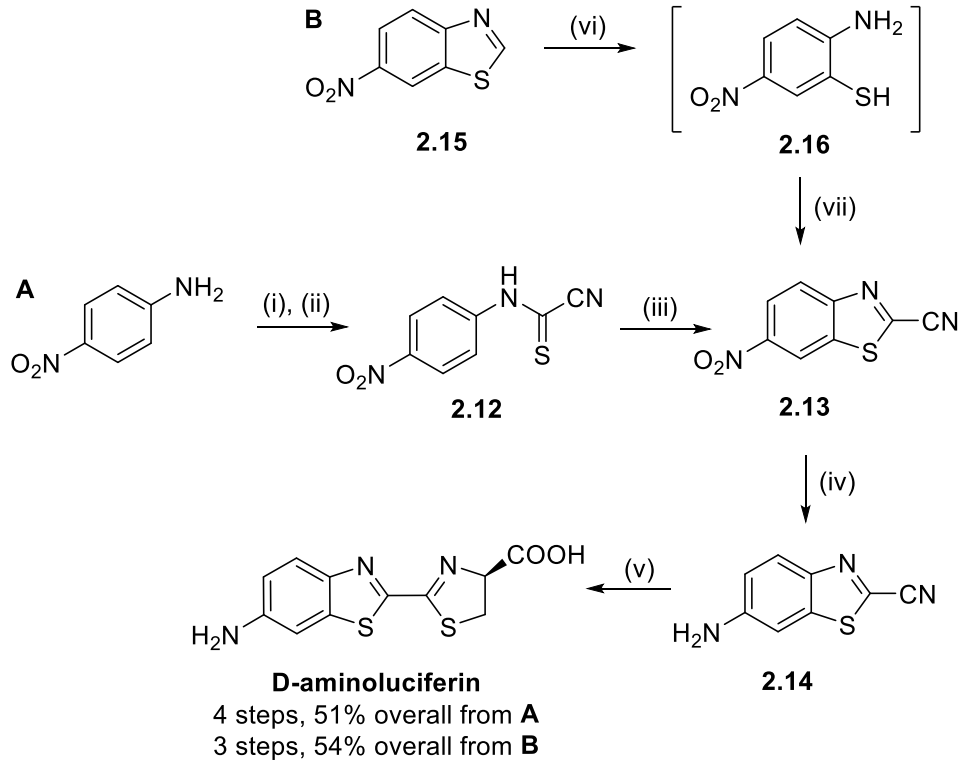

Scheme 1.7. McCutcheon *et al.* synthesis of D-aminoluciferin from **(A)** *p*-nitroaniline and **(B)** hydrazine.[91] Reagents and conditions: (i) **1**, MeCN:THF (2:1), (ii) $Na_2S_2O_3$ (3 eq), H_2O, rt, 3 h, (80%), (iii) $PdCl_2$ (10 mol %), CuI (50 mol %), TBAB (2 eq), DMF:DMSO (1:1), 130 °C, 3 h, (74%), (iv) Zn, NH_4Cl, MeOH, rt, 30 min, (95%), (v) D-cysteine, K_2CO_3, MeCN:H_2O (4:1), rt, 20 min, (91%), (vi) $NH_2NH_2.H_2O$, EtOH, rt 12 h, (vii) **1**, DCM, reflux 12 h (62%).

1.2.3 C-6 Heteroatom substitution of D-luciferin

With the first synthesis of D-luciferin and its 6-amino analogue by White *et al*., a new era of bioluminescence assays and BLI was ushered in. This advancement led to a surge in luciferin-based assays, where the amine functionality served as a handle for constructing probes via amide hydrolysis. Since then, numerous derivatives have been developed by various research groups to create new bioluminogenic substrates and imaging probes. However, these derivatives are all based on modifications of either natural (6′-hydroxy) D-luciferin or D-aminoluciferin, thereby restricting the chemistry to *O*- and *N*-linked variants.[93]

Previously, Ohulchanskyy *et al*. investigated how replacing the oxygen atom in tetramethylrosamine (TMR-O) dyes with sulphur (TMR-S) or selenium (TMR-Se) affects their photophysical properties, particularly fluorescence, triplet state behaviour, and singlet oxygen generation.[94] They found that while substituting oxygen with sulphur or selenium leads to a

decrease in fluorescence efficiency, bathochromic shifts in both absorption and emission spectra were observed (Figure **1.3**). The results strongly demonstrate the heavy-atom effect, where increased atomic mass (O → S → Se) enhances spin-orbit coupling, boosts intersystem crossing, and alters excited-state dynamics.[95]

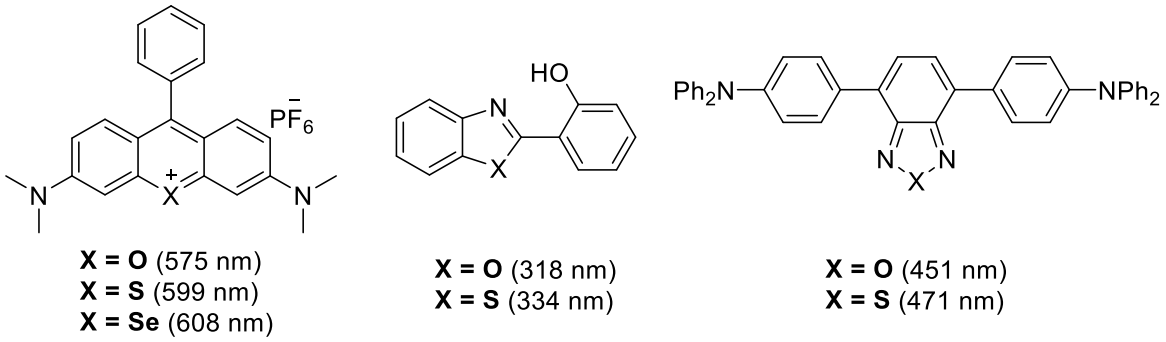

X = O (575 nm)
X = S (599 nm)
X = Se (608 nm)

X = O (318 nm)
X = S (334 nm)

X = O (451 nm)
X = S (471 nm)

Figure 1.3. Compounds with varying fluorescence emission maxima due to heteroatom substitution, illustrating the heavy atom effect.

In addition, several time-dependent density functional theory (TD-DFT) investigations have explored how heteroatom substitution influences the photophysical properties of heteroaromatic fluorescent molecules (Figure **1.3**).[96, 97] These studies consistently report that replacing oxygen with sulphur leads to bathochromic shifts in fluorescence emission maxima. This shift is attributed to a reduced energy gap between the ground and excited states.

It has been established that the energies of the highest occupied molecular orbitals (HOMOs) and lowest unoccupied molecular orbitals (LUMOs) in both states are critical not only for determining spectral properties but also for influencing chemical reactivity. Since the same energy differences that affect fluorescence also govern bioluminescence emission maxima, findings from fluorescent systems are directly relevant to bioluminescent ones.

While the influence of C-6 nitrogen substitution on bioluminescent activity has already been studied, introducing sulphur at the C-6 position, offers new insights into how the 6′-heteroatom affects the photobiological properties of D-luciferin (Figure **1.4**). Furthermore, this bioluminescent thiol analogue could pave the way for a new class of bioluminescent probes with potential applications that extend beyond the capabilities of conventional D-luciferin and D-aminoluciferin systems.

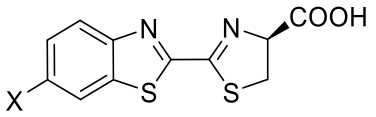

X = OH, D-luciferin
X = NH, D-aminoluciferin
X = SH, D-thioluciferin

Figure 1.4. Structures of C-6 heteroatom-substituted luciferins.

1.2.4 D-Thioluciferin, a novel thio-analogue of D-luciferin

(i) Jardine - Rylands Method

In 2018 Rylands *et al.* reported the synthesis of a novel luciferin analogue, namely D-thioluciferin.[93] This analogue was unique in that it demonstrated a bioluminescence emission maximum with a red-shift λ_{max} (599 nm) relative to D-luciferin (557 nm) and D-aminoluciferin (593 nm) upon treatment with purified *Photinus pyralis* (Ppy) luciferase (Luc). Moreover, cancer cells have been shown to undergo abnormal redox homeostasis, resulting in oxidative stress.[98] This lead to the hypothesis that cancer cells expressing fLuc would oxidise the thiol group of D-thioluciferin to the disulphide in vivo. Theoretically, this would cause cancer cells to produce a less intense bioluminescence signal as opposed to healthy cells.

The Rylands *et al.* synthesis relies on the aryl thioacrylate as a sulphur protecting group. As such, using thiol-yne click chemistry, aryl thioacrylate **5.2** was obtained via a chemoselective reaction between benzyl propiolate **5.1** and *p*-aminothiophenol. This, he reported, resulted in a separable *E/Z* thioacrylate mixture of **5.2** and **5.3**. The cis isomer **5.2** was isolated and subsequently reacted with Appel's salt **1** to yield *N*-aryliminodithiazole **5.4**. Subsequent nucleophilic attack of thiophilic DBU converted *N*-aryliminodithiazole **5.4** into cyanoformanilide **5.5**. Thereafter, intramolecular C-S coupling using palladium chloride formed the cyclised carbonitrile **5.6**. Following the addition of 2 mol equivalents of D-cysteine, a one pot D-cysteine condensation as well as thioacrylate deprotection of carbonitrile **5.7** released D-thioluciferin in an overall yield of 14% (Scheme **1.8**).[93]

The limitations of the Rylands method, however manifested in the penultimate step of the synthetic sequence. In previous attempts of replicating the synthetic route, it appeared that the cis isomer is stable as the D-thioluciferin acrylate **5.7**.[99] It was found that in the presence of organic bases, the cis isomer **5.2** undergoes conversion to a mixture of *E/Z* isomers following a Michael addition-elimination mechanism. Shiu *et al*. investigated the modification of cysteine-containing peptides in which they found that thiol-protection of cysteine using electron-deficient alkynes favoured formation of the *Z*-isomer.[100] Attempts made to isolate the trans isomer **5.3** to ascertain whether the uncaging was isomer-dependent were unsuccessful,

with the dominant cis isomer **5.2** forming in low yield. It was thus concluded that the *E*-isomer was stable to a thio-Michael addition-elimination reaction.[99]

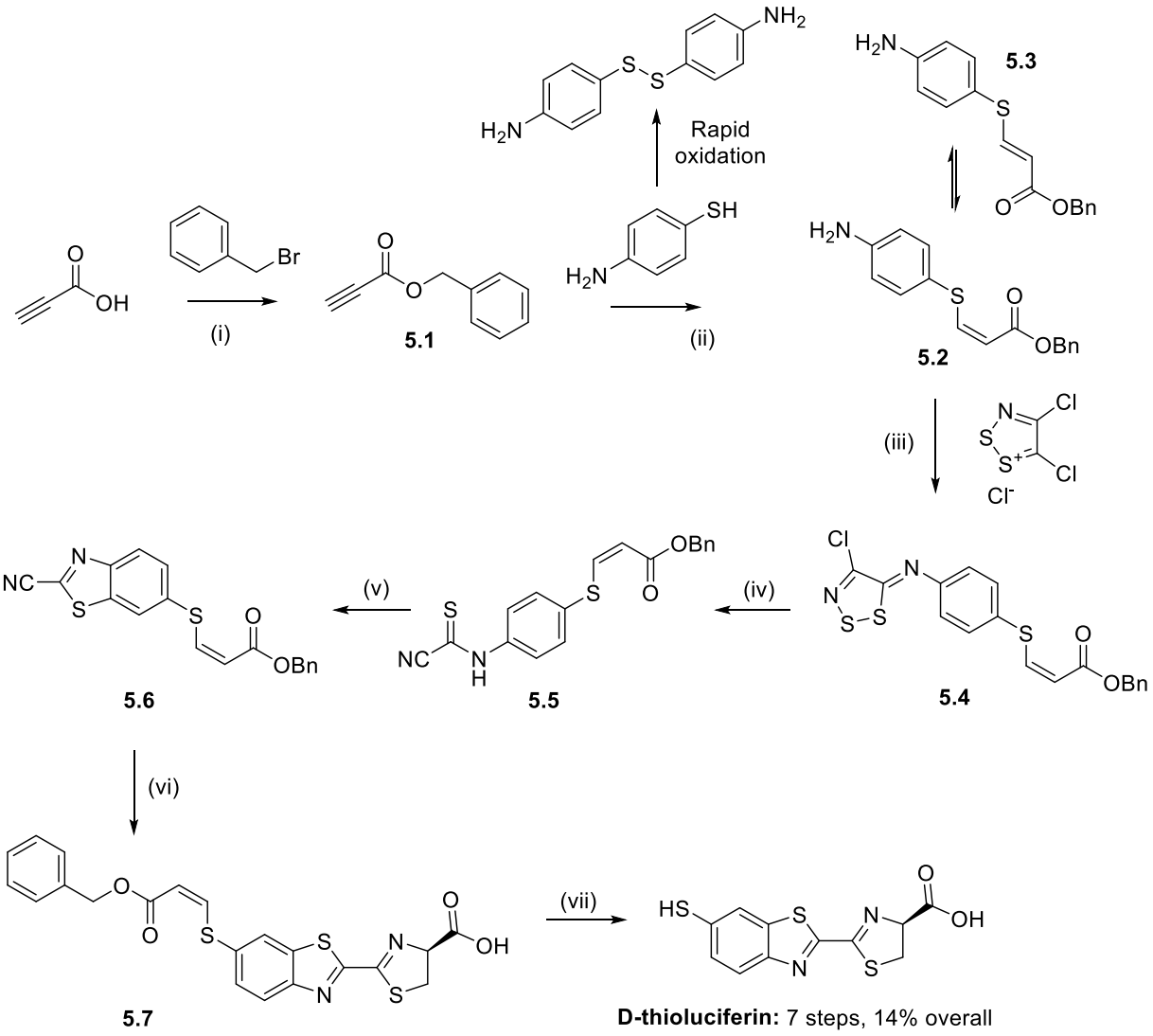

Scheme 1.8. Synthetic route toward D-thioluciferin.[101] Reagents and conditions: i) Cs_2CO_3, BnBr, DMF, 0° C, (99%), (ii) *p*-aminothiophenol, DMF, 24 hrs, 0° C, N_2, (39%), (iii) Appel's salt **1**, pyridine, DMF, rt, N_2, (99%), (iv) DBU, DMSO, rt, N_2, (61%), (v) $PdCl_2$, CuI, TBAB, DMSO, 120° C, N_2, (62%), (vi) D-cysteine, K_2CO_3, DMSO, 0 °C, N_2, (98%).

As a result, D-thioluciferin was not obtained which warranted the exploration of an alternate route. To this end, Rylands reported that the synthesis of 2-cyano-6-iodobenzothiazole **14** was a key intermediate in future D-thioluciferin synthetic routes.[93] The reasoning being that the iodine functionality would act as a surrogate group to access the thiol moiety. In his attempts, he succeeded in synthesising 6-iodo-2-cyanobenzothiazole **14**,[101] however, was not able to obtain the thio derivative **7** (Scheme **1.9**). This, he presumed, was due to the C-2 nitrile functionality which reacted with the sulphur reagent. This argument is supported by the claims

of Sharma *et al* who also stated that the C-2 nitrile functionality presented a challenge on C-6 halide substitution.[102] Attempts made at improved synthesis of 6-iodo-2-cyanobenzothiazole are discussed in detail in **Chapter 2**.

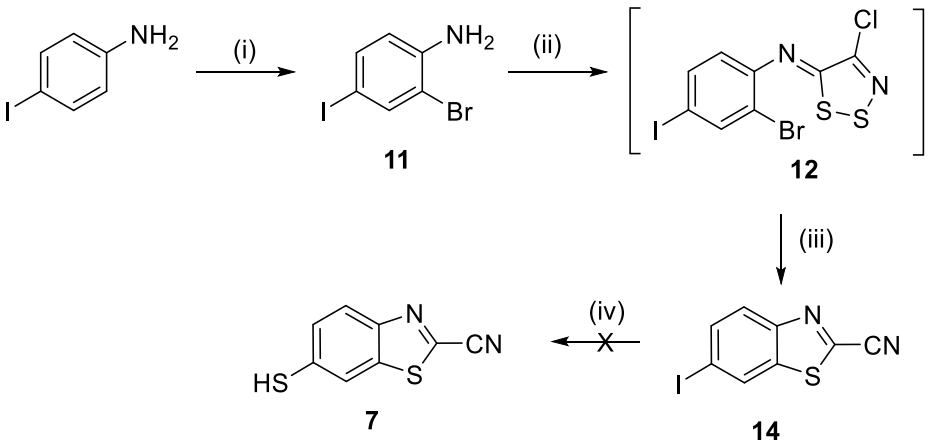

Scheme 1.9. One pot, metal-free base-mediated cyclisation from *o*-bromoaniline.[93] Reagents and conditions: (i) $NaBO_3$, KBr, AcOH, rt, 16 h, (78%), (ii) Appel's salt **1**, DCM, 3 h, (iii) DBU, DCM, 5 °C, 3-4 h, (67%), (iv) CuI, Sulfur powder, K_2CO_3, DMF, 90 °C, $NaBH_4$.

(ii) Sharma synthesis of D-alkylthioluciferins

In 2017, Sharma *et al.* published a paper on a new synthetic approach for accessing a wide range of 6′-substituted firefly luciferin analogues, expanding the scope of known luciferase substrates.[102] The researchers developed a route that included nucleophilic aromatic substitution (S_NAr) and Buchwald-Hartwig[103] amination of 6-fluoro- and 6-bromo-2-cyanobenzothiazoles respectively. The latter methodology effected the introduction of diverse electron-donating groups at the 6′-position of the D-luciferin core. Furthermore, the work enabled the synthesis of novel "caged" amide and azetidine analogues, luminogenic aryl amine derivatives as well as thioether luciferase inhibitors.

Some key thioether analogues the authors investigated included methanethiol-substituted analogue **19** (obtained in an overall yield of 34%) which was expected to be highly fluorescent, as well as its sulfoxide derivative **21**, obtained in an overall yield of 24%. Their luciferin analogues **20** and **22** were obtained in overall yields of 17% and 13% respectively. (Scheme **1.10**).

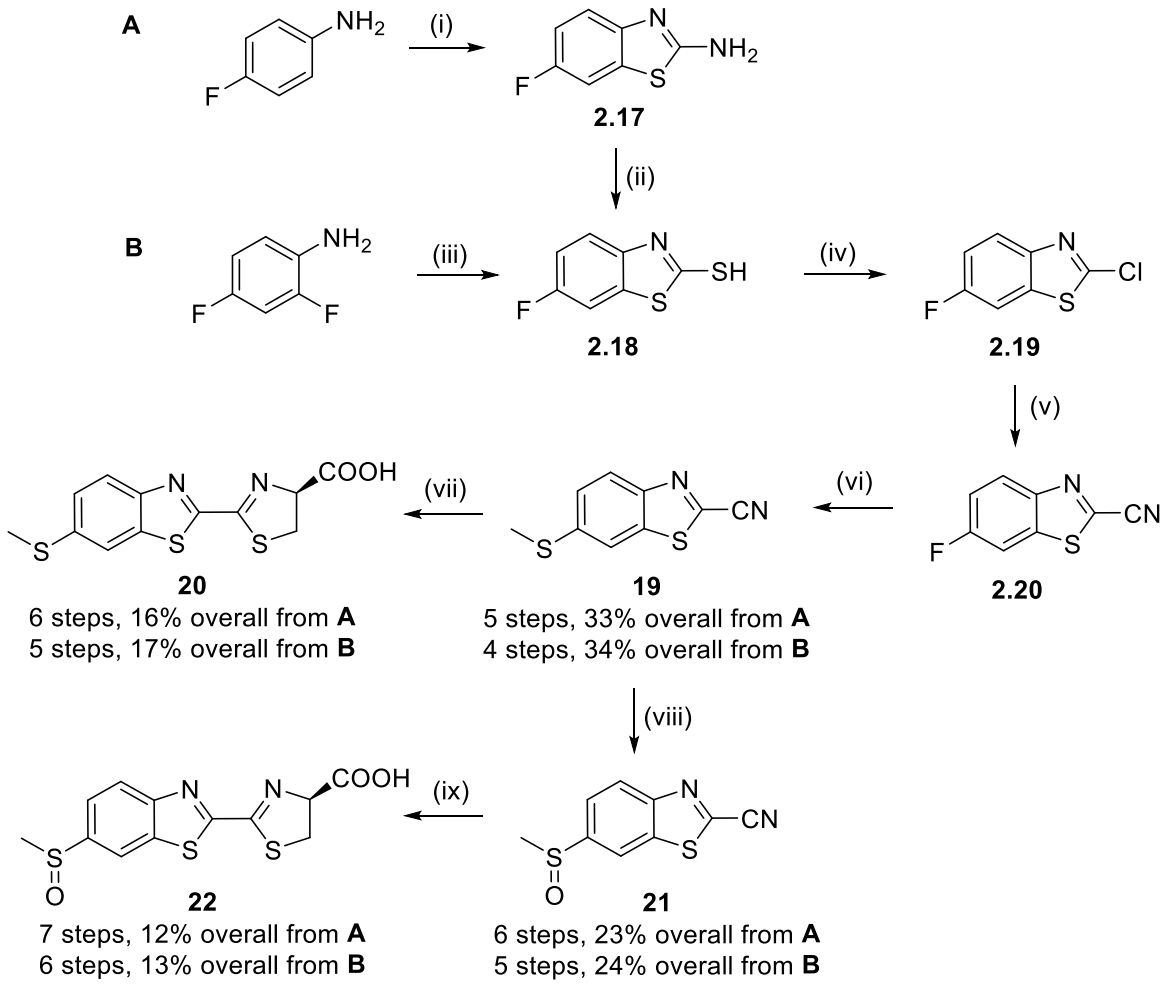

Scheme 1.10. Sharma's synthetic route to thiomethyl **20** and methylsulfinyl-substituted luciferin **22** from **(A)** 4-fluoroaniline and **(B)** 2,4-difluoroaniline.[102] Reagents and conditions: (i) Br (s), KSCN, acetic acid, rt, 21 h, (94%), (ii) t-butyl nitrite, $CuCl_2$, CH_3CN, rt – 65 °C, 3 h, (95%), (iii) Potassium ethyl xanthogenate, DMF, 95 °C, 4 h, Ar (g), (93%), (iv) SO_2Cl_2, rt, 2 h, N_2 (g), (95%), (v) KCN, DMSO, 80 °C, 6 h, (81%), (vi) Sodium thiomethoxide, DMF, 60 °C, 8 h, (48%), (vii) D-cysteine, Na_2PO_4, rt, 1 h, Ar (g), (50%), (viii) Oxone, ethanol, 60 °C, 8 h, (71%), (ix) D-cysteine, Na_2PO_4 (aq), methanol, 1 h, Ar (g) (53%).

Bioluminescence evaluation revealed that thioether **20** is a potent luciferase inhibitor, while thiomethyl sulfoxide **22** is only weakly inhibitory. The authors suggest these results could provide a potential strategy for constructing bioluminescent sensors of S-oxidation based on relief of luciferase inhibition.[102] While this may be the case, the overall yields of the aforementioned target compounds are quite low. Additionally, the use of the asphyxiant potassium cyanide is highly unfavourable due to the substantial risks related to toxicity and potential oxygen displacement in confined laboratory environments. Attempts at a high yielding, condensed method for the synthesis of these compounds is thus explored in **Chapter 3**.

(iii) Pirrung synthesis of D-thioluciferin

More recently, Pirrung *et al.* published a completely new synthetic route to D-thioluciferin from (allylthio)aniline.[104] This synthetic route comprises of a sequence of steps incorporating the general luciferin synthesis developed by Prescher[90, 91] as well as a Mislow-Evans[105] type rearrangement mediated by triphenylphosphite.

Pirrung and co-workers employed an *S*-allyl protecting group in their synthetic strategy. The sequence begins with the condensation of 4,5-dichloro-1,2,3-dithiazolium chloride (Appel's salt) **1** and amine **2** to generate imine **3**. This intermediate then undergoes DBU-mediated dithiazole fragmentation to yield thioformamide **4**. A copper(I) iodide/palladium(II) chloride-catalysed C–S cross-coupling of thioformamide **4** produces benzothiazole **5**. Subsequent non-asymmetric oxidation of **5** using sodium periodate affords sulfoxide **6**, which undergoes a Mislow–Evans-type *[2,3]*-sigmatropic rearrangement. This is followed by triphenylphosphite [$P(OPh)_3$]-mediated cleavage of the sulfenate intermediate to give thiobenzothiazole **7**. The final step involves a standard luciferin condensation with D-cysteine to afford the desired product, D-thioluciferin (Scheme **1.11**). Overall, this route is one step shorter than that reported by Rylands *et al*. and proceeds in a higher overall yield of 23%.

Optical analyses by the authors revealed that D-thioluciferin exhibited a blue-shifted absorption and fluorescence emission maxima compared to D-luciferin which they attributed to reduced conjugation due to the sulphur atom's larger orbital size. Bioluminescence evaluation of the product revealed it to be a modest substrate with very low light output, while displaying substrate inhibition at higher concentrations. These findings are consistent with the thioether luciferin analogues developed by Sharma *et al*.[102] The authors attributed the diminished bioluminescence due to poor orbital overlap between the thiolate and the aromatic system, making D-thioluciferin more like non-luminescent deoxyluciferin. However, despite the low emission, D-thioluciferin was found to bind tightly to luciferase (Km = 0.16 μM; Ki = 0.07 μM).[104]

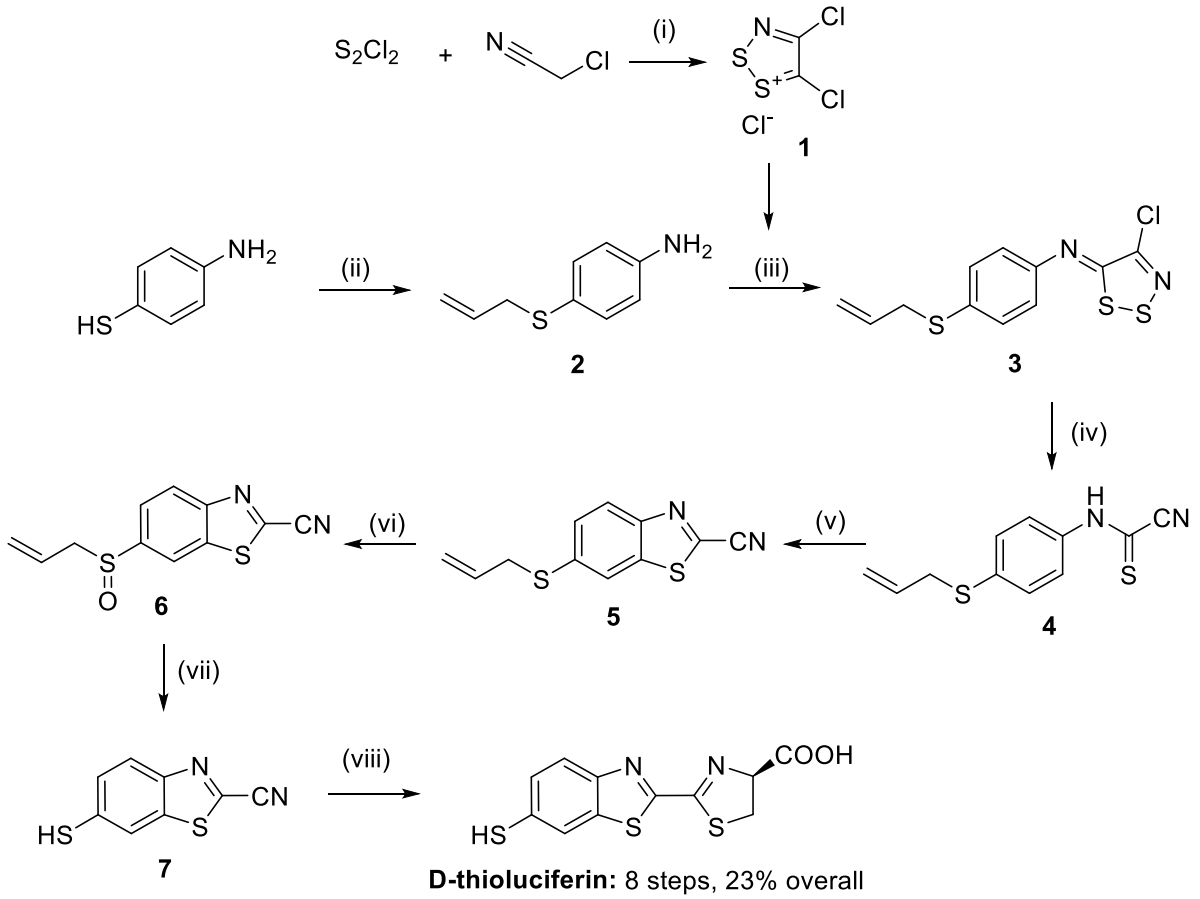

Scheme 1.11. Linear synthetic route for the synthesis of D-thioluciferin.[104] Reagents and conditions: (i) DCM, rt, 24 h, (ii) Allyl bromide, K_2CO_3, acetone, rt, 18 h, (90%), (iii) Appel's salt, DCM, anhydrous pyridine, rt, 3 h, (77%), (iv) DCM, DBU, -5 ℃, 1 h, (83%), (v) $PdCl_2$ (10 mol %), CuI (50 mol %), TBAB (2 eq), DMF:DMSO (1:1), 120 ℃, 1 h, (65%), (vi) DCM:MeOH (1:5), $NaIO_4$, 0 ℃, 12 h, (90%), (vii) $P(OPh)_3$, THF, H_2O, 18 h, (79%), (viii) D-Cysteine, K_2CO_3, MeOH:H_2O, rt, 30 min (87%).

Furthermore, D-thioluciferin easily forms a disulphide in solution, however this oxidised form is non-bioluminescent as expected. Since the reduced form is required for bioluminescent activity, it was stabilised with tris(2-carboxyethyl)phosphine (TCEP).[104] Although the low light output of D-thioluciferin limits immediate application, the authors suggest its unique redox sensitivity and enzyme binding possess potential as a redox probe in future engineered luciferase systems or modified assay conditions. To further analyse D-thioluciferin, this synthetic route was attempted, with the results obtained discussed in **Chapter 3**.

1.3 Motivation for the synthesis of C-6 modified luciferin derivatives

Previous attempts at D-thioluciferin and D-alkylthioluciferin syntheses were unfavourable due to the low yields and use of a toxic asphyxiant. The general plan of this research project is thus to elucidate a condensed, high yielding synthetic route to D-thioluciferin and D-alkylthioluciferin to be used as bioluminescent probes in cancer cell lines. The availability of thioluciferin will also enable the synthesis of cephalosporin conjugates in a β-lactamase activation strategy as previously demonstrated by the Bluco probe (Figure **1.5**).

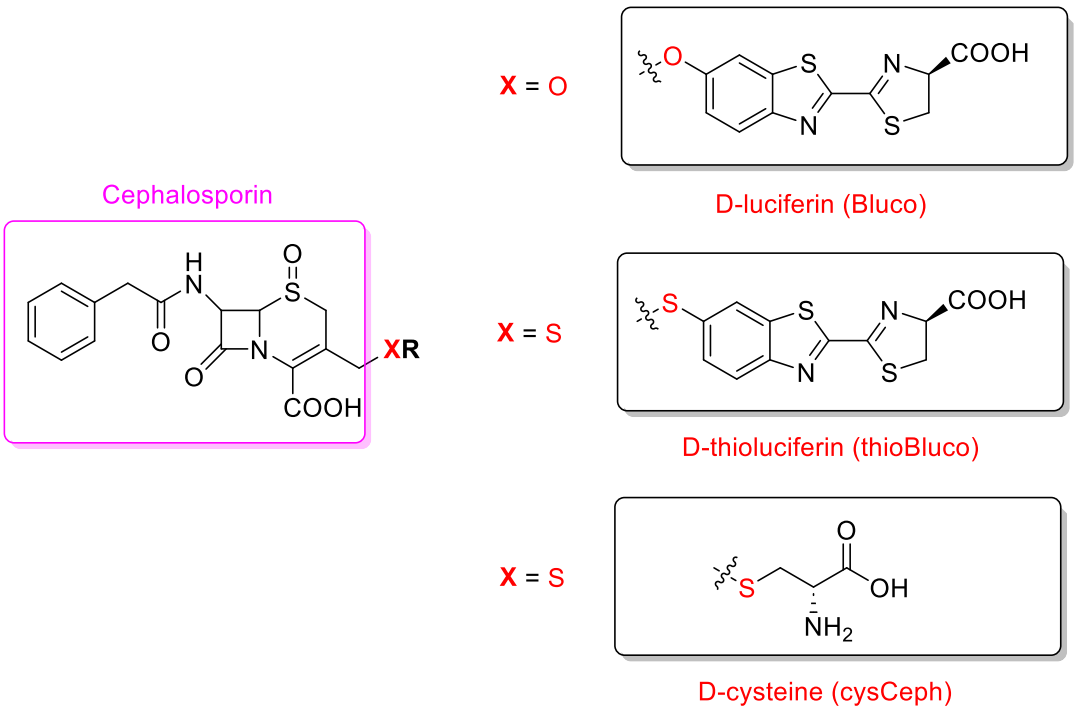

Figure 1.5. Structures of C-6 heteroatom-substituted luciferins.

Additionally, forming a D-cysteine-cephalosporin conjugate (cysCeph) would allow for the release of free D-cysteine once the conjugate is hydrolysed by β-lac. Uncoupled 6-substituted benzothiazoles could react with D-cysteine and subsequently produce a bioluminescence emission in cells expressing the fLuc enzme (Scheme **1.12**).

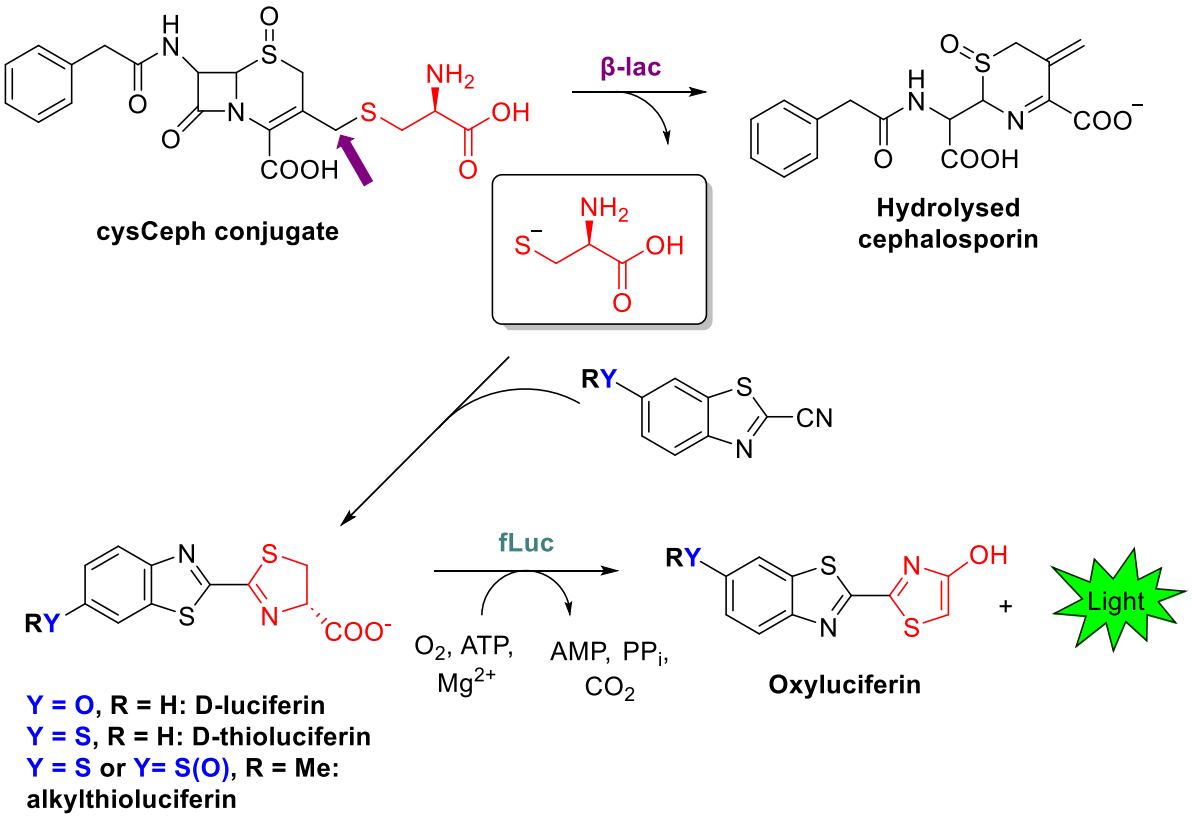

Scheme 1.12. Proposed β-lactamase activation strategy with D-cysteine.

1.4 Aims and Objectives

1.4.1 Aims

The overall aim of this project is to develop an improved synthetic route towards D-thioluciferin and alkylthioluciferins, and in doing so improve the synthesis of the key intermediate 6-iodo-2-cyanobenzothiazole. Improving the aqueous solubility of luciferin analogues by developing synthetic routes to aza-luciferin analogues has also been highlighted as part of the aims of this project as aza-analogues hold potential for further development. These results are discussed in **Chapter 4**. The availability of D-thioluciferin will enable the synthesis of β-lactam probes such as Bluco. Lastly, all target compounds were to be analysed for their potential fluorescence, bioluminescence and cytotoxic activity and are discussed in **Chapter 5**.

1.4.2 Objectives

Objective 1: Synthesise and characterise 6-iodo-2-cyanobenzothiazole.

Objective 2: Synthesise and characterise D-thioluciferin.

Objective 3: Synthesise and characterise alkylthioluciferins.

Objective 4: Synthesise and characterise aza-luciferin analogues.

Objective 5: Evaluate the fluorescence emission of the target compounds.

Objective 6: Evaluate the bioluminescence emission of the target compounds.

Objective 7: Evaluate the possible cytotoxic effects of the target compounds in cancer cell lines.

1.5 References

(1) Yun, S. H.; Kwok, S. J. Light in diagnosis, therapy and surgery. *Nature biomedical engineering* **2017**, *1* (1), 0008.

(2) Lee, G.-H.; Moon, H.; Kim, H.; Lee, G. H.; Kwon, W.; Yoo, S.; Myung, D.; Yun, S. H.; Bao, Z.; Hahn, S. K. Multifunctional materials for implantable and wearable photonic healthcare devices. *Nature Reviews Materials* **2020**, *5* (2), 149-165.

(3) Kim, H.; Jung, S. O.; Lee, S.; Lee, Y. Bioluminescent Systems for Theranostic Applications. *International Journal of Molecular Sciences* **2024**, *25* (14), 7563.

(4) Wolfbeis, O. S. An overview of nanoparticles commonly used in fluorescent bioimaging. *Chemical Society Reviews* **2015**, *44* (14), 4743-4768.

(5) Wang, S.; Li, B.; Zhang, F. Molecular fluorophores for deep-tissue bioimaging. *ACS central science* **2020**, *6* (8), 1302-1316.

(6) De Freitas, L. F.; Hamblin, M. R. Proposed mechanisms of photobiomodulation or low-level light therapy. *IEEE Journal of selected topics in quantum electronics* **2016**, *22* (3), 348-364.

(7) Hamblin, M. R. Photobiomodulation or low-level laser therapy. *Journal of biophotonics* **2016**, *9* (11-12), 1122.

(8) Wang, Z.; Li, H.; She, W.; Zhang, X.; Liu, Y.; Liu, Y.; Jiang, P. 3-Bromopyruvate-loaded Ti3C2 MXene/Cu2O nanosheets for photoacoustic imaging-guided and hypoxia-relieving enhanced photothermal/chemodynamic therapy. *Analytical Chemistry* **2023**, *95* (2), 1710-1720.

(9) Pham, T. C.; Nguyen, V.-N.; Choi, Y.; Lee, S.; Yoon, J. Recent strategies to develop innovative photosensitizers for enhanced photodynamic therapy. *Chemical reviews* **2021**, *121* (21), 13454-13619.

(10) Wang, M.; Rao, J.; Wang, M.; Li, X.; Liu, K.; Naylor, M. F.; Nordquist, R. E.; Chen, W. R.; Zhou, F. Cancer photo-immunotherapy: from bench to bedside. *Theranostics* **2021**, *11* (5), 2218.

(11) Chen, D.; Tang, Y.; Zhu, J.; Zhang, J.; Song, X.; Wang, W.; Shao, J.; Huang, W.; Chen, P.; Dong, X. Photothermal-pH-hypoxia responsive multifunctional nanoplatform for cancer photo-chemo therapy with negligible skin phototoxicity. *Biomaterials* **2019**, *221*, 119422.

(12) Arany, P. R.; Cho, A.; Hunt, T. D.; Sidhu, G.; Shin, K.; Hahm, E.; Huang, G. X.; Weaver, J.; Chen, A. C.-H.; Padwa, B. L. Photoactivation of endogenous latent transforming growth factor–β1 directs dental stem cell differentiation for regeneration. *Science translational medicine* **2014**, *6* (238), 238ra269-238ra269.

(13) Peng, J.; Zhao, J.; Tang, Q.; Wang, J.; Song, W.; Lu, X.; Huang, X.; Chen, G.; Zheng, W.; Zhang, L. Low intensity near-infrared light promotes bone regeneration via circadian clock protein cryptochrome 1. *International Journal of Oral Science* **2022**, *14* (1), 53.

(14) Sordillo, L. A.; Pu, Y.; Pratavieira, S.; Budansky, Y.; Alfano, R. R. Deep optical imaging of tissue using the second and third near-infrared spectral windows. *Journal of biomedical optics* **2014**, *19* (5), 056004-056004.

(15) Choi, J.; Lee, I. S.; Lee, J. S.; Jeon, S.; Yun, W. S.; Yang, S.; Moon, Y.; Kim, J.; Kim, J.; Choy, S. Implantable micro-scale LED device guided photodynamic therapy to potentiate antitumor immunity with mild visible light. *Biomaterials Research* **2022**, *26* (1), 56.

(16) Ran, Y.; Xu, Z.; Chen, M.; Wang, W.; Wu, Y.; Cai, J.; Long, J.; Chen, Z. S.; Zhang, D.; Guan, B. O. Fiber-optic theranostics (FOT): interstitial fiber-optic needles for cancer sensing and therapy. *Advanced science* **2022**, *9* (15), 2200456.

(17) Wang, D.; Kuzma, M. L.; Tan, X.; He, T.-C.; Dong, C.; Liu, Z.; Yang, J. Phototherapy and optical waveguides for the treatment of infection. *Advanced drug delivery reviews* **2021**, *179*, 114036.

(18) Haddock, S. H.; Moline, M. A.; Case, J. F. Bioluminescence in the sea. *Annual review of marine science* **2010**, *2* (1), 443-493.

(19) Widder, E. A. Bioluminescence in the ocean: origins of biological, chemical, and ecological diversity. *Science* **2010**, *328* (5979), 704-708.

(20) Herring, P. J. Bioluminescence of marine organisms. *Nature* **1977**, *267* (5614), 788-793.

(21) Shimomura, O. *Bioluminescence: chemical principles and methods*; World Scientific, 2006.

(22) Inouye, S. Firefly luciferase: an adenylate-forming enzyme for multicatalytic functions. *Cellular and molecular life sciences* **2010**, *67* (3), 387-404.

(23) Wilson, T.; Hastings, J. W. Bioluminescence. *Annual review of cell and developmental biology* **1998**, *14* (1), 197-230.

(24) Syed, A. J.; Anderson, J. C. Applications of bioluminescence in biotechnology and beyond. *Chemical Society Reviews* **2021**, *50* (9), 5668-5705.

(25) Adams Jr, S. T.; Miller, S. C. Enzymatic promiscuity and the evolution of bioluminescence. *The FEBS journal* **2020**, *287* (7), 1369-1380.

(26) Jiang, T.; Du, L.; Li, M. Lighting up bioluminescence with coelenterazine: Strategies and applications. *Photochemical & Photobiological Sciences* **2016**, *15*, 466-480.

(27) Xu, Y.; Piston, D. W.; Johnson, C. H. A bioluminescence resonance energy transfer (BRET) system: application to interacting circadian clock proteins. *Proceedings of the National Academy of Sciences* **1999**, *96* (1), 151-156.

(28) Pfleger, K. D.; Eidne, K. A. Illuminating insights into protein-protein interactions using bioluminescence resonance energy transfer (BRET). *Nature methods* **2006**, *3* (3), 165-174.

(29) Kaskova, Z. M.; Tsarkova, A. S.; Yampolsky, I. V. 1001 lights: luciferins, luciferases, their mechanisms of action and applications in chemical analysis, biology and medicine. *Chemical Society Reviews* **2016**, *45* (21), 6048-6077.

(30) d'Enfert, C.; Vecchiarelli, A.; Brown, A. J. Bioluminescent fungi for real-time monitoring of fungal infections. *Virulence* **2010**, *1* (3), 174-176.

(31) Luker, K. E.; Smith, M. C.; Luker, G. D.; Gammon, S. T.; Piwnica-Worms, H.; Piwnica-Worms, D. Kinetics of regulated protein–protein interactions revealed with firefly luciferase complementation imaging in cells and living animals. *Proceedings of the National Academy of Sciences* **2004**, *101* (33), 12288-12293.

(32) Prescher, J. A.; Contag, C. H. Guided by the light: visualizing biomolecular processes in living animals with bioluminescence. *Current opinion in chemical biology* **2010**, *14* (1), 80-89.

(33) Hawes, J. J.; Reilly, K. M. Bioluminescent approaches for measuring tumor growth in a mouse model of neurofibromatosis. *Toxicologic pathology* **2010**, *38* (1), 123-130.

(34) McCaffrey, A.; Kay, M. A.; Contag, C. H. Advancing molecular therapies through in vivo bioluminescent imaging. *Molecular imaging* **2003**, *2* (2), 15353500200303124.

(35) Markova, S. V.; Larionova, M. D.; Vysotski, E. S. Shining light on the secreted luciferases of marine copepods: Current knowledge and applications. *Photochemistry and photobiology* **2019**, *95* (3), 705-721.

(36) Hunt, E. A.; Moutsiopoulou, A.; Ioannou, S.; Ahern, K.; Woodward, K.; Dikici, E.; Daunert, S.; Deo, S. K. Truncated variants of Gaussia luciferase with tyrosine linker for site-specific bioconjugate applications. *Scientific reports* **2016**, *6* (1), 26814.

(37) Close, D.; Xu, T.; Smartt, A.; Rogers, A.; Crossley, R.; Price, S.; Ripp, S.; Sayler, G. The evolution of the bacterial luciferase gene cassette (lux) as a real-time bioreporter. *Sensors* **2012**, *12* (1), 732-752.

(38) Tinikul, R.; Chunthaboon, P.; Phonbuppha, J.; Paladkong, T. Bacterial luciferase: Molecular mechanisms and applications. In *The enzymes*, Vol. 47; Elsevier, 2020; pp 427-455.

(39) Lu, L.; Li, B.; Ding, S.; Fan, Y.; Wang, S.; Sun, C.; Zhao, M.; Zhao, C.-X.; Zhang, F. NIR-II bioluminescence for in vivo high contrast imaging and in situ ATP-mediated metastases tracing. *Nature communications* **2020**, *11* (1), 4192.

(40) Yao, Z.; Zhang, B. S.; Steinhardt, R. C.; Mills, J. H.; Prescher, J. A. Multicomponent bioluminescence imaging with a π-extended luciferin. *Journal of the American Chemical Society* **2020**, *142* (33), 14080-14089.

(41) Tamaki, S.; Kitada, N.; Kiyama, M.; Fujii, R.; Hirano, T.; Kim, S. B.; Maki, S. Color-tunable bioluminescence imaging portfolio for cell imaging. *Scientific Reports* **2021**, *11* (1), 2219.

(42) Evans, M. S.; Chaurette, J. P.; Adams Jr, S. T.; Reddy, G. R.; Paley, M. A.; Aronin, N.; Prescher, J. A.; Miller, S. C. A synthetic luciferin improves bioluminescence imaging in live mice. *Nature methods* **2014**, *11* (4), 393-395.

(43) Kuchimaru, T.; Iwano, S.; Kiyama, M.; Mitsumata, S.; Kadonosono, T.; Niwa, H.; Maki, S.; Kizaka-Kondoh, S. A luciferin analogue generating near-infrared bioluminescence achieves highly sensitive deep-tissue imaging. *Nature communications* **2016**, *7* (1), 11856.

(44) Iwano, S.; Sugiyama, M.; Hama, H.; Watakabe, A.; Hasegawa, N.; Kuchimaru, T.; Tanaka, K. Z.; Takahashi, M.; Ishida, Y.; Hata, J. Single-cell bioluminescence imaging of deep tissue in freely moving animals. *Science* **2018**, *359* (6378), 935-939.

(45) Su, Y.; Walker, J. R.; Park, Y.; Smith, T. P.; Liu, L. X.; Hall, M. P.; Labanieh, L.; Hurst, R.; Wang, D. C.; Encell, L. P. Novel NanoLuc substrates enable bright two-population bioluminescence imaging in animals. *Nature Methods* **2020**, *17* (8), 852-860.

(46) Yang, Y.; Shao, Q.; Deng, R.; Wang, C.; Teng, X.; Cheng, K.; Cheng, Z.; Huang, L.; Liu, Z.; Liu, X. In vitro and in vivo uncaging and bioluminescence imaging by using photocaged upconversion nanoparticles. *Angewandte Chemie International Edition* **2012**, *51* (13), 3125-3129.

(47) Heffern, M. C.; Park, H. M.; Au-Yeung, H. Y.; Van de Bittner, G. C.; Ackerman, C. M.; Stahl, A.; Chang, C. J. In vivo bioluminescence imaging reveals copper deficiency in a murine model of nonalcoholic fatty liver disease. *Proceedings of the National Academy of Sciences* **2016**, *113* (50), 14219-14224.

(48) Jiang, T.; Yang, X.; Li, G.; Zhao, X.; Sun, T.; Müller, R.; Wang, H.; Li, M.; Zhang, Y. Bacteria-based live vehicle for in vivo bioluminescence imaging. *Analytical Chemistry* **2021**, *93* (47), 15687-15695.

(49) Sykes, R.; Matthew, M. The β-lactamases of gram-negative bacteria and their role in resistance to β-lactam antibiotics. *Journal of Antimicrobial Chemotherapy* **1976**, *2* (2), 115-157.

(50) Yao, H.; So, M. K.; Rao, J. A bioluminogenic substrate for in vivo imaging of beta-lactamase activity. *Angew Chem Int Ed Engl* **2007**, *46* (37), 7031-7034.

(51) Ozawa, T.; Yoshimura, H.; Kim, S. B. Advances in fluorescence and bioluminescence imaging. *Analytical chemistry* **2013**, *85* (2), 590-609.

(52) Chen, F.; Warnock, R. L.; Van der Meer, J. R.; Wegner, S. V. Bioluminescence-triggered photoswitchable bacterial adhesions enable higher sensitivity and dual-readout bacterial biosensors for mercury. *ACS sensors* **2020**, *5* (7), 2205-2210.

(53) Viviani, V. R.; Pelentir, G. F.; Bevilaqua, V. R. Bioluminescence color-tuning firefly luciferases: engineering and prospects for real-time intracellular pH imaging and heavy metal biosensing. *Biosensors* **2022**, *12* (6), 400.

(54) Xiong, M.; Wu, Y.; Kong, G.; Lewis, W.; Yang, Z.; Zhang, H.; Xu, L.; Liu, Y.; Liu, Q.; Zhao, X. A semisynthetic bioluminescence sensor for ratiometric imaging of metal ions in vivo using DNAzymes conjugated to an engineered nano-luciferase. *Angewandte Chemie* **2023**, *135* (37), e202308086.

(55) Michielsen, C. M.; van Aalen, E. A.; Merkx, M. Ratiometric bioluminescent zinc sensor proteins to quantify serum and intracellular free Zn2+. *ACS Chemical Biology* **2022**, *17* (6), 1567-1576.

(56) Aird, E. J.; Tompkins, K. J.; Ramirez, M. P.; Gordon, W. R. Enhanced molecular tension sensor based on bioluminescence resonance energy transfer (BRET). *ACS sensors* **2019**, *5* (1), 34-39.

(57) Yang, Y.; Hou, W.; Liu, S.; Sun, K.; Li, M.; Wu, C. Biodegradable polymer nanoparticles for photodynamic therapy by bioluminescence resonance energy transfer. *Biomacromolecules* **2018**, *19* (1), 201-208.

(58) Yan, H.; Forward, S.; Kim, K.-H.; Wu, Y.; Hui, J.; Kashiparekh, A.; Yun, S.-H. All-natural-molecule, bioluminescent photodynamic therapy results in complete tumor regression and prevents metastasis. *Biomaterials* **2023**, *296*, 122079.

(59) Al-Ani, A. W.; Zhang, L.; Ferreira, L.; Turyanska, L.; Bradshaw, T. D.; Thomas, N. R. Listeria innocua Dps as a nanoplatform for bioluminescence based photodynamic therapy utilizing Gaussia princeps luciferase and zinc protoporphyrin IX. *Nanomedicine* **2019**, *20*, 102005.

(60) Lin, W.; Gong, J.; Fang, L.; Jiang, K. A photodynamic system based on endogenous bioluminescence for in vitro anticancer studies. *Zeitschrift für anorganische und allgemeine Chemie* **2019**, *645* (18-19), 1161-1164.

(61) Kim, E. H.; Park, S.; Kim, Y. K.; Moon, M.; Park, J.; Lee, K. J.; Lee, S.; Kim, Y.-P. Self-luminescent photodynamic therapy using breast cancer targeted proteins. *Science Advances* **2020**, *6* (37), eaba3009.

(62) Shramova, E. I.; Filimonova, V. P.; Frolova, A. Y.; Pichkur, E. B.; Fedotov, V. R.; Konevega, A. L.; Deyev, S. M.; Proshkina, G. M. HER2-specific liposomes loaded with proteinaceous BRET pair as a promising tool for targeted self-excited photodynamic therapy. *European Journal of Pharmaceutics and Biopharmaceutics* **2023**, *193*, 208-217.

(63) Hsu, C.-Y.; Chen, C.-W.; Yu, H.-P.; Lin, Y.-F.; Lai, P.-S. Bioluminescence resonance energy transfer using luciferase-immobilized quantum dots for self-illuminated photodynamic therapy. *Biomaterials* **2013**, *34* (4), 1204-1212.

(64) Kim, Y. R.; Kim, S.; Choi, J. W.; Choi, S. Y.; Lee, S.-H.; Kim, H.; Hahn, S. K.; Koh, G. Y.; Yun, S. H. Bioluminescence-activated deep-tissue photodynamic therapy of cancer. *Theranostics* **2015**, *5* (8), 805.

(65) Yang, K.; Wang, C.; Liu, C.; Ding, S.; Tian, F.; Li, F. Bioluminescence-initiated photodynamic therapy bridged on high-luminescent carbon dots-conjugated protoporphyrin IX. *Journal of Materials Science* **2019**, *54* (4), 3383-3391.

(66) Shramova, E. I.; Chumakov, S. P.; Shipunova, V. O.; Ryabova, A. V.; Telegin, G. B.; Kabashin, A. V.; Deyev, S. M.; Proshkina, G. M. Genetically encoded BRET-activated photodynamic therapy for the treatment of deep-seated tumors. *Light: Science & Applications* **2022**, *11* (1), 38.

(67) Yang, Z.; Zhu, Y.; Dong, Z.; Hao, Y.; Wang, C.; Li, Q.; Wu, Y.; Feng, L.; Liu, Z. Engineering bioluminescent bacteria to boost photodynamic therapy and systemic anti-tumor immunity for synergistic cancer treatment. *Biomaterials* **2022**, *281*, 121332.

(68) White, E. H.; Wörther, H.; Seliger, H. H.; McElroy, W. D. Amino Analogs of Firefly Luciferin and Biological Activity Thereof1. *Journal of the American Chemical Society* **1966**, *88* (9), 2015-2019.

(69) Takakura, H.; Kojima, R.; Urano, Y.; Terai, T.; Hanaoka, K.; Nagano, T. Aminoluciferins as functional bioluminogenic substrates of firefly luciferase. *Chemistry–An Asian Journal* **2011**, *6* (7), 1800-1810.

(70) Reddy, G. R.; Thompson, W. C.; Miller, S. C. Robust light emission from cyclic alkylaminoluciferin substrates for firefly luciferase. *Journal of the American Chemical Society* **2010**, *132* (39), 13586-13587.

(71) Conley, N. R.; Dragulescu-Andrasi, A.; Rao, J.; Moerner, W. E. A Selenium Analogue of Firefly D-Luciferin with Red-Shifted Bioluminescence Emission. *Angewandte Chemie International Edition* **2012**, *51* (14), 3350-3353.

(72) Branchini, B. R.; Murtiashaw, M. H.; Magyar, R. A.; Portier, N. C.; Ruggiero, M. C.; Stroh, J. G. Yellow-Green and Red Firefly Bioluminescence from 5,5-Dimethyloxyluciferin. *Journal of the American Chemical Society* **2002**, *124* (10), 2112-2113.

(73) Takakura, H.; Sasakura, K.; Ueno, T.; Urano, Y.; Terai, T.; Hanaoka, K.; Tsuboi, T.; Nagano, T. Development of Luciferin Analogues Bearing an Amino Group and Their Application as BRET Donors. *Chemistry – An Asian Journal* **2010**, *5* (9), 2053-2061.

(74) Iwano, S.; Obata, R.; Miura, C.; Kiyama, M.; Hama, K.; Nakamura, M.; Amano, Y.; Kojima, S.; Hirano, T.; Maki, S.; et al. Development of simple firefly luciferin analogs emitting blue, green, red, and near-infrared biological window light. *Tetrahedron* **2013**, *69* (19), 3847-3856.

(75) Miura, C.; Kiyama, M.; Iwano, S.; Ito, K.; Obata, R.; Hirano, T.; Maki, S.; Niwa, H. Synthesis and luminescence properties of biphenyl-type firefly luciferin analogs with a new, near-infrared light-emitting bioluminophore. *Tetrahedron* **2013**, *69* (46), 9726-9734.

(76) Jathoul, A. P.; Grounds, H.; Anderson, J. C.; Pule, M. A. A dual-color far-red to near-infrared firefly luciferin analogue designed for multiparametric bioluminescence imaging. *Angewandte Chemie International Edition* **2014**, *53* (48), 13059-13063.

(77) Steinhardt, R. C.; O'Neill, J. M.; Rathbun, C. M.; McCutcheon, D. C.; Paley, M. A.; Prescher , J. A. Design and Synthesis of an Alkynyl Luciferin Analogue for Bioluminescence Imaging. *Chemistry – A European Journal* **2016**, *22* (11), 3671-3675.

(78) Woodroofe, C. C.; Shultz, J. W.; Wood, M. G.; Osterman, J.; Cali, J. J.; Daily, W. J.; Meisenheimer, P. L.; Klaubert, D. H. N-Alkylated 6′-Aminoluciferins Are Bioluminescent Substrates for Ultra-Glo and QuantiLum Luciferase: New Potential Scaffolds for Bioluminescent Assays. *Biochemistry* **2008**, *47* (39), 10383-10393. DOI: 10.1021/bi800505u.

(79) Branching, B. R.; Hayward, M. M.; Bamfor, S.; M. Brennan, P.; Lajiness, E. J. Naphthyl - and Quinolylluciferin: Green and Red Light Emitting Firefly Luciferin Analogues. *Photochemistry and Photobiology* **1989**, *49* (5), 689-695.

(80) Woodroofe, C. C.; Meisenheimer, P. L.; Klaubert, D. H.; Kovic, Y.; Rosenberg, J. C.; Behney, C. E.; Southworth, T. L.; Branchini, B. R. Novel Heterocyclic Analogues of Firefly Luciferin. *Biochemistry* **2012**, *51* (49), 9807-9813.

(81) Shinde, R.; Perkins, J.; Contag, C. H. Luciferin Derivatives for Enhanced in Vitro and in Vivo Bioluminescence Assays. *Biochemistry* **2006**, *45* (37), 11103-11112.

(82) Li, J.; Chen, L.; Du, L.; Li, M. Cage the firefly luciferin! – a strategy for developing bioluminescent probes. *Chemical Society Reviews* **2013**, *42* (2), 662-676, 10.1039/C2CS35249D.

(83) Xia, T.; Cheng, X.; Zhan, W.; Liang, G. Activity-Based Luciferase-Luciferin Bioluminescence System for Bioimaging Applications. *Analysis & Sensing* **2021**, *1* (4), 138-147.

(84) White, E. H.; Rapaport, E.; Seliger, H. H.; Hopkins, T. A. The chemi- and bioluminescence of firefly luciferin: An efficient chemical production of electronically excited states. *Bioorganic Chemistry* **1971**, *1* (1), 92-122.

(85) Meroni, G.; Rajabi, M.; Santaniello, E. D-Luciferin, derivatives and analogues: synthesis and in vitro/in vivo luciferase-catalyzed bioluminescent activity. *ARKIVOC: Online Journal of Organic Chemistry* **2009**.

(86) White, E. H.; McCapra, F.; Field, G. F. The structure and synthesis of firefly luciferin. *Journal of the American Chemical Society* **1963**, *85* (3), 337-343.

(87) Sun, Y.-C.; Shi, W.-X.; Kuo, W.-C.; Hsiang, Y.-R.; Lo, W.-L.; Chen, L.-C.; Farn, S.-S.; Lin, Y.-F.; Chen, K.-T. Cyanopyridoimidazole/1,2-Aminothiol Click Reaction: A Novel Bioorthogonal Reaction for Synthesis of Radiotracers. *Bioconjugate Chemistry* **2024**, *35* (1), 107-114.

(88) Seto, S. Ogura. K., and Nishiyama, Y.(1963) B/t. *Chem. Sot. Jap 36*, 332-341.

(89) Nyoni, D.; Lobb, K.; Kaye, P.; Caira, M. DBU-mediated Cleavage of Aryl- and Heteroaryl Disulphides. *ARKIVOC: archive for organic chemistry* **2012**, *2012*, 245-252.

(90) McCutcheon, D. C.; Paley, M. A.; Steinhardt, R. C.; Prescher, J. A. Expedient Synthesis of Electronically Modified Luciferins for Bioluminescence Imaging. *Journal of the American Chemical Society* **2012**, *134* (18), 7604-7607.

(91) McCutcheon, D. C.; Porterfield, W. B.; Prescher, J. A. Rapid and scalable assembly of firefly luciferase substrates. *Org Biomol Chem* **2015**, *13* (7), 2117-2121.

(92) Rakitin, O. A.; Rees, C. W.; Vlasova, O. G. Direct Synthesis of 2-Cyanobenzimidazoles and the Generation of S2. *Tetrahedron letters* **1996**, *37* (26), 4589-4592.

(93) Rylands, M. PhD thesis, unpublished. University of Cape Town, **2018**.

(94) Ohulchanskyy, T. Y.; Donnelly, D. J.; Detty, M. R.; Prasad, P. N. Heteroatom Substitution Induced Changes in Excited-State Photophysics and Singlet Oxygen Generation in Chalcogenoxanthylium Dyes: Effect of Sulfur and Selenium Substitutions. *The Journal of Physical Chemistry B* **2004**, *108* (25), 8668-8672.

(95) Solov'ev, K. N.; Borisevich, E. A. Intramolecular heavy-atom effectin the photophysics of organic molecules. *Physics-Uspekhi* **2005**, *48* (3), 231.

(96) Hu, B.; Yao, C.; Wang, Q.; Zhang, H.; Yu, J. CH 2, NH, and O heteroatom substitution effects on the electronic, optical, and charge transport properties of a 2, 1, 3-benzothiadiazole-based derivative: Insights from theory. *Science China Chemistry* **2012**, *55*, 1364-1369.

(97) Manojai, N.; Daengngern, R.; Kerdpol, K.; Ngaojampa, C.; Kungwan, N. Heteroatom effect on photophysical properties of 2-(2′-hydroxyphenyl) benzimidazole and its derivatives as fluorescent dyes: A TD-DFT study. *Journal of Luminescence* **2017**, *188*, 275-282.

(98) Hayes, J. D.; Dinkova-Kostova, A. T.; Tew, K. D. Oxidative Stress in Cancer. *Cancer Cell* **2020**, *38* (2), 167-197.

(99) Jackson, K. MSc thesis, unpublished. University of Cape Town, **2020**.

(100) Shiu, H. Y.; Chan, T. C.; Ho, C. M.; Liu, Y.; Wong, M. K.; Che, C. M. Electron-deficient alkynes as cleavable reagents for the modification of cysteine-containing peptides in aqueous medium. *Chemistry–A European Journal* **2009**, *15* (15), 3839-3850.

(101) Rylands, M.; Jardine, A. Synthesis and evaluation of D-thioluciferin, a bioluminescent 6'-thio analog of D-luciferin. *ARKIVOC* **2021**, *2020* (5), 176-189.

(102) Sharma, D. K.; Adams, S. T., Jr.; Liebmann, K. L.; Miller, S. C. Rapid Access to a Broad Range of 6'-Substituted Firefly Luciferin Analogues Reveals Surprising Emitters and Inhibitors. *Org Lett* **2017**, *19* (21), 5836-5839.

(103) Heravi, M. M.; Kheilkordi, Z.; Zadsirjan, V.; Heydari, M.; Malmir, M. Buchwald-Hartwig reaction: An overview. *Journal of Organometallic Chemistry* **2018**, *861*, 17-104.

(104) Pirrung, M. C.; Carlson, A. D.; De Howitt, N.; Liao, J. Synthesis and bioluminescence of thioluciferin. *Bioorg Med Chem Lett* **2019**, *29* (19), 126591.

(105) Rayner, D. R.; Miller, E. G.; Bickart, P.; Gordon, A. J.; Mislow, K. Mechanisms of Thermal Racemization of Sulfoxides1. *Journal of the American Chemical Society* **1966**, *88* (13), 3138-3139.

Chapter 2 : Benzothiazole core and its reactivity

2.1 Literature overview

2.1.1 Synthesis of 2-cyanobenzothiazoles

As outlined in Chapter 1, Rylands reported the synthesis of 6-iodo-2-cyanobenzothiazole **14** as a crucial intermediate in the preparation of D-thioluciferin.[1] Given its significance, the efficient synthesis of this key benzothiazole intermediate **14** was identified as a strategic starting point for the development of a more concise and streamlined synthetic route to D-thioluciferin. In the proposed approach, *p*-iodoaniline was initially subjected to bromination at the C-2 position to enable intramolecular cyclisation in the subsequent step. This was followed by the general condensation with 4,5-dichloro-1,2,3-dithiazolium chloride (Appel's salt) as developed by Prescher[2] and finally, the optimal conditions of ring closure were investigated (Scheme **2.1**).

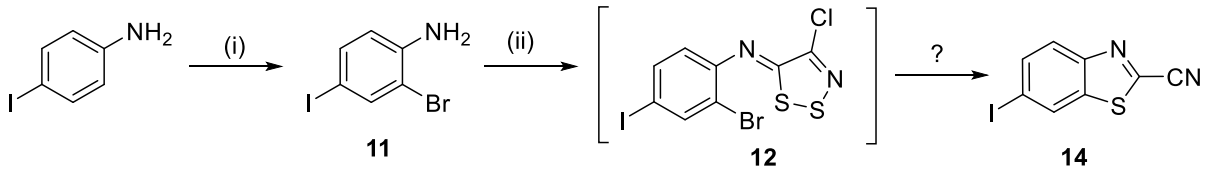

Scheme 2.1. Proposed route for the synthesis of 6-iodo-2-cyanobenzothiazole **14**. Reagents and conditions: (i) $NaBO_3$, KBr, acetic acid, rt, 16 h, (ii) Appel's salt, DCM, 3 h.

An array of methods to mediate benzothiazole ring closure has been reported in literature (Scheme **2.2**). Previous publications from Besson and Rees explored the reactivity of Appel's salt with various anilines.[3] They generated iminodithiazole intermediates and converted them into 2-cyanobenzothiazoles and cyanoimidoyl chlorides through thermolysis (250 °C) or oxidation (*m*-CPBA). By 1997, English reported that product distribution depends on the electronic nature of the substituents, with electron-donating groups (EDG) promoting cyclisation while electron-withdrawing groups (EWG) promoting fragmentation.[4] A year later Besson and coworkers employed microwave irradiation at atmospheric pressure in pyridine containing cuprous iodide and were able to form various benzothiazole derivatives in moderate to high yields.[5] Later publications also reported a productive and more eco-friendly methodology for 2-cyanobenzothiazoles synthesis via graphite/microwave interaction.[6] By 2014 Deau and coworkers had published an optimised method on the microwave-assisted copper(I)-mediated cyclisation of ortho-halogenated *N*-aryliminodithiazoles which produced a number of novel *N*-(4-phenylthiazol-2-yl)-benzo[*d*]thiazole-, thiazolo[4,5-*b*]pyridine-, thiazolo[5,4-*b*]pyridine and benzo[*d*]oxazole-2-carboximidamides.[7] In their synthetic

procedure, a stirred solution of the appropriate aryliminodithiazole and copper iodide in dry pyridine was heated under microwave irradiation (400 W) at 115 °C for 30 min at atmospheric pressure. This reaction illustrated much potential as the benzothiazole derivatives reported were synthesised from imines structurally similar to **12** (i.e. *o*-brominated imines).

Rylands had also reported a one-pot metal free cyclisation reaction incorporating five equivalents of DBU at a slightly elevated temperature of 40 °C.[1] The imine derivative used was also *o*-brominated on the C-2 position to facilitate ring closure, with an EWG on its C-4 position. This reaction was thus identified as a suitable approach as it could be applied directly to imine **12**.

The procedure developed by McCutcheon *et al*., was also deemed to be reliable route in the synthesis of C-6 substituted benzothiazoles. However, their initial method[2] incorporated the use of a combination of metal catalysts which do not function ideally in upscaled reactions. Their subsequent scalable and condensed method was suitable for upscaled reactions, however their mechanism for benzothiazole formation relied on the presence of an electron donating (OMe) group substituent on the C-4 position of its imine derivative.[8]

Interestingly, in 2022 Broudic and coworkers revised the initial metal-catalysed reaction developed by McCutcheon[2] and reported the cyclisation of cyanothioformamides and the synthesis of 2-cyanobenzothiazoles in the presence of air, using two equivalents of an inorganic additive (KI).[9] Furthermore, they reported that the reaction led to a sole product in most cases which was regioselectively obtained and in good yield. Of the many benzothiazoles they generated, 6-chloro- and 6-bromo-2-cyanobenzothiazlole were also reported in yields of 71% and 54% respectively. Considering their successful synthesis of novel C-6 halogenated 2-cyanobenzothiazoles, this method was also identified as a possible route to the synthesis of 6-iodo-2-cyanobenzothiazole **14**. However, due to the incorporation of the expensive metal catalysts and the extra synthetic step requiring cyanothioformamide formation, it was decided that this method would only be attempted if the DBU reaction by Rylands[1] and the microwave reaction by Deau[7] were not successful.

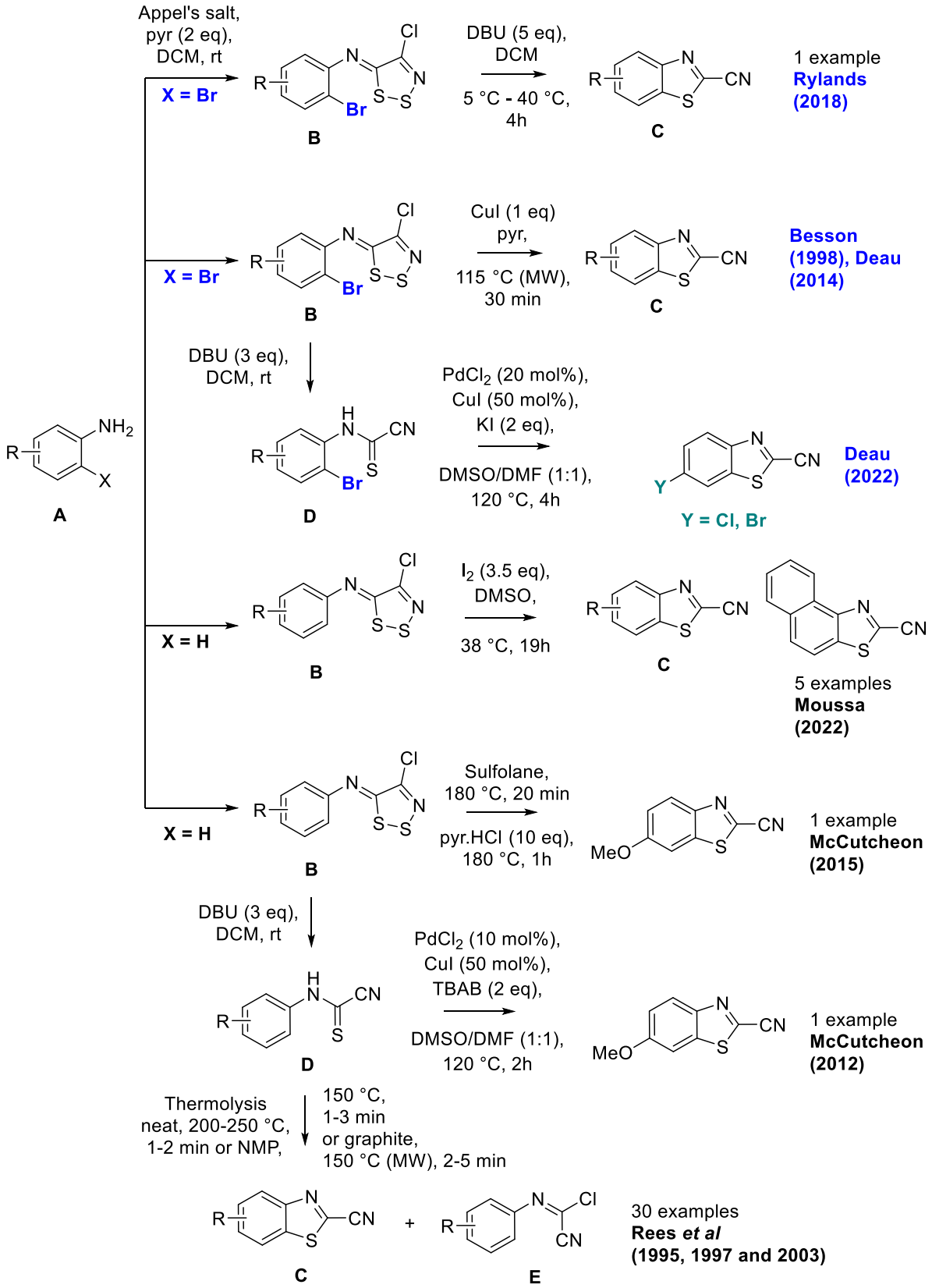

Scheme 2.2. Overview of the different strategies for benzothiazole ring closure reported in literature.

Another publication in 2022 by Moussa and colleagues reported the development of a mild and scalable method for converting *N*-arylcyanothioformamides into *N*-arylcyanoformamides using a simple iodine (I_2) and DMSO oxidative system.[10] The thione group (C=S) in the starting material was oxidised to a carbonyl group (C=O), forming the desired cyanothioformamide. To the authors surprise, they discovered some substrates underwent intramolecular cyclisation instead of simple oxidation, producing 2-cyanobenzothiazoles. They reported their synthesis as high yielding and scalable to gram quantities, providing a green, efficient route to important molecular scaffolds. Although Moussa's findings were biologically relevant and useful in designing luciferin analogues, their method relied on the presence of EDGs on the imine derivative (Scheme **2.3**). In contrast, an electron withdrawing iodine group was present on the C-4 position of the imine at hand. As such, Moussa's method was not attempted on imine **12**.

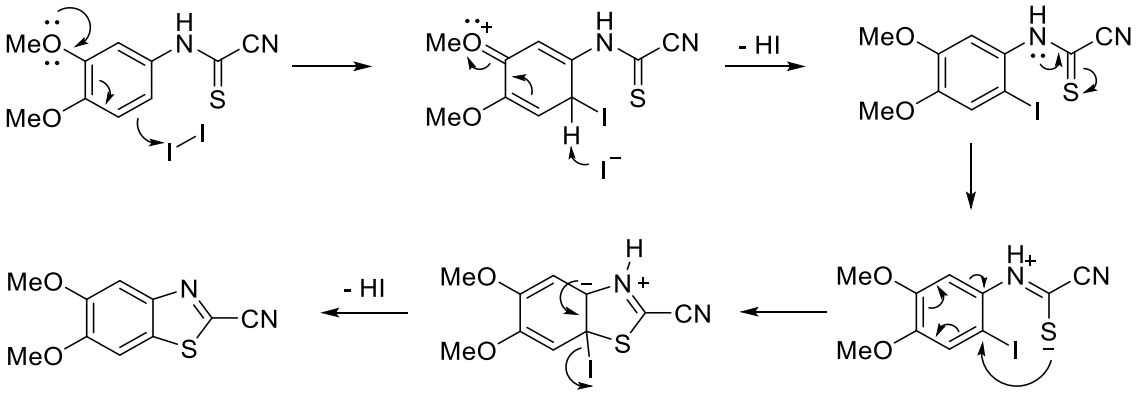

Scheme 2.3. Proposed mechanism for the formation of 2-cyanobenzothiazoles from *N*-arylcyanothioformamide containing -OMe substituents on the aromatic ring as an example.[10]

2.1.2 Synthesis of 6-thio-2-cyanobenzothiazole (7)

Following the formation of the benzothiazole ring, the next key intermediate in the synthesis of D-thioluciferin was identified as the C-6 sulphur-substituted benzothiazole **7**. Rylands previously reported significant challenges in accessing this intermediate, which he attributed to the presence of the electron withdrawing nitrile group at the C-2 position of the benzothiazole ring.[1] In 2019, Pirrung and co-workers reported a successful synthesis of 6-thio-2-cyanobenzothiazole **7** using triphenylphosphite.[11] However, their approach involved a Mislow–Evans rearrangement[12] from an allylic sulfoxide benzothiazole, a strategy that could not be applied to 6-iodo-2-cyanobenzothiazole **14**, thereby limiting its general utility in this context (Scheme **2.4**).

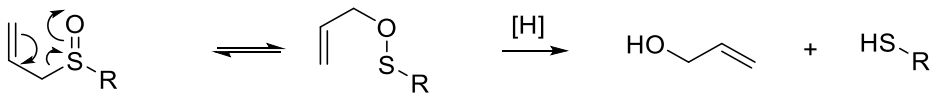

Scheme 2.4. Proposed Mislow-Evans rearrangement of an allylic sulfoxide to unmask the thiol group and produce allylic alcohol.[11]

In 2013, Soria-Castro and Peñéñory reported a strategy to overcome the synthetic challenges posed by the nitrile functional group.[13] In their study, they successfully synthesised S-(4-cyanophenyl) thioacetate from 4-iodobenzonitrile using cost-effective potassium thioacetate under a base-free copper/ligand catalytic system (Scheme **2.5**). This approach demonstrated that C–S bond formation in the presence of an EWG nitrile group is feasible under carefully optimised conditions.

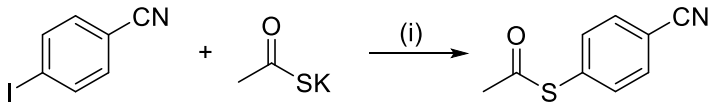

Scheme 2.5. Synthesis of *S*-(4-cyanophenyl) thioacetate from 4-iodobenzonitrile.[13] Reagents and conditions: (i) CuI (10 mol %), 1,10-phenanthroline (20 mol %), potassium thioacetate (1.5 eq), toluene, 100 °C, 24 h.

Aromatic carbon–sulphur (C–S) bond formation via C–X (X = halide, pseudohalide) activation is a key strategy in synthesising aryl sulphides. Copper-catalysed Ullmann-Type Reactions[14] are useful, especially for aryl iodides and bromides. This study showed promise, as it was anticipated that it could be extended to the benzothiazole ring of 2-cyano-6-iodobenzothiazole **14** to yield the desired thiol **7** (Scheme **2.6**).

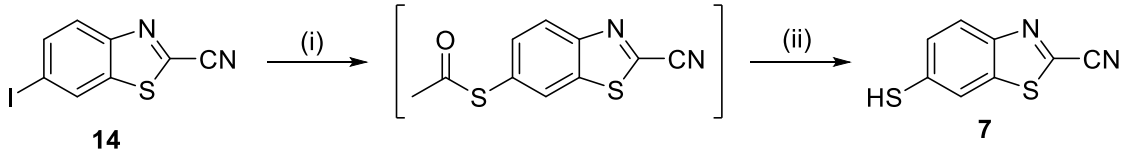

Scheme 2.6. Proposed synthesis of thiol **7**. Reagents and conditions: (i) CuI (10 mol %), 1,10-phenanthroline (20 mol), potassium thioacetate (1.5 eq), toluene, 100 °C, 24 h.

2.2 Research rationale and motivation

With the synthetic strategies of the two key benzothiazoles in place, a complete retrosynthetic route targeting D-thioluciferin was thus constructed (Scheme **2.7**). The starting material *p*-iodoaniline would be brominated using potassium bromide in an electrophilic substitution reaction, forming 2-bromo-4-iodoaniline **11**. Thereafter the general Appel's salt condensation[2] reaction was to be followed to form imine **12**, without isolation. Copper iodide-mediated ring closure would facilitate the formation of key benzothiazole **14** followed by a novel reaction

with potassium thioacetate to yield thiobenzothiazole **7**. Lastly, the standard luciferin reaction would be conducted to form D-thioluciferin.

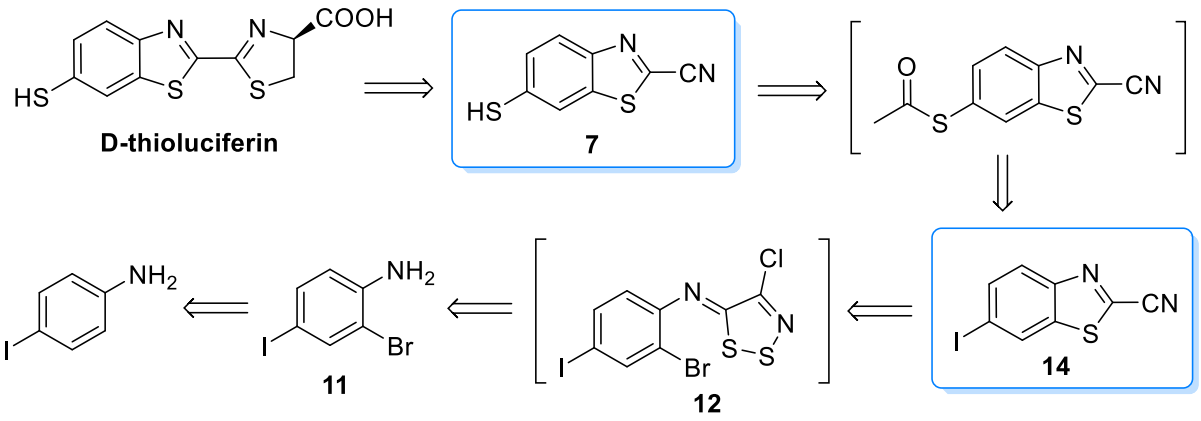

Scheme 2.7. Proposed retrosynthetic route for the synthesis of D-thioluciferin from *p*-iodoaniline.

2.3 Results and Discussion

2.3.1 Model study

To evaluate the thioacetylation protocol reported by Soria *et al.*,[13] a preliminary model study was conducted to establish optimal thioacetylation conditions on the benzothiazole scaffold. Commercially available benzothiazoles **7.1a** and **7.1b** were selected as convenient starting materials. These substrates were subjected to halogenation using sodium iodide and potassium bromide to afford C-6 substituted benzothiazole derivatives **7.2a**, **7.2b**, **7.2c**, and **7.2d** via electrophilic substitution (Scheme **2.8**). Both iodination and bromination were employed to assess the potential influence of halogen electronegativity and atomic radius on the reaction rate. Following halogenation, the resulting 6-substituted benzothiazoles were reacted with potassium thioacetate, copper(I) iodide, and 1,10-phenanthroline to afford the corresponding thioacetate-substituted benzothiazoles **7.3a** and **7.3b** through a nucleophilic substitution reaction. To initiate the synthetic sequence, four parallel reactions were carried out to prepare the halogenated benzothiazole derivatives **7.2a**, **7.2b**, **7.2c**, and **7.2d** (Scheme **2.8**).

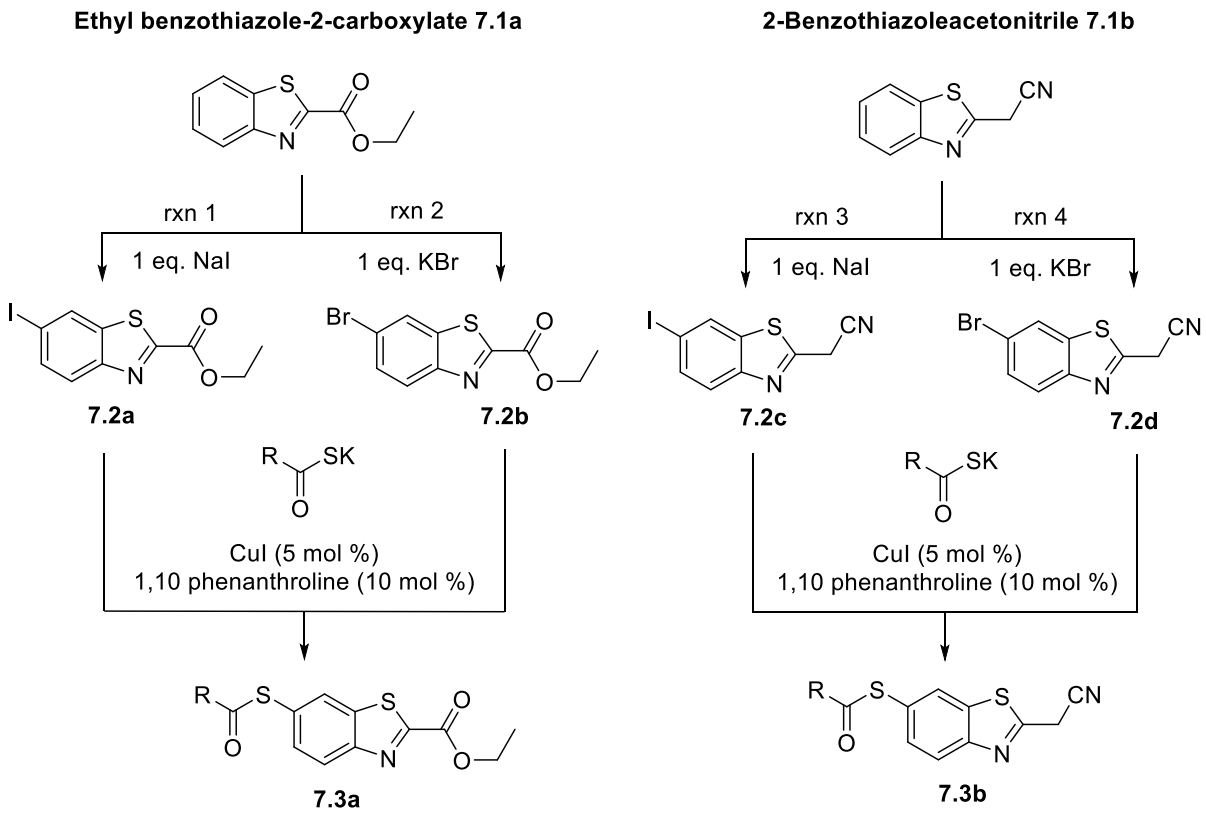

Scheme 2.8. Overview of the four proposed reaction pathways to synthesise thioacetate-benzothiazoles **3a** and **3b**.

After 24 hours, thin-layer chromatography (TLC) revealed no change in the R_f values for reactions 1 and 2, indicating that compound **7.1a** did not undergo reaction with either sodium iodide or potassium bromide. This observation was confirmed by ^{1}H NMR spectroscopy, which showed that ethyl benzothiazole-2-carboxylate **7.1a** remained unreacted. These results suggest that the electron-withdrawing carboxylate group in **7.1a** significantly deactivates the aromatic ring, rendering it less susceptible to electrophilic substitution.

In contrast, new products were observed in reactions 3 and 4 after only 3 hours. After 24 hours, the starting material in both reactions was fully consumed, and the halogenated products were successfully isolated. In comparison to the starting material (Figure **2.1a**), the ^{1}H NMR spectrum of reaction 3 revealed the complete disappearance of the methylene proton signals, while the aromatic proton signals remained unchanged (Figure **2.1b**). This suggests regioselective iodination at the methylene position rather than the aromatic ring. In reaction 4, however, a residual methylene proton signal was still present, and the aromatic region exhibited two distinct sets of signals, indicative of the formation of two regio-isomeric bromo-substituted products (Figure **2.1c**). In both halogenation reactions with **7.1b**, downfield shifts of the aromatic proton signals were observed, consistent with the decreased electron density resulting

from halogen substitution. The electron-withdrawing nature of the halogen atoms reduces local shielding, thus accounting for the observed chemical shift changes.

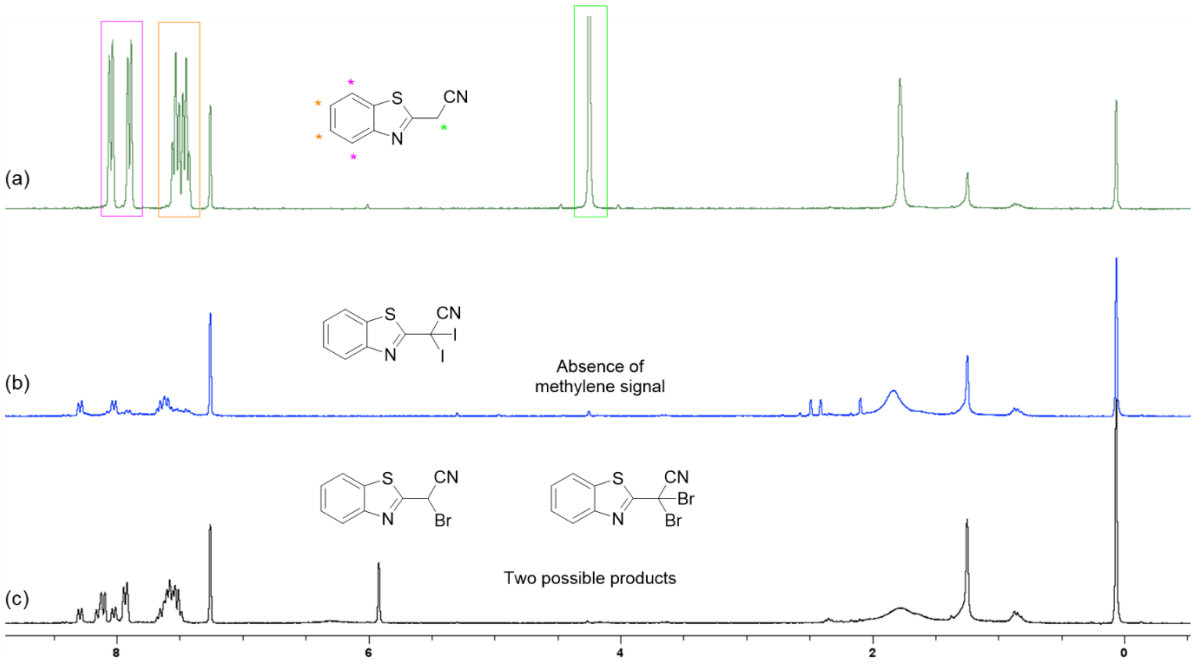

Figure 2.1. Stacked expansion of crude ^{1}H NMR spectra for **(a)** 2-benzothiazoleacetonitrile 1b with all protons annotated according to colour, **(b)** Reaction 1: product formed with 1b and 1 eq NaI and **(c)** products formed with 1b and 1 eq KBr in $CDCl_3$.

Given that halogenation predominantly occurred at the methylene carbon rather than on the aromatic ring of **7.1b**, the halogen equivalents were increased from one to three in reactions 1 and 2 to promote halogenation at both the methylene and aromatic positions (Table **2.1**). In reaction 5, despite the increased iodine equivalents, ^{1}H NMR analysis of the isolated product revealed selective iodination at the methylene carbon, with no evidence of substitution on the aromatic ring (Figure **2.2**). This suggests the formation of 2-benzothiazole-2,2-diiodoacetonitrile **9** rather than the anticipated aromatic iodinated benzothiazole **7.2e**. Although a sufficient quantity of the compound was obtained for further analysis (98.7 mg, 30% yield), ^{13}C NMR spectroscopy could not be performed due to the compound's pronounced air sensitivity.

Table 2.1. Summary of reactions 5 and 6.

Reaction	Starting material	Halogen source	Halogen molar eq.	Target Product
5	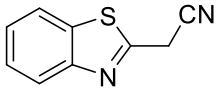 **7.1b**	NaI	3	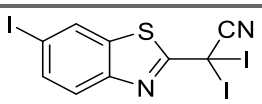 **7.2e** Not obtained
6	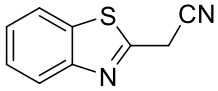 **7.1b**	KBr	3	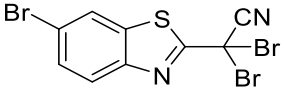 **7.2f** Not obtained

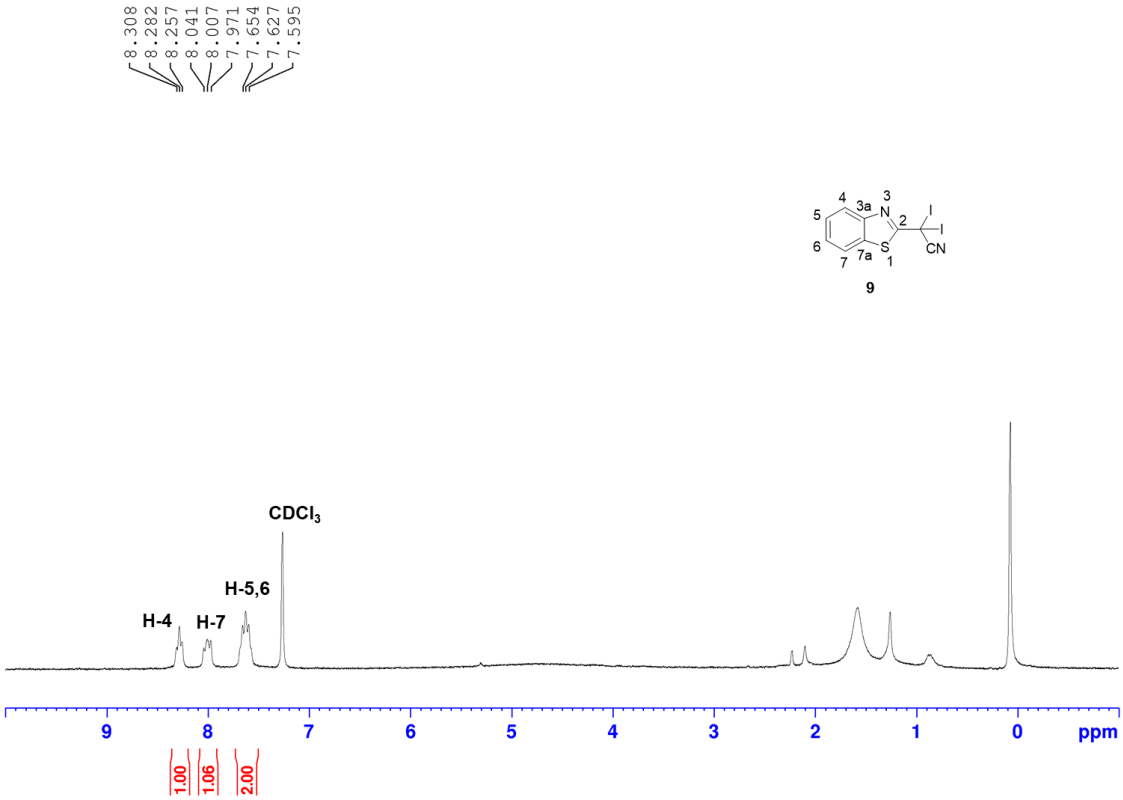

Figure 2.2. ^{1}H NMR spectrum of **9** in $CDCl_3$.

Similarly, the major product obtained from reaction 6 was found to be halogenated exclusively at the methylene carbon, with no evidence of substitution on the aromatic ring, as confirmed by ^{1}H NMR analysis (Figure **2.3**). Comparative IR analysis of compounds **9** and **10** revealed a characteristic absorption band consistent with the presence of a nitrile functional group in **9**

and a loss of the nitrile group in **10** (Figure **2.4**). Based on these observations, the product is tentatively assigned as 2-(tribromomethyl)benzo[d]thiazole **10**, with further characterisation by mass spectroscopy required to confirm the structure.

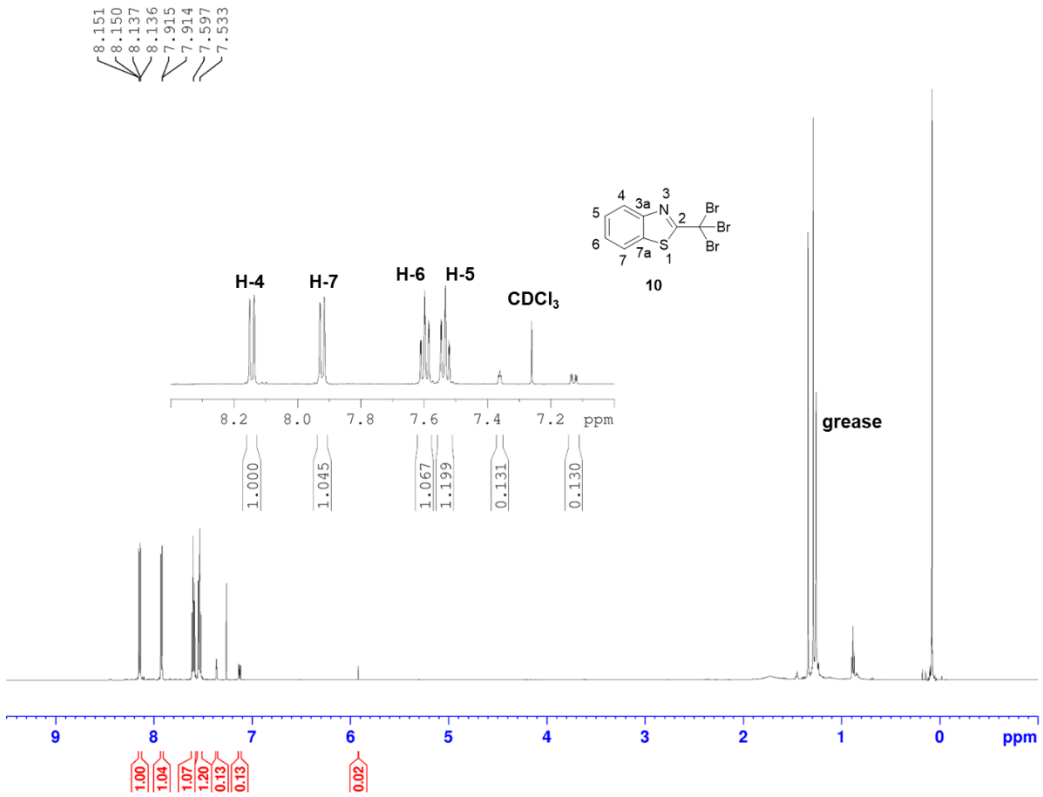

Figure 2.3. ^{1}H NMR spectrum of 2-benzothiazole-2,2-dibromoacetonitrile **2h** in $CDCl_3$.

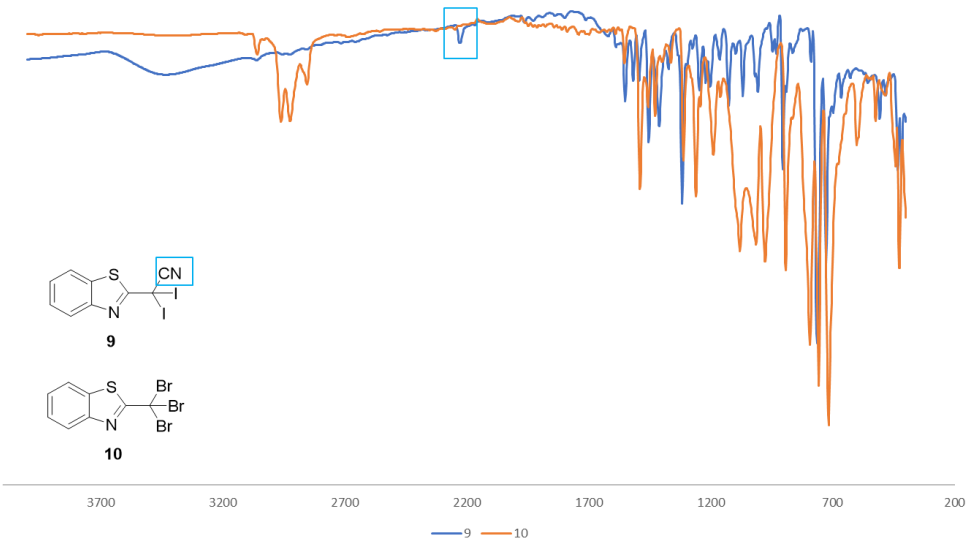

Figure 2.4. Stacked IR spectra of **9** and **10** with the nitrile group highlighted in light blue.

2.3.2 Improved synthesis of 6-iodo-2-cyanobenzothiazole (14)

Although initial attempts at halogenation of the benzothiazole core were unsuccessful, it was hypothesised that thioacetylation of 6-iodo-2-cyanobenzothiazole **14** might still be feasible. As such, bromination of *p*-iodoaniline proceeded smoothly, affording the desired amine **11** in excellent yield (96%). The crude product was of sufficient purity to be used directly in subsequent steps without further purification. In contrast, the synthesis of imine **12** resulted in a markedly lower yield of 13%. This significant decrease was attributed to the compound's sensitivity, likely leading to degradation during purification on silica gel. Given the poor yield of imine **12**, it became clear that a more efficient strategy was required to access the ring-closed product **14**. An initial approach involved a metal-free cyclisation using five equivalents of DBU, as described by Rylands (Scheme **2.2**).[1] However, this methodology was unsuccessful, yielding only the intermediate thioformamide **13** (Sceme **2.9**).

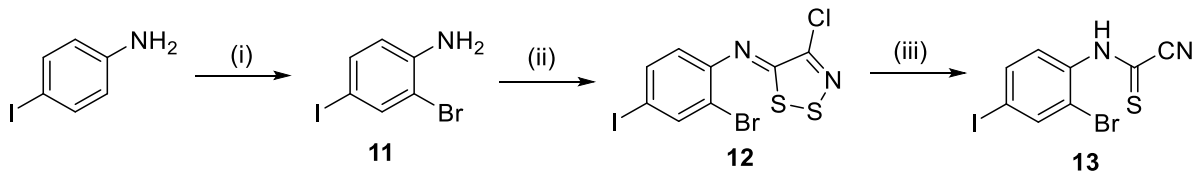

Scheme 2.9. *p*-Iodoaniline synthetic route. Reagents and conditions: (i) KBr, $NaBO_3$, CH_3COOH, rt, 18 h, (96%), (ii) Appel's salt, DCM, Anhydrous pyridine (2 eq), rt, 3 h, (13% when isolated), (iii) DBU (5 eq), DCM, -5 °C, 1 h, (60-80%).

The formation of **13** was suggested by IR spectroscopy, with the appearance of a characteristic nitrile stretch (Figure **2.5**).^{1}H NMR spectroscopy confirmed the product, with the appearance of the NH/SH peak due to the thione **13** and thiol **13'** tautomer formation (Figure **2.6**).

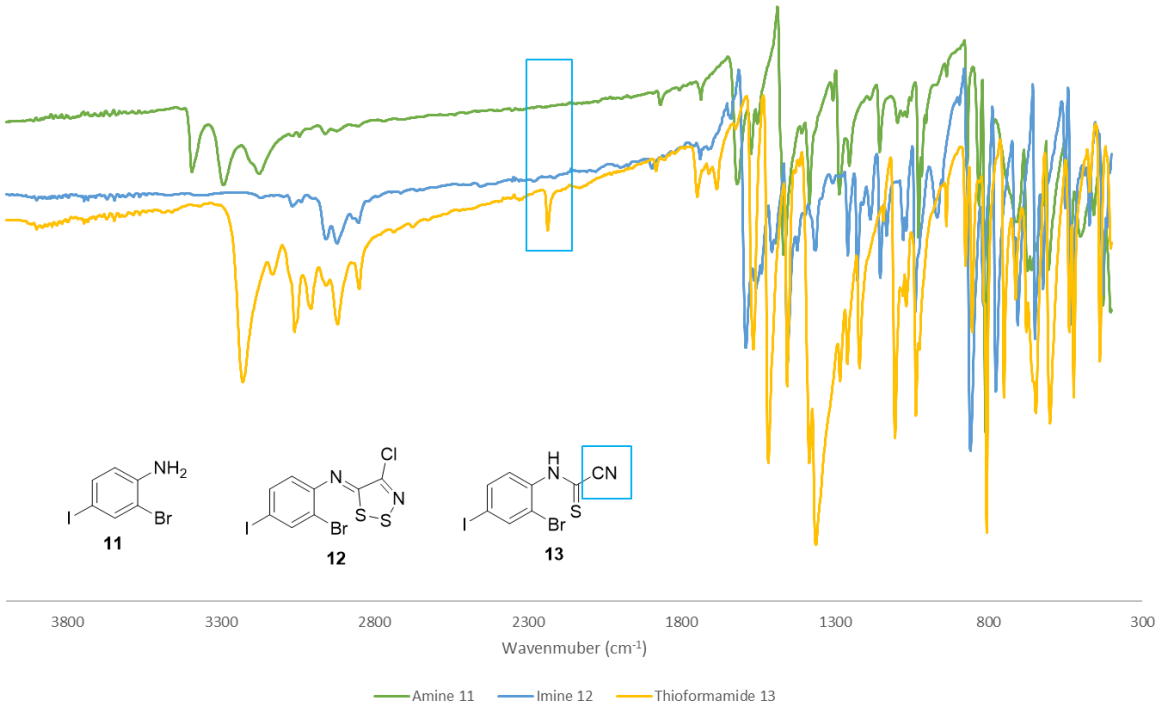

Figure 2.5. Stacked IR spectra of **11**, **12** and **13** with the nitrile group highlighted in blue.

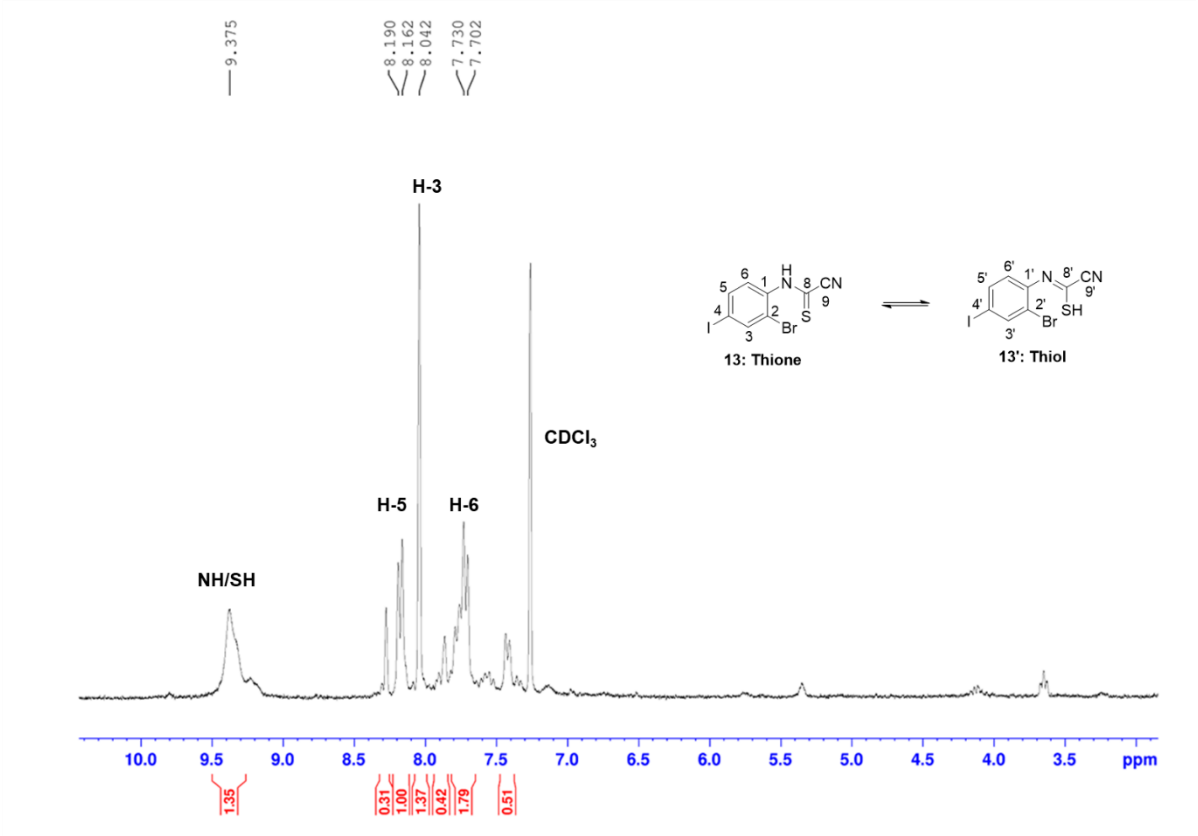

Figure 2.6. ^{1}H NMR spectrum of thione **13** and thiol **13'** formation.

Subsequently, the focus shifted to the microwave-assisted method reported by Deau and colleagues. In their synthetic procedure, a stirred solution of the appropriate

aryliminodithiazole and copper iodide in dry pyridine was heated under microwave irradiation (400 W) at 115 °C for 30 min at atmospheric pressure.[7] This method was applied to the *p*-iodoaniline series in which crude imine **12** and copper iodide in anhydrous pyridine were sealed in a microwave tube and subjected to microwave irradiation at 115 °C. After 30 min the tube was allowed to cool and removed for workup. TLC analysis indicated the presence of a new product (R_f = 0.42 with 10% diethyl ether / petroleum ether) which was purified via column chromatography to afford benzothiazole **14** in moderate yield (60%). This method proved to be superior as it could be conducted on crude imine **12** and still produce the desired benzothiazole **14** in moderate yield. The method was also repeated using sulfolane, a higher boiling point solvent in an attempt to improve the yield, but produced a similar moderate yield (54%). It was rationalised that the electrocyclisation and fragmentation process, previously reported by Besson,[3, 5] may be facilitated by halogen complexation (Scheme **2.9**)

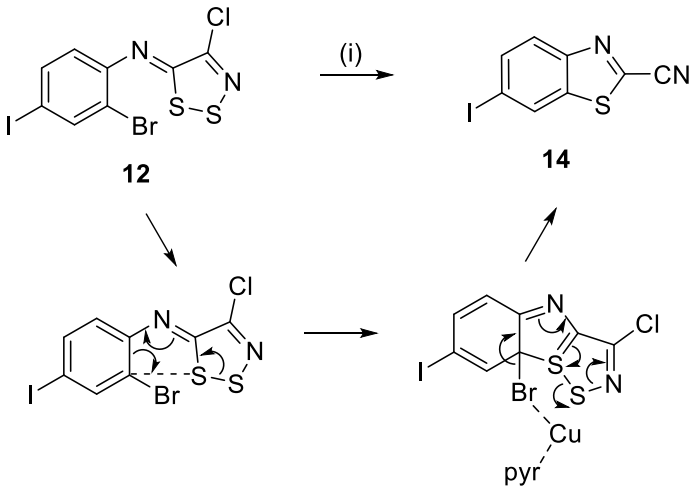

Scheme 2.10. Proposed mechanism of benzothiazole **14** formation through electrocyclisation and fragmentation. Reagents and conditions: (i) CuI (1 eq), pyr, 115 °C (MW), 30 min.

Interestingly, benzothiazole **14** did not possess any fluorescent activity, a common trait of benzothiazoles. This is thought to be due to the iodine group in the 6-position of the benzothiazole ring increasing intersystem crossing (ISC) due to the heavy atom effect.

^{1}H NMR analysis of the isolated material revealed the three aromatic protons H-7, H-4 and H-5 as a singlet, doublet and doublet as expected. Despite attempting to separate the material via column chromatography, there were still some impurities such as iodobenzene present in the spectrum (Figure **2.7**). LCMS analysis of the isolated material confirmed the appropriate mass of the product and the iodobenzene by-product (Supplementary materials, page 38).

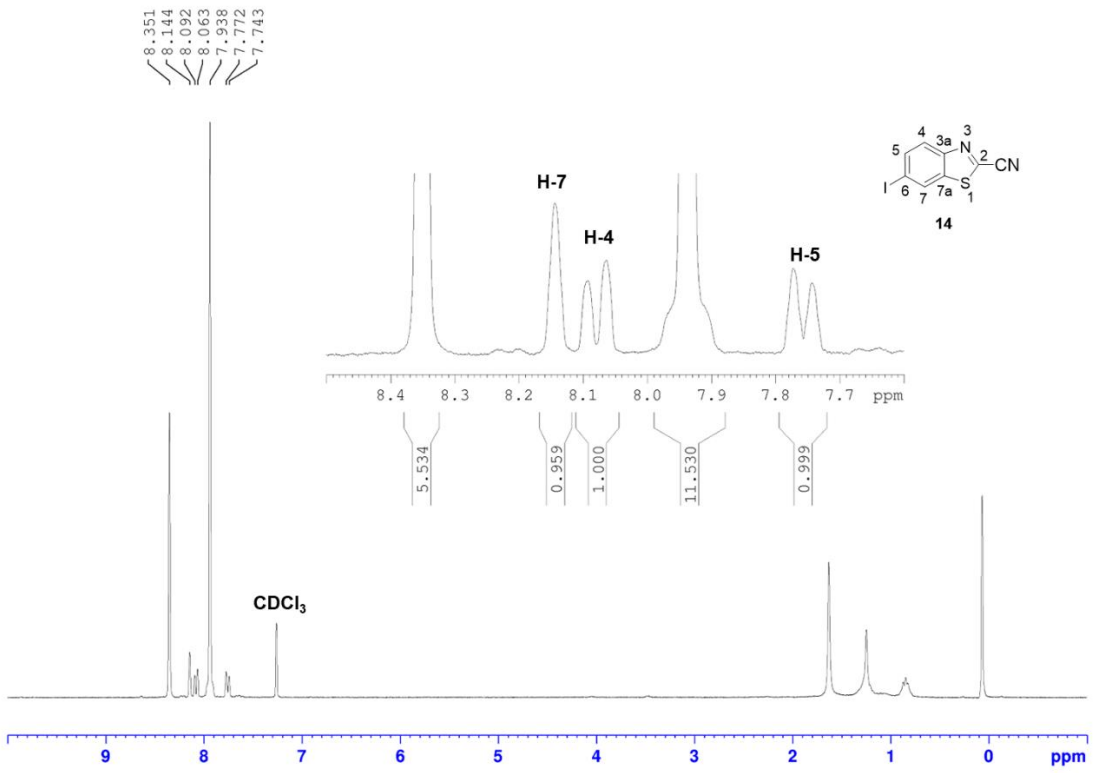

Figure 2.7. ^{1}H NMR spectrum of **14** in $CDCl_3$.

2.3.3 Thioacetylation reaction on 6-iodo-2-cyanobenzothiazole (14)

Following the successful synthesis of benzothiazole **14**, the thioacetylation reaction was attempted once more. A mixture of impure benzothiazole **14**, 10 mol% CuI, 1,10-phenanthroline and potassium thioacetate in toluene was heated under reflux at 110 °C according to the literature method.[15] After 48 h the crude reaction mixture was purified via column chromatography on silica gel, with the primary product of the reaction eluting with 70% ethyl acetate/hexane in moderate yield (52%). ^{1}H NMR analysis of the isolated material **15** was promising as it indicated that the aromatic ring remained substituted at the 6-position with a doublet, singlet and doublet of doublets splitting pattern (Figure **2.8**). However, when analysing the material via IR spectroscopy, surprisingly there was an absence of the nitrile functional group (Figure **2.9**). This suggested that the nitrile group was in fact not maintained during the reaction and that the thioacetylation reagents may have reacted on the C-2 position of the benzothiazole ring, instead of the C-6 position.

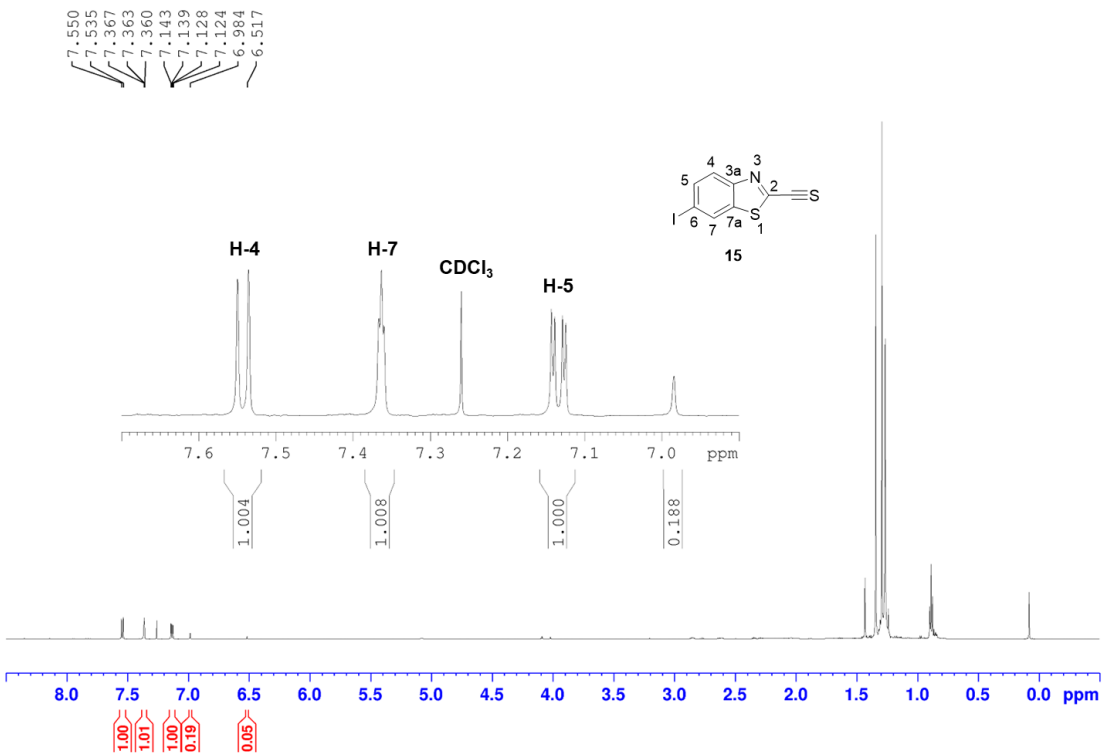

Figure 2.8. ^{1}H NMR spectrum of **15** in $CDCl_3$.

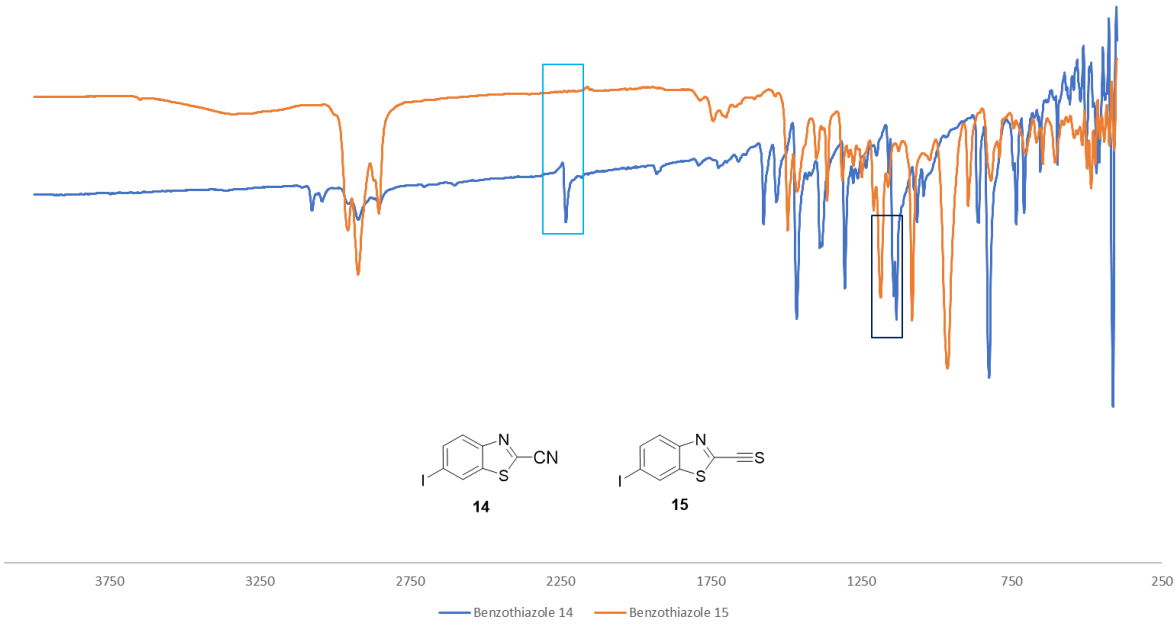

Figure 2.9. Stacked IR spectra of benzothiazole **14** and benzothiazole **15** showing the loss of the nitrile group.

LCMS analysis confirmed that indeed the iodine functional group was not substituted, instead the C-2 position of the benzothiazole ring was substituted. The calculated mass of the product was 304.88, while 304.9 was found (Supplementary materials page 39). Other masses of side

products were found in the LCMS spectrum as well; however, these also corresponded to thioacetylation occurring on the nitrile group. With that result it was evident that the thioacetylation reaction was not successful on benzothiazole **14** and would most likely not be successful in substituting benzothiazoles at the 6-position.

2.4 Conclusion

Halogenation of ethyl benzothiazole-2-carboxylate **7.1a** was unsuccessful, which is attributed to the electron-withdrawing nature of the carboxylate group, rendering the aromatic ring deactivated towards electrophilic substitution. This finding suggests that commercially available 2-cyanobenzothiazole would likewise be unsuitable as an intermediate in luciferin synthesis, due to its analogous reactivity profile. In contrast, halogenation of 2-benzothiazoleacetonitrile **7.1b** occurred preferentially at the methylene carbon, consistent with the relatively high acidity of the methylene protons and their susceptibility to electrophilic substitution. Even upon increasing the halogen equivalents from one to three, no substitution at the aromatic ring was observed, thereby leading to the discontinuation of this model study.

In the alternative synthetic approach based on *p*-iodoaniline, four intermediates were successfully synthesised. Although a metal-free method for benzothiazole ring closure was not achieved, Deau *et al.*'s microwave-assisted, copper(I)-mediated cyclisation protocol[7] was found to be effective when applied to the novel imine intermediate **12**, affording benzothiazole **14** in an overall yield of 7%. The low overall yield was attributed to the instability and degradation of intermediate **12** on silica during purification. However, performing the cyclisation directly on crude **12** afforded **14** in an isolated yield of 60%, indicating this as a preferred approach for future synthesis.

Attempts to thioacetylate benzothiazole **14** at the C-6 position were unsuccessful. The reaction instead occurred at the more reactive C-2 position, resulting in the formation of benzothiazole **15**. Further modifications to enforce substitution on the aromatic ring were not pursued, due to the concurrent loss of the essential nitrile group. Despite this limitation, a new and effective route to benzothiazole **14** was established and could serve as the foundation for further synthetic efforts (Scheme **2.10**). These findings justified the exploration of an alternative route to D-thioluciferin, involving the incorporation of alkyl-sulphur substituents. The outcomes of this investigation are detailed in **Chapter 3**.

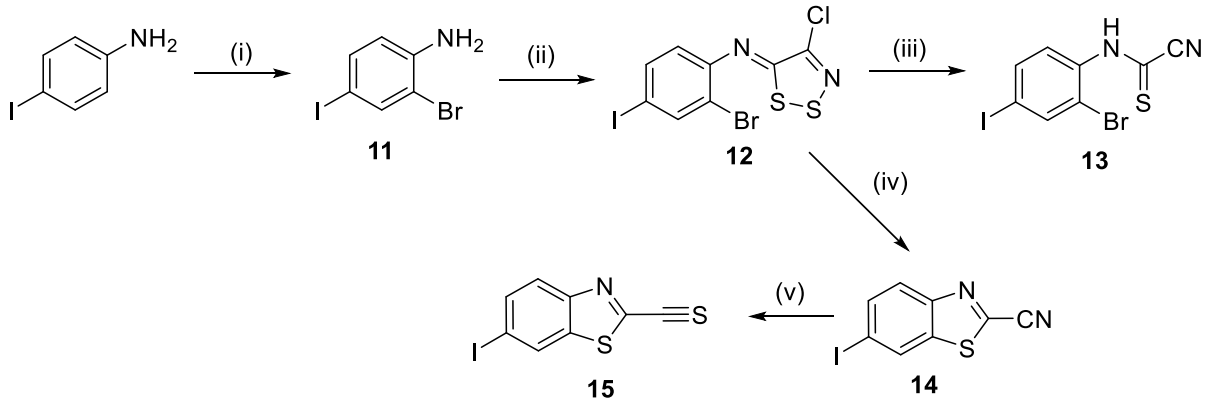

Scheme 2.11. *p*-Iodoaniline synthetic route. Reagents and conditions: (i) KBr, $NaBO_3$, CH_3COOH, rt, 18 h, (96%), (ii) Appel's salt, DCM, Anhydrous pyridine (2 eq), rt, 3 h, (13% when isolated), (iii) DBU (5 eq), DCM, -5 °C, 1 h, (60-80%), (iv) CuI (1 eq.), pyr, 115 °C, 30 min, (59%), (v) CuI (10 mol %), 1,10-phenanthroline (20 mol %), AcS^-K^+, toluene, 110 °C, 2 h (52%).

2.5 References

(1) Rylands, M. PhD thesis, unpublished. University of Cape Town, **2018**.

(2) McCutcheon, D. C.; Paley, M. A.; Steinhardt, R. C.; Prescher, J. A. Expedient Synthesis of Electronically Modified Luciferins for Bioluminescence Imaging. *Journal of the American Chemical Society* **2012**, *134* (18), 7604-7607. DOI: 10.1021/ja301493d.

(3) Besson, T.; Rees, C. W. Some chemistry of 4, 5-dichloro-1, 2, 3-dithiazolium chloride and its derivatives. *Journal of the Chemical Society, Perkin Transactions 1* **1995**, (13), 1659-1662.

(4) English, R. F.; Rakitin, O. A.; Rees, C. W.; Vlasova, O. G. Conversion of imino-1, 2, 3-dithiazoles into 2-cyanobenzothiazoles, cyanoimidoyl chlorides and diatomic sulfur. *Journal of the Chemical Society, Perkin Transactions 1* **1997**, (3), 201-206.

(5) Besson, T.; Dozias, M.-J.; Guillard, J.; Rees, C. W. New route to 2-cyanobenzothiazoles via N-arylimino-1, 2, 3-dithiazoles. *Journal of the Chemical Society, Perkin Transactions 1* **1998**, (23), 3925-3926.

(6) Frère, S.; Thiéry, V.; Besson, T. Eco-Friendly microwave-assisted scaleable synthesis of 2-cyanobenzothiazoles via N-arylimino-1, 2, 3-dithiazoles. *Synthetic communications* **2003**, *33* (21), 3795-3804.

(7) Deau, E.; Dubouilh-Benard, C.; Levacher, V.; Besson, T. Microwave-assisted synthesis of novel N-(4-phenylthiazol-2-yl)-benzo[d]thiazole-, thiazolo[4,5-b]pyridine-, thiazolo[5,4-b]pyridine- and benzo[d]oxazole-2-carboximidamides inspired by marine topsentines and nortopsentines. *Tetrahedron* **2014**, *70* (35), 5532-5540.

(8) McCutcheon, D. C.; Porterfield, W. B.; Prescher, J. A. Rapid and scalable assembly of firefly luciferase substrates. *Org Biomol Chem* **2015**, *13* (7), 2117-2121.

(9) Broudic, N.; Pacheco-Benichou, A.; Fruit, C.; Besson, T. Synthesis of 2-Cyanobenzothiazoles via Pd-Catalyzed/Cu-Assisted CH Functionalization/Intramolecular CS Bond Formation from N-Arylcyanothioformamides. *Molecules* **2022**, *27* (23), 8426.

(10) Moussa, Z.; Judeh, Z. M. A.; Alzamly, A.; Ahmed, S. A.; Tomah Al-Masri, H.; Al-Hindawi, B.; Rasool, F.; Saada, S. Iodine-DMSO mediated conversion of N-arylcyanothioformamides to N-arylcyanoformamides and the unexpected formation of 2-cyanobenzothiazoles. *RSC Advances* **2022**, *12* (10), 6133-6148, 10.1039/D2RA00049K.

(11) Pirrung, M. C.; Carlson, A. D.; De Howitt, N.; Liao, J. Synthesis and bioluminescence of thioluciferin. *Bioorg Med Chem Lett* **2019**, *29* (19), 126591.

(12) Evans, D. A.; Andrews, G. C. Allylic sulfoxides. Useful intermediates in organic synthesis. *Accounts of Chemical Research* **1974**, *7* (5), 147-155.

(13) Soria, S.; Peñéñory, A. Efficient Cu-catalyzed base-free C-S coupling under conventional and microwave heating. A simple access to S-heterocycles and sulfides. *Beilstein journal of organic chemistry* **2013**, *9*, 467-475.

(14) Ullmann, F. A new presentation method of phenyl ether salic acid. *Berichte Der Deutschen Chemischen Gesellschaft* **1904**, *37*, 853-854.

(15) Soria-Castro, S. M.; Peñéñory, A. B. Efficient Cu-catalyzed base-free C–S coupling under conventional and microwave heating. A simple access to S-heterocycles and sulfides. *Beilstein Journal of Organic Chemistry* **2013**, *9*, 467-475.

Chapter 3 : Improved synthesis of alkylthioether luciferins

3.1 Literature overview

3.1.1 Thioether luciferin synthesis by Sharma

Due to the limitations encountered in the metal-free synthetic route to D-thioluciferin,[1] as outlined in the preceding chapter, it became necessary to explore an alternative strategy for the synthesis of D-thioluciferin and related thioether luciferins. As discussed in the introduction, the synthetic approach developed by Sharma and co-workers for thioether luciferins[2] was reviewed, along with its associated applications and limitations. The former included a promising platform for the design of bioluminescent probes responsive to sulphur oxidation, based on the alleviation of luciferase inhibition. However, the method was hindered by a low overall yield and the use of potassium cyanide, a hazardous and toxic reagent. These drawbacks highlighted the need for a more efficient and safer synthetic route.

A key transformation in the synthesis of D-thioluciferin is the preparation of 6-thio-2-cyanobenzothiazole **7**. Pirrung and co-workers previously achieved this intermediate through a Mislow–Evans rearrangement[3, 4] of an allylic sulfoxide.[5] However, this strategy was not applicable to methyl(thio)-substituted benzothiazole **21**, due to the absence of an allylic functional group (Scheme **3.1**). Additionally, efforts to introduce the thiol functionality via potassium thioacetate under a base-free copper/ligand catalytic system[6] proved ineffective for 2-cyanobenzothiazoles, as detailed in **Chapter 2**. Consequently, an alternative synthetic approach to this key intermediate was required.

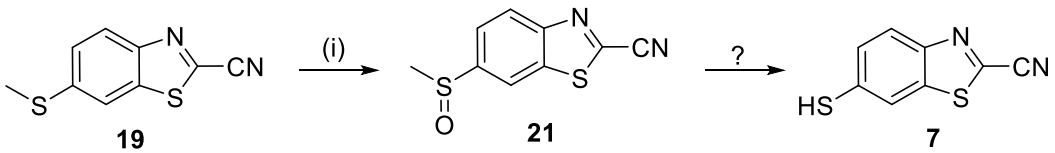

Scheme 3.1. Synthetic challenges posed for the synthesis of 6-thio-2-cyanobenzothiazole **7**. Reagents and conditions: (i) *m*-CPBA, DCM, rt, 12 h.

3.1.2 Unmasking the thiol group

The Pummerer rearrangement[7] is a well-established transformation in organic synthesis, wherein a sulfoxide is converted into an α-acyloxy sulphide (or α-thioether) in the presence of an acid anhydride or acid chloride. The mechanism involves nucleophilic activation of the sulfoxide oxygen, followed by elimination to form a sulfonium intermediate and subsequent addition of the acyloxy group to the carbon α to the sulphur atom (Scheme **3.2**).

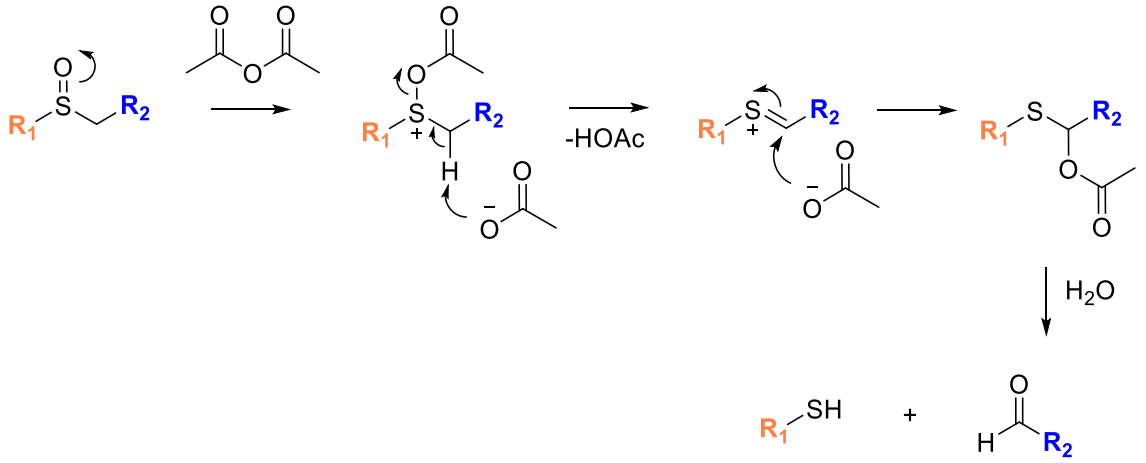

Scheme 3.2. Pummerer rearrangement of sulfoxides into aldehydes or ketones and free thiols.

This reaction has been effectively applied in the synthesis of various sulphur-containing compounds, including alkoxysulfonium salts,[8] enantiomerically pure β-hydroxy-γ-sulfenyl-γ-butyrolactones,[9] (11,12)-dihydrodibenzo[c,g][1,2]dithiocine,[10] and alkylthiomethyl esters.[11]

In a 2004 study, Wyatt and Hudson reported the synthesis of (11,12)-dihydrodibenzo[c,g][1,2]dithiocine via two distinct approaches, both originating from a common dibromide intermediate **3.1**.[10] The first strategy involved sequential incorporation of two sulphur atoms. The dibromide was first subjected to double lithiation, followed by treatment with dimethyl disulphide (Me_2S_2), affording the methylated disulphide intermediate **3.2** in high yield. Oxidation of this intermediate to the corresponding sulfoxide, followed by a double Pummerer rearrangement, afforded intermediate **3.3**. Subsequent treatment with methanol and ammonia produced the dithiol compound **3.4**, which was then oxidised with potassium triiodide (KI_3) to yield the final product **3.5** (Scheme **3.3**). Despite the multi-step route, the overall yield of 28% demonstrated its viability.

In contrast, the second approach employed disulphur diimidazole (S_2Im_2) as a bis-electrophilic sulphur donor, allowing for the simultaneous introduction of both sulphur atoms. Treatment of the lithiated dibromide with S_2Im_2 enabled direct access to the target dithiocine in a single step,

affording the product in an impressive 85% yield. Although the second method was superior in terms of both efficiency and operational simplicity, the study underscored the value of the Pummerer rearrangement in heterocyclic sulphur chemistry, particularly when utilising methyl(sulfoxide)-substituted intermediates.

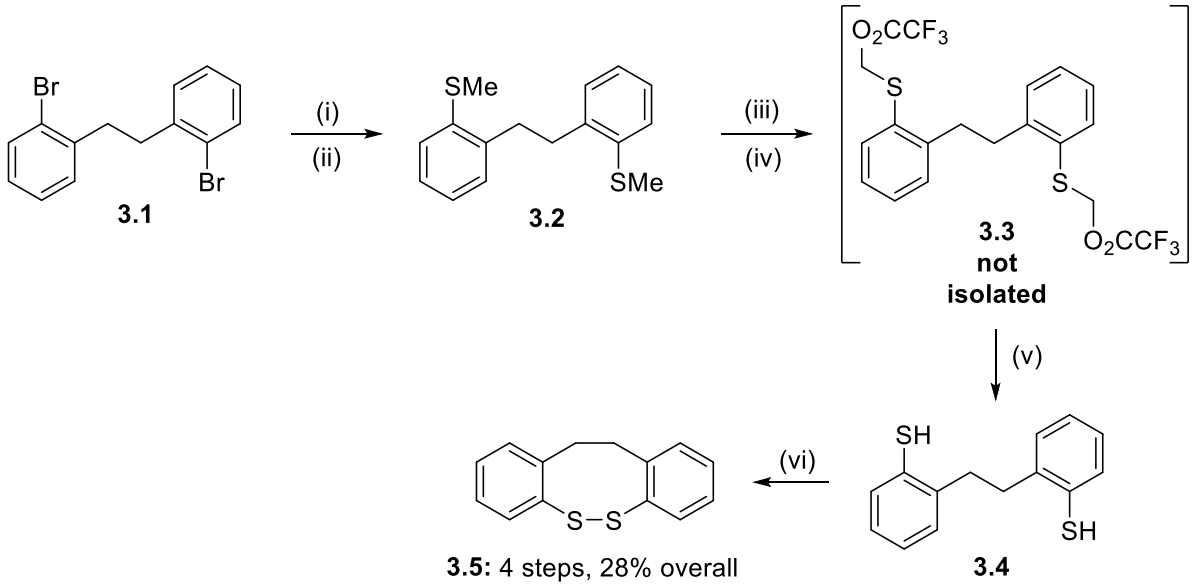

Scheme 3.3. Double Pummerer rearrangement of 1,2-bis(2-bromophenyl)ethane **3.1**.[10] Reagents and conditions: (i) *n*-BuLi (2 eq), THF, 78 °C, 30 min, (92%), (ii) Me_2S_2 (6 eq), 78 °C-rt, 12 h, (iii) *m*-CPBA, sodium sulphite, rt, 10 min, (iv) TFAA, 40 °C, 30 min, (30%), (v) 1:1 MeOH / Et_3N (30%), (vi) KI_3, chloroform (94%).

3.2 Research rationale and motivation

Commercially available 4-(methylthio)aniline was selected as a suitable starting material. This compound was to undergo the standard Appel salt condensation,[12] followed by intramolecular cyclisation via thermolysis,[13] to afford benzothiazole **19**. The efficient synthesis of benzothiazole **19** was of particular importance, as it served as a pivotal intermediate en route to benzothiazole derivatives **21** and **7**, and ultimately to the corresponding luciferin analogues **20**, **22**, and D-thioluciferin (Scheme **3.4**).

Subsequently, the Pummerer rearrangement conditions described by Wyatt and Hudson were to be applied to benzothiazole **21** in order to obtain the key thio derivative **7**. To ensure structural confirmation of both 6-thio-2-cyanobenzothiazole **7** and D-thioluciferin, the linear synthetic route reported by Pirrung and co-workers[5] would also be replicated. This validation step would be conducted prior to the synthesis of the thioether luciferin analogues.

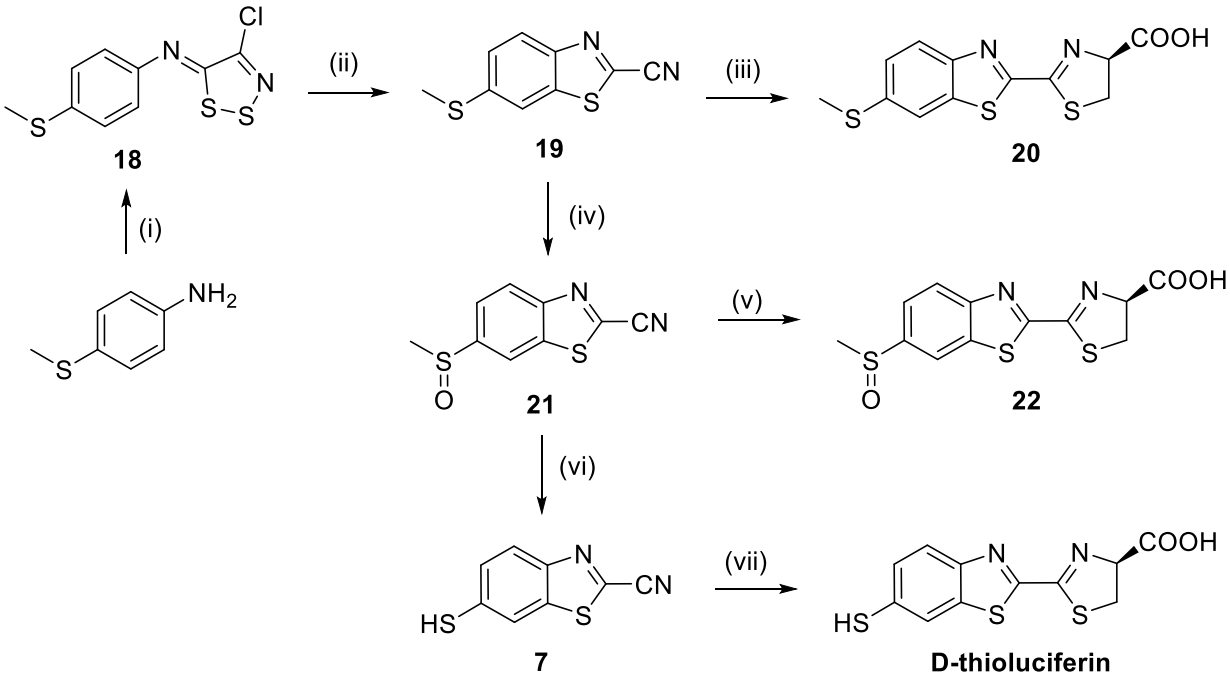

Scheme 3.4. Proposed synthetic route to D-thioluciferin and its methyl(thio) analogues. Reagents and conditions: (i) Appel's salt, DCM, anhydrous pyridine, rt, 3 h, (ii) Sulfolane, 180 °C, 30 min (iii) D-Cysteine, K_2CO_3, MeOH:H_2O, rt, 30 min, (iv) *m*-CPBA, DCM, rt, 12 h, (v) D-Cysteine, K_2CO_3, MeOH:H_2O, rt, 30 min (vi) TFAA, 40 °C, 30 min, 1:1 MeOH / Et_3N, (vii) D-Cysteine, K_2CO_3, MeOH:H_2O, rt, 30 min.

Furthermore, it was proposed that the resulting luciferin derivatives be evaluated as substrates for firefly luciferase (fLuc), in order to assess their bioluminescent activity and potential utility in sensing applications (Scheme **3.5**).

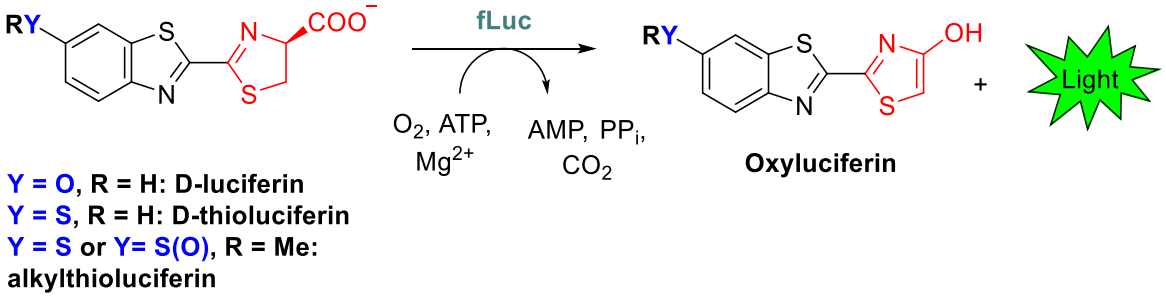

Scheme 3.5. Structures of different sulphur-containing luciferin analogues for potential bioluminescent emission analysis.

3.3 Results and Discussion

3.3.1 Challenges with the Pirrung synthesis of D-thioluciferin

Similar to the Rylands approach which was previously attempted,[14] the synthetic route reported by Pirrung and co-workers[5] was also successful up to the penultimate step. All intermediates leading up to the synthesis of D-thioluciferin were successfully synthesised in moderate to high yields until the synthesis of 6-thio-2-cyanobenzothiazole **7** (Scheme **3.6**).

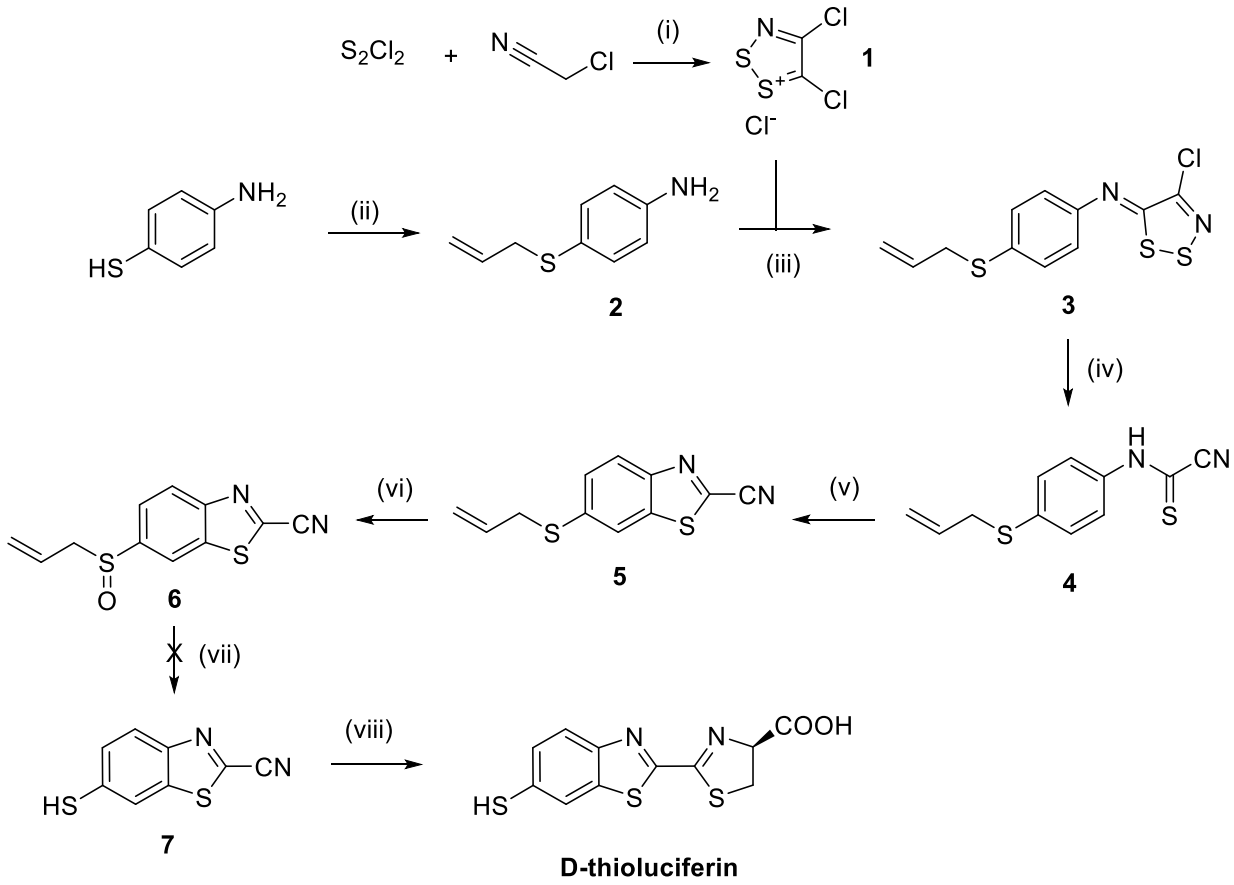

Scheme 3.6. Linear synthetic route for the synthesis of D-thioluciferin. Reagents and conditions: (i) DCM, rt, 24 h, (84%), (ii) Allyl bromide, K_2CO_3, Acetone, rt, 18 h, (90%), (iii) Appel's salt, DCM, Anhydrous pyridine, rt, 3 h, (81%), (iv) DCM, DBU, -5 °C, 1 h, (57%), (v) $PdCl_2$, CuI, TBAB, DMF:DMSO (1:1), 120 °C, 1 h, (56%), (vi) DCM:MeOH (1:5), $NaIO_4$, 0 °C, 12 h, (82%), (vii) $P(OPh)_3$, THF, H_2O, 18 h, (viii) D-Cys, K_2CO_3, MeOH:H_2O, rt, 30 min.

The conversion of sulfoxide **6** to thiol **7** was proposed to proceed via a Mislow–Evans rearrangement,[3, 4] as originally described by the authors.[5] The initial transformation involves a *[2,3]*-sigmatropic rearrangement of sulfoxide **6**, carried out at an elevated temperature of 72 °C for 16 hours. This step yields the intermediate sulfenate ester **6.1**. Nucleophilic addition of triphenylphosphite to this intermediate subsequently generates a thiolate salt **6.2**, which upon hydrolysis with water affords 6-thio-2-cyanobenzothiazole **7** (Scheme **3.7**).

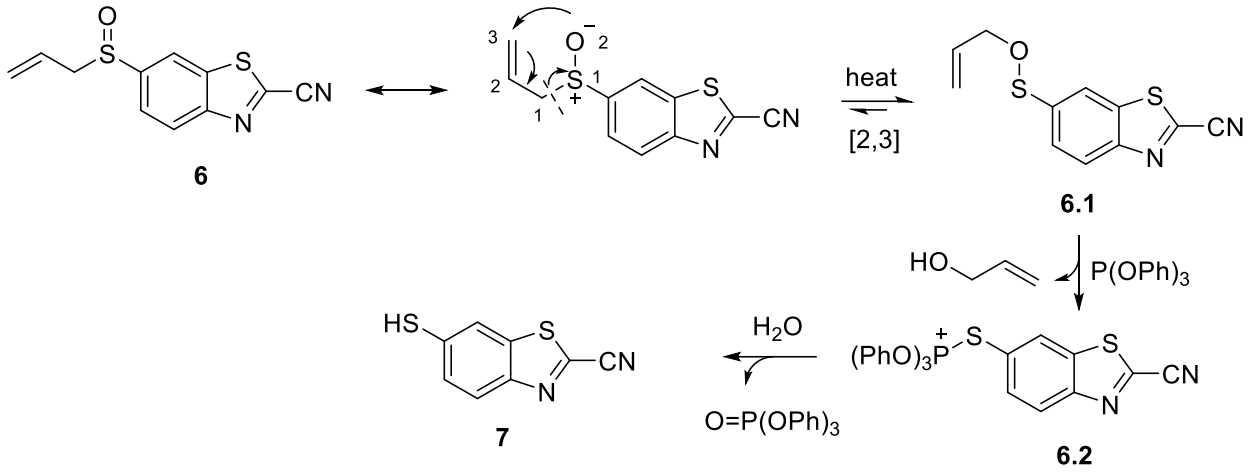

Scheme 3.7. Proposed mechanism for the formation of aryl thiol **7**. Reaction conditions (i) $P(OPh)_3$, THF, H_2O, 18 h.

Following hydrolysis and 30 minutes of stirring with water, thin-layer chromatography (TLC) analysis indicated the formation of a new product with an R_f value of 0.50 (30% ethyl acetate/hexane). The crude yellow oil was subjected to normal-phase column chromatography on silica gel using 5% ethyl acetate in hexane to isolate the target compound. However, upon solvent removal under reduced pressure the expected yellow solid had not formed, precluding an accurate determination of the reaction yield.

Nevertheless, analytical data provided some insight into the reaction outcome. ^{1}H NMR analysis of the isolated material revealed multiple signals in the aromatic region (6.7–7.5 ppm), which are attributed to the phosphine oxide. Additionally, lower-intensity signals observed between 7.6–8.3 ppm were consistent with the aromatic proton resonances reported for thiol **7**.[4] Furthermore, signals in the 4.0–6.0 ppm region were tentatively assigned to the allylic protons of sulfenate ester **6.1**, suggesting the presence of multiple reaction intermediates in the crude product mixture (Figure **3.1**).

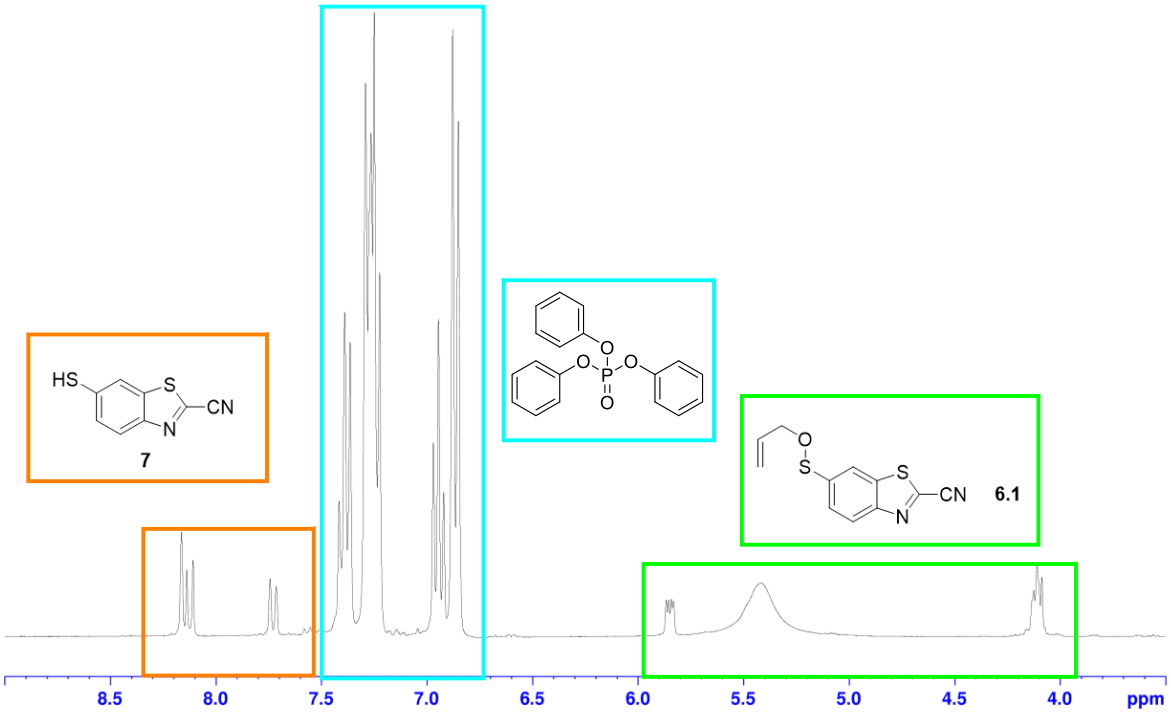

Figure 3.1. ^{1}H NMR spectrum of **6.1**, **7** and phosphine oxide in $CDCl_3$.

LCMS analysis of the isolated material revealed a molecular ion peak at *m/z* 193.0, consistent with the expected mass of thiol **7**.[5] This observation suggests that thiol **7** may have formed via hydrolysis of the thiolate salt intermediate **6.2** during column chromatography. Additional peaks at *m/z* 270.3 and 263.0 were observed and are attributed to degradation products of triphenylphosphite (Figure **3.2c**). Taken together with the ^{1}H NMR data, these results indicate that the reaction may not have proceeded to full completion, instead halting at the formation of the thiolate intermediate **6.2**, prior to hydrolysis. This interpretation is supported by the limited aqueous work-up time, as the reaction mixture was stirred in water for only 30 minutes.

To address this, the reaction was repeated three additional times, with variations in the duration of the heating step. However, the resulting ^{1}H NMR spectra were largely similar across trials, showing no significant improvement in the conversion to thiol **7**. A persistent challenge during purification was the presence of excess triphenylphosphite, which consistently co-eluted with the presumed product, complicating isolation.

At this stage, the cause of the incomplete conversion remained unclear. In an effort to better understand the reaction profile and to monitor the progression of key intermediates, an NMR kinetic study was undertaken. The findings of this investigation are presented in the following section of this chapter.

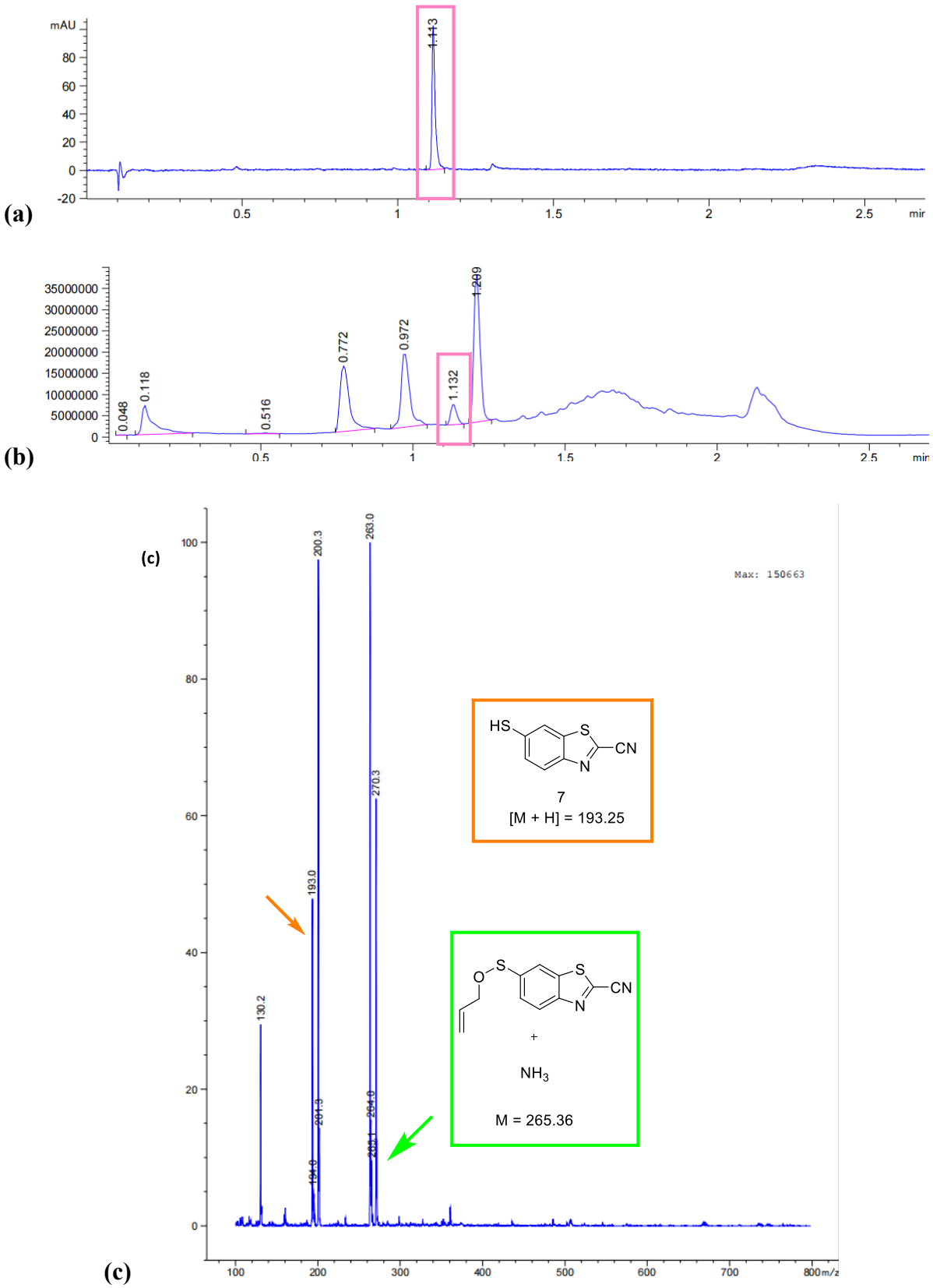

Figure 3.2. (a) LC spectrum of the isolated material at 290 nm. **(b)** TIC spectrum with the peak of interest highlighted in pink. **(c)** MS spectrum of the isolated material.

To ascertain where the potential problem in the synthesis of thiol **7** was, sulfoxide **6** and triphenylphosphite were reacted in deuterated tetrahydrofuran (THF) and monitored via ^{1}H, ^{13}C and ^{31}P NMR periodically over two days. At the time of submission (t=0) all the reactants were added and the sulfoxide **6** proton peaks, highlighted in red, are clearly visible (Figure **3.3**).

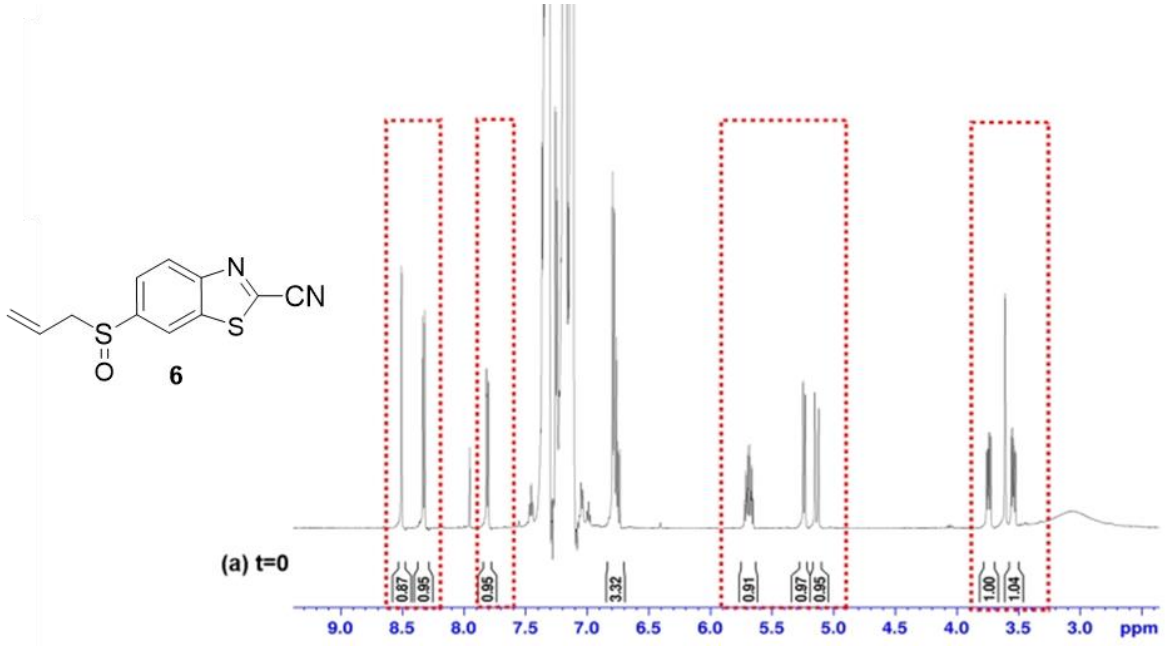

Figure 3.3. ^{1}H NMR spectrum for sulfoxide 6 and $P(OPh)_3$ in THF-d8 at the time of submission (t=0).

As time progressed, signals corresponding to the starting material **6** (Figure **3.4a**) became less intense. Instead, peaks corresponding to the rearranged intermediate, sulfenate ester **6.1** highlighted in green, became visible (Figure **3.4b**). Interestingly, these peaks appeared without the introduction of heat to the reaction system This is further confirmed by HSQC analysis of the reaction mixture, 18 hours after submission whilst still at 303 K (Figure **3.5**). After 10 h of reacting at 323 K, the starting material peaks had diminished almost entirely (Figure **3.4c**).

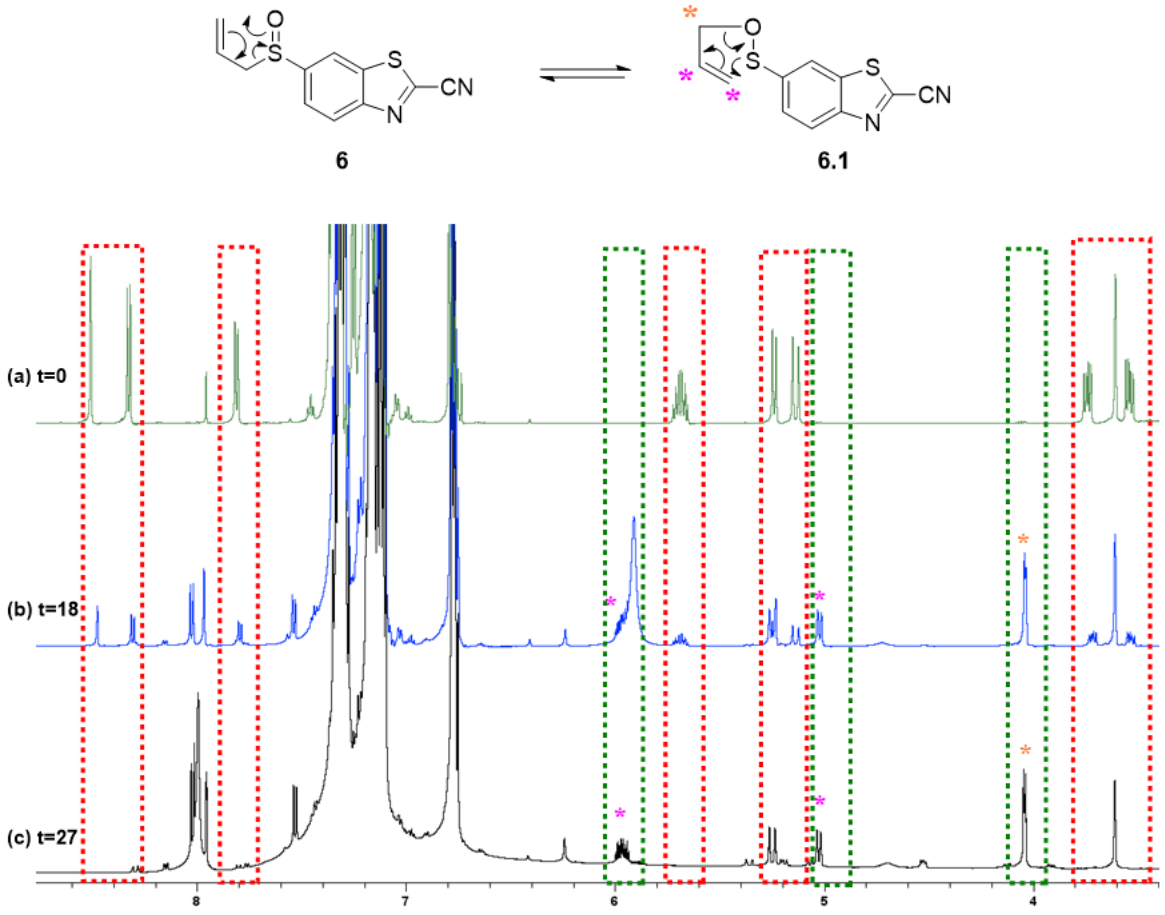

Figure 3.4. Stacked ^{1}H NMR spectra of sulfoxide **6** and triphenylphosphite reaction mixture in THF-d8 at **(a)** 303K immediately after mixing, **(b)** 303K after 18 h, **(c)** 323K for 10 h.

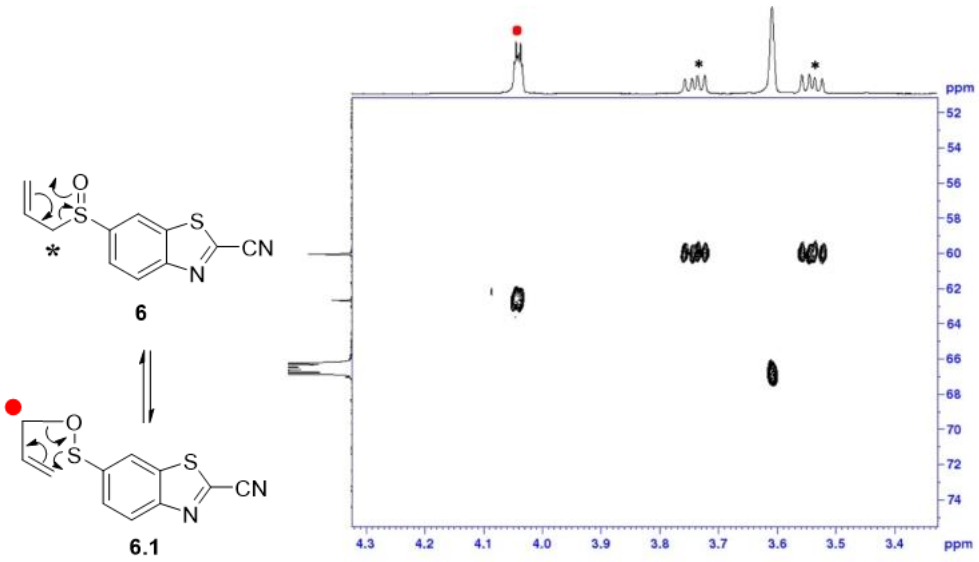

Figure 3.5. Expanded HSQC spectrum of sulfoxide **6** and triphenylphosphite reaction mixture in THF-d8 at 303 K.

Similarly, from ^{13}C NMR analysis, the signal for the methylene carbon of sulfoxide **6** became less intense as the reaction proceeded, whilst the signal for the *O*-allyl residue **6.1** became visible (Figure **3.6**).

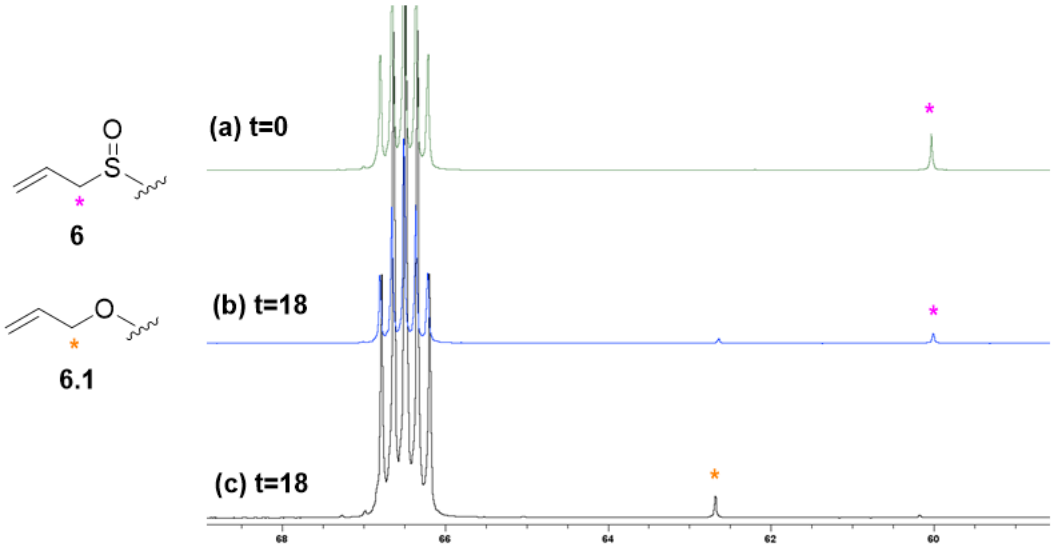

Figure 3.6. Stacked expansion of ^{13}C NMR spectra of sulfoxide **6** and triphenylphosphite reaction mixture in THF-d8 at **(a)** 303 K immediately after mixing, **(b)** 303 K 18 h after mixing, **(c)** 323 K, with THF as an intensity reference.

As the reaction progressed even further, the proton peaks for sulfoxide **6** diminished almost entirely (Figure **3.7d**). However, at t=36 after 18 hours of heating the proton peaks for the sulfenate ester were still present in the reaction mixture (Figure **3.7e**). The reaction remained unchanged after an additional 18 h of heating and quenching with D_2O (Figure **3.7f**). This indicated that intermediate **6.1** was not fully converted into the next intermediate, the thiolate salt **6.2**.

Additionally, triphenylphosphite and its breakdown products were also tracked via the ^{31}P NMR analysis (Figure **3.8**). By t=36, after the addition of D_2O, all triphenylphosphite in the reaction mixture seems to have been broken down into triphenyl phosphate (Figure **3.8d**). This seems plausible as the addition of water into the reaction system should hydrolyse intermediate **6.2**.

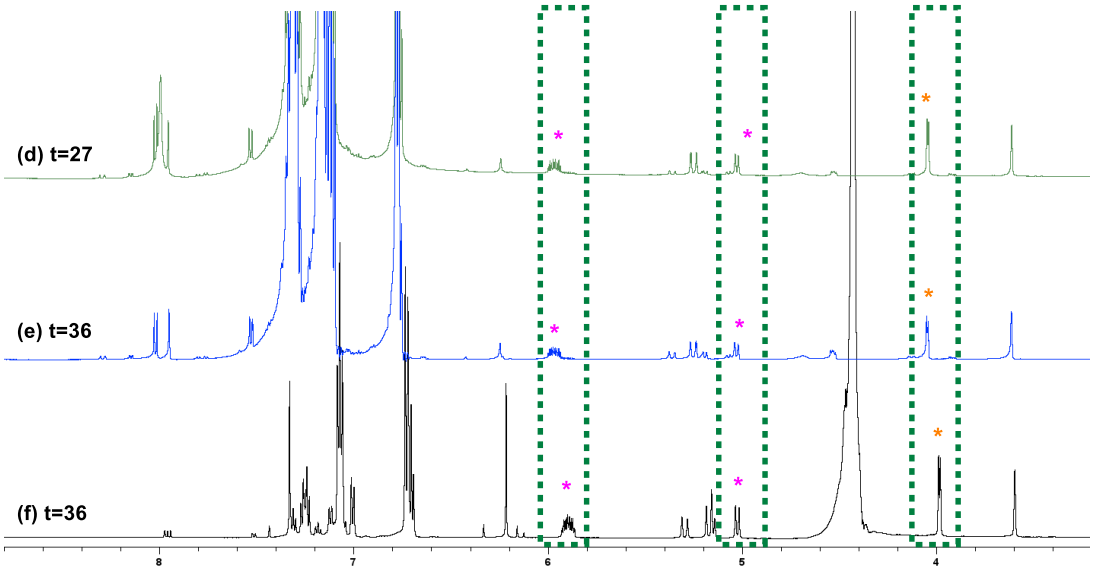

Figure 3.7. Stacked expansion of ^{1}H NMR spectra of sulfoxide **6** and triphenylphosphite reaction mixture in THF-d8 at **(d)** 323 K, **(e)** 323 K for 18 h, **(f)** 323 K for 36 h in 0.4 mL D_2O.

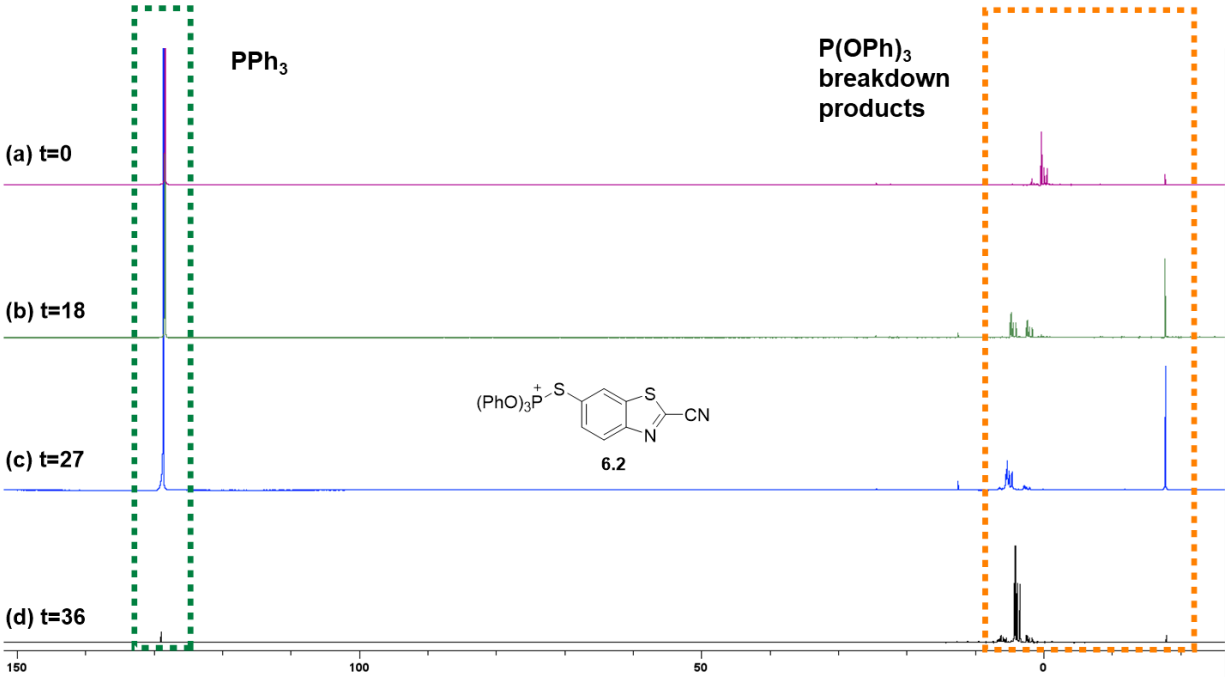

Figure 3.8. Stacked expansion of ^{31}P NMR spectra of sulfoxide **6** and triphenylphosphite reaction mixture in THF-d8 at **(a)** 303 K immediately after mixing, **(b)** 303 K after 18 h, **(c)** heated at 323 K for 10 h, **(d)** 323 K in 0.4 mL D_2O.

When examining the aromatic region of the final ^{1}H NMR spectrum, there does appear to be some peaks emerging which could correspond to those of thiobenzothiazole **7** since the intermediate **6.2** is thought to be quite short-lived (Figure **3.9**). This indicated that this reaction may require a much longer heating period than what was reported in literature.

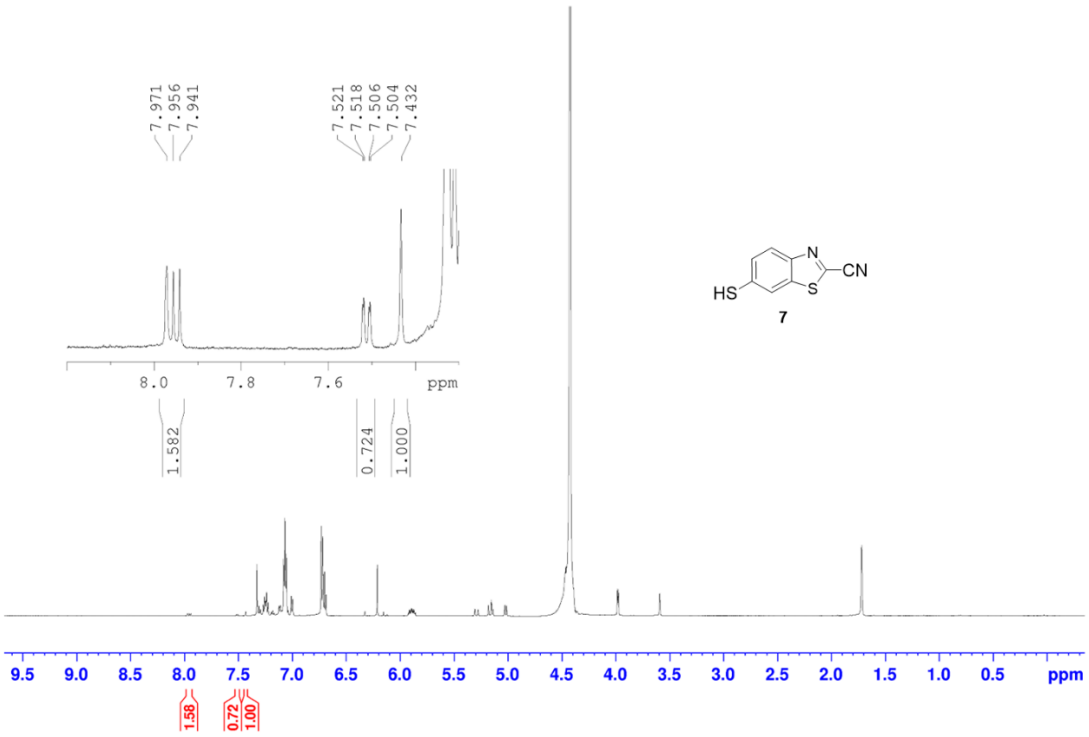

Figure 3.9. ^{1}H NMR spectrum of sulfoxide **6** and triphenylphosphite reaction mixture in THF-d8 at 323K in 0.4 mL D_2O with THF as an intensity reference.

The synthetic obstacle in this reaction is thought to have arisen from the extraction part of the methodology. When examining the extraction mixture, both phases were fluorescent (indicative of the benzothiazole ring closure). This could indicate that the desired product is entering the aqueous water layer as a sulphide, rather than the free thiol. The THF:H_2O reaction mixture was therefore reduced and resuspended in saturated ammonium chloride solution, then extracted with chloroform. The extract was subjected to column chromatography, however the phosphite remained present in the fractions collected. In the interest of time, no further attempts at synthesising thiol **7** and D-thioluciferin were made from this methodology. Instead, the alkyl(thio)-luciferins synthesised by Sharma *et al.*[2] was attempted.

3.3.2 Improved synthesis of thioether luciferins

Due to the failed attempts at synthesising D-thioluciferin in the abovementioned route, it was clear a new method had to be employed. By utilising the ring closure methodology developed by McCutcheon *et al.*,[13] it was proposed that the synthesis of benzothiazole **19** could be condensed to one step as opposed to Sharma's four-step method.[2] As such, 4-methylthioaniline and Appel's salt were allowed to stir for 1 h at room temperature followed by the slow addition of anhydrous pyridine which afforded imine **18** after 2 h. About 100 mg of this crude reaction mixture was subjected to column chromatography to obtain a pure sample of the intermediate

18, which was confirmed by ^{1}H NMR analysis. As the imine is symmetrical, two doublets corresponding to H-3 and H-2 were expected to be located in the aromatic region of the spectrum. However, evidence of a doublet of doublets (dd) splitting pattern was observed which indicated that the imine formed was present as a mixture of *E* and *Z* isomers (Figure **3.10**).

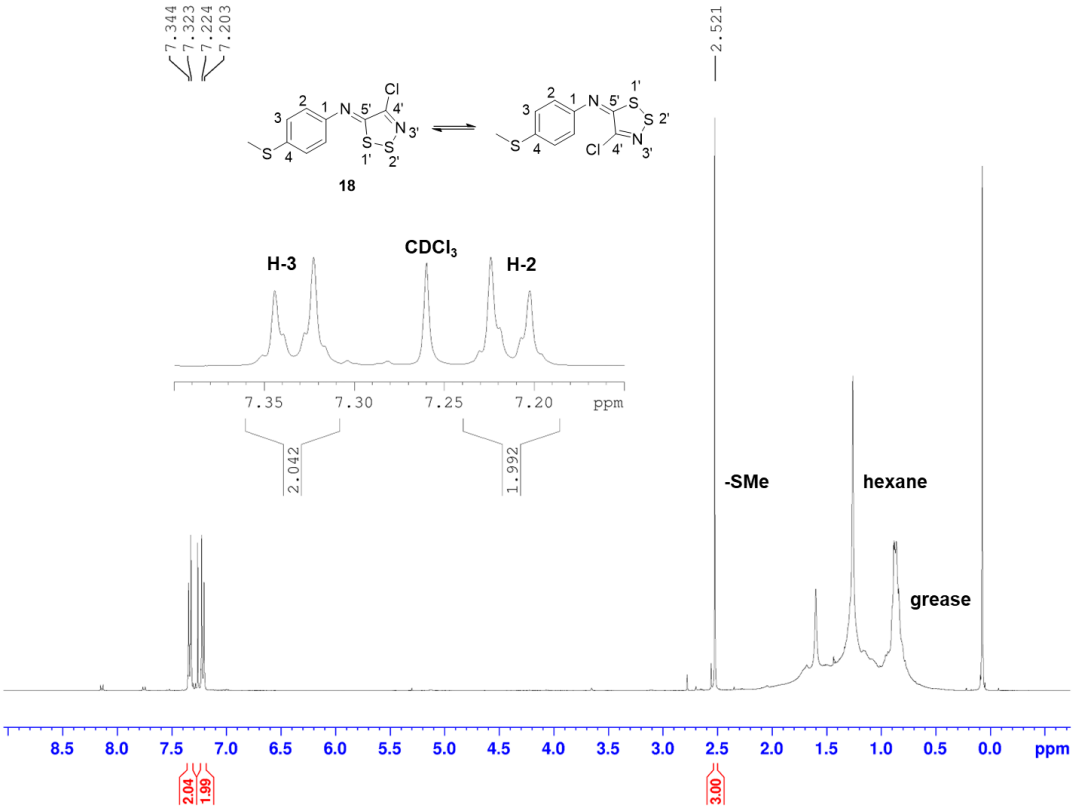

Figure 3.10. ^{1}H NMR spectrum of imine **18** in $CDCl_3$.

After confirmation of the successful formation of imine **18**, the remaining imine was not purified but instead, DCM was removed under reduced pressure and replaced with sulfolane, a higher boiling point solvent. The reaction mixture was heated at 180 °C which afforded benzothiazole **19** in an impressive time of 30 min and in high yield (79%). All protons for this key intermediate were accounted for by ^{1}H NMR analysis (Figure **3.11**).

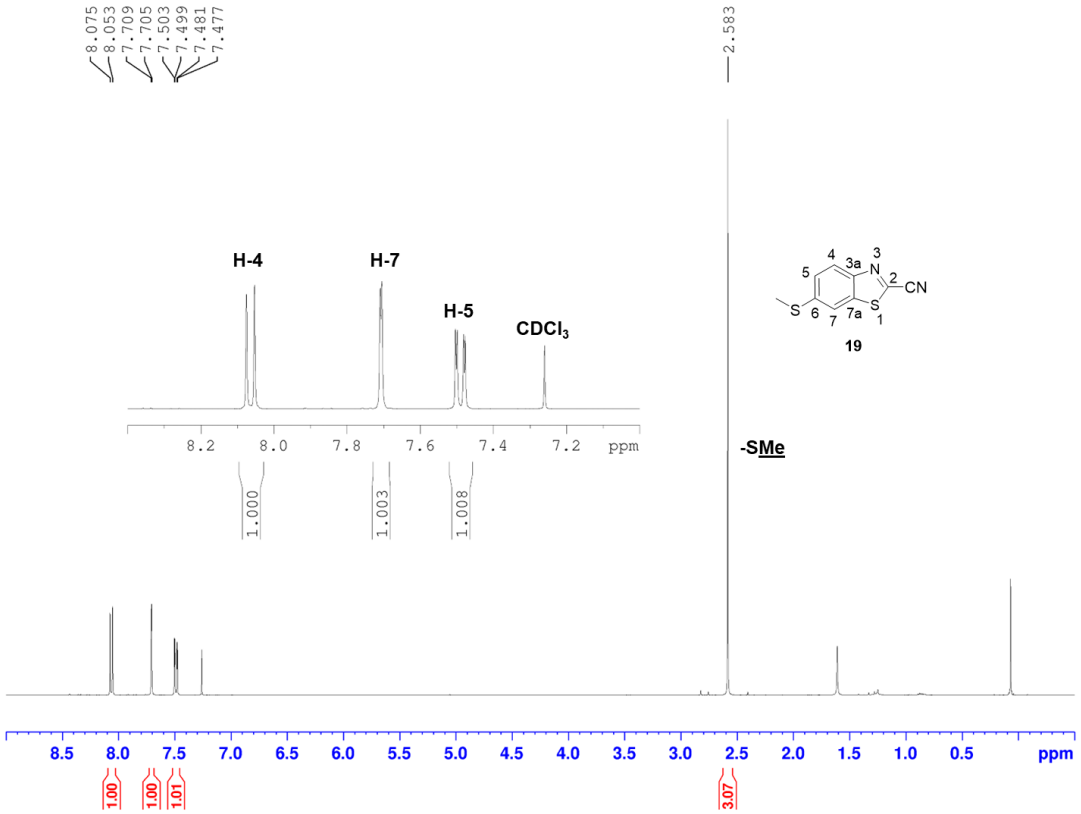

Figure 3.11. ^{1}H NMR spectrum of benzothiazole **19** in $CDCl_3$.

Once purified, benzothiazole **19** was reacted with one equivalent of *m*-CPBA to afford the oxidation product **21**. This method differed from the literature reported by Sharma in which they reported that one equivalent of *m*-CPBA would produce the sulfone intermediate.[2]

The rearrangement of sulfoxides into α-acylated sulfides under acidic conditions, commonly referred to as the Pummerer rearrangement[7] has been previously reported in literature to oxidise the methylthio functionality to free thiols via their sulfoxide derivatives.[10, 15] The mechanism is thought to occur as follows; Sulfoxide **21** reacts with trifluoroacetic anhydride (TFAA) to form the sulfonium intermediate (R-S(+)-OAc), making the α-carbon more electrophilic. The acetate anion deprotonates the α-position, leading to the formation of a positively charged sulphur intermediate. A 1,2-migration occurs where the adjacent alkyl group shifts from sulphur to the α-carbon. This leads to the formation of an α-acylated sulfide. Nucleophilic attack of methanol further modifies the product to afford benzothiazole **7** (Scheme **3.8)**.

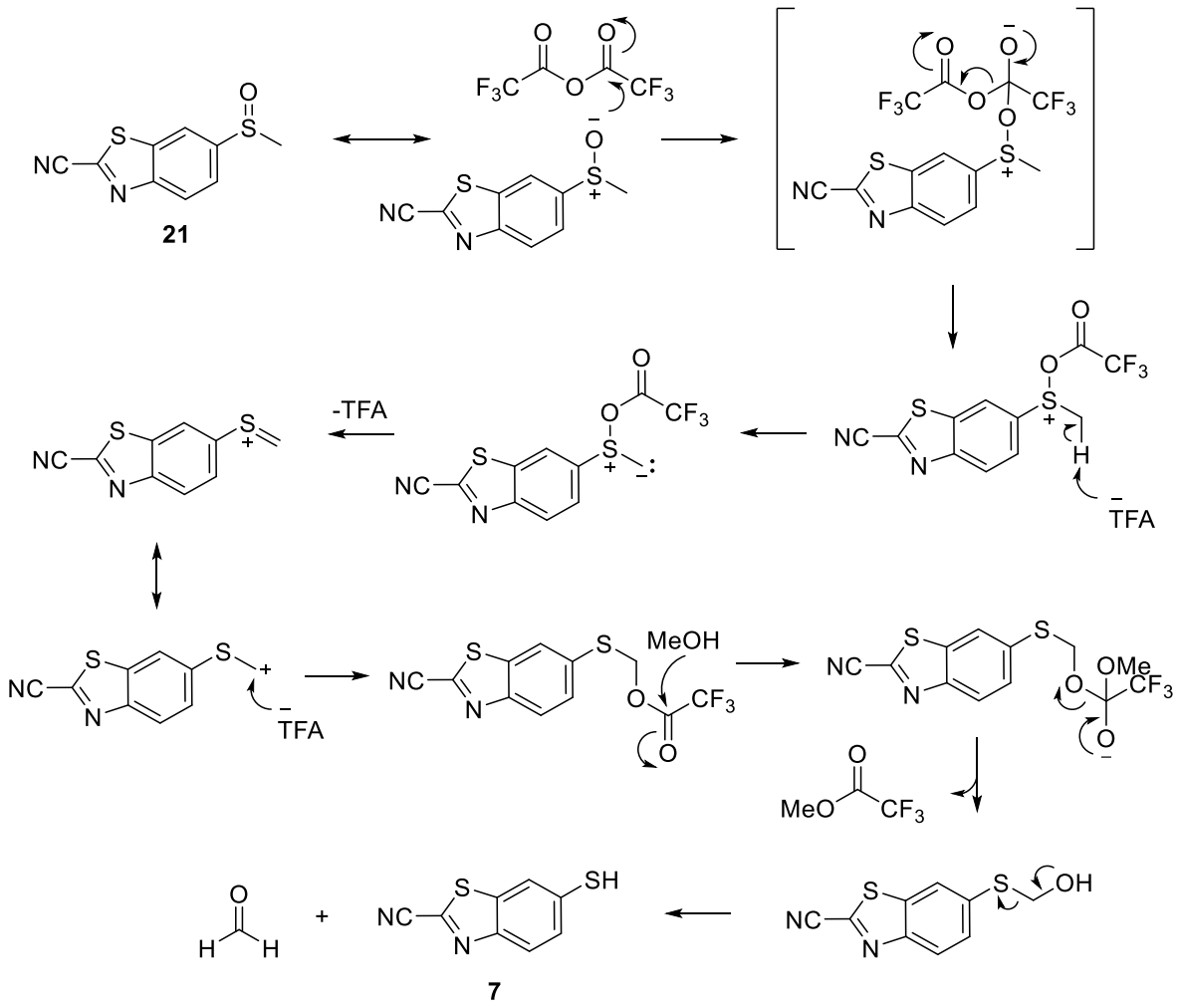

Scheme 3.8. Proposed reaction mechanism for the formation of thiol **7** from sulfoxide **21** via the Pummerer rearrangement.

When attempting this reaction on sulfoxide **21**, a one-pot method was used, as reported in literature.[10] Sulfoxide **21** was dissolved in TFAA and heated at 40 °C for 30 min. After removing the TFAA under reduced pressure, the crude mixture was dissolved in 1:1 methanol and triethylamine. TLC analysis of the reaction mixture revealed a new bright green fluorescence signal on the baseline of the TLC plate as well as a blue fluorescent signal corresponding to the R_f of benzothiazole **19**. Isolation of the reaction mixture proved challenging as a purified product could not be obtained. However, ^{1}H NMR analysis of the crude precipitate confirmed that benzothiazole **19** was indeed present in the reaction mixture, as well as a new product. IR analysis of the crude reaction mixture revealed a thiol stretch at 2595 cm^{-1} (Figure **3.12**). Similarly, LCMS analysis confirmed that thiol **7** was forming, however the main product of the reaction appeared to be the oxidised disulphide (Figure **3.13**).

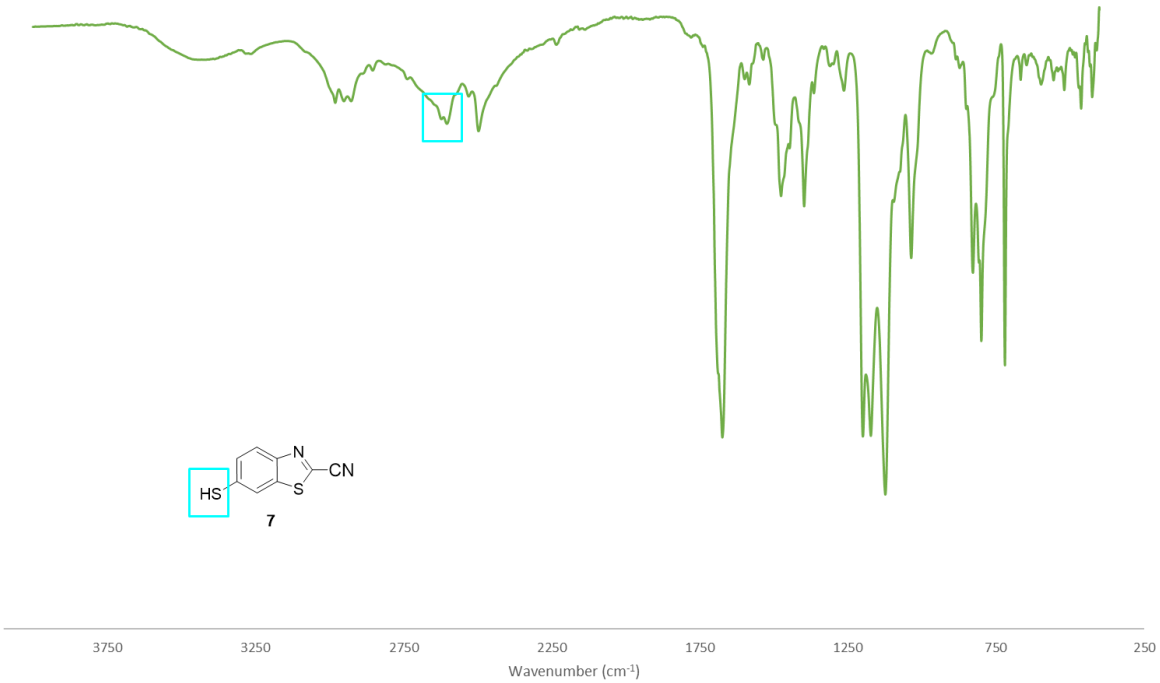

Figure 3.12. IR spectrum of crude thiol **7**.

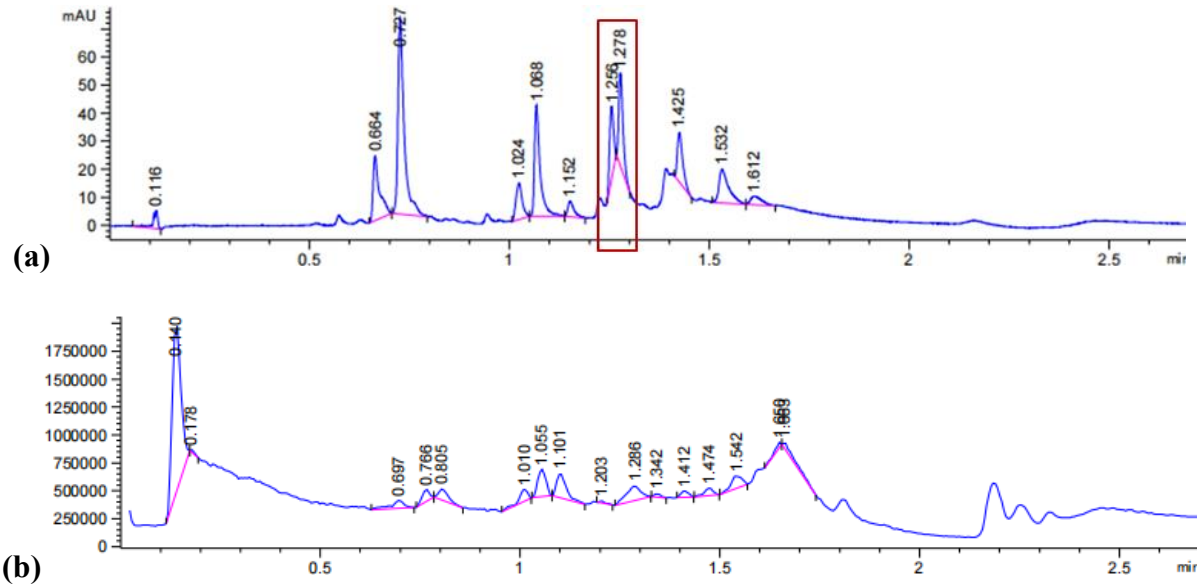

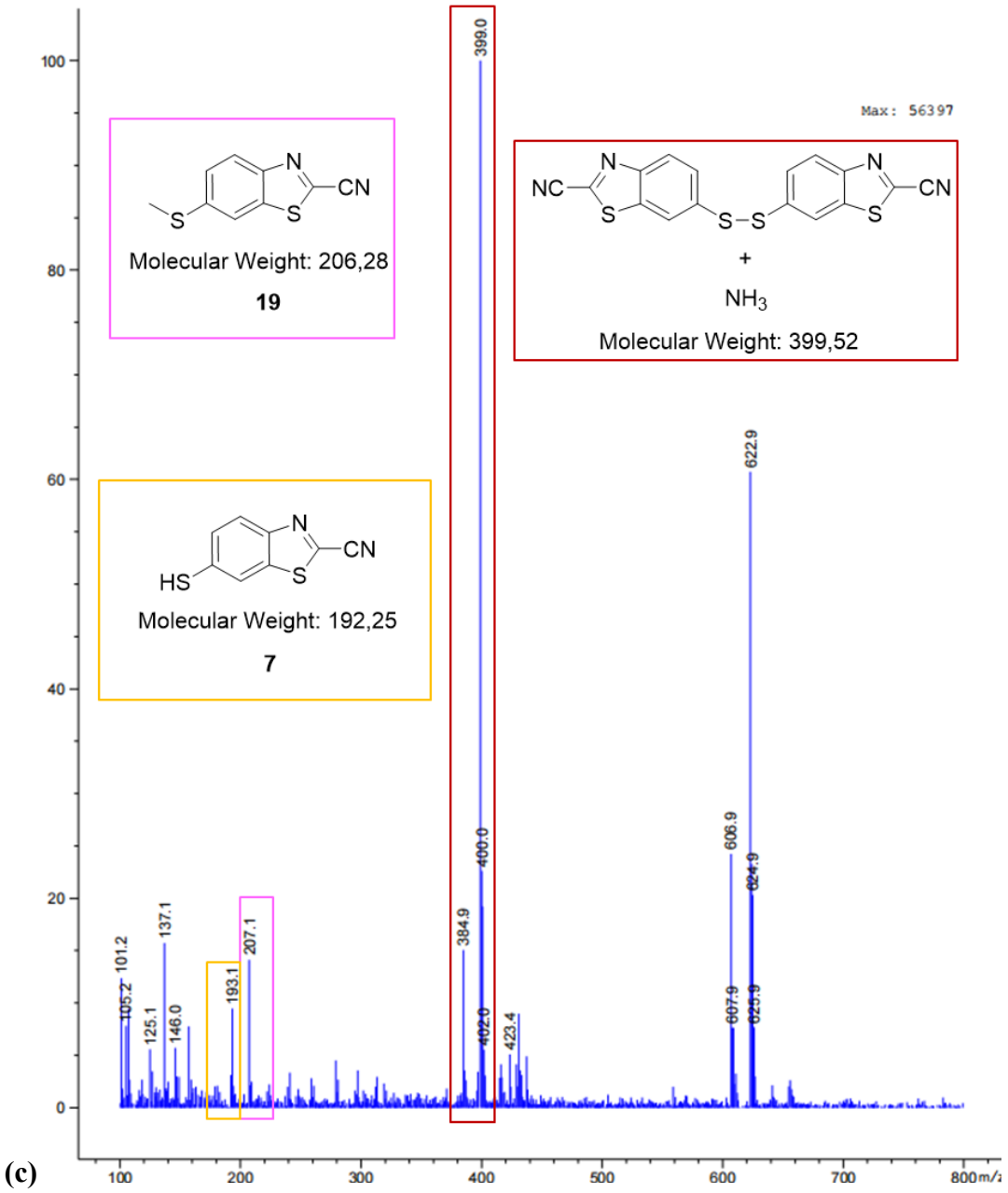

(c)

Figure 3.13. (a) LC spectrum of the isolated material at 290 nm. **(b)** TIC spectrum. **(c)** MS spectrum of the isolated material with the peak of interest highlighted in orange.

Despite the challenges presented in this reaction, benzothiazoles **19** and **21** were reacted with D-cysteine to form the respective luciferin analogues **20** and **22** (Scheme **3.9**). All these steps were moderate to high yielding, with a significant increase in the overall yield of benzothiazoles **19** and **20** and their luciferin analogues **20** and **22**, compared to the literature values.[2] Furthermore, implementing McCutcheon's method of thermolysis[13] aided facile ring closure and condensed the synthetic route to one step from the starting material 4-(methylthio)aniline to benzothiazole **19**.

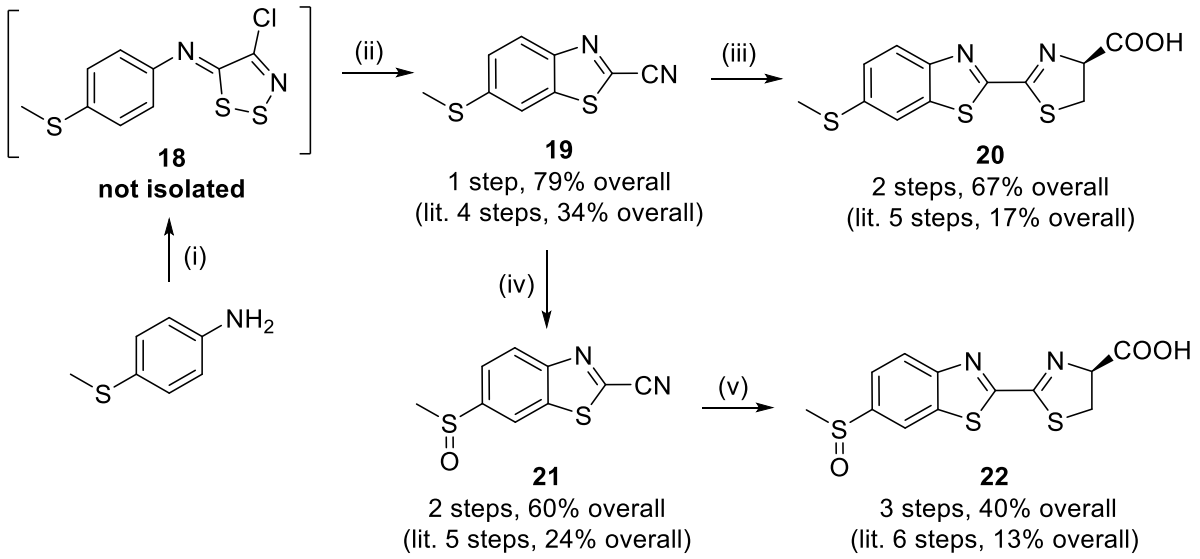

Scheme 3.9. Condensed synthetic route to methylthio-substituted benzothiazoles and luciferins. Reagents and conditions: (i) Appel's salt, DCM, anhydrous pyridine, rt, 3 h, (ii) Sulfolane, 180 °C, 30 min (70%), (iii) D-Cys, K_2CO_3, MeOH:H_2O, rt, 30 min (85%), (iv) *m*-CPBA, DCM, rt, 12 h (75%), (v) D-Cys, K_2CO_3, MeOH:H_2O, rt, 30 min (50%).

3.4 Conclusion

From the Pirrung method; six intermediates in the synthetic sequence for D-thioluciferin were successfully synthesised and characterised via different spectroscopic techniques. ^{1}H NMR and LCMS analyses indicated that transformation of sulfoxide **6** produced intermediates on route to the target product **7**, which was confirmed by an NMR kinetic study. The rearrangement of **6.1** is reversible and is the rate limiting step, followed by phosphite mediated reduction. Despite increasing the reaction time and subjecting the material to multiple rounds of purification, the triphenylphosphite breakdown products continued to coelute with thiol **7**. It is thought that subsequent aqueous hydrolysis may also require a longer reaction time for optimisation or more aggressive basic breakdown. However, in the interest of time this route was also abandoned.

From the Sharma method; four intermediates on route to D-thioluciferin were successfully synthesised and characterised. Using commercially available 4-(methylthio)aniline as a starting material and elevated temperature to facilitate ring closure allowed the synthetic route to be condensed by three steps with an increase in the overall yield of compounds **19**, **20**, **21** and **22**. Unfortunately, the Pummerer rearrangement of sulfoxide **21** into thiol **7** was unsuccessful as a one-pot method. The analytical data strongly suggests that this reaction needs to be performed in two steps rather than the one pot method. In such a case the sulphonium intermediate would be purified and characterised before subjecting it to nucleophilic attack with methanol and

triethyl amine. Alternatively, the reaction could proceed as a one-pot method to yield the disulphide intermediate. Subsequent reduction with a reducing agent such as dithiothreitol (DTT) may yield the free thiol **7**.

Due to the interesting change in fluorescence properties of benzothiazoles **19** and **21** and luciferins **20** and **22**, all four compounds were subjected to UV, fluorescence, bioluminescence and cell viability assays which will be discussed in **Chapter 5**.

3.5 References

(1) Rylands, M.; Jardine, A. Synthesis and evaluation of D-thioluciferin, a bioluminescent 6'-thio analog of D-luciferin. *ARKIVOC* **2021**, *2020* (5), 176-189.

(2) Sharma, D. K.; Adams, S. T., Jr.; Liebmann, K. L.; Miller, S. C. Rapid Access to a Broad Range of 6'-Substituted Firefly Luciferin Analogues Reveals Surprising Emitters and Inhibitors. *Org Lett* **2017**, *19* (21), 5836-5839.

(3) Rayner, D. R.; Miller, E. G.; Bickart, P.; Gordon, A. J.; Mislow, K. Mechanisms of Thermal Racemization of Sulfoxides1. *Journal of the American Chemical Society* **1966**, *88* (13), 3138-3139.

(4) Evans, D. A.; Andrews, G. C. Allylic sulfoxides. Useful intermediates in organic synthesis. *Accounts of Chemical Research* **1974**, *7* (5), 147-155.

(5) Pirrung, M. C.; Carlson, A. D.; De Howitt, N.; Liao, J. Synthesis and bioluminescence of thioluciferin. *Bioorg Med Chem Lett* **2019**, *29* (19), 126591.

(6) Soria, S.; Peñéñory, A. Efficient Cu-catalyzed base-free C-S coupling under conventional and microwave heating. A simple access to S-heterocycles and sulfides. *Beilstein journal of organic chemistry* **2013**, *9*, 467-475.

(7) Pummerer, R. Über Phenylsulfoxy-essigsäure. (II.). *Berichte der deutschen chemischen Gesellschaft* **1910**, *43* (2), 1401-1412.

(8) Findlay, J. B.; Fishwick, C. W.; Kersey, I. D.; Ward, P. Neighbouring group participation in Pummerer-type rearrangements of ortho-substituted arylmethyl sulphoxides. *Tetrahedron letters* **1995**, *36* (13), 2299-2302.

(9) Solladié, G.; Wilb, N.; Bauder, C. Highly stereoselective synthesis of enantiomerically pure β-hydroxy-γ-sulfenyl-γ-butyrolactone by asymmetric Pummerer type cyclization. *Tetrahedron Letters* **2000**, *41* (21), 4189-4192.

(10) Wyatt, P.; Hudson, A. Two routes to (11,12)-dihydrodibenzo[c,g][1,2]dithiocine. *Org Biomol Chem* **2004**, *2* (10), 1528-1530.

(11) Xing, H.; Chen, L.; Jia, Y.; Jiang, Z.; Yang, Z. Fe2O3-catalyzed Pummerer rearrangement of acyl chlorides and sulfoxides: Facile synthesis of alkylthiomethyl ester. *Tetrahedron Letters* **2017**, *58* (23), 2199-2202.

(12) McCutcheon, D. C.; Paley, M. A.; Steinhardt, R. C.; Prescher, J. A. Expedient Synthesis of Electronically Modified Luciferins for Bioluminescence Imaging. *Journal of the American Chemical Society* **2012**, *134* (18), 7604-7607.

(13) McCutcheon, D. C.; Porterfield, W. B.; Prescher, J. A. Rapid and scalable assembly of firefly luciferase substrates. *Org Biomol Chem* **2015**, *13* (7), 2117-2121.

(14) Jackson, K. MSc thesis, unpublished. University of Cape Town, 2020.

(15) Isabel, E.; Black, W. C.; Bayly, C. I.; Grimm, E. L.; Janes, M. K.; McKay, D. J.; Nicholson, D. W.; Rasper, D. M.; Renaud, J.; Roy, S.; et al. Nicotinyl aspartyl ketones as inhibitors of caspase-3. *Bioorg Med Chem Lett* **2003**, *13* (13), 2137-2140.

Chapter 4 : Synthesis of Aza-luciferin analogues

4.1 Literature Overview

4.1.1 General synthetic strategies towards pyridone aza-luciferin analogues

As discussed in Chapter 1, luciferin is the natural substrate of luciferase, the enzyme responsible for the bioluminescence in organisms like fireflies.[1-4] Aza-luciferin analogues are synthetic derivatives of luciferin in which one or more carbon atoms in the heterocyclic ring are replaced by nitrogen atoms. These derivatives possess some interesting properties which are of interest in the biological sense.[5, 6] In 2018 Zhang *et al.* developed new pyridone-based luciferins and evaluated their compatibility with native and mutant firefly luciferases (Fluc).[7] These two regioisometric pyridine luciferins are structurally similar to D-luciferin but incorporate a pyridone core (Figure **4.1**).

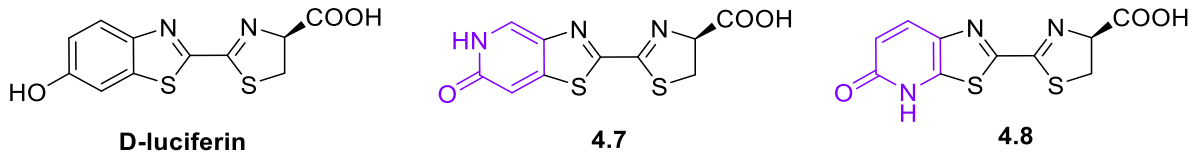

Figure 4.1. D-luciferin and luciferin analogues **4.7** and **4.8**, possessing pyridone moieties (purple).[7]

Computational DFT analysis performed by the authors showed expected emission shifts due to differences in HOMO-LUMO energy gaps between pyridone and hydroxypyridine tautomers (Figure **4.2**). The study proposed that light emission arises from excited-state tautomerisation, leading to distinct spectral properties. The authors thus hypothesised that the pyridine core could improve chemical stability and modulate light emission.

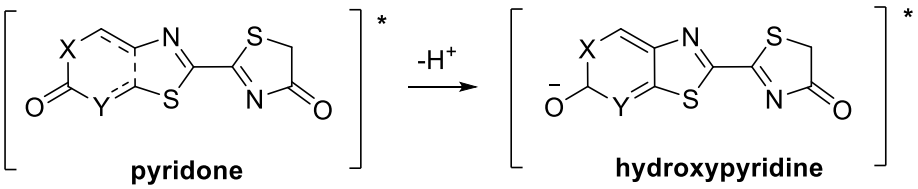

Figure 4.2. Pyridone and hydroxypyridine tautomers.[7]

Pyridone luciferins **4.7** and **4.8** were thus synthesised from a common precursor using a robust previously developed chemical route.[8, 9] As in the previous methods, this method also relied on the dithiazolium reagent, Appel's salt,[10] to access the annulated thiazole of the luciferin core.

Aniline **4.1** was first condensed with Appel's salt and the resulting dithiazole **4.2** was subsequently fragmented[11] using sodium thiosulphate to access cyanothioformamide **4.3**. Oxidative cyclisation of **4.3** with a palladium catalyst[12] provided intermediates **4.4a** and **4.4b**. These regioisomers were separated by flash column chromatography. The methyl protecting groups of the cyclised isomers were then removed by subjecting them to pyridine hydrochloride at elevated temperatures. Some undesired *N*-methylation byproducts were readily separated from the desired cyanobenzothiazoles upon treatment with acetic anhydride and subsequent chromatography. Finally, condensation of **4.5** and **4.6** with D-cysteine afforded luciferins **4.7** and **4.8** in an overall yield of 14% and 2% respectively (Scheme **4.1**).

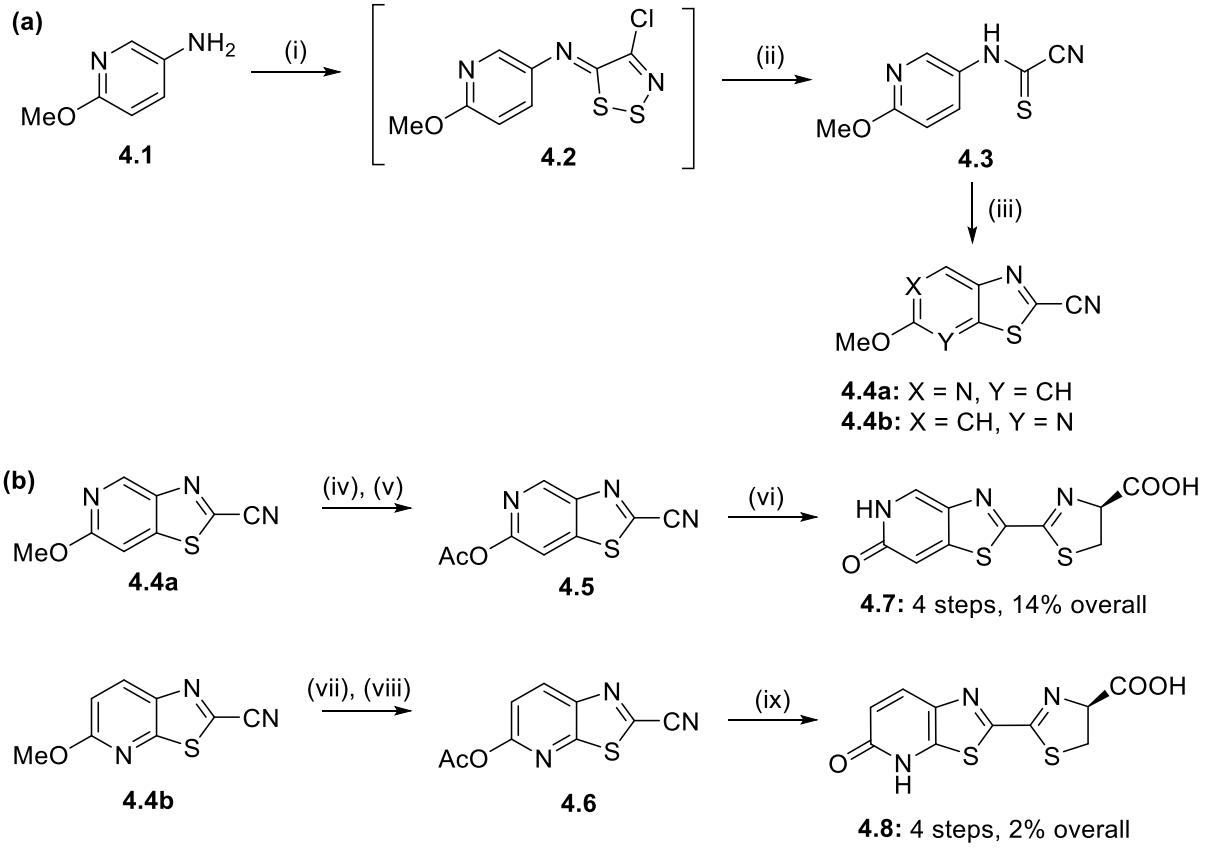

Scheme 4.1. Synthesis of pyridone luciferins.[7] **(a)** Formation of the thiazolo-pyridyl core. Reagents and conditions: (i) THF, pyr (2 eq), rt, 19 h, (ii) $Na_2S_2O_3$ (2 eq), H_2O, RT, 4.5 h, (71%), (iii) $PdCl_2$ (20 mol %), CuI (50 mol %), $(nBu)_4NBr$ (2 eq), DMF:DMSO (1:1), 120 °C, 1 h, (**4.4a** = 44% and **4.4b** = 9%). **(b)** Condensations with D-cysteine provided the desired analogues. Reagents and conditions: (iv) pyr·HCl (10 eq), 160 °C, 15 min, (v) DMAP (20 mol %), Ac_2O (10 eq), pyr (20 eq), rt, 1 h, (77%), (vi) K_2CO_3 (2 eq), MeCN:H_2O (6:1), rt, 1.5 h, (62%), (vii) pyr·HCl (10 eq), 160 °C, 30 min, (viii) DMAP (20 mol %), Ac_2O (10 eq), pyr (20 eq), rt, 1 h, (73%), (ix) K_2CO_3 (2 eq), MeCN:H_2O (2:1), rt, 10 min (53%).

From the study it was found that compounds **4.7** and **4.8** emitted light at 570 nm and 530 nm respectively. The emissions were distinct and resolvable, supporting potential for dual-colour

imaging.[13-15] Both luciferins were cell-permeable and functional in HEK293 cells expressing Fluc. However, their photon output was lower than native D-luciferin, about 1-3% in vitro and 3-20% in cells.[16] Further screening of 166 Fluc mutants led to the discovery of two mutants that significantly boosted light output. These mutants restored light emission levels to those seen with native Fluc/D-luciferin pairs in cells (up to 80x for compound **4.8**).

This combination of engineered luciferins and mutant luciferases expands the bioluminescent imaging toolkit. These new tools can be used for multi-component, spectrally resolved imaging,[17, 18] potentially enabling more complex in vivo experiments.

4.1.2 General synthetic approaches towards heteroarenethiazoles

To expand the synthesis of aza-luciferin analogues, the synthesis of heteroazine fused thiazoles (heteroarenothiazoles) needed to be investigated. Unlike benzothiazoles[19-23] which contain a bicyclic ring system, synthetic routes to heteroarenothiazoles are less well developed.[20, 21] This being despite the fact that these and related compounds have displayed interesting biological activity including anticoagulant behaviour.[24, 25]

The thermolysis of [(4-chloro-5H-1,2,3-dithiazol-5-ylidene)-amino]arenes **4.9** primarily yields arene-fused thiazole-2-carbonitriles, with benzothiazole-2-carbonitriles **4.10** being the main products (Scheme **4.2**). These reactions also generate elemental sulfur (S_8), and when the aniline substituent is electron-deficient, arylcarbonocyanidimidic chlorides **4.11** are formed as well. A mechanistic explanation for the formation of both products has been proposed by Rees.[26, 27]

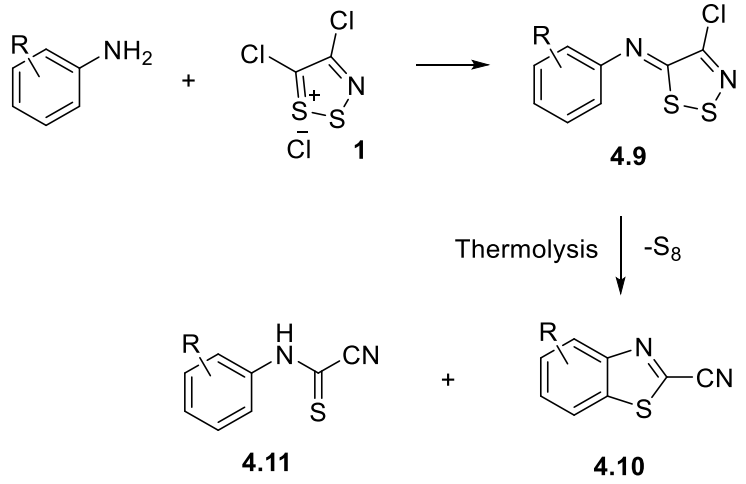

Scheme 4.2. Thermolysis of dithiazoles to give arene-fused carbonitriles.

Drawing on the precedent of benzothiazole-2-carbonitrile **4.10** formation (Scheme **4.2**), Koutentis and colleagues hypothesised that thermolysis of their previously synthesized [(4-chloro-5H-1,2,3-dithiazol-5-ylidene)amino]azines[28] could offer a facile route to azine-fused thiazole-2-carbonitriles.[29]

Initial efforts by the authors employed thermolysis of *N*-(4-chloro-5H-1,2,3-dithiazol-5-ylidene)pyridin-n-amines. This yielded the desired thiazolopyridine-2-carbonitriles, but in low to moderate yields, alongside by-products like elemental sulphur. A more efficient transformation was developed using a thiophile-mediated ANRORC (Addition of Nucleophile, Ring Opening, and Ring Closure) mechanism (Scheme **4.3**).[30] Benzyltriethylammonium iodide (BnEt3NI) was used to catalyse the ring transformation. This method produced 14 different azine-fused thiazole-2-carbonitriles in moderate to near-quantitative yields. Further optimisation found that reactions performed in dry, degassed chlorobenzene under an argon atmosphere gave the best results. Similarly, catalytic (5 mol%) amounts of $BnEt_3NI$ were sufficient, although required longer reaction times.

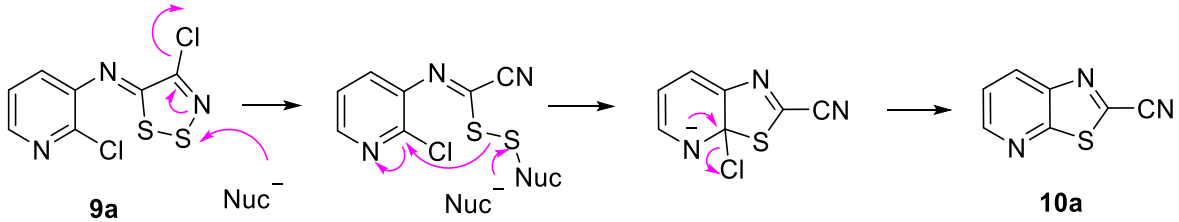

Scheme 4.3. Proposed ANRORC strategy for the synthesis of thiazolo[5,4-b]pyridine-2-carbonitrile **10a**.[29]

Of particular interest was the synthesis of 5-chlorothiazolo[5,4-b]-pyridine-2-carbonitrile **17**. Considering the success in the ANRORC strategy, the authors prepared (*Z*)-2,6-Dichloro-N-(4-chloro-5H-1,2,3-dithiazol-5-ylidene)-pyridin-3-amine **9i** using the standard method for the condensation of Appel salt with 2,6-dichloropyridin-3-amine. The resulting dithiazole **9i** was then treated with the optimized conditions for ring closure and the desired heteroarenothiazole-2-carbonitrile **17** was obtained in moderate yield (40%) along with isothiocyanate **11b** (13%) (Scheme **4.4**). Interestingly, no further application studies were performed on the synthesised compounds by the authors.

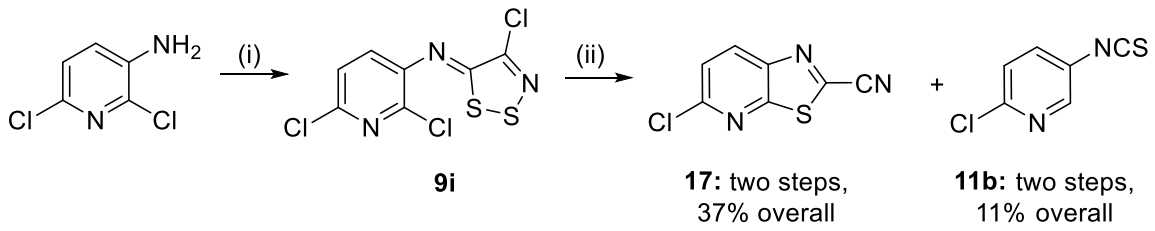

Scheme 4.4. Synthesis of **17**.[29] Reagents and conditions: (i) Appel salt, 2-6 lutidene (2 eq), DCM, rt, 3 h, (85%), (ii) $BnEt_3NI$ (5 mol%), dry PhCl, 132 °C, Ar (g), **17** = 43% and **11b** = 13%.

Overall this method expands the utility of Appel salt in heterocycle synthesis which represents a promising avenue for drug discovery.[31] The study presents a reliable, two-step synthetic route for creating heteroarenothiazole-2-carbonitriles. These compounds are notable for their biological potential[24, 25] and material properties.[32, 33] In addition to tuning light output, these analogues often exhibit improved chemical stability and solubility compared to natural luciferin, enhancing their bioavailability within cells. A further benefit is their selective interaction with engineered luciferases[7]; some aza-luciferins are specifically designed to work only with these tailored enzymes, enabling orthogonal reporter systems in which multiple distinct light signals in a single experiment without signal interference.

4.2 Research rationale and motivation

While there has been considerable successful synthesis and application of numerous luciferin analogs[9, 34, 35], the synthesis and properties of aza-lucfiferin analogues have not fully been exploited. Commercially available starting material, 3-amino-2,6-dichloropyridine was considered ideal to open new directions in the synthesis of a pyridyl benzothiazole intermediate that will allow access to novel aza D-luciferin analogues (Scheme **4.5**). Additionally, the ring closure reaction would be attempted with DBU instead of $BnEt_3NI$ with an aim of improving the overall yield of the ring-closed product **17** and its luciferin derivative **17a**.

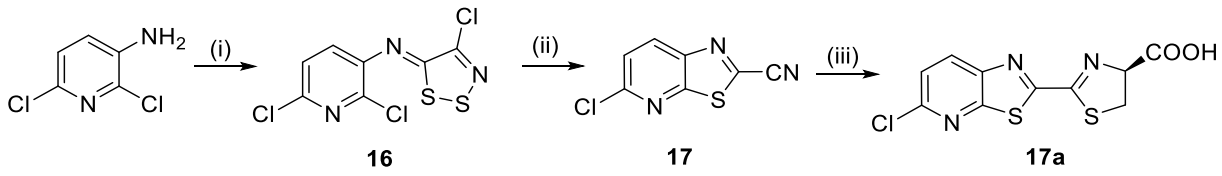

Scheme 4.5. Attempted synthesis of a pyridine-luciferin analogue **17a**. Reagents and conditions: (i) Appel's salt, DCM, anhydrous pyr, rt, 3 h, (ii) CuI (1 eq), anhydrous pyr, 115 °C, 30 min, (iii) D-Cysteine, K_2CO_3, MeOH:H_2O, rt, 30 min.

It was hypothesised that the structural modification of aza-luciferin analogue **17a** would alter the molecule's electronic properties, resulting in a red-shifted emission compared to native D-

luciferin. This is particularly advantageous for deep-tissue imaging in biological systems. Overall, this would open a library of new aza-D-luciferin analogues with functional group diversity at the 6-position (Scheme **4.6**).

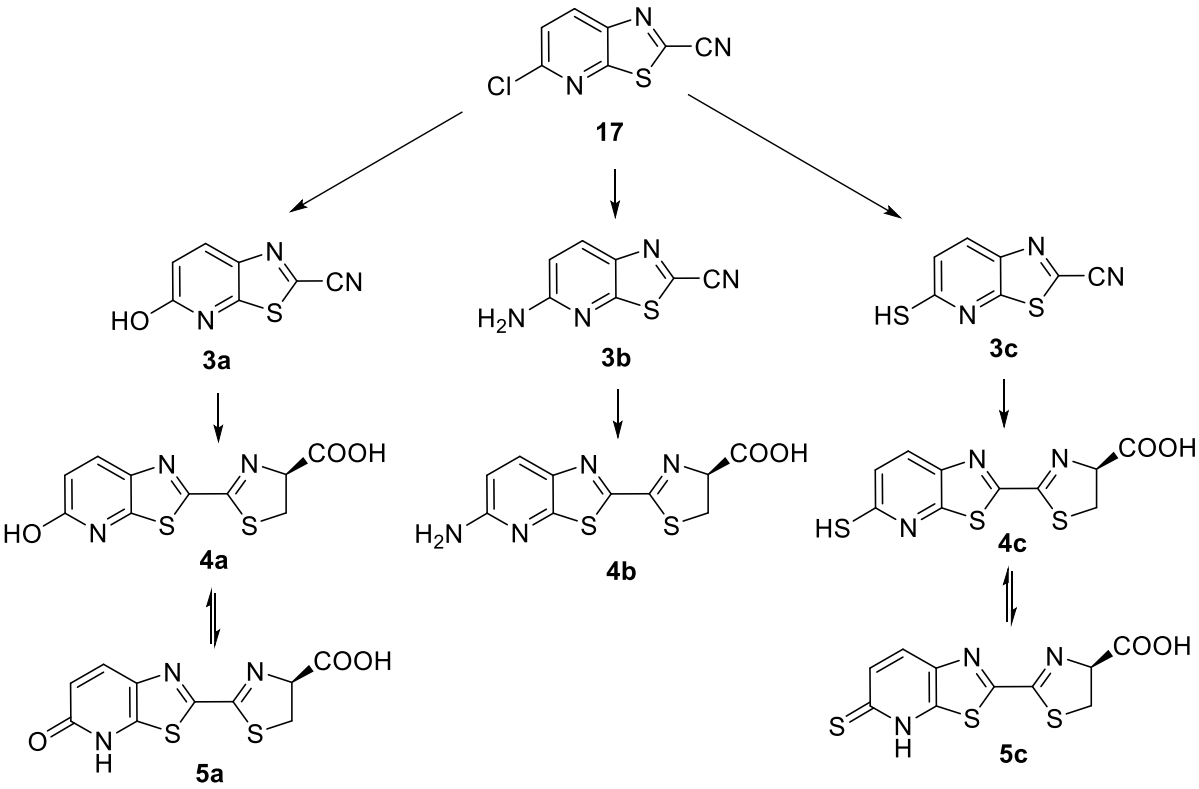

Scheme 4.6. Proposed library of novel aza D-luciferin analogues from **17**.

4.3 Results and Discussion

4.3.1 Synthesis of dithiazole (16)

Commercially available 3-amino-2,6-dichloropyridine was reacted in slight excess of previously synthesised Appel's salt **1** in a solution of DCM at room temperature. After the brown mixture was left to stir for 1 h, two equivalents of anhydrous pyridine were added drop-wise and the resulting mixture was left to stir for another 2 h. This deviates from the published synthesis in which two equivalents of 2,6-lutidene were used.[29] The reaction was then monitored by TLC which showed the complete conversion of pyridine starting material into a new product (R_f = 0.70 with 20% diethyl ether / pet ether). The crude precipitate was purified via normal phase column chromatography on silica gel eluting with pet ether and isolated to afford dithiazole **16** as a bright yellow solid in moderate yield (62%). The reaction forming

dithiazole **16** is thought to proceed via a nucleophilic substitution involving pyridine and Appel's salt **1** (Scheme **4.7**).

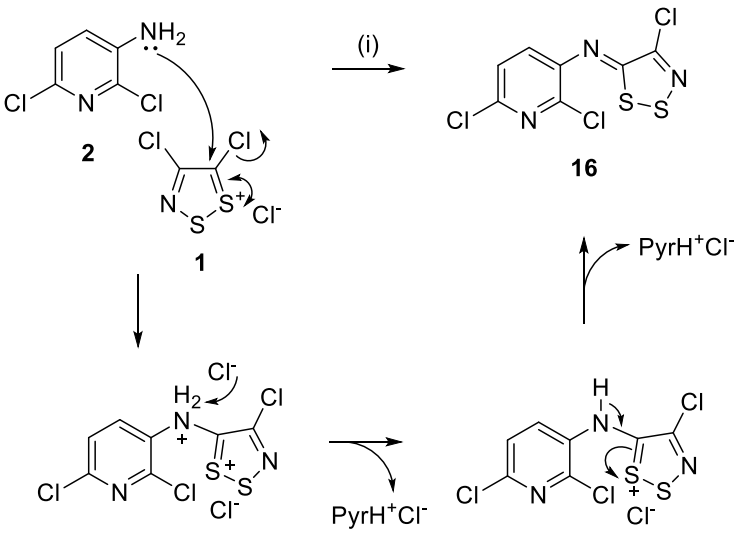

Scheme 4.7. Proposed reaction mechanism for the formation of dithiazole **16**. Reagents and conditions: (i) Appel's salt, DCM, anhydrous pyridine, rt, 3 h (62%).

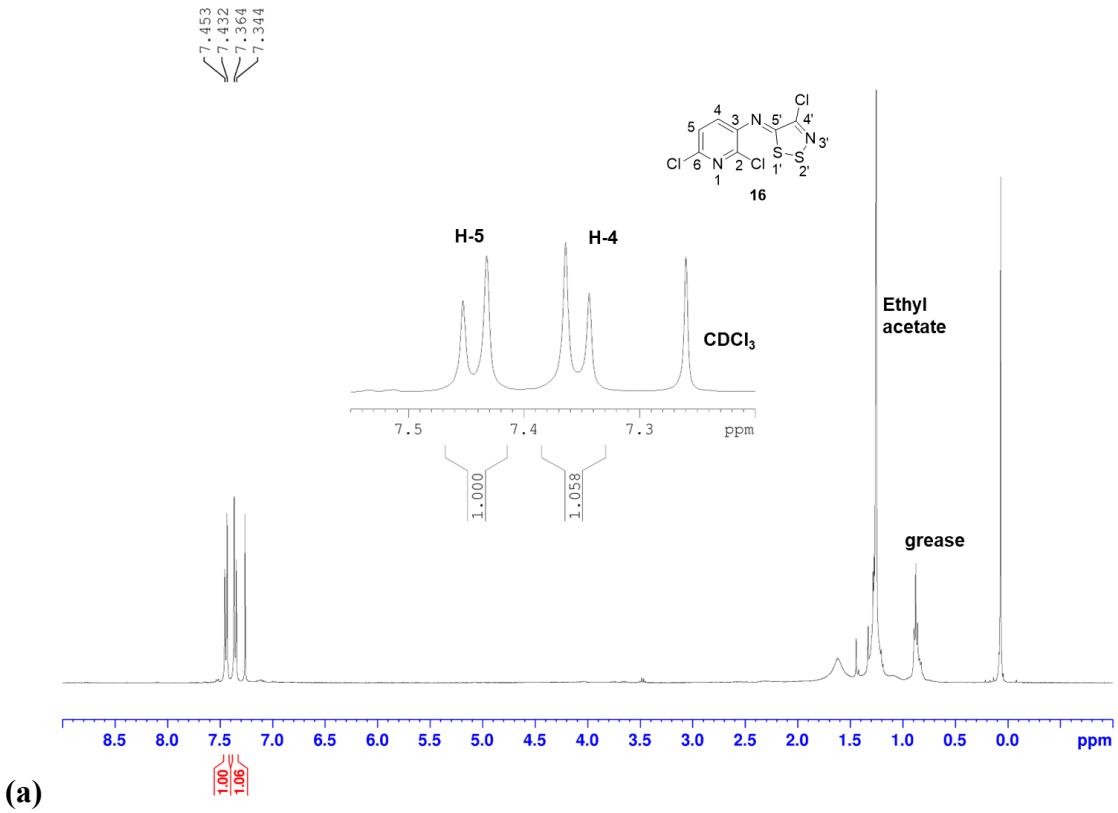

(a)

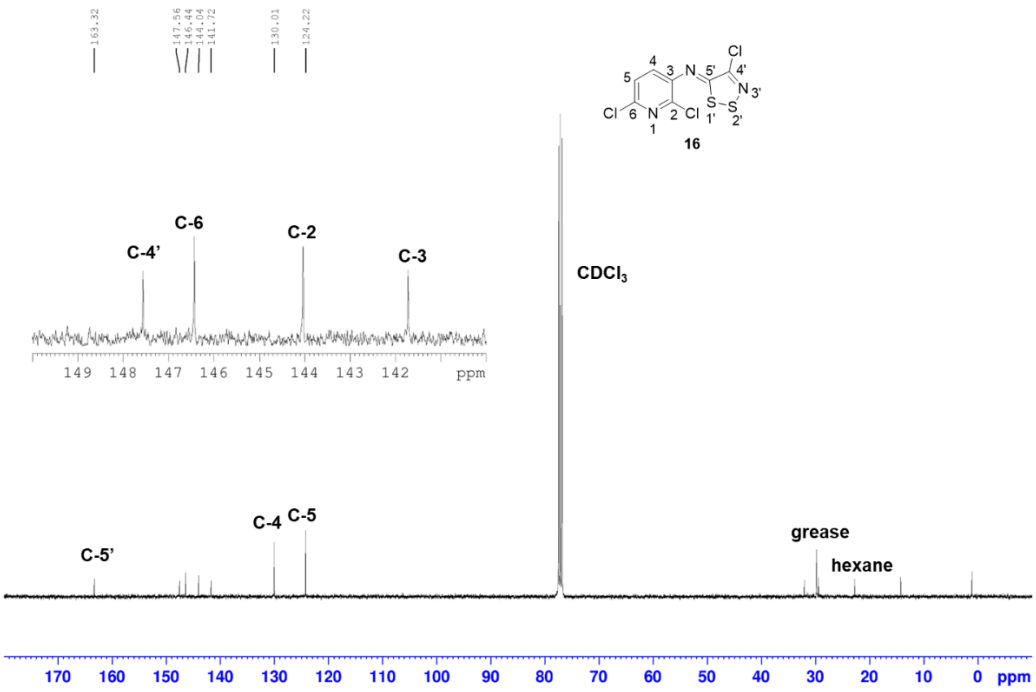

(b)

Figure 4.3. (a) 1H NMR spectrum of **16** in $CDCl_3$. **(b)** 13C NMR spectrum of **16** in $CDCl_3$.

^{1}H NMR analysis of the isolated product confirmed the formation of dithiazole **16**. Two doublets were observed corresponding to the two aromatic protons H-5 (J = 8.1 Hz) and H-4 (J = 8.1 Hz), with H-5 being the most deshielded due to the presence of the ortho chlorine (Figure **4.3a**). ^{13}C NMR was able to further confirm the presence of the product as a total of seven carbon signals were observed, as expected (Figure **4.3b**).

4.3.2 Synthesis of carbonitrile (17)

The ring closure of dithiazole **16** yielded intriguing results. Rather than employing $BnEt_3NI$[29] as a catalyst, it was hypothesised that the reaction could proceed via a DBU-mediated ring closure without the need for a catalyst.[36] As such, a solution of 3-amino-2,6-dichloropyridine and Appel's salt in DCM was cooled to below 5 °C. and one equivalent of DBU was added. After allowing the reaction mixture to stir overnight at room temperature, an additional two equivalents of DBU were added and the reaction mixture was left to heat under reflux in DMSO overnight. The title compound **17** was purified by column chromatography, eluting with hexanes as a colourless solid in low yield (17%). ^{1}H NMR analysis of the isolated material was consistent with that found in literature,[29] revealing two doublets corresponding to H-7 (J = 8.6 Hz) and H-6 (J = 8.6 Hz) respectively (Figure **4.5**). Some side product corresponding to the formation of 2-chloro-5-isothiocyanatopyridine **11b** had coeluted with **17** and was also visible

in the ^{1}H NMR spectrum (7.0 – 7.6 ppm). However, due to the limiting amount of material obtained, no further attempts at purifying the sample were performed.

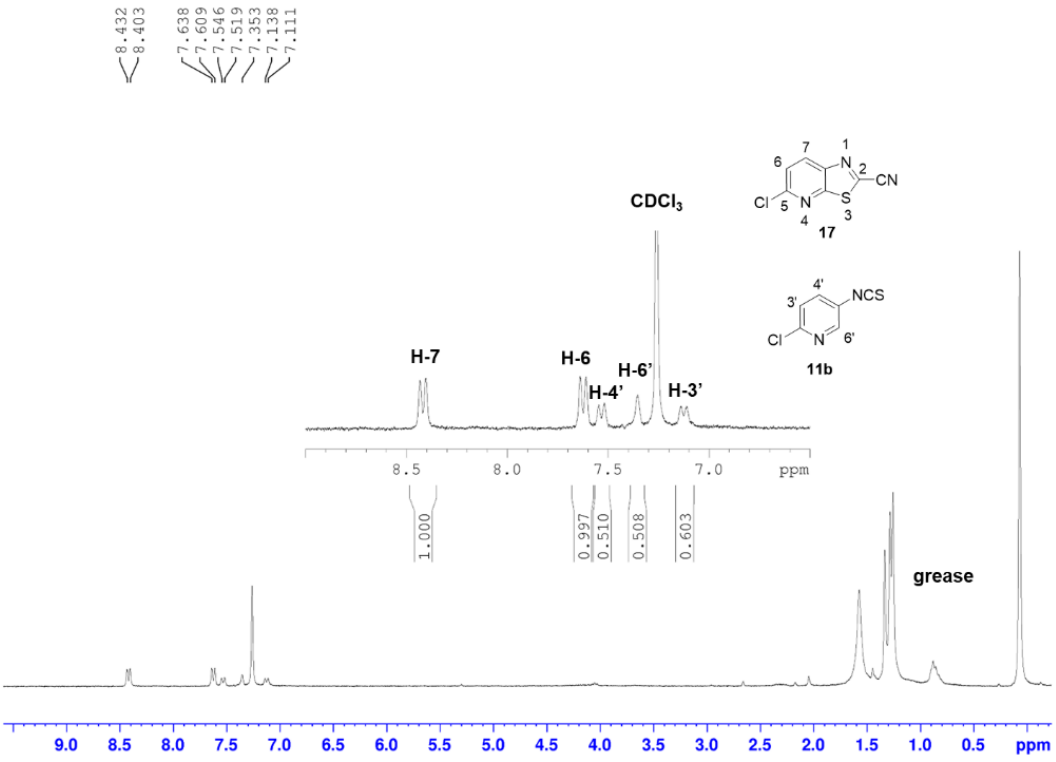

Figure 4.4. ^{1}H NMR spectrum of **17** in $CDCl_3$.

Notably, subsequent attempts to reproduce this reaction did not yield the desired compound. Due to time constraints, a limiting amount of starting material and an absence of $BnEt_3NI$,[29] it was evident that a new method of ring closure had to be employed.

As a last attempt at obtaining the ring closed material, a small-scale reaction was performed. A stirred solution of dithiazole **16** and copper iodide in anhydrous pyridine was heated at 115 °C for 30 min.[37] Surprisingly, TLC analysis of the reaction mixture revealed product formation (R_f = 0.70 in 20% hexane / DCM) and the ring closed product **17** was isolated via column chromatography eluting with hexanes in low yield (24%). The isolated material was promptly submitted for LCMS analysis, which revealed a *m/z* peak at 196.0, closely matching the calculated $[M+H]^+$ value of 195.9731 for $C_7H_2N_3SCl$ (Figure **4.6**).

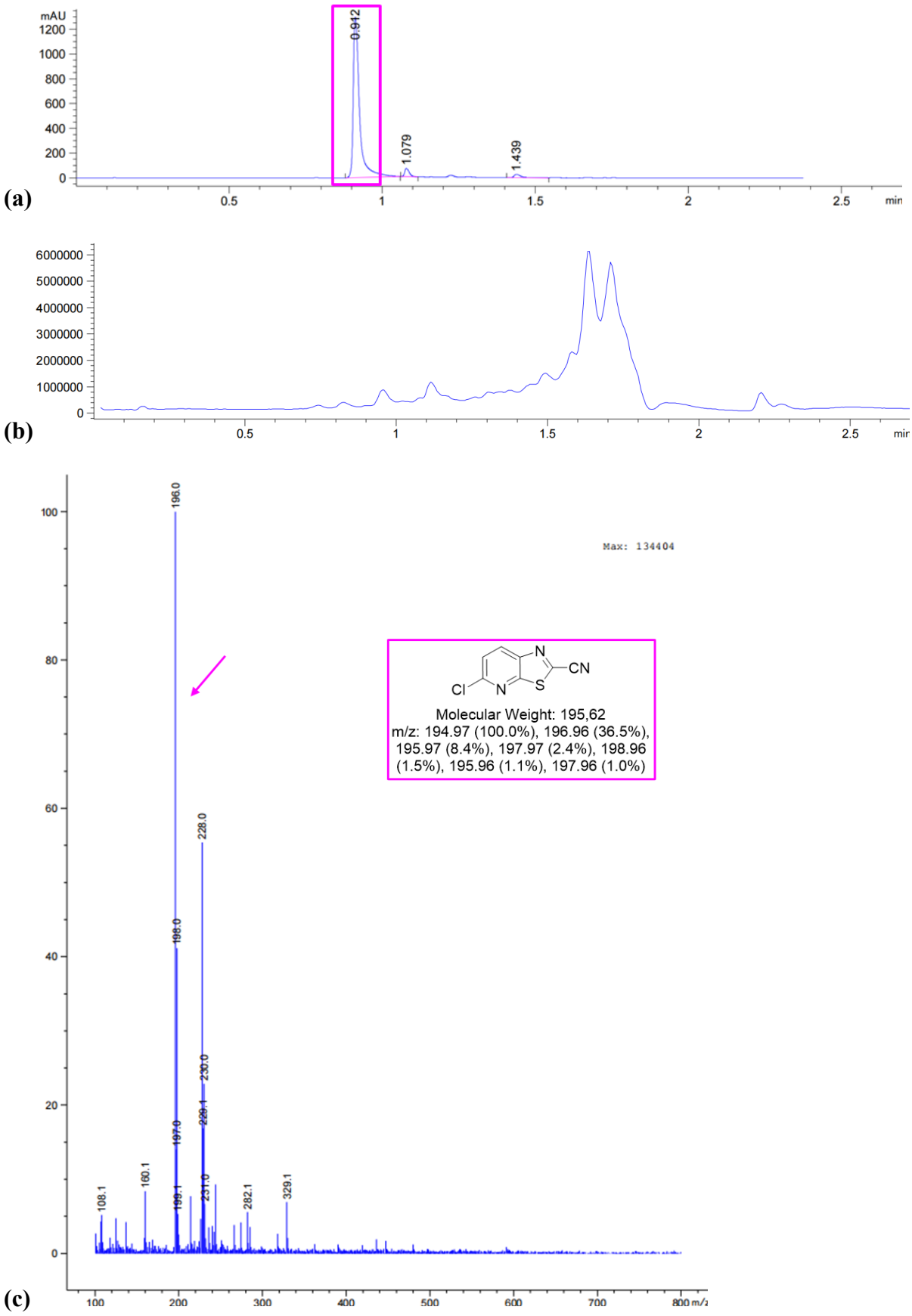

Figure 4.5. LCMS spectrum of **17**. **(a)** LC spectrum of the isolated material at 290 nm. **(b)** TIC spectrum. **(c)** MS spectrum of the isolated material with the peak of interest highlighted in pink.

4.4 Conclusion

Two intermediates in the aza-lucifeirn analogue series were successfully synthesised and characterised. The synthesis of dithiazole **16** was successful, despite deviating from the literature method by using 2 equivalents of anhydrous pyridine instead of 2,6-lutidene. Similarly, the synthesis of heteroarenothiazole **17** proceeded using copper iodide instead of $BnEt_3NI$ (Scheme **4.8**). The ring closed reaction was also successful using three equivalents of DBU, however attempts at repeating the experiment with DBU were unsuccessful. As such, it is proposed that future reactions forming **17** should proceed using copper iodide instead.

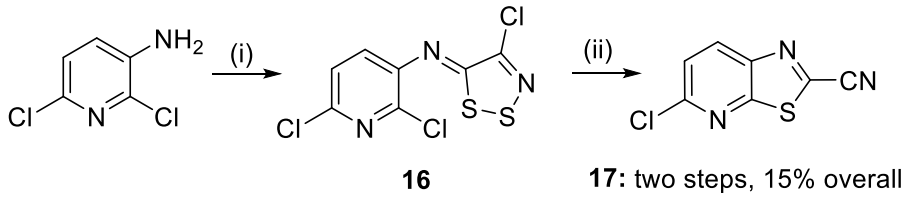

Scheme 4.8. Synthesis of heteroarenothiazole **17**. Reagents and conditions: (i) Appel's salt, DCM, anhydrous pyr, rt, 3 h (62%), (ii) CuI (1 eq), anhydrous pyr, 115 °C, 30 min, (24%).

Due to time constraints and a depletion of the starting material, the upscaling of the successful ring closure method using copper iodide could not be repeated. For the same reasons, reaction optimisation could not be performed to improve the yield of **16** and **17**. However, new directions were opened in the synthesis of a pyridyl intermediate that will allow future generation of aza D-luciferin analogues.

4.5 References

(1) McElroy, W. D. The Energy Source for Bioluminescence in an Isolated System. *Proceedings of the National Academy of Sciences* **1947**, *33* (11), 342-345.

(2) McElroy, W. D. Properties of the Reaction Utilizing Adenosinetriphosphate for Bioluminescence. *Journal of Biological Chemistry* **1951**, *191* (2), 547-557.

(3) Marques, S. M.; Esteves da Silva, J. C. G. Firefly bioluminescence: A mechanistic approach of luciferase catalyzed reactions. *IUBMB Life* **2009**, *61* (1), 6-17.

(4) White, E. H.; Rapaport, E.; Seliger, H. H.; Hopkins, T. A. The chemi- and bioluminescence of firefly luciferin: An efficient chemical production of electronically excited states. *Bioorganic Chemistry* **1971**, *1* (1), 92-122.

(5) Massoud, T. F.; Gambhir, S. S. Molecular imaging in living subjects: seeing fundamental biological processes in a new light. *Genes & development* **2003**, *17* (5), 545-580.

(6) Paley, M. A.; Prescher, J. A. Bioluminescence: a versatile technique for imaging cellular and molecular features. *MedChemComm* **2014**, *5* (3), 255-267.

(7) Zhang, B. S.; Jones, K. A.; McCutcheon, D. C.; Prescher, J. A. Pyridone luciferins and mutant luciferases for bioluminescence imaging. *ChemBioChem* **2018**, *19* (5), 470-477.

(8) McCutcheon, D. C.; Paley, M. A.; Steinhardt, R. C.; Prescher, J. A. Expedient Synthesis of Electronically Modified Luciferins for Bioluminescence Imaging. *Journal of the American Chemical Society* **2012**, *134* (18), 7604-7607. DOI: 10.1021/ja301493d.

(9) McCutcheon, D. C.; Porterfield, W. B.; Prescher, J. A. Rapid and scalable assembly of firefly luciferase substrates. *Org Biomol Chem* **2015**, *13* (7), 2117-2121.

(10) Appel, R.; Janssen, H.; Siray, M.; Knoch, F. Synthese und Reaktionen des 4,5-Dichlor-1,2,3-dithiazolium-chlorids. *Chemische Berichte* **1985**, *118* (4), 1632-1643.

(11) Michaelidou, S. S.; Koutentis, P. A. The synthesis of 2-cyano-cyanothioformanilides from 2-(4-chloro-5H-1, 2, 3-dithiazol-5-ylideneamino) benzonitriles using DBU. *Synthesis* **2009**, *2009* (24), 4167-4174.

(12) Inamoto, K.; Hasegawa, C.; Hiroya, K.; Doi, T. Palladium-catalyzed synthesis of 2-substituted benzothiazoles via a C− H functionalization/intramolecular C− S bond formation process. *Organic Letters* **2008**, *10* (22), 5147-5150.

(13) Mofford, D. M.; Reddy, G. R.; Miller, S. C. Aminoluciferins extend firefly luciferase bioluminescence into the near-infrared and can be preferred substrates over D-luciferin. *Journal of the American Chemical Society* **2014**, *136* (38), 13277-13282.

(14) Jones, K. A.; Porterfield, W. B.; Rathbun, C. M.; McCutcheon, D. C.; Paley, M. A.; Prescher, J. A. Orthogonal luciferase–luciferin pairs for bioluminescence imaging. *Journal of the American Chemical Society* **2017**, *139* (6), 2351-2358.

(15) Rathbun, C. M.; Porterfield, W. B.; Jones, K. A.; Sagoe, M. J.; Reyes, M. R.; Hua, C. T.; Prescher, J. A. Parallel screening for rapid identification of orthogonal bioluminescent tools. *ACS central science* **2017**, *3* (12), 1254-1261.

(16) Branchini, B. R.; Murtiashaw, M. H.; Magyar, R. A.; Portier, N. C.; Ruggiero, M. C.; Stroh, J. G. Yellow-green and red firefly bioluminescence from 5, 5-dimethyloxyluciferin. *Journal of the American Chemical Society* **2002**, *124* (10), 2112-2113.

(17) Mezzanotte, L.; Que, I.; Kaijzel, E.; Branchini, B.; Roda, A.; Löwik, C. Sensitive dual color in vivo bioluminescence imaging using a new red codon optimized firefly luciferase and a green click beetle luciferase. *PloS one* **2011**, *6* (4), e19277.

(18) Gammon, S. T.; Leevy, W. M.; Gross, S.; Gokel, G. W.; Piwnica-Worms, D. Spectral unmixing of multicolored bioluminescence emitted from heterogeneous biological sources. *Analytical chemistry* **2006**, *78* (5), 1520-1527.

(19) Facchinetti, V.; da R Reis, R.; RB Gomes, C.; RA Vasconcelos, T. Chemistry and biological activities of 1, 3-benzothiazoles. *Mini-Reviews in Organic Chemistry* **2012**, *9* (1), 44-53.

(20) Koutentis, P. A.; Koyioni, M.; Michaelidou, S. S. The conversion of [(4-chloro-5 H-1, 2, 3-dithiazol-5-ylidene) amino] azines into azine fused thiazole-2-carbonitriles. *Organic & Biomolecular Chemistry* **2013**, *11* (4), 621-629.

(21) Katritzky, A. R.; Ramsden, C. A.; Scriven, E. F.; Taylor, R. J. Comprehensive heterocyclic chemistry III. In *V1 3-memb. Heterocycl., together with all Fused Syst. contain. a 3-memb. Heterocycl. Ring. V2 4-memb. Heterocycl. together with all Fused Syst. contain. a 4-memb. Heterocycl. Ring. V3 Five-memb. Rings with One Heteroat. together with their Benzo and other Carbocycl.-fused Deriv. V4 Five-memb. Rings with Two Heteroat., each with their Fused Carbocycl. Deriv.*, Elsevier, 2008; pp 1-13718.

(22) Gupta, A.; Rawat, S. Synthesis and cyclization of benzothiazole. *J Curr Pharm Res* **2010**, *3*, 13-23.

(23) Koyioni, M.; Manoli, M.; Manolis, M. J.; Koutentis, P. A. Reinvestigating the Reaction of 1 H-Pyrazol-5-amines with 4, 5-Dichloro-1, 2, 3-dithiazolium Chloride: A Route to Pyrazolo [3, 4-c] isothiazoles and Pyrazolo [3, 4-d] thiazoles. *The Journal of Organic Chemistry* **2014**, *79* (9), 4025-4037.

(24) Komoriya, S.; Kobayashi, S.; Osanai, K.; Yoshino, T.; Nagata, T.; Haginoya, N.; Nakamoto, Y.; Mochizuki, A.; Nagahara, T.; Suzuki, M. Design, synthesis, and biological activity of novel factor Xa inhibitors: Improving metabolic stability by S1 and S4 ligand modification. *Bioorganic & medicinal chemistry* **2006**, *14* (5), 1309-1330.

(25) Haginoya, N.; Kobayashi, S.; Komoriya, S.; Yoshino, T.; Nagata, T.; Hirokawa, Y.; Nagahara, T. Design, synthesis, and biological activity of non-amidine factor Xa inhibitors containing pyridine N-oxide and 2-carbamoylthiazole units. *Bioorganic & medicinal chemistry* **2004**, *12* (21), 5579-5586.

(26) Rees, C. W. Polysulfur-nitrogen heterocyclic chemistry. *Journal of heterocyclic chemistry* **1992**, *29* (3), 639-651.

(27) Besson, T.; Rees, C. W. Some chemistry of 4, 5-dichloro-1, 2, 3-dithiazolium chloride and its derivatives. *Journal of the Chemical Society, Perkin Transactions 1* **1995**, (13), 1659-1662.

(28) Koutentis, P. A.; Koyioni, M.; Michaelidou, S. S. Synthesis of [(4-Chloro-5 H-1, 2, 3-dithiazol-5-ylidene) amino] azines. *Molecules* **2011**, *16* (11), 8992-9002.

(29) Koutentis, P. A.; Koyioni, M.; Michaelidou, S. S. The conversion of [(4-chloro-5H-1,2,3-dithiazol-5-ylidene)amino]azines into azine fused thiazole-2-carbonitriles. *Organic & Biomolecular Chemistry* **2013**, *11* (4), 621-629, 10.1039/C2OB26993G.

(30) Van Der Plas, H. C.; Woźniak, M.; Van Den Haak, H. J. Reactivity of naphthyridines toward nitrogen nucleophiles. In *Advances in Heterocyclic Chemistry*, Vol. 33; Elsevier, 1983; pp 95-146.

(31) Kalogirou, A. S.; Oh, H. J.; Asquith, C. R. The Synthesis and Biological Applications of the 1, 2, 3-Dithiazole Scaffold. *Molecules* **2023**, *28* (7), 3193.

(32) Barclay, T. M.; Cordes, A. W.; Beer, L.; Oakley, R. T.; Preuss, K. E.; Taylor, N. J.; Reed, R. W. Sterically protected 1, 2, 3-dithiazolyl radicals: preparation and structural characterization of 4-chloro-5-pentafluorophenyl-1, 2, 3-dithiazolyl. *Chemical Communications* **1999**, (6), 531-532.

(33) Beer, L.; Cordes, A. W.; Haddon, R. C.; Itkis, M. E.; Oakley, R. T.; Reed, R. W.; Robertson, C. M. A π-stacked 1, 2, 3-dithiazolyl radical. Preparation and solid state characterization of (Cl 2 C 3 NS)(ClC 2 NS 2). *Chemical Communications* **2002**, (17), 1872-1873.

(34) Meroni, G.; Rajabi, M.; Santaniello, E. D-Luciferin, derivatives and analogues: synthesis and in vitro/in vivo luciferase-catalyzed bioluminescent activity. *ARKIVOC: Online Journal of Organic Chemistry* **2009**.

(35) Sharma, D. K.; Adams, S. T., Jr.; Liebmann, K. L.; Miller, S. C. Rapid Access to a Broad Range of 6'-Substituted Firefly Luciferin Analogues Reveals Surprising Emitters and Inhibitors. *Org Lett* **2017**, *19* (21), 5836-5839.

(36) Rylands, M. PhD thesis, unpublished. University of Cape Town, **2018**.

(37) Deau, E.; Dubouilh-Benard, C.; Levacher, V.; Besson, T. Microwave-assisted synthesis of novel N-(4-phenylthiazol-2-yl)-benzo[d]thiazole-, thiazolo[4,5-b]pyridine-, thiazolo[5,4-b]pyridine- and benzo[d]oxazole-2-carboximidamides inspired by marine topsentines and nortopsentines. *Tetrahedron* **2014**, *70* (35), 5532-5540.

Chapter 5 : Evaluation of luciferins as probes for anticancer drug discovery

5.1 Literature Overview

Bioluminescence is a chemical reaction within a living organism that creates light, while fluorescence involves a molecule absorbing light and re-emitting it at a different wavelength. Bioluminescence relies on chemical energy within the organism while fluorescence requires an external light source to excite the molecule. Considering the facile click reaction between cysteines and benzothiazoles, it is prudent to investigate and exploit both properties in vivo where possible.

5.1.1 Fluorescent properties of benzothiazoles

In recent years, fluorescence imaging technology has emerged as one of the most effective tools for detecting and visualising biological molecules in living cells, due to its excellent temporal and spatial resolution, high sensitivity, and non-destructive nature.[1-5] However, despite these advancements, most probes that have been developed contain defects such as short emission wavelength, small Stokes shift (<100 nm), complicated probe synthesis and are susceptible to interference by biomolecules.[6-8]

Benzothiazoles are a class of chemical compounds which possess a strong electron-withdrawing property. This characteristic arises from the electron-deficient nature of the benzothiazole ring, created by the presence of the nitrogen and sulphur atoms. As a result, benzothiazoles serve as excellent electron acceptors, particularly in donor–acceptor systems. This facilitates intramolecular charge transfer (ICT), which plays a crucial role in enhancing fluorescence and producing large Stokes shifts.[9-13] Due to these advantageous chemical properties, benzothiazoles are often used as fluorescent probes.[14-16] In a previous study, Hrobárik *et al*. presented the design and synthesis of a series of triphenylamine-based chromophores incorporating benzothiazole units arranged in either a matched (reverse polarity) or mismatched fashion (Figure **5.1**).[17] This was done to systematically study their impact on linear and nonlinear optical properties, especially two-photon absorption (TPA). By tuning the electron-withdrawing strength through additional substituents at the C2 and C6 positions of the benzothiazole ring, the authors demonstrated that “matched” configurations significantly enhance TPA cross-sections, shift absorption/emission to longer wavelengths, and increase charge-transfer efficiency. These findings presented the “matched” setup as a powerful strategy

for developing efficient nonlinear optical (NLO)-active chromophores for applications like two-photon microscopy and optical imaging.

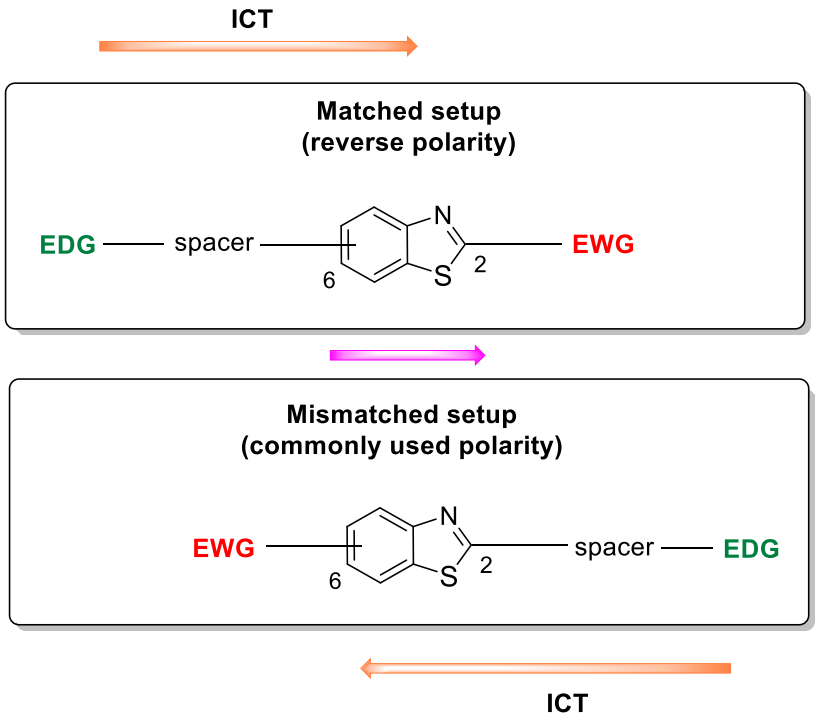

Figure 5.1. Structure of benzothiazoles with matched and mismatched alignment with respect to electron-donating (EDG) and electron withdrawing (EWG) groups.[17]

Benzothiazoles are chemically and photophysically stable, meaning they do not degrade easily under light exposure. This is crucial for applications like real-time imaging or long-term tracking in biological systems. An example of this is their bright and colourful emission. Benzothiazole derivatives can emit light in the blue to red wavelength range (450 to 750 nm). They often display high fluorescence quantum yields, making them bright and easy to detect at low concentrations.[16, 18]

Some applications of benzothiazole based fluorescent probes include fluorescent sensors for metal ions or pH,[14, 18, 19] bioimaging agents in cancer research, theranostic probes and two-photon fluorescent dyes for deep tissue imaging.[17, 20, 21]

5.1.2 Use of benzothiazoles as probes in anticancer research

Benzothiazoles are often used in cancer research due to their excellent bioavailability and cell membrane permeability. Their strong fluorescence signal and photostability enables them to emit light in the visible to near infrared (NIR) range which is ideal for non-invasive imaging. In addition to this, benzothiazoles can be easily modified to bind specific targets like receptors, DNA, or enzymes.

There are several examples of benzothiazole-based probes in cancer research including those used as selective anticancer agents and imaging probes. These have been shown to selectively bind to oestrogen receptor-positive breast cancer cells, possessing strong fluorescence and high cytotoxicity in cancer cells but low in normal cells.[22] Benzothiazole–cyanine dyes have been used in NIR imaging of live animal tumours. These dyes are often functionalized to target cancer-specific receptors. An example of this is benzothiazole–Cy5 conjugates which is used for fluorescence-guided surgery.[23]

Cancer cells often have altered mitochondrial activity. Due to this, lipophilic cations attached to benzothiazoles help target mitochondria in cancer cells. These probes can differentiate cancer cells from normal cells due to metabolic differences. Benzothiazole-based Aβ (amyloid-β) probes which were originally developed for imaging amyloid-β plaques in Alzheimer's have been repurposed to detect this activity.[24] Furthermore, enzymes like matrix metalloproteinases (MMPs) or cathepsins are overexpressed in tumours. Benzothiazole–fluorophore conjugates have been used to detect these enzymes through enzymatic cleavage.[25]

Another promising probe on the horizon is BPN-01, designed to assist in cancer detection and tissue biopsy analysis.[26] BPN-01 was synthesized using a benzothiazole-phenylamide scaffold linked to nitrobenzoxadiazole (NBD), a visible light-emitting fluorophore. The compound was engineered for optical imaging of cancer cells with the possibility of future modifications (e.g., NIR dyes or radiolabeling). Moreover, the probe specifically stained prostate (DU-145) and melanoma (B16-F10) cancer cells and did not stain normal muscle cells (C2C12), suggesting selectivity for cancer cells with the best staining results observed at lower concentrations (0.01 mM).

A summary of the abovementioned benzothiazole probes with their corresponding structures has been made in Table **5.1**. There are also numerous other benzothiazole-based fluorescent probes used in anticancer research recorded in literature.[18, 27]

Table 5.1. Summary of several known benzothiazole probes used in anticancer research.

Probe Type	Application	Structure
2-(4′-Aminophenyl)benzothiazole (PBZ) Derivatives[22]	Breast cancer imaging and therapy.	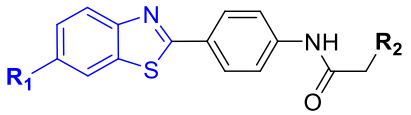 **R**$_1$ = H, CH_3 **R**$_2$ = $C_{12}H_8N_2O_5$ **M** = Re, ^{99m}Tc
Benzothiazole–Cyanine Dyes[23]	NIR tumour imaging.	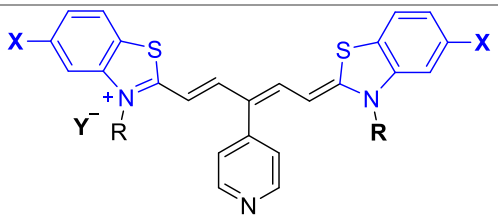 **X** = Me, **R** = Me, **Y** = I **X** = F, **R** = Me, **Y** = I **X** = H, **R** = Et, **Y** = I **X** = H, **R** = PhPr, **Y** = Br
Benzothiazolium-Based Probes[24]	Mitochondrial pH imaging in cancer cells.	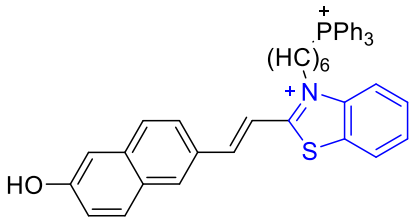
Benzothiazole-Based Enzyme-Activated Probes[25]	Detection of tumour-associated enzymes.	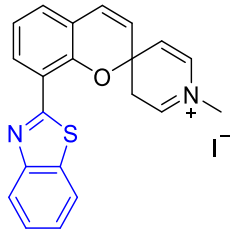
Benzothiazole-phenylamide moiety featuring nitrobenzoxadiazole (NBD) BPD-01[26]	Fluorescence image-guided surgery (FIGS).	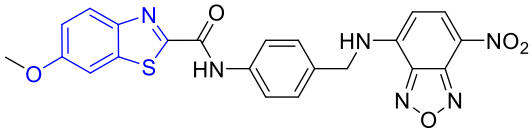

5.1.3 Bioluminescent properties of luciferins

Bioluminescence imaging (BLI) is a widely adopted non-invasive technique used to visualise molecular and cellular processes in living organisms.[28] Compared to fluorescence imaging, BLI offers the advantage of a lower background signal, resulting in a higher signal-to-noise ratio.

D-Luciferin is the natural substrate of the enzyme luciferase (Luc). This enzyme catalyses the production of the characteristic yellow-green bioluminescent light seen in fireflies,[29] which are part of a broader group of bioluminescent insects capable of emitting light in a range of wavelengths from yellow-green (around 560 nm) up to red (620 nm).[30] Interestingly, all of these enzymes use the same substrate: D-luciferin. The variation in light colour is due to subtle differences in the structure of luciferase active sites. These structural nuances can shift the emitted wavelength, and in firefly luciferases, the balance between green and red light is further regulated by a pH-sensitive mechanism.[31]

Among these enzymes, the luciferase from the North American firefly *Photinus pyralis* (fLuc) is one of the best characterised. It is widely used in mammalian cell research and in vivo imaging, thus becoming a standard tool in optical molecular imaging.[32] Additionally, it is often employed as a reporter gene in transgenic animals or as a cellular tag in transplantation studies.[33] Functionally, fLuc catalyses a multistep reaction with D-luciferin. It first forms luciferyl adenosine monophosphate (AMP) and inorganic pyrophosphoric acid (PPi) in a process similar to that of acyl-adenylate synthetases.[34] The reaction proceeds with oxygen interacting with the thiazoline ring of luciferin, producing a dioxetane intermediate through a mechanism known as intramolecular chemically initiated electron-exchange luminescence (CIEEL).[35, 36]

The final step involves the release of CO_2, which leads to the formation of oxyluciferin in an electronically excited state. As it relaxes back to the ground state, it emits yellow-green light in the 530 to 640 nm wavelength range, peaking at a wavelength of about 560 nm. (Scheme **5.1**). This detailed understanding of fLuc has helped researchers unravel the complex chemistry behind bioluminescence and continues to support its widespread use in scientific and medical applications.

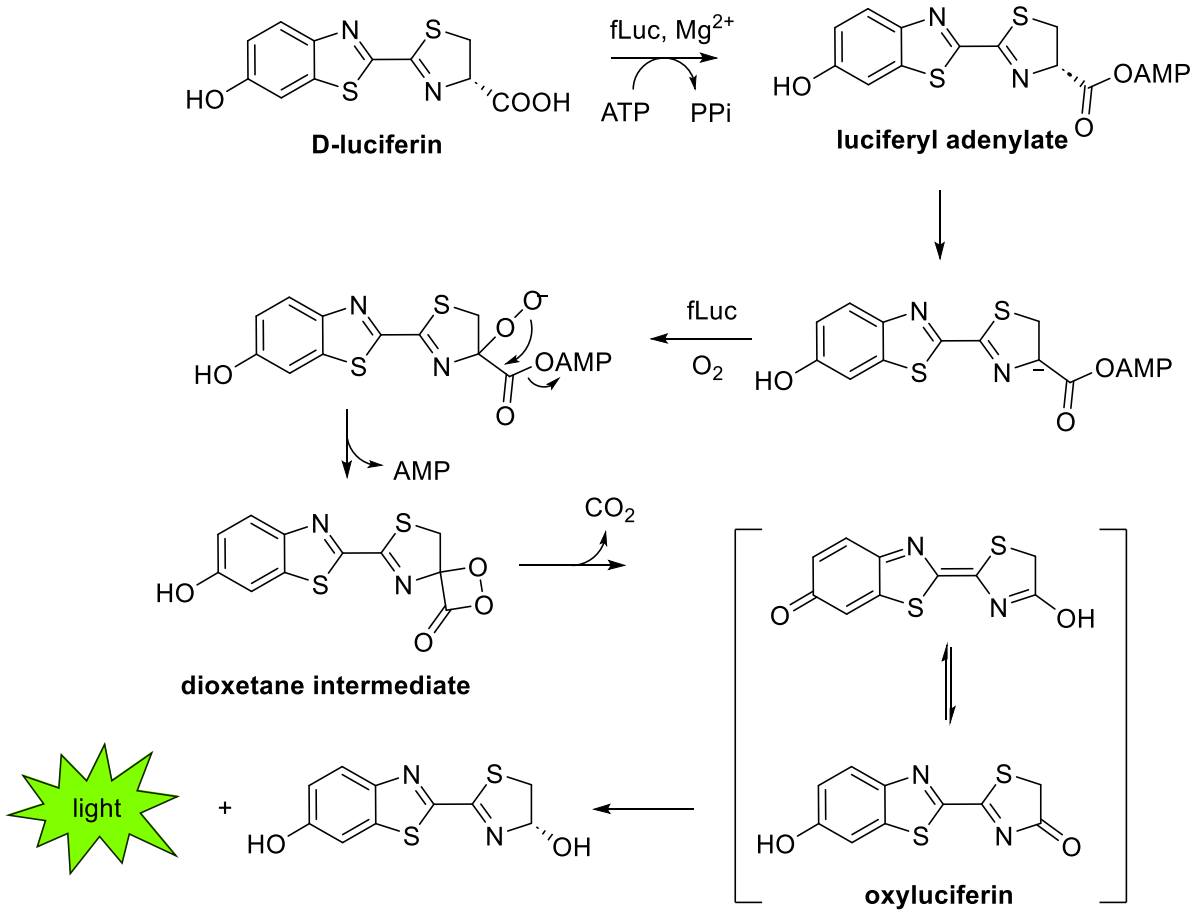

Scheme 5.1. Mechanism of fLuc-catalysed transformation of D-luciferin-based bioluminescence.[37, 38]

5.1.4 Caged luciferins

To date, bioluminescent imaging systems based on D-luciferin and luciferase have been widely employed to visualise biological analytes[39, 40] and monitor cellular processes.[41, 42] A common design strategy involves “caging” D-luciferin with specific functional groups, rendering it inactive. Upon interaction with a target biological analyte, the protecting group is cleaved, triggering a bioluminescent signal. This "turn-on" mechanism enables real-time imaging of the corresponding biological events. The most employed design of the luciferin–luciferase system for biomolecule detection involves the use of caged D-luciferin. Typically, the caging occurs at either the 6- or 4’-position of the luciferin molecule (Scheme **5.2**).

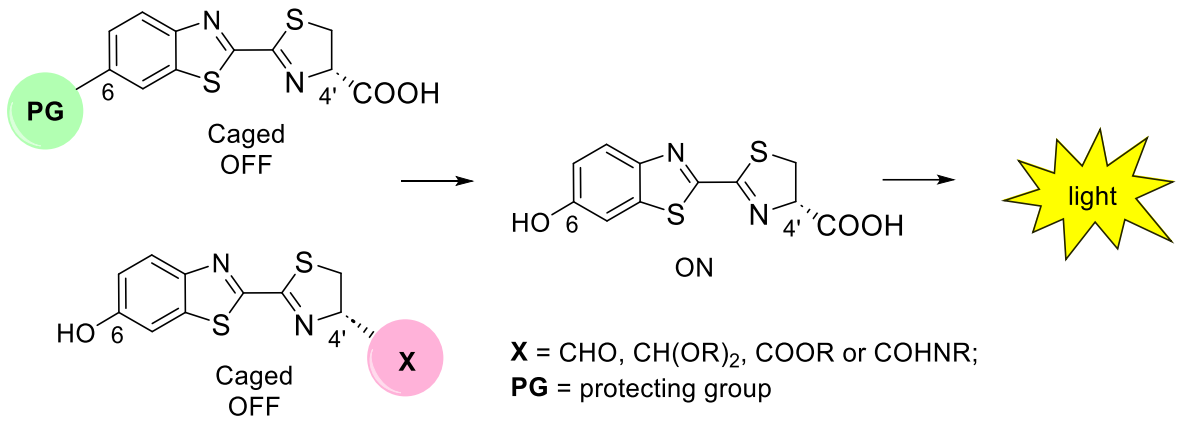

Scheme 5.2. General strategy for the design of caged luciferin bioluminescence probes.[38]

The 6-hydroxy or 6-amino functional group in D-luciferin or D-aminoluciferin, respectively is essential for luciferase binding and the subsequent enzyme-catalysed bioluminescent reaction.[28, 43] Conversely, the 4'-carboxyl group serves as the site for adenylation which is the initial step in the luciferase-mediated reaction.[44, 45] By strategically placing caging groups at the 6- or 4'-position, the interaction between luciferin and luciferase is inhibited, effectively turning "off" the bioluminescence. Upon exposure to specific biological targets such as enzymes, bioactive small molecules, or metal ions, the caging group is cleaved, releasing free D-luciferin. This restored luciferin can then undergo oxidation by luciferase, producing a bioluminescent signal.

A representative example has been displayed in the work by Chen *et al*., who developed a bioluminescent probe, Gly-Gly-Arg-aminoluciferin (GGR-amLuc), for detecting urokinase-type plasminogen activator (uPA).[38] In this probe, the 6-amino group of aminoluciferin was replaced with the uPA-recognised tripeptide GGR. Upon enzymatic cleavage of the GGR moiety by uPA, free aminoluciferin was released, enabling the emission of a bioluminescent signal and thus allowing for real-time imaging of uPA activity (Scheme **5.3**). Based on this strategy of caging and uncaging luciferins, a variety of biological molecule-responsive bioluminescent probes have been designed. Moreover, they have been successfully applied to evaluate the activity of a variety of enzymes or small molecules.[40, 46-49]

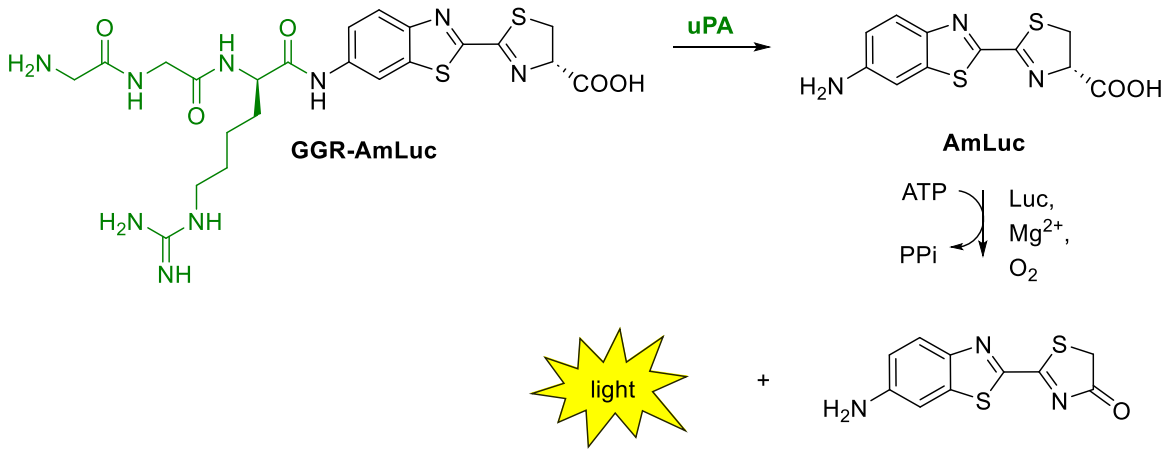

Scheme 5.3. uPA-triggered bioluminescence generation of the bioluminescent probe GGR-AmLuc.[38]

5.1.5 Use of luciferins as probes in anticancer research

Luciferins have also been used in anticancer drug discovery, though not as direct anticancer agents, but rather as tools for imaging, monitoring, and screening. Luciferins are widely used in combination with luciferase enzymes in preclinical cancer research such as tumour tracking and drug efficacy. One of the earlier studies using D-luciferin tested how effective Topotecan, a chemotherapy drug which inhibits topoisomerase 1, is at treating cancer using two human cancer cell lines DU-145 (prostate cancer) and MCF-7 (breast cancer).[50] To make it easier to track tumour growth and shrinkage, researchers modified these cancer cell lines by stably transfecting them with plasmid pcDNA3.1-Luc expressing fLuc. This allowed them to visually track tumour growth and metastasis via light emission. This is significant as BLI allows non-invasive, real-time monitoring of how tumours respond to anticancer drugs over time. This makes luciferins essential in in vivo screening for identifying potential anticancer drugs.

Luciferase-luciferin systems are also used in high-throughput assays to screen for compounds that affect cancer cell viability, apoptosis, or specific oncogenic pathways. For example, ATP assays based on luciferin-luciferase are used to measure cell viability in response to drug candidates. This is perfectly illustrated in the work by Zhang *et al.*, in which researchers developed a BLI-based high-throughput assay to identify inhibitors of the ABCG2 transporter, which is associated with tumour resistance to chemotherapeutic drugs.[51] By using HEK293 cells engineered to express both ABCG2 and fLuc, they screened a library of FDA-approved drugs. Since D-luciferin is also a substrate of ABCG2, compounds that inhibited ABCG2 increased intracellular D-luciferin concentrations, thereby enhancing the bioluminescence

signal. This method efficiently identified several potential ABCG2 inhibitors, including previously unrecognised ones.

Similar high-throughput firefly luciferase assays have also been used to assess tumour angiogenesis in mice using dynamic bioluminescence imaging (DBLI)[52] and to identify inhibitors of the heat shock protein 90 (Hsp90).[53] Sun *et al*. illustrated that increasing bioluminescence intensity correlated with tumour mass and vascular changes, providing insights into the dynamics of tumour angiogenesis over time.[52] Similarly, Sadikot *et al*. illustrated that by measuring luciferase refolding in cancer cells, compounds like ethoxyquin and biperiden could be identified as significant inhibitors of Hsp90.[53]

Alternatively, *Gaussia* luciferase (GLuc) has also been used to monitor cell viability in glioblastoma multiforme (GBM) cells using a screening assay. This assay enabled the identification of small-molecule drugs that sensitized GBM cells to apoptosis induced by tumour necrosis factor-related apoptosis-inducing ligand (TRAIL).[54]

In recent years, Wang *et al*. developed a novel bioluminescent probe AcAH-Luc that allows for the simultaneous imaging of esterase (CES) and histone deacetylase (HDAC) activity in tumours.[55] This probe was engineered to release D-luciferin, in response to enzyme activity. The probe showed high sensitivity and selectivity in vitro, with limits of detection of 0.495 nM for CES and 1.14 nM for HDAC6. Cell and animal studies using human breast cancer (MDA-MB-231) cells demonstrated that the bioluminescence signal was primarily due to CES and HDAC activity, contributing approximately half and one-third of the signal, respectively.

As shown in Scheme **5.4**, AcAH-Luc was carefully designed with two key components: (1) a D-luciferin core responsible for generating bioluminescence, and (2) a 6-acetamidohexanoic acid (AcHA) group, connected via an ester bond, which allowed the probe to respond to both CES and HDAC enzyme activity. In its intact form, AcAH-Luc does not emit light due to the hydroxyl group of D-luciferin being caged. However, when in the presence of CES, the ester bond of the prove is hydrolysed, releasing free D-luciferin. Subsequently, a bioluminescent signal is produced in the presence of fLuc (Scheme **5.4 a**). Alternatively, when HDAC is present, it removes the acetyl group from the AcHA moiety, triggering a self-immolated intramolecular cyclisation reaction that also liberates D-luciferin, resulting in bioluminescence (Scheme **5.4 b**).

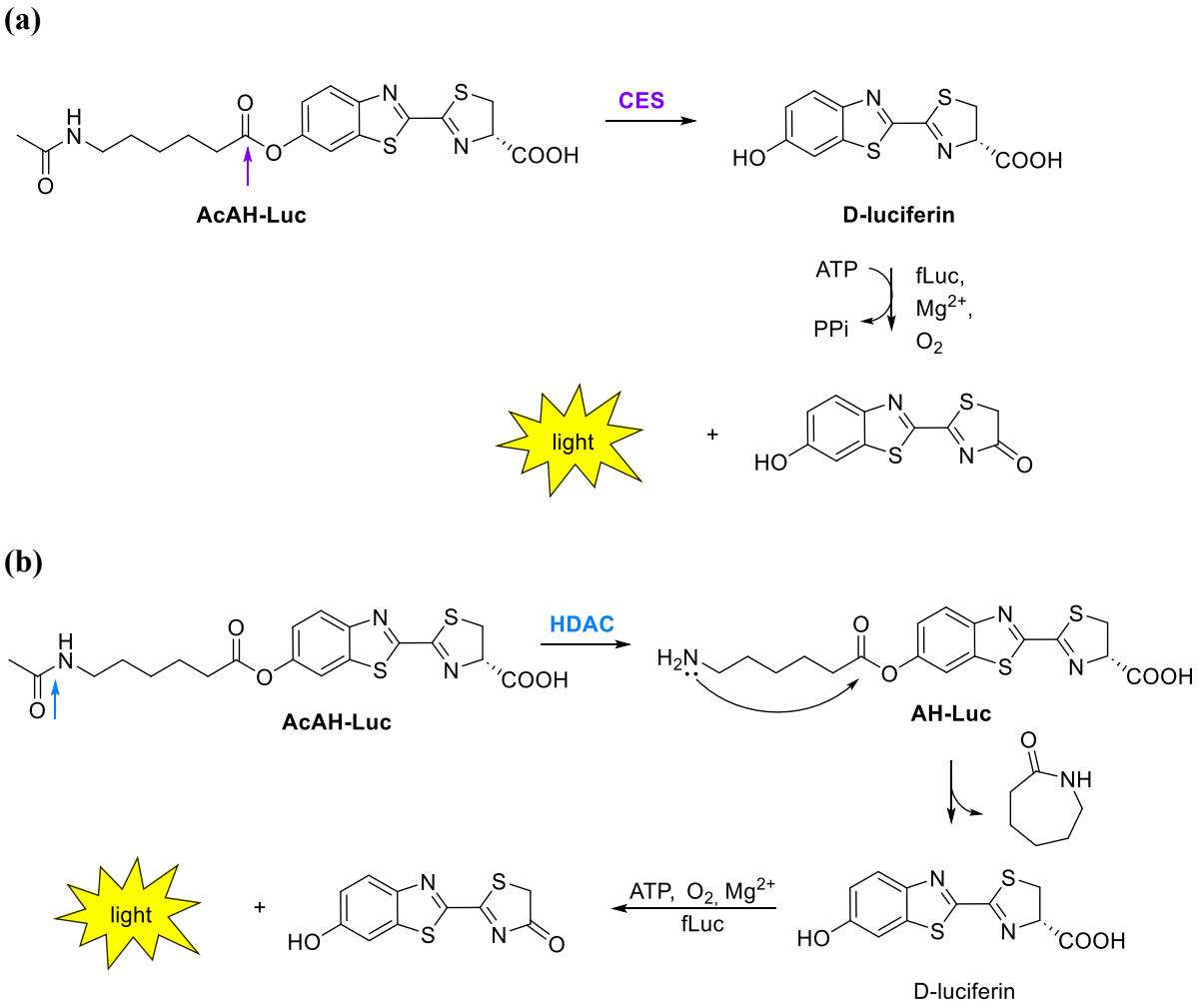

Scheme 5.4. (a) CES-triggered and **(b)** HDAC-triggered bioluminescence emission of AcAH-Luc.[55]

This work highlights AcAH-Luc as a promising tool for non-invasive imaging of tumour enzyme activity, offering potential applications in early and accurate cancer diagnosis.

In summary, luciferins are not used as drugs themselves, but are indispensable tools in anticancer research for imaging, screening, and evaluating drug candidates. As such, researchers are constantly trying to develop newer synthetic luciferins with better properties such as red-shifted light emission for deeper tissue imaging, which further enhances their usefulness in drug discovery and cancer biology.

5.2 Research rationale and motivation

As previously demonstrated by Sharma *et al*., the thioether luciferin analogue **20** was identified as a potent inhibitor of luciferase activity, whereas its oxidised sulfoxide derivative **22** exhibited only weak inhibitory effects, compared to the natural D-luciferin substrate.[56] Complementary absorbance and fluorescence spectroscopy studies performed on these luciferin analogues revealed notable photophysical changes upon oxidation. Specifically, oxidation of the sulphur atom of the sulphide **20** to the sulfoxide **22** resulted in a reduction in absorbance and a complete quenching of fluorescence (Figure **5.2**). Notably, the authors did not report corresponding data for the benzothiazole derivatives **19** and **21**, although it is presumed that these compounds may exhibit analogous trends in their absorbance and emission properties.

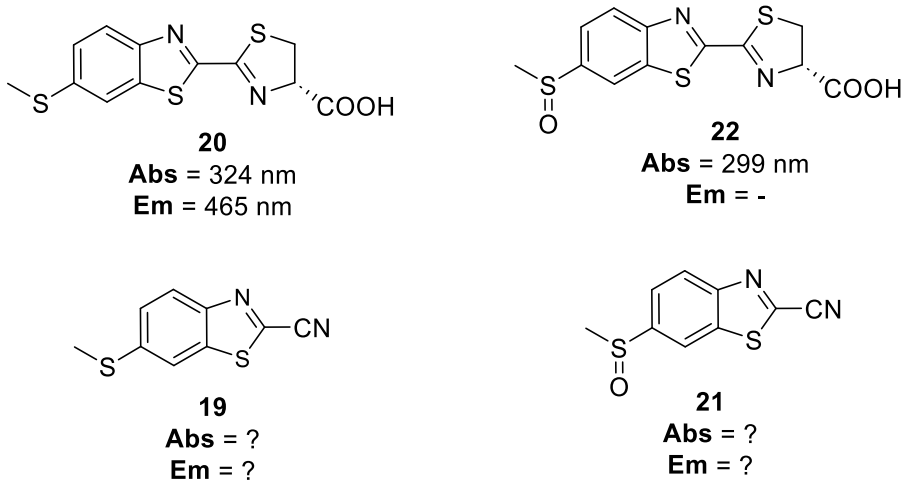

Figure 5.2. Photophysical properties of the selected luciferin analogues, reported in methanol.

The authors proposed that the observed alteration in bioluminescence emission of **20** and **22** may serve as a basis for the development of bioluminescent probes capable of sensing *S*-oxidation events, through a mechanism involving the alleviation of luciferase inhibition. This may be applicable to sulphur redox chemistry occurring in cancer cells; thus, these compounds may be exploited as redox probes. From a redox status point of view, normal and cancer cells differ significantly due to variations in metabolism, reactive oxygen species (ROS) handling, and antioxidant capacity.

5.3 Results and Discussion

5.3.1 UV-Vis properties of benzothiazole and luciferin derivatives

Absorption spectra for 6-(methylthio)benzo[d]thiazole **19** and its derivatives **20**, **21** and **22** were recorded using a Varian Cary 60 UV-Vis spectrophotometer, using 1cm path length quartz cell cuvettes. Benzothiazole samples **19** and **21** were prepared as 0.1 mM ethanol solutions while luciferin samples **20** and **22** were prepared as 0.1 mM H_2O solutions. These samples were scanned from 200 nm to 800 nm. Absorption spectra for **19** and **21** revealed a λ_{max} of 343 nm and 299 nm respectively (Figure **5.3**). The distinct shift in λ_{max} for the two samples is indicative of the addition of the sulfoxide functional group.

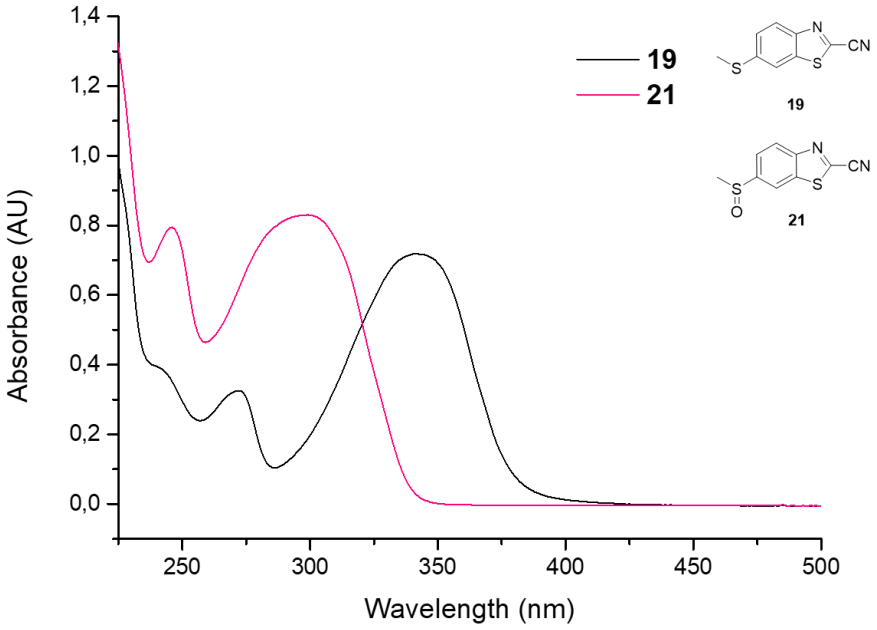

Figure 5.3. UV spectrum of 19 (λ_{max} = 343 nm) and 21 (λ_{max} = 299 nm) in ethanol.

Similarly, the absorption spectra for luciferin derivatives **20** and **22** revealed a λ_{max} of 346 nm and 308 nm respectively (Figure **5.4**). This shift in λ_{max} is also thought to be due to the oxidation of sulphur which pulls electron density away from the adjacent aromatic ring.

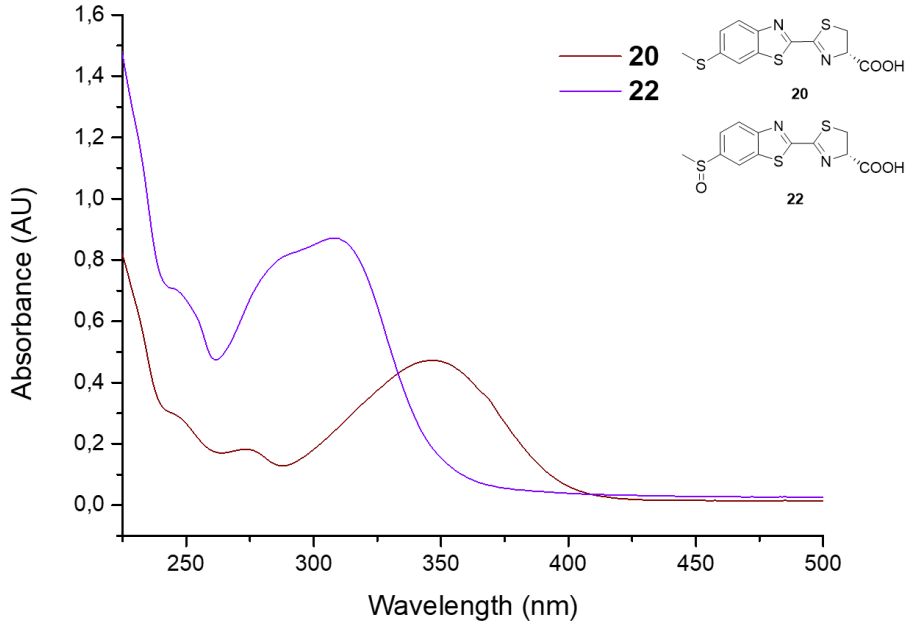

Figure 5.4. UV spectrum of **20** (λ_{max} = 346 nm) and **22** (λ_{max} = 308 nm) in H_2O.

5.3.2 Fluorescent properties of benzothiazole and luciferin derivatives

After completion of the UV-vis analysis of the four samples, the fluorescence studies were conducted. Excitation and emission spectra were recorded on a TECAN infinite M200 fluorometer using a NanoQuant plate. The samples were scanned from 280 nm to 850 nm. Emission spectra were recorded at the excitation wavelength corresponding to previously recorded absorption maxima. Benzothiazole **19** and its luciferin derivative **21** were prepared as 0.01 mM ethanol and H_2O solutions respectively while benzothiazole **20** and its luciferin derivative **22** were prepared as 0.1 mM ethanol and H_2O solutions respectively. The concentration of **19** and **21** had to be prepared 10-fold more dilute than **20** and **22** due to their higher fluorescence quantum yield.

As in the case with the UV-vis spectra, the fluorescence emission spectra of benzothiazoles **19** and **21** were distinctly different (Figure **5.5**). Both benzothiazoles were excited at their UV absorption maxima of 343 nm and 299 nm respectively, however only benzothiazole **19** displayed an emission wavelength (λ_{em} = 450 nm). Similarly, luciferin derivatives **20** and **22** were excited at their UV absorption maxima of 346 nm and 208 nm respectively (Figure **5.6**). Once more, only luciferin derivative **20** displayed a fluorescence emission wavelength (λ_{em} = 500 nm).

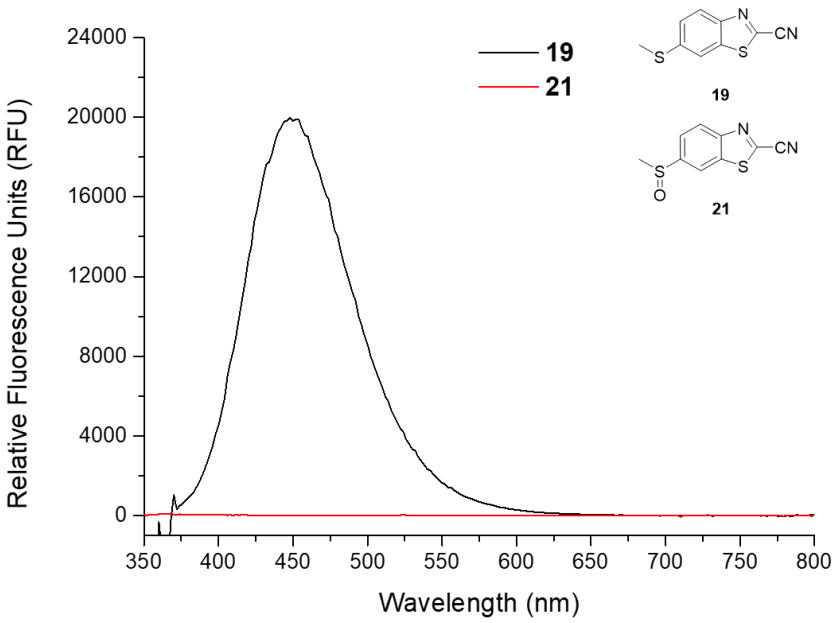

Figure 5.5. Fluorescence emission spectrum of **19** (λ_{ex} = 343 nm, λ_{em} = 450 nm) and 21 in ethanol.

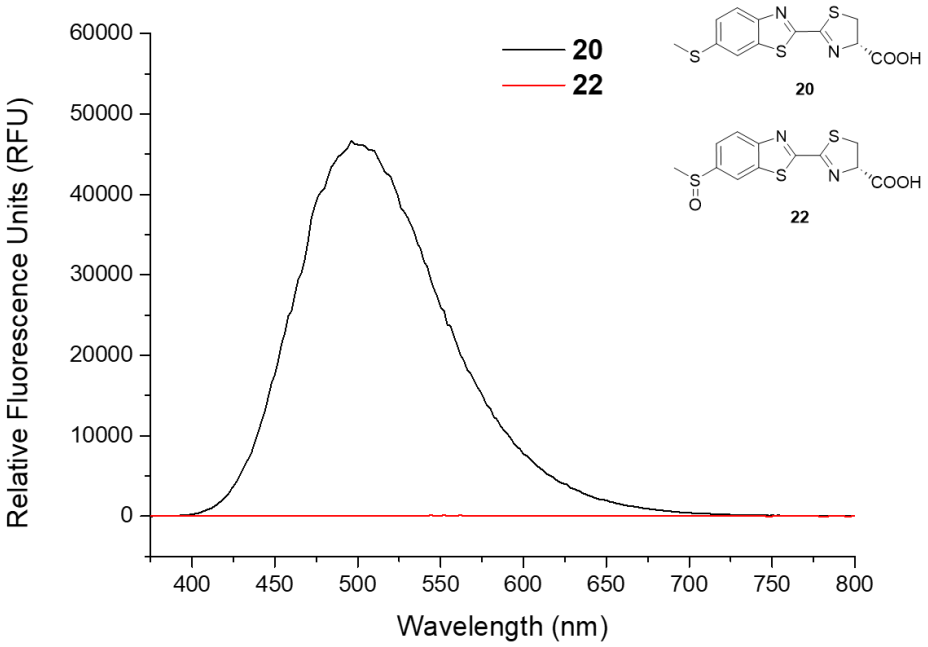

Figure 5.6. Fluorescence emission spectrum of **20** (λ_{ex} = 346 nm, λ_{em} = 500 nm) and **22** in H_2O.

The observed photophysical changes in the sulphide and sulfoxide analogues can be related back to the "matched" and "mismatched" setups observed in benzothiazole systems. In benzothiazole **19**, electrons on the sulphur atom of the sulphide EDG are available to resonate into the adjacent benzene ring. This facilitates an efficient charge transfer where a virtual dipole is created between the electron rich benzothiazole ring and the electron poor nitrile group at

the C-2 position. The virtual dipole is thus in the same direction of the ICT which reinforces the excited-state dipole moment. As such, a strong fluorescence emission is observed for benzothiazole **19** and its sulphide luciferin derivative **20**. Conversely, the electron-withdrawing sulfoxide functional group in compounds **21** and **22** pulls electrons away from the adjacent aromatic ring. Efficient charge transfer is not facilitated as there are EWGs on the C-2 (nitrile) and C-6 (sulfoxide) positions of the benzothiazole ring (Figure **5.7**). As such, no fluorescence emission is observed for these two compounds.

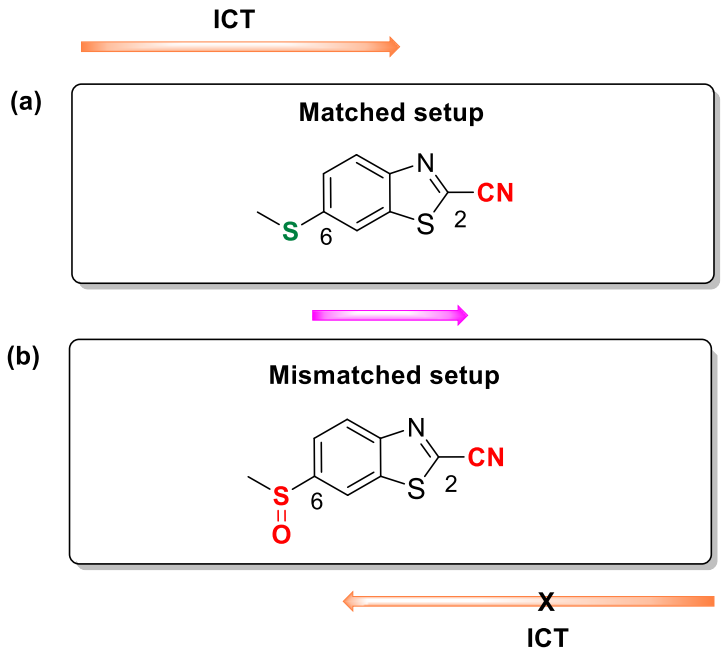

Figure 5.7. Schematic structure of **(a)** matched alignment of the benzothiazole core with respect to the sulphide (EDG) and **(b)** mismatched alignment of the benzothiazole core with respect to the sulfoxide (EWG).

5.3.3 5.3.3 Bioluminescent properties of luciferin analogues

Initial findings by Sharma and colleagues indicated that thioether luciferin analogue **20** exhibited strong luciferase inhibitory activity, whereas the thiomethyl sulfoxide **22** displayed only weak inhibition.[56] However, in the present study, luciferase inhibition assays conducted on the synthesised analogues revealed the inverse to be true. Compound **20** demonstrated only weak inhibitory effects, while compound **22** emerged as a potent luciferase inhibitor (Figure **5.8**).

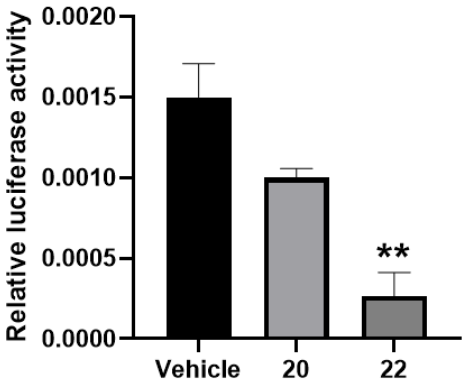

Figure 5.8. Inhibition of firefly luciferase by luciferin analogues **20** and **22**.

5.3.4 5.3.4 Cell viability assays

The National Cancer Institute (NCI) states that a promising therapeutic agent should have an initial single dose effect below 10 μM, after which, the ability of the drugs to inhibit additional cancer hallmarks can be assessed.[57] Therefore, to assess if compounds **19**, **20**, **21** and **22** may have cytotoxic effects MTT cell viability assays were performed in the most frequently used and most well established cervical cancer cell lines, HeLa and CaSki at 10 μM. In addition, cisplatin (Cis), a platinum-based chemotherapy drug commonly used to treat various cancers, including cervical cancer, was included as a positive control in these assays.

The cytotoxic profiles of the compounds of interest against HeLa and CaSki cancer cells at a 10 μM concentration are shown in Figure **5.9**. The average percentage cell viability recorded for the drugs was well above 75% in both cell lines, with only the positive control having a percentage viability of 68.42% in HeLa cells and 62.68% in CaSki cells. These findings revealed that none of the test compounds had any significant suppressing effect on the growth of either cervical cancer cell lines including the control, cisplatin. The cisplatin result is not surprising as these cell lines have exhibited variable resistance to cisplatin.[58, 59] This was further supported by the morphological analysis of both cancer cell lines. No changes in cell morphology or evidence of apoptosis were observed at this concentration (Figure **5.10**). Similarly, the fluorescence output at this concentration in both cell lines was very low. Only slight fluorescence was observed for compounds **19** and **20** while no fluorescence was observed for compounds **21** and **22**, as expected (Figure **5.11**).

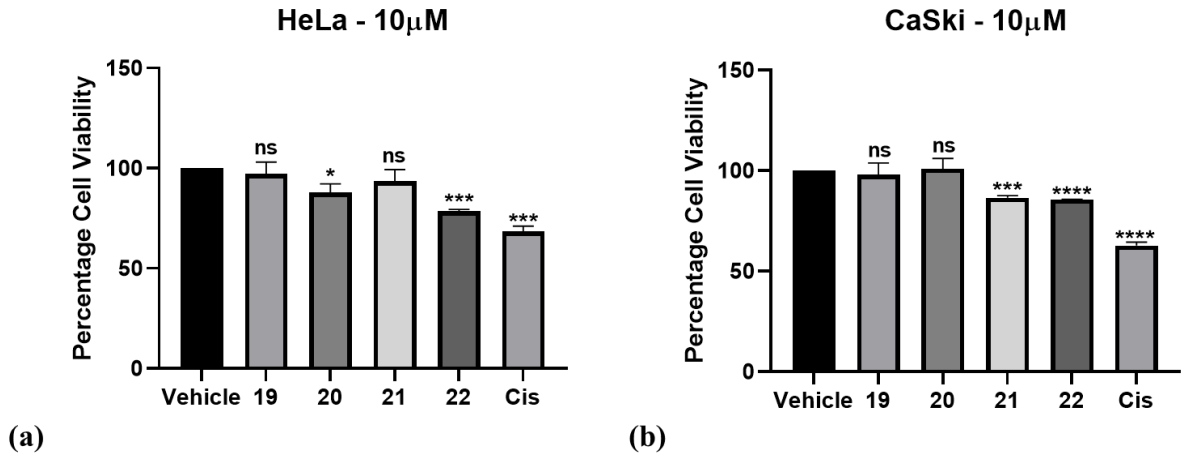

Figure 5.9. MTT cell viability assays of human cervical cancer cell lines, **(a)** HeLa and **(b)** CaSki, treated with 10 μM of compounds **19**, **20**, **21** and **22** for 72 hours. Graphs show mean cell viability as a percentage of vehicle control ± SEM for each treatment determine.

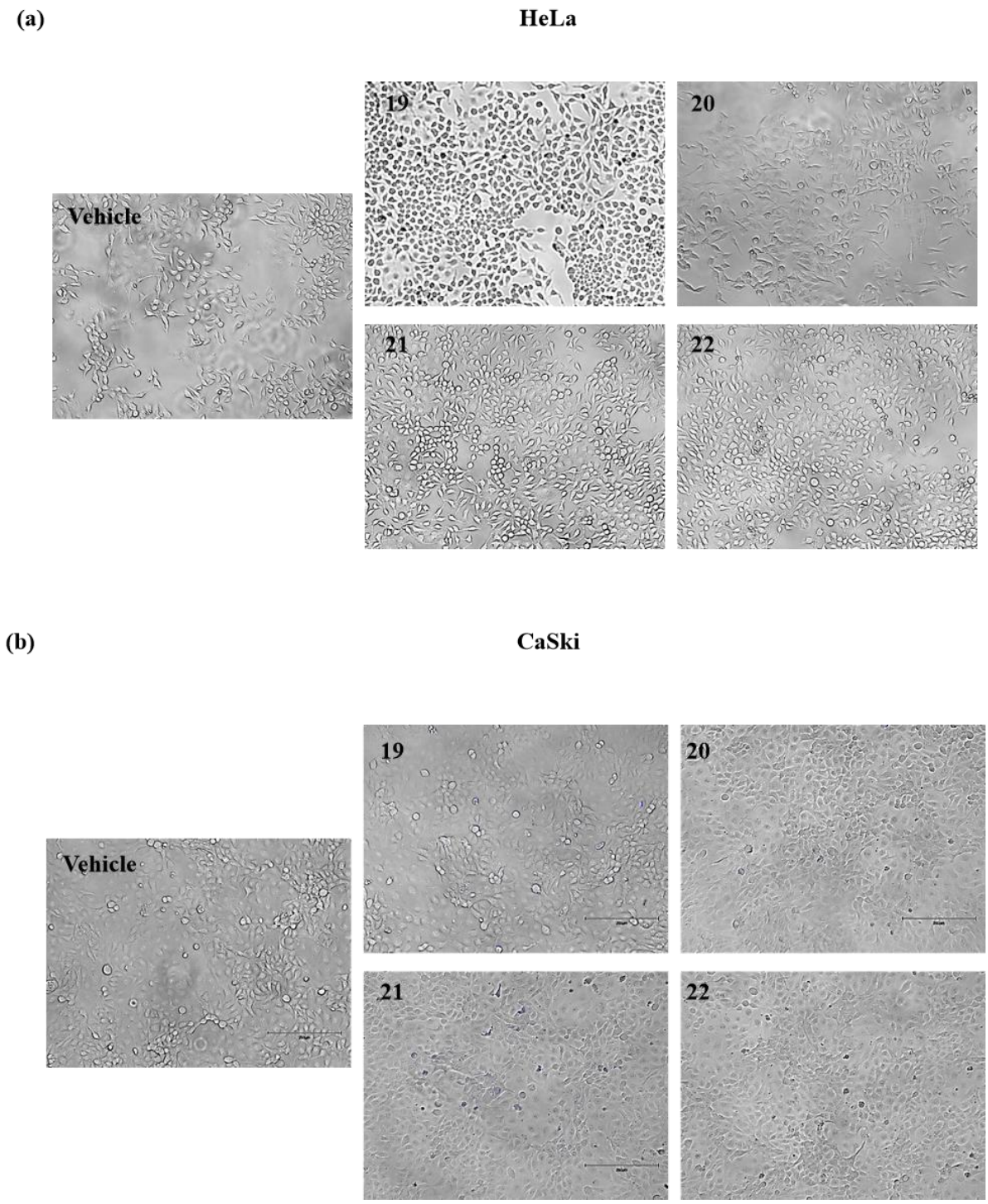

Figure 5.10. Representative light microscopy images (×200; EVOS M5000) of **(a)** HeLa and **(b)** CaSki cell lines treated with 10 μM of compounds **19**, **20**, **21**, **22** or vehicle for 72 h.

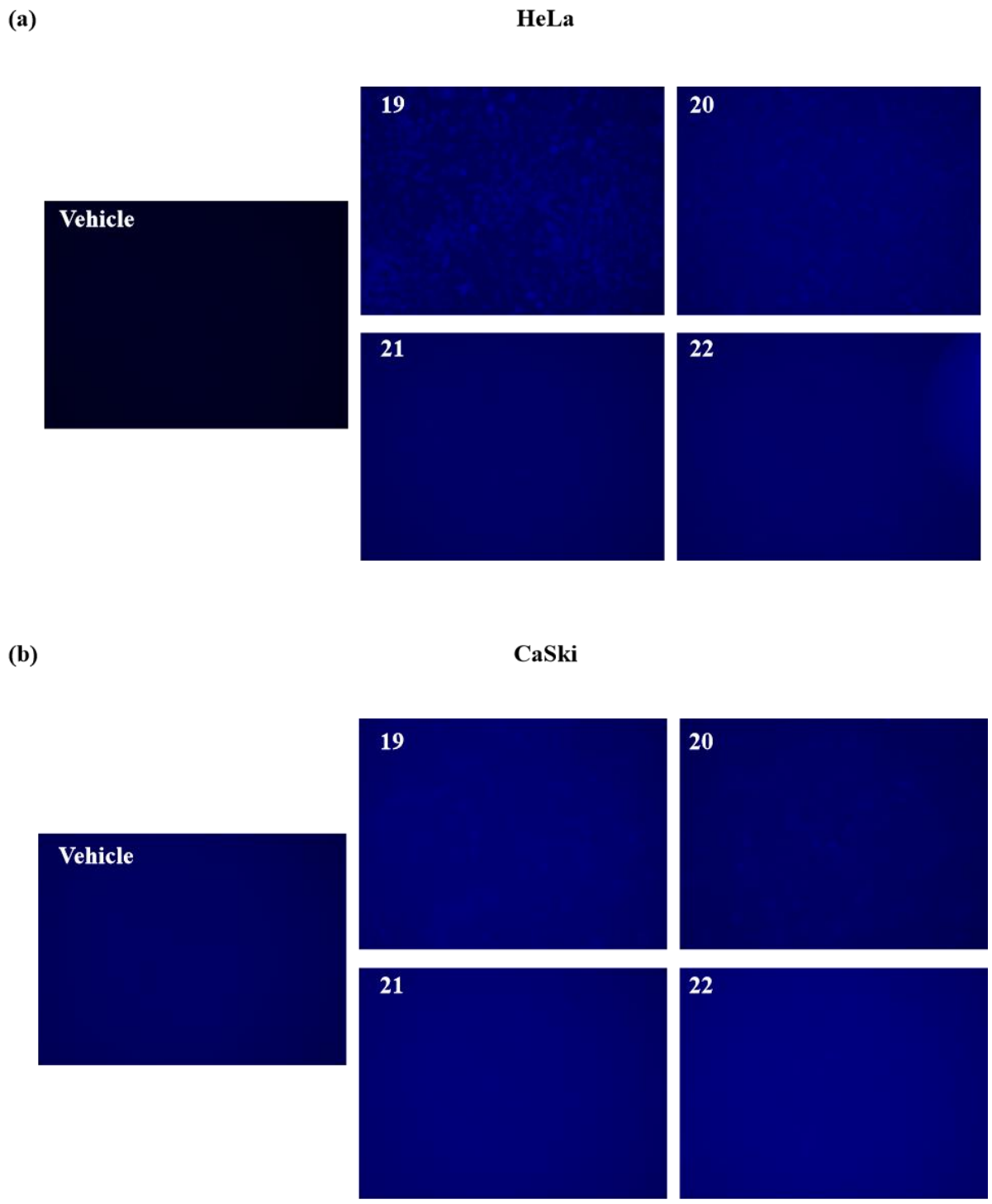

Figure 5.11. Representative fluorescent microscopy images of **(a)** HeLa and **(b)** CaSki cell lines treated with 10 μM of compounds **19**, **20**, **21**, **22** or vehicle for 72 h. Images obtained in the DAPI channel (×200; EVOS M5000).

Due to the resistant nature of these cells, the concentration of all the compounds were increased to 100 μM. This concentration was chosen as this ensured that the final DMSO concentration, the dissolving reagent, was below the 1% threshold. Interestingly, at this concentration there was a considerable reduction in the viability in both cell lines (Figure **5.12**). The average

percentage cell viability recorded for compounds **19**, **20** and **21** was below 50% in both cell lines, while being just over 50% for compound **22** (50.67% in HeLa cells and 50.94% in CaSki cells). Compound **19** had the lowest percentage cell viability in HeLa cells (41.80%), while compound **21** had the lowest cell percent viability in CaSki cells (41.56%). The viability of cells treated with the cisplatin control remained below 30% in both cell lines.

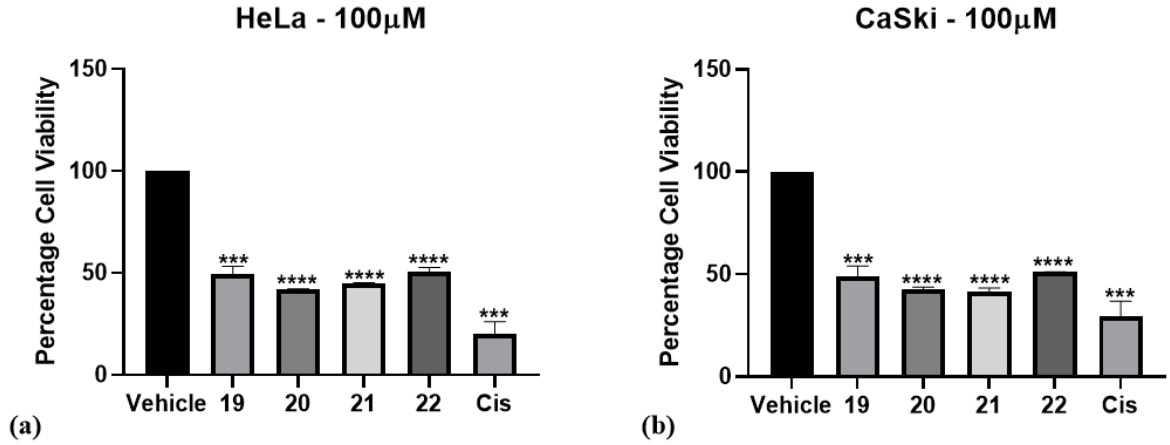

Figure 5.12. MTT cell viability assays of human cervical cancer cell lines, (a) HeLa and (b) CaSki, treated with 100 µM of compounds 19, 20, 21 and 22 for 72 hours. Graphs show mean cell viability as a percentage of vehicle control ± SEM for each treatment determin

These findings were further supported by the morphological analyses of both cancer cell lines. Significant changes in cell morphology and evidence of apoptosis were observed at the increased concentration in both cell lines (Figure **5.13**). Furthermore, the fluorescence output at this concentration increased significantly for compounds **19** and **20** in HeLa cells, while fluorescence in CaSki cells was only observed for compound **20** (Figure **5.14**). No fluorescence was observed for compounds **21** and **22** in both cell lines, as expected.

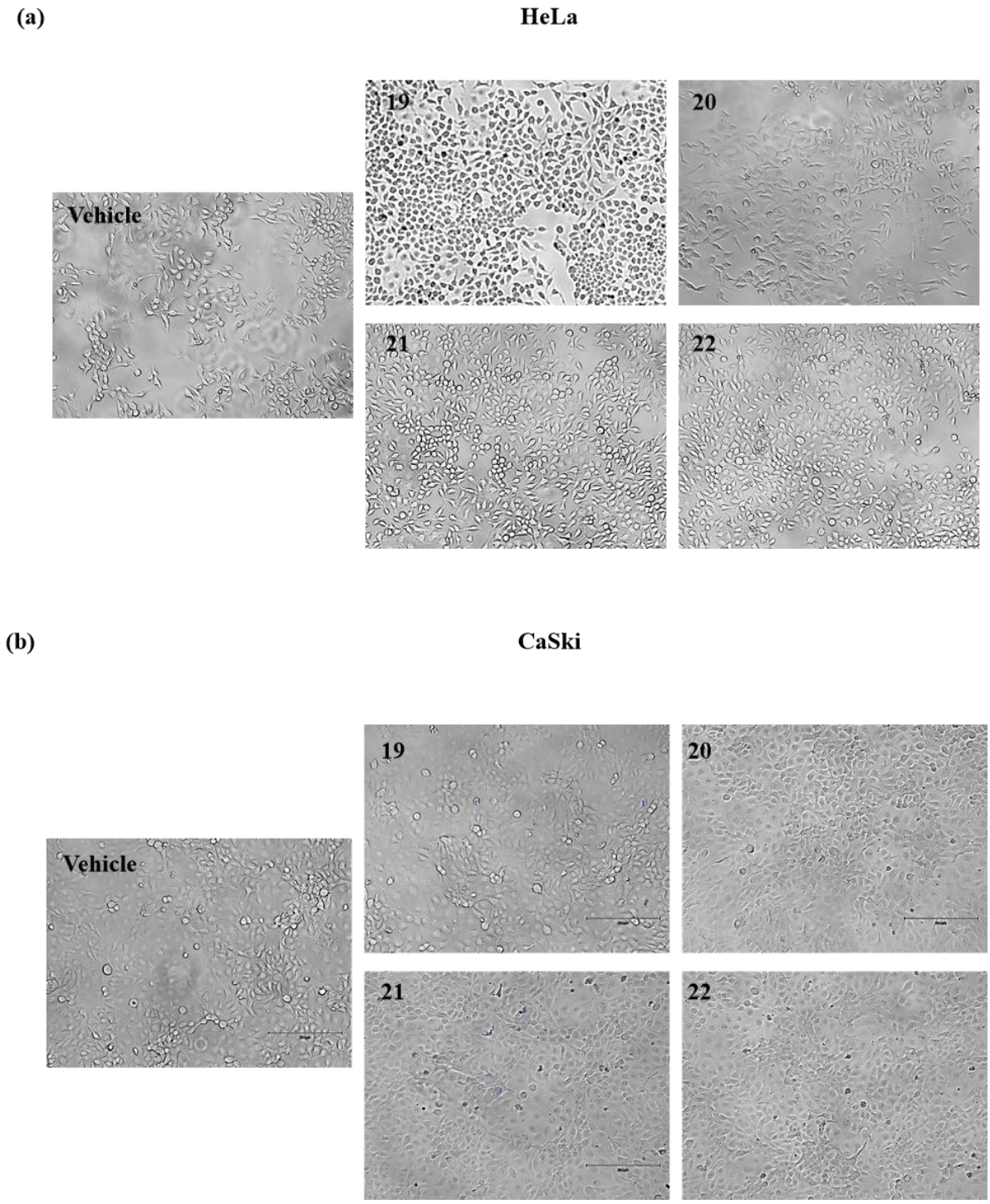

Figure 5.13. Representative light microscopy images (×200; EVOS M5000) of (a) HeLa and (b) CaSki cell lines treated with 100 μM of compounds 19, 20, 21, 22 or vehicle for 72 h.

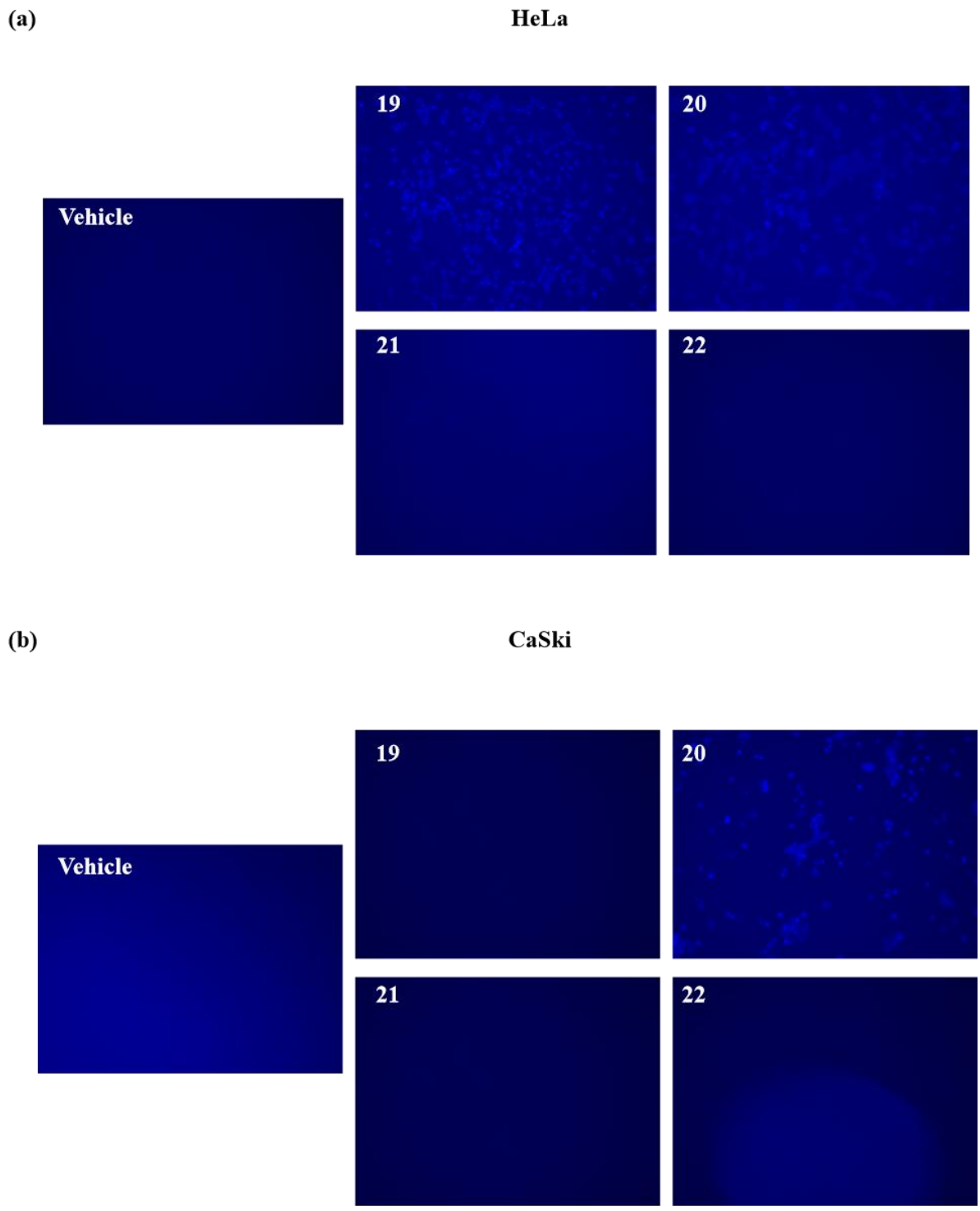

Figure 5.14. Representative fluorescent microscopy images of **(a)** HeLa and **(b)** CaSki cell lines treated with 100 μM of compounds **19**, **20**, **21**, **22** or vehicle for 72 h. Images obtained in the DAPI channel (×200; EVOS M5000).

5.4 Conclusion

Fluorescence studies revealed that thiomethyl derivative **19** and its corresponding sulfoxide **21** exhibited trends comparable to those observed for the luciferin analogues **20** and **22**, as reported by Sharma. For both the benzothiazole and luciferin derivatives, oxidation of the sulphur atom resulted in a reduction in the maximum absorbance and a complete quenching of fluorescence (Figure **5.15**).

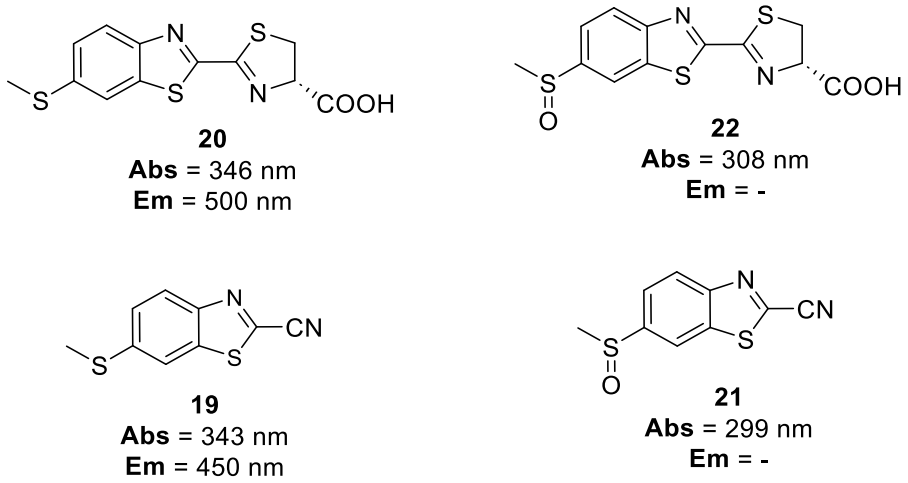

Figure 5.15. Photophysical properties of the selected luciferin (**20** and **22**) and benzothiazole (**19** and **21**) analogues, reported in H_2O and ethanol respectively.

Bioluminescence analysis of the luciferin analogues exhibited the opposite properties to what was previously reported in literature. From this study, thioether **20** weakly inhibited luciferase activity, while compound **22** emerged as a potent luciferase inhibitor.

The potential cytotoxic effects of compounds **19**, **20**, **21**, and **22** on cancer cells were assessed using MTT assays. At a concentration of 10 μM, these compounds exhibited negligible anti-proliferative activity against HeLa and CaSki cell lines, with no observable changes in cell morphology or indications of apoptosis. Correspondingly, fluorescence emission at this concentration was minimal in both cell lines.

In contrast, increasing the concentration to 100 μM resulted in a considerable reduction in cell viability for both HeLa and CaSki cells. Significant morphological alterations and clear signs of apoptosis were evident at this higher concentration. Notably, fluorescence output also increased substantially for compounds **19** and **20** in HeLa cells, whereas only compound **20** displayed fluorescence in CaSki cells. As anticipated, compounds **21** and **22** did not exhibit any detectable fluorescence in either cell line.

5.5 References

(1) Bi, K.; Tan, R.; Hao, R.; Miao, L.; He, Y.; Xianghua, W.; Zhang, J.; Rui, X. A carbazole-hemicyanine dye based ratiometric fluorescent probe for selective detection of bisulfite (HSO3−) in cells and C. elegans. *Chinese Chemical Letters* **2019**, *30* (3), 545-548.

(2) Han, X.; Zhai, Z.; Yang, X.; Zhang, D.; Tang, J.; Zhu, J.; Zhu, X.; Ye, Y. A FRET-based ratiometric fluorescent probe to detect cysteine metabolism in mitochondria11Electronic supplementary information (ESI) available. See DOI: 10.1039/d0ob00002g. *Organic & Biomolecular Chemistry* **2020**, *18* (7), 1487-1492.

(3) Tang, L.; Zhou, L.; Yan, X.; Zhong, K.; Gao, X.; Li, J. A new NIR-emissive fluorescence turn-on probe for Hg2+ detection with a large Stokes shift and its multiple applications. *Journal of Photochemistry and Photobiology A: Chemistry* **2020**, *387*, 112160.

(4) Zhao, F.; Zhai, Z.; Tang, J.; Zhang, B.; Yang, X.; Song, X.; Ye, Y. A bond energy transfer based difunctional fluorescent sensor for Cys and bisulfite. *Talanta* **2020**, *214*, 120884.

(5) Zhong, K.; Zhou, S.; Yan, X.; Hou, S.; Li, X.; Tang, L. A novel D-π-A type NBD-based fluorescent probe for ultrafast and distinguishable detection of Hcy/Cys and its bioimaging application. *Journal of Luminescence* **2020**, *224*, 117330.

(6) Diwan, U.; Kumar, V.; Mishra, R. K.; Rana, N. K.; Koch, B.; Upadhyay, K. Harvesting red fluorescence through design specific tuning of ICT and ESIPT: an efficient optical detection of cysteine and live cell imaging. *RSC advances* **2016**, *6* (98), 95722-95728.

(7) Feng, B.; Liu, Y.; Huang, S.; Huang, X.; Huang, L.; Liu, M.; Wu, J.; Du, T.; Wang, S.; Feng, X.; et al. Highly selective discrimination of cysteine from glutathione and homo-cysteine with a novel AIE-ESIPT fluorescent probe. *Sensors and Actuators B: Chemical* **2020**, *325*, 128786.

(8) Liu, H.; Wang, X.; Xiang, Y.; Tong, A. Fluorescence turn-on detection of cysteine over homocysteine and glutathione based on "ESIPT" and "AIE". *Analytical Methods* **2015**, *7* (12), 5028-5033.

(9) Henary, M. M.; Fahrni, C. J. Excited state intramolecular proton transfer and metal ion complexation of 2-(2 '-Hydroxyphenyl) benzazoles in aqueous solution. *The Journal of Physical Chemistry A* **2002**, *106* (21), 5210-5220.

(10) Mutai, T.; Tomoda, H.; Ohkawa, T.; Yabe, Y.; Araki, K. Switching of Polymorph-Dependent ESIPT Luminescence of an Imidazo[1,2-a]pyridine Derivative. *Angewandte Chemie International Edition* **2008**, *47* (49), 9522-9524.

(11) Wang, R.; Liu, D.; Xu, K.; Li, J. Substituent and solvent effects on excited state intramolecular proton transfer in novel 2-(2′-hydroxyphenyl)benzothiazole derivatives. *Journal of Photochemistry and Photobiology A: Chemistry* **2009**, *205* (1), 61-69.

(12) Kwon, J. E.; Park, S. Y. Advanced Organic Optoelectronic Materials: Harnessing Excited-State Intramolecular Proton Transfer (ESIPT) Process. *Advanced Materials* **2011**, *23* (32), 3615-3642..

(13) Qian, Y.; Li, S.; Wang, Q.; Sheng, X.; Wu, S.; Wang, S.; Li, J.; Yang, G. A nonpolymeric highly emissive ESIPT organogelator with neither dendritic structures nor long alkyl/alkoxy chains. *Soft Matter* **2012**, *8* (3), 757-764.

(14) Gong, X.; Ding, X.; Jiang, N.; Zhong, T.; Wang, G. Benzothiazole-based fluorescence chemosensors for rapid recognition and "turn-off" fluorescence detection of Fe3+ ions in aqueous solution and in living cells. *Microchemical Journal* **2020**, *152*, 104351.

(15) Pan, Y.; Ban, L.; Li, J.; Liu, M.; Tang, L.; Yan, X. Cysteine recognition by a benzothiazole-derived fluorescent probe with "AIE+ ESIPT" characteristics. *Dyes and Pigments* **2022**, *203*, 110305.

(16) Ren, Y.; Fan, D.; Ying, H.; Li, X. Rational design of the benzothiazole-based fluorescent scaffold for tunable emission. *Tetrahedron Letters* **2019**, *60* (15), 1060-1065.

(17) Hrobárik, P.; Hrobáriková, V.; Sigmundová, I.; Zahradník, P.; Fakis, M.; Polyzos, I.; Persephonis, P. Benzothiazoles with tunable electron-withdrawing strength and reverse polarity: a route to triphenylamine-based chromophores with enhanced two-photon absorption. *The Journal of organic chemistry* **2011**, *76* (21), 8726-8736.

(18) Tang, J.; Li, F.; Liu, C.; Shu, J.; Yue, J.; Xu, B.; Liu, X.; Zhang, K.; Jiang, W. Attractive benzothiazole-based fluorescence probe for the highly efficient detection of hydrogen peroxide. *Analytica Chimica Acta* **2022**, *1214*, 339939.

(19) Yan, F.; Sun, J.; Zang, Y.; Sun, Z.; Zhang, H.; Wang, X. Benzothiazole applications as fluorescent probes for analyte detection. *Journal of the Iranian Chemical Society* **2020**, *17*, 3179-3203.

(20) Sun, L.; Wang, X.; Fleurat-Lessard, P.; Gros, C. P.; Bolze, F.; Xu, H. Synthesis, photophysical properties and two-photon absorption of benzothiazole/benzoxazole π-expanded carbazole dyes. *Dyes and Pigments* **2022**, *204*, 110447.

(21) Sun, Y. T.; Zhang, C.; Gao, L. X.; Liu, M. M.; Yang, Y.; Shao, A.; Zhou, Y. B.; Zhu, Y. L.; Li, J.; Wang, W. L. Design, synthesis and evaluation of fluorescent properties of benzothiazole derivatives. *ChemPhysChem* **2023**, *24* (17), e202300159.

(22) Tzanopoulou, S.; Sagnou, M.; Paravatou-Petsotas, M.; Gourni, E.; Loudos, G.; Xanthopoulos, S.; Lafkas, D.; Kiaris, H.; Varvarigou, A.; Pirmettis, I. C.; et al. Evaluation of Re and 99mTc Complexes of 2-(4′-Aminophenyl)benzothiazole as Potential Breast Cancer Radiopharmaceuticals. *Journal of Medicinal Chemistry* **2010**, *53* (12), 4633-4641.

(23) Lovett, W. R.; Al Hamd, A.; Casa, S.; Henary, M. Synthesis of pH-sensitive benzothiazole cyanine dye derivatives containing a pyridine moiety at the meso position. *Dyes and Pigments* **2021**, *190*, 109268.

(24) Lin, B.; Fan, L.; Zhou, Y.; Ge, J.; Wang, X.; Dong, C.; Shuang, S.; Wong, M. S. A benzothiazolium-based fluorescent probe with ideal pK(a) for mitochondrial pH imaging and cancer cell differentiation. *J Mater Chem B* **2020**, *8* (46), 10586-10592.

(25) Das, S.; Indurthi, H. K.; Asati, P.; Saha, P.; Sharma, D. K. Benzothiazole based fluorescent probes for the detection of biomolecules, physiological conditions, and ions responsible for diseases. *Dyes and Pigments* **2022**, *199*, 110074.

(26) Wongso, H.; Goenawan, H.; Lesmana, R.; Mahendra, I.; Kurniawan, A.; Wibawa, T. H.; Nuraeni, W.; Rosyidiah, E.; Setiadi, Y.; Sylviana, N. Synthesis and biological evaluation of new fluorescent probe BPN-01: a model molecule for fluorescence image-guided surgery. *Journal of Fluorescence* **2023**, *33* (5), 1827-1839.

(27) Jin, Y.; Wang, S.; Zhang, Y.; Song, B. Highly selective fluorescent chemosensor based on benzothiazole for detection of Zn2+. *Sensors and Actuators B: Chemical* **2016**, *225*, 167-173.

(28) Li, J.; Chen, L.; Du, L.; Li, M. Cage the firefly luciferin! – a strategy for developing bioluminescent probes. *Chemical Society Reviews* **2013**, *42* (2), 662-676, 10.1039/C2CS35249D.

(29) White, E. H.; Rapaport, E.; Seliger, H. H.; Hopkins, T. A. The chemi- and bioluminescence of firefly luciferin: An efficient chemical production of electronically excited states. *Bioorganic Chemistry* **1971**, *1* (1), 92-122.

(30) Viviani, V. R. The origin, diversity, and structure function relationships of insect luciferases. *Cellular and Molecular Life Sciences CMLS* **2002**, *59*, 1833-1850.

(31) Seliger, H.; McElroy, W. The colors of firefly bioluminescence: enzyme configuration and species specificity. *Proceedings of the National Academy of Sciences* **1964**, *52* (1), 75-81.

(32) Luker, G. D.; Luker, K. E. Optical imaging: current applications and future directions. *Journal of Nuclear Medicine* **2008**, *49* (1), 1-4.

(33) Contag, C. H.; Bachmann, M. H. Advances in in vivo bioluminescence imaging of gene expression. *Annual review of biomedical engineering* **2002**, *4* (1), 235-260.

(34) McElroy, W.; DeLuca, M.; Travis, J. Molecular Uniformity in Biological Catalyses: The enzymes concerned with firefly luciferin, amino acid, and fatty acid utilization are compared. *Science* **1967**, *157* (3785), 150-160.

(35) McCapra, F. Chemical mechanisms in bioluminescence. *Accounts of chemical research* **1976**, *9* (6), 201-208.

(36) Schuster, G. B. Chemiluminescence of organic peroxides. Conversion of ground-state reactants to excited-state products by the chemically initiated electron-exchange luminescence mechanism. *Accounts of Chemical Research* **1979**, *12* (10), 366-373.

(37) Meroni, G.; Rajabi, M.; Santaniello, E. D-Luciferin, derivatives and analogues: synthesis and in vitro/in vivo luciferase-catalyzed bioluminescent activity. *ARKIVOC: Online Journal of Organic Chemistry* **2009**.

(38) Xia, T.; Cheng, X.; Zhan, W.; Liang, G. Activity-Based Luciferase-Luciferin Bioluminescence System for Bioimaging Applications. *Analysis & Sensing* **2021**, *1* (4), 138-147.

(39) Zhang, M.; Wang, L.; Zhao, Y.; Wang, F.; Wu, J.; Liang, G. Using Bioluminescence Turn-On To Detect Cysteine in Vitro and in Vivo. *Analytical Chemistry* **2018**, *90* (8), 4951-4954.

(40) Zheng, Z.; Li, G.; Wu, C.; Zhang, M.; Zhao, Y.; Liang, G. Intracellular synthesis of D-aminoluciferin for bioluminescence generation. *Chemical Communications* **2017**, *53* (25), 3567-3570.

(41) Luker, K. E.; Smith, M. C.; Luker, G. D.; Gammon, S. T.; Piwnica-Worms, H.; Piwnica-Worms, D. Kinetics of regulated protein–protein interactions revealed with firefly luciferase complementation imaging in cells and living animals. *Proceedings of the National Academy of Sciences* **2004**, *101* (33), 12288-12293.

(42) Prescher, J. A.; Contag, C. H. Guided by the light: visualizing biomolecular processes in living animals with bioluminescence. *Current opinion in chemical biology* **2010**, *14* (1), 80-89.

(43) Mezzanotte, L.; van't Root, M.; Karatas, H.; Goun, E. A.; Löwik, C. W. In vivo molecular bioluminescence imaging: new tools and applications. *Trends in biotechnology* **2017**, *35* (7), 640-652.

(44) White, E. H.; Steinmetz, M. G.; Miano, J. D.; Wildes, P. D.; Morland, R. Chemi-and bioluminescence of firefly luciferin. *Journal of the American Chemical Society* **1980**, *102* (9), 3199-3208.

(45) Naumov, P.; Ozawa, Y.; Ohkubo, K.; Fukuzumi, S. Structure and spectroscopy of oxyluciferin, the light emitter of the firefly bioluminescence. *Journal of the American Chemical Society* **2009**, *131* (32), 11590-11605.

(46) Li, S.; Hu, R.; Wang, S.; Guo, X.; Zeng, Y.; Li, Y.; Yang, G. Specific imaging of tyrosinase in vivo with 3-hydroxybenzyl caged D-luciferins. *Analytical Chemistry* **2018**, *90* (15), 9296-9300.

(47) Bellini, M.; Riva, B.; Tinelli, V.; Rizzuto, M. A.; Salvioni, L.; Colombo, M.; Mingozzi, F.; Visioli, A.; Marongiu, L.; Frascotti, G. Engineered ferritin nanoparticles for the bioluminescence tracking of nanodrug delivery in cancer. *Small* **2020**, *16* (39), 2001450.

(48) Yuan, Y.; Wang, F.; Tang, W.; Ding, Z.; Wang, L.; Liang, L.; Zheng, Z.; Zhang, H.; Liang, G. Intracellular self-assembly of cyclic d-luciferin nanoparticles for persistent bioluminescence imaging of fatty acid amide hydrolase. *ACS nano* **2016**, *10* (7), 7147-7153.

(49) Tian, X.; Liu, X.; Wang, A.; Lau, C.; Lu, J. Bioluminescence imaging of carbon monoxide in living cells and nude mice based on Pd0-mediated Tsuji–Trost reaction. *Analytical chemistry* **2018**, *90* (9), 5951-5958.

(50) Caceres, G.; Zankina, R.; Zhu, X.; Jiao, J.-a.; Wong, H.; Aller, A.; Andreotti, P. Determination of chemotherapeutic activity in vivo by luminescent imaging of luciferase-transfected human tumors. *Anti-cancer drugs* **2003**, *14* (7), 569-574.

(51) Zhang, Y.; Byun, Y.; Ren, Y. R.; Liu, J. O.; Laterra, J.; Pomper, M. G. Identification of Inhibitors of ABCG2 by a Bioluminescence Imaging–Based High-Throughput Assay. *Cancer research* **2009**, *69* (14), 5867-5875.

(52) Sun, A.; Hou, L.; Prugpichailers, T.; Dunkel, J.; Kalani, M. A.; Chen, X.; Kalani, M. Y.; Tse, V. Firefly luciferase-based dynamic bioluminescence imaging: a noninvasive technique to assess tumor angiogenesis. *Neurosurgery* **2010**, *66* (4), 751-757; discussion 757.

(53) Sadikot, T.; Swink, M.; Eskew, J. D.; Brown, D.; Zhao, H.; Kusuma, B. R.; Rajewski, R. A.; Blagg, B. S.; Matts, R. L.; Holzbeierlein, J. M.; et al. Development of a high-throughput screening cancer cell-based luciferase refolding assay for identifying Hsp90 inhibitors. *Assay Drug Dev Technol* **2013**, *11* (8), 478-488.

(54) Badr, C. E.; Wurdinger, T.; Tannous, B. A. Functional drug screening assay reveals potential glioma therapeutics. *Assay Drug Dev Technol* **2011**, *9* (3), 281-289.

(55) Wang, C.; Du, W.; Zhang, T.; Liang, G. A bioluminescent probe for simultaneously imaging esterase and histone deacetylase activity in a tumor. *Analytical Chemistry* **2020**, *92* (23), 15275-15279.

(56) Sharma, D. K.; Adams, S. T., Jr.; Liebmann, K. L.; Miller, S. C. Rapid Access to a Broad Range of 6'-Substituted Firefly Luciferin Analogues Reveals Surprising Emitters and Inhibitors. *Org Lett* **2017**, *19* (21), 5836-5839.

(57) Burger, A. M.; Fiebig, H.-H. Preclinical screening for new anticancer agents. *Handbook of anticancer pharmacokinetics and pharmacodynamics* **2013**, 23-38.

(58) Ćwiklińska-Jurkowska, M.; Wiese-Szadkowska, M.; Janciauskiene, S.; Paprocka, R. Disparities in Cisplatin-Induced Cytotoxicity—A Meta-Analysis of Selected Cancer Cell Lines. *Molecules* **2023**, *28* (15), 5761.

(59) Fang, J.; Wang, Y.; Li, C.; Liu, W.; Wang, W.; Wu, X.; Wang, Y.; Zhang, S.; Zhang, J. A hypoxia-derived gene signature to suggest cisplatin-based therapeutic responses in patients with cervical cancer. *Comput Struct Biotechnol J* **2024**, *23*, 2565-2579.

Chapter 6 : Conclusion and Future Outlook

6.1 Overall Summary and Conclusions

The primary synthetic target of this project was the preparation of D-thioluciferin, aimed at achieving red-shifted light emission for tumour imaging. A key intermediate in the synthetic route, 2-cyano-6-iodobenzo[d]thiazole **14**, was successfully synthesised using microwave irradiation. However, attempts to substitute the iodine functional group with a thiol group were unsuccessful. As a result, alternative synthetic approaches toward D-thioluciferin had to be explored.

Efforts to repeat the method reported by Pirrung and co-workers were successful up to the penultimate step. Multiple attempts to synthesise 2-cyano-6-mercaptobenzo[d]thiazole **7** via a Mislow-Evans rearrangement were unsuccessful. An in-depth NMR kinetic study revealed that the reaction stalled at the formation of the thiolate salt intermediate **6.2**. It was suggested that a stronger base might be required to cleave the salt from the benzothiazole ring. However, due to time constraints, no further optimisation of this route was pursued.

Given the challenges associated with unmasking the thiol group, the synthesis of the free thiol **7** was identified as a key intermediate en route to D-thioluciferin. Consequently, a new strategy involving 4-(methylthio)aniline was developed for the synthesis of methylthio-luciferins. By applying the thermolysis method previously reported by McCutheon, the synthetic sequence was shortened and the overall yield significantly improved. However, attempts to convert the sulfoxide **20** to the free thiol **7** under reported Pummerer rearrangement conditions were unsuccessful. However, it is hypothesised that the transformation may proceed via a stepwise process rather than a one-pot reaction, as originally described.

Subsequent UV-Vis and fluorescence studies of the methylthio derivatives **19**, **20**, **21** and **22** revealed notable changes in their photophysical properties. Upon oxidation of the sulphide derivatives **19** and **21** to their corresponding sulfoxides **20** and **22**, a hypsochromic shift in λ_{max} was observed in the UV-Vis spectra, accompanied by complete quenching of fluorescence.

6.2 Future Outlook

Given that the primary aim of this study was the synthesis of D-thioluciferin and its subsequent evaluation as a bioluminescent probe for anticancer drug discovery, it was necessary to critically assess the synthetic route toward the target compound. Although literature reports support the application of the Pummerer rearrangement in related systems, the transformation proved unsuccessful when applied to 6-(methylsulfinyl)benzo[d]thiazole-2-carbonitrile **21** for unmasking the C-6 thiol functionality. This limitation is likely attributable to the C-2 nitrile substituent on the benzothiazole ring being sensitive to the strong acidic medium. To potentially circumvent this challenge, a modified approach may be considered in which a chlorine atom is introduced at the C-6 position, as demonstrated by Sharma and co-workers. This would allow for the Pummerer rearrangement to reveal the C-6 thiol group, followed by nucleophilic substitution with potassium cyanide to install the C-2 nitrile moiety (Scheme **6.1**).

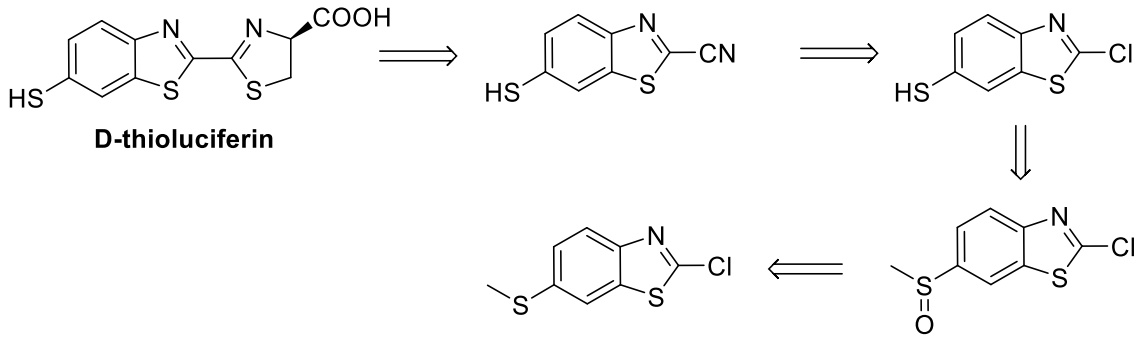

Scheme 6.1. Proposed retrosynthetic pathway to the synthesis of D-thioluciferin incorporating a C-2 chlorine functional group on the benzothiazole ring.

Additionally, new directions were opened in the aza-luciferin series which would possibly allow a future generation of aza D-luciferin analogues with functional group diversity at the C-6 position.

Chapter 7 : Experimental Procedures

7.1 General synthetic procedures

All reactions were carried out in oven-dried glassware under an inert nitrogen atmosphere, unless otherwise stated. Reagents were obtained from commercial sources (Sigma–Aldrich, Merck, Kimix) and used as received unless otherwise stated. Solvents were evaporated under reduced pressure at 40 °C using a Buchi Rotavapor, unless otherwise stated. Reaction temperatures were achieved with heat/silicone oil (for > 25 ºC) and ice/NaCl salt (for 0 and -5 °C). Aqueous solutions were prepared using distilled water. All reactions were monitored by TLC using aluminium-backed Sigma Aldrich silica-gel 60 F254 plates, and compounds were visualised on TLC under a UV-lamp at 254 and 365nm. Normal phase column chromatography was carried out using silica-gel (Fluka Silica Gel 60, 40-63 microns) and compounds eluted with the appropriate solvent mixtures. All compounds were dried under vacuum before yields were determined and spectroscopic analyses performed.

Nuclear Magnetic Resonance (NMR) spectra (^{1}H and ^{13}C) were recorded on a Bruker 400 UltrashieldPlus spectrometer (Bruker Biospin, Rheinstetten, Germany) equipped with a 5 mm BBO probe or a Bruker Avance III 600 MHz NMR spectrometer (Bruker Biospin, Rheinstetten, Germany) equipped with a BBO Prodigy cryoprobe and processed using Bruker processing software (Topspin 4.2.0). All NMR were recorded in $CDCl_3$, CD_3OD or DMSO-d6 as the solvents, unless otherwise stated. Chemical shifts (δ) and J coupling values were reported in units of ppm and Hz respectively. Chemical shifts for ^{1}H and ^{13}C were recorded using tetramethylsilane (TMS) as the internal standard. Assignments were confirmed by COSY or HSQC analysis, when required.

Infrared (IR) spectroscopy was performed on a Perkin-Elmer Spectrum One FT-IR Spectrometer using Attenuated Total Reflectance (ATR) with bond variations measured in reciprocal centimetres (cm^{-1}) and analysed using Microsoft Excel.

Melting points were obtained using a Reichert-Jung Thermovar hot stage microscope (HSM) and are uncorrected.

LCMS analyses were carried out with a UPLC Agilent 1290 Infinity Diode Array Detector FS (Germany), accurate mass spectrometer Agilent 6150 single quadrupole mass spectrometer equipped with an Agilent jet stream ionisation source (positive ionisation mode) (ESI+) and column (Kinetex 1.7µm EVO C18 100Å, 50 x 2.1mm).

7.1.1 Attempted synthesis of D-thioluciferin using the Pirrung *et al* route

(Appel salt) 4,5-Dichloro-1,2,3-dithiazol-1-ium chloride (1)[1]

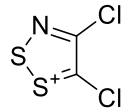

1

Sulfur monochloride (26 mL, 316 mmol), was added to a solution of chloroacetonitrile (4 mL, 63.2 mmol) in DCM (30.0 mL) in a flask equipped with a stopper and gas outlet. The reaction mixture was allowed to swirl for a few seconds and then left to stand for 24 h at room temperature under nitrogen. The resulting brown precipitate that had formed was agitated by stirring for 5 min at room temperature. The precipitate was filtered under vacuum and washed with DCM (4 x 200 mL) to afford Appel's salt as a dark-green solid (8.94 g, 84.3%).

4-(Allylthio)aniline (2)[2]

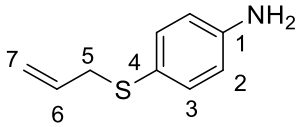

2

Potassium carbonate (4.27 g, 30.9 mmol) was suspended in a solution of 4-aminothiophenol (5.00 g, 39.9 mmol) in acetone (80 mL). Allyl bromide (1.7 mL, 20.0 mmol) was then injected, and the reaction mixture was allowed to stir for 18 h under a nitrogen atmosphere. The mixture was then filtered under vacuum and the solvent removed under reduced pressure. The concentrated filtrate was dissolved in DCM (20 mL) and washed with 1 M NaOH (20 mL), then water (20 mL). The organic layer was collected and dried over $MgSO_4$, filtered and the solvent removed under reduced pressure. The crude residue was subjected to column chromatography on silica gel (10% ethyl acetate / hexane) to afford **2** as a yellow oil (2.99 g, 91%). **R_f = 0.53** with 30% ethyl acetate / hexane. **^{1}H NMR** (600 MHz, $CDCl_3$): δ (ppm) 7.23 (d, J = 8.2 Hz, 2H, H-3), 6.66 (d, J = 8.2 Hz, 2H, H-2), 5.79 – 5.88 (m, 1H, H-6), 5.02 – 4.95 (m, 2H, H-7), 4.05-3.61 (br s, 2H, NH_2), 3.39 (d, J = 7.1 Hz, 2H, H-5). **^{13}C NMR** (100.6 MHz, $CDCl_3$) δ (ppm): 144.8 (C-1), 134.3 (C-3), 131.9 (C-6), 123.8 (C-4), 117.1 (C-7), 116.0 (C-2), 39.7 (C-5).

4-Chloro-5-[(4-(allylthio)phenyl)imino]-5H-1,2,3-dithiazole (3)[2]

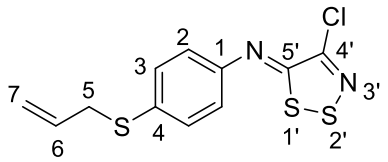

3

Appel's salt (4.98 g, 21.7 mmol) was added to a solution of **1** (2.99 g, 18.1 mmol) in DCM (20 mL). The brown mixture was stirred for 1 h under a nitrogen atmosphere. Anhydrous pyridine (2.94 mL, 36.3 mmol) was added dropwise and the resulting reddish-brown mixture was allowed to stir for an additional 2 h. Thereafter, the solvent was removed under reduced pressure and the crude product was purified by flash chromatography on silica gel (10% ethyl acetate / hexane) with gradient elution to afford compound **3** as a red-orange solid (4.41 g, 81%). **R_f = 0.65** (30% ethyl acetate / hexane). **M.p.**: 77 – 83 °C (lit. 80 – 83 °C).[2] **^{1}H NMR** (600 MHz, $CDCl_3$) δ (ppm) 7.40 (d, J = 8.6 Hz, 2H, H-3), 7.16 (d, J = 8.6 Hz, 2H, H-2), 5.81 – 5.92 (m, 1H, H-6), 5.11 (dd, J = 15.7, 1.2 Hz, 1H, H-7a), 5.07 (dd, J = 10.0, 0.7 Hz, 1H, H-7b), 3.55 (d, J = 6.9 Hz, 2H, H-5). **^{13}C NMR** (100.6 MHz, $CDCl_3$) δ (ppm): 157.8 (C-4'), 148.8 (C-1), 148.2 (C-5'), 134.5 (C-4), 133.3 (C-6), 131.1 (C-2), 120.3 (C-3), 117.9 (C-7), 37.9 (C-5).

***N*-(*p*-(Allylthio)phenyl)cyanothioformamide (4)[2]**

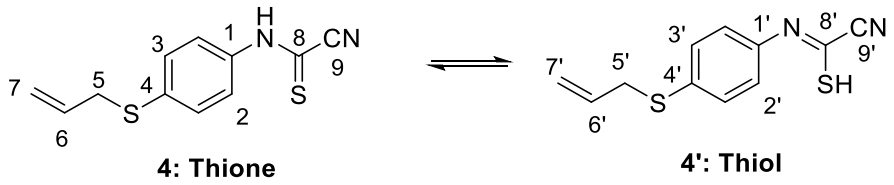

4: Thione **4': Thiol**

A solution of **3** (4.41 g, 18.83 mmol) in dry DCM (40 mL) was cooled to -5 °C. DBU (8.43 mL, 56.50 mmol) was added dropwise followed by stirring for 1 h under a nitrogen atmosphere. The solution was washed thrice with 1 M $NaHSO_4$, water and then brine. The organic layer was dried over anhydrous $MgSO_4$, filtered and the solvent removed under reduced pressure. The crude product was subjected to column chromatography on silica gel (10% ethyl acetate / hexane) elution to obtain the title compound **4** as a dark red solid (1.96 g, 57%). **R_f = 0.54** (30% ethyl acetate / hexane). **Thione**; **^{1}H NMR** (600 MHz, $CDCl_3$) δ (ppm) 9.72 (s, 1H, NH), 7.73 (d, J = 8.5 Hz, 1H, H-3), 7.36 (d, J = 8.5 Hz, 2H, H-2), 5.88 – 5.82 (m, 1H, H-6), 5.18

(dd, J = 11.3, 3.9 Hz, H-7a), 5.11 (dd, J = 6.7, 5.5 Hz, 1H, H-7b), 3.58 (d, J = 6.4 Hz, 2H, H-5). **^{13}C NMR** (100.6 MHz, $CDCl_3$) δ (ppm): 165.2 (C-8), 138.0 (C-1), 134.9 (C-4), 132.92 (C-6), 130.0 (C-3), 122.9 (C-2), 118.4 (C-7), 113.5 (C-9), 36.6 (C-5). **Thiol**; **^{1}H NMR** (400 MHz, $CDCl_3$) δ (ppm) 9.51 (s, 1H, SH), 7.34 (d, J = 8.6 Hz, 1H, H-3'), 7.28 (d, J = 8.5 Hz, 2H, H-2'), 5.86 (m, 1H, H-6'), 5.18 (dd, J = 11.3, 3.9 Hz, H-7a'), 5.11 (dd, J = 6.7, 5.5 Hz, 1H, H-7b'), 3.58 (d, J = 6.4 Hz, 2H, H-5). **^{13}C NMR** (100.6 MHz, $CDCl_3$) δ (ppm): 161.1 (C-8'), 136.9 (C-1'), 134.6 (C-4'), 132.8 (C-6'), 129.5 (C-3'), 122.4 (C-2'), 118.3 (C-7'), 112.0 (C-9'), 36.6 (C-5').

2-Cyano-6-(allylthio)benzo[d]thiazole (5)[2]

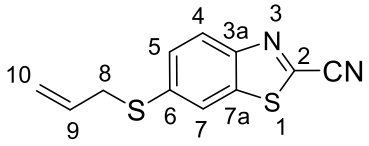

5

N-(*p*-(Allylthio)phenyl)cyanothioformamide **4** (509 mg, 2.13 mmol), palladium chloride (37.8 mg, 0.213 mmol), copper(I) iodide (203 mg, 1.02 mmol) and tetrabutylammonium bromide (1.37 g, 4.26 mmol) was suspended in 1:1 DMF:DMSO (20 mL). The resulting mixture was allowed to stir under nitrogen at 120 °C for 1 h. The reaction mixture was diluted with ethyl acetate (60 mL) and washed four times with water (40 mL). The organic layer was dried over anhydrous $MgSO_4$, filtered and the solvent removed under reduced pressure. The title compound **5** was obtained from the crude residue by column chromatography on silica gel (10% ethyl acetate / hexane) as a dark orange solid (1.12 g, 57%). **R_f = 0.61** (10% ethyl acetate / hexane). **M.p.**: 107 – 111 °C (lit. 102 – 105 °C).[2] **^{1}H NMR** (600 MHz, $CDCl_3$) δ (ppm) 8.10 (d, J = 8.7 Hz, 1H, H-4), 7.84 (s, 1H, H-7), 7.57 (d, J = 8.7 Hz, 1H, H-5), 5.92 (m, 1H, H-9), 5.26 (d, J = 16.7 Hz, 1H, H-10a), 5.17 (d, J = 10.1 Hz, 1H, H-10b), 3.70 (d, J = 6.6 Hz, 2H, H-8). **^{13}C NMR** (100.6 MHz, $CDCl_3$) δ (ppm): 150.4 (C-2), 139.1 (C-3a), 136.3 (C-6), 135.4 (C-7a), 132.5 (C-9), 128.9 (C-4), 125.0 (C-5), 120.2 (C-7), 118.8 (C-10), 113.0 (C≡N), 36.6 (C-8). **FT-IR** (ATR) ν_{max} (cm^{-1}): 2224 (nitrile, -CN).

2-Cyano-6-(allylsulfinyl)benzo[d]thiazole (6)[2]

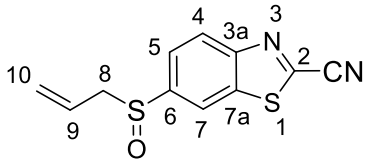

6

A solution of 2-cyano-6-(allylthio)benzothiazole **5** (1.12 g, 4.83 mmol) in 1:5 DCM:MeOH (25 mL) was cooled to 0 °C followed by dropwise addition of a solution of $NaIO_4$ (1.03 g, 4.83 mmol) in water (10 mL). The reaction mixture was allowed to reach room temperature and stirred for 10 h. The solvent was then removed under reduced pressure. Water (50 mL) was added, and the mixture was extracted thrice with ethyl acetate (30 mL). The organic layer was dried over $MgSO_4$, filtered, and concentrated under reduced pressure. The title compound **6** was isolated from this residue by column chromatography on silica gel (50% ethyl acetate/hexanes) as an off-white solid (978 mg, 82%). $\mathbf{R_f}$ **= 0.19** with 50% ethyl acetate/hexanes. **^{1}H NMR** (600 MHz, $CDCl_3$) δ (ppm) 8.33 (d, J = 1.1 Hz, 1H, H-7), 8.30 (d, J = 8.6 Hz, H-4), 7.69 (dd, J = 8.6, 1.6 Hz, 1H, H-5), 5.62 (m, 1H, H-9), 5.33 (dd, J = 10.1 Hz, 1H, H-10a), 5.16 (dd, J = 17.0, 1.0 Hz, H-10b), 3.68 (dd, J = 13.0, 7.4 Hz, 1H, H-8a), 3.54 (dd, J = 13.0, 7.5 Hz, 1H, H-8b). **^{13}C NMR** (100.6 MHz, $CDCl_3$) δ (ppm): 153.7 (C-2), 144.3 (C-3a), 138.8 (C-6), 136.1 (C-7a), 125.7 (C-4), 124.7 (C-5), 124.3 (C-7), 123.4 (C-9), 118.8 (C-10), 112.5 (C≡N), 60.7 (C-8). **FT-IR** (ATR) ν_{max} (cm^{-1}): 2228 (nitrile, -CN), 1046 (sulfoxide, -S=O).

2-Cyano-6-mercaptobenzo[d]thiazole (7)[2]

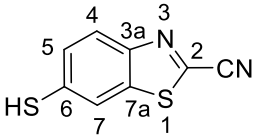

7

Triphenylphosphite (360 µL, 1.37 mmol) was added to a solution of 2-cyano-6-(allylsulfinyl)benzothiazole **6** (34.0 mg, 0.137 mmol) in THF (2 mL). The resulting mixture was heated at reflux under nitrogen for 16 h. Water (1 mL) was added and the reaction mixture was allowed to stir for 30 min. This mixture was extracted twice with diethyl ether (8 mL). The combined organic phase was washed twice with brine (10 mL), dried over anhydrous $MgSO_4$,

filtered through celite, and concentrated under reduced pressure. The title compound **7** was isolated from this residue by column chromatography on silica gel (ethyl acetate/hexanes gradient) as a yellow oil 151.2 mg (crude, largely triphenyl phosphate). **R_f = 0.50** (20% ethyl acetate/hexane). **MS (ESI+)**: *m/z* Calculated for $C_8H_5N_2S_2$ $[M+H]^+$192.99, found 193.00.

7.1.2 Model Study

2-Benzo[d]thiazole -2,2-dibromoacetonitrile (9)

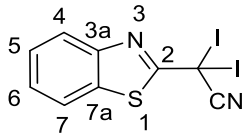

9

NaI (0.253g, 1.68 mmol, 2.8 eq) and $NaBO_3.4H_2O$ (0.265 g, 2.25 mmol, 3.77 eq.) were suspended in acetic acid (5 mL) whilst allowed to stir at room temperature under a nitrogen atmosphere. The resulting solution was added dropwise to a suspension of 2-(benzo[d]thiazol-2-yl)acetonitrile (0.104 g, 0.597 mmol, 1 eq) in acetic acid (3 mL) at 0 °C. The reaction mixture was maintained at 5 °C throughout the addition. Thereafter, it was allowed to warm to room temperature and left to stir overnight. The reaction mixture was poured into chilled water and the resulting precipitate filtered and washed with 50 mL of chilled water to afford **9** as a brown solid (98.7 mg, 30%). **^{1}H NMR** (600 MHz, $CDCl_3$): δ (ppm) 8.39 – 8.18 (m, 1H, H-4), 8.10 – 7.90 (m, 1H, H-7), 7.75 – 7.50 (m, 2H, H-5,6). **FT-IR** (ATR) ν_{max} (cm^{-1}): 2227 (nitrile, -CN).

2-Benzo[d]thiazole-2,2-dibromoacetonitrile (10)

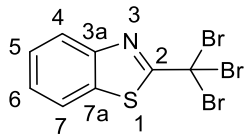

10

KBr (0.202g, 1.70 mmol, 2.8 eq) and $NaBO_3.4H_2O$ (0.269 g, 1.75 mmol, 2.9 eq) were suspended in acetic acid (5 mL) whilst allowed to stir at room temperature under a nitrogen atmosphere. The resulting solution was added dropwise to a suspension of 2-(benzo[d]thiazol-2-yl)acetonitrile (0.105 g, 0.602 mmol, 1 eq) in acetic acid (3 mL) at 0 °C. The reaction mixture was maintained at 5 °C throughout the addition. Thereafter, it was allowed to warm to room

temperature and left to stir overnight. The reaction mixture was poured into chilled water and the resulting precipitate filtered and washed with 50 mL of chilled water. The crude material was purified by silica gel chromatography eluting with hexanes to afford the corresponding 2-benzothiazole-2,2-dibromoacetonitrile **10** as a light brown solid (0.140 g, 75%). $\mathbf{R_f = 0.70}$ (20% ethyl acetate / hexane). **^{1}H NMR** (600 MHz, $CDCl_3$): δ (ppm) 8.14 (d, *J* = 8.2 Hz, 1H, H-4), 7.92 (d, *J* = 8.1 Hz, 1H, H-7), 7.67 – 7.47 (m, 2H, H-6, H-5). **^{13}C NMR** (100.6 MHz, $CDCl_3$) δ (ppm): 165.6 (C-2), 151.8 (C-3a), 137.1 (C-7a), 127.7 (C-6), 127.7 (C-5), 125.2 (C-4), 122.0 (C-7), 22.9 (C-Br_3). **FT-IR** (ATR) ν_{max} (2250 cm^{-1}): (nitrile, -CN).

7.1.3 *p*-Iodoaniline synthetic route

2-Bromo-4-iodoaniline (11)[3]

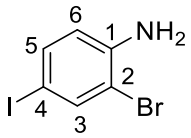

11

KBr (2.82 g, 21 mmol, 1 eq) and $NaBO_3$ (3.65 g, 21 mmol, 1 eq) were suspended and left to stir in acetic acid (11 mL) at room temperature. The resulting solution was added dropwise to a suspension of *p*-iodoaniline (4.54 g, 21 mmol, 1 eq) in acetic acid (3 mL) cooled to below 0 °C. The reaction mixture was maintained below 0 °C throughout the addition. Thereafter, it was allowed to equilibrate to room temperature and left to stir overnight. The reaction mixture was poured into chilled water and the resulting precipitate filtered and washed with copious amounts of water (4 x 100 mL) to afford the brominated product **11** as a brown solid (6.01, 96.4%). **^{1}H NMR** (600 MHz, DMSO): δ (ppm) 7.58 (d, *J* = 1.9 Hz, 1H, H-3), 7.30 (dd, *J* = 8.5, 2.0 Hz, 2H, H-5), 6.61 (d, *J* = 8.5 Hz, H-6), 5.44 (s, 1H, NH_2). **^{13}C NMR** (100.6 MHz, $CDCl_3$) δ (ppm): 146.0 (C-1), 139.3 (C-3), 137.0 (C-5), 117.8 (C-6), 108.7 (C-2), 76.3 (C-4). **MS (ESI+)**: *m/z* Calculated for C_6H_6NBrI $[M+H]^+$ 297.92, found 298.9.

(*Z*)-*N*-(2-bromo-4-iodophenyl)-4-chloro-5*H*-1,2,3-dithiazol-5-imine (12)

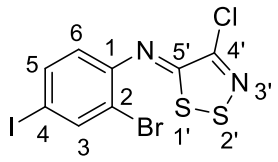

12

Method A: 2-Bromo-4-iodoaniline **11** (49.3 mg, 0.165 mmol) was added to DCM (6 mL) and Appel's salt (35.1 mg, 0.168 mmol). The solution was cooled to 0 °C and DBU (25.0 µL, 0.167 mmol) was added dropwise to the reaction mixture. The reaction mixture was allowed to stir for 24 hrs at room temperature under a nitrogen atmosphere. Thereafter, the reaction mixture was washed with water and extracted with ethyl acetate. The organic layer was dried over anhydrous $MgSO_4$, filtered through celite and the solvent removed under reduced pressure. The crude product was purified via column chromatography eluting with hexanes to afford the dithiazole **12** as a yellow solid (12.3 mg, 17.2%).

Method B: Appel's salt **1** (1.25g, 6.00 mmol) was added to a solution of 2-bromo-4-iodoaniline **11** (0.613 g, 0.547 mmol) in DCM (20 mL) in a 100 mL round-bottom flask. The reaction mixture was allowed to stir for 4.5 hrs at room temperature under a nitrogen atmosphere. Pyridine (0.8 mL, 9.91 mmol) was added slowly, and the resulting mixture was left to stir overnight. The solvent was removed under reduced pressure. The crude mixture was purified via column chromatography eluting with hexanes, to afford the dithiazole **12** as a yellow solid (19.7 mg, 0.76%). **R_f = 0.70** (15% ethyl acetate / hexane). **^{1}H NMR** (300 MHz, $CDCl_3$): δ (ppm) 8.02 (s, 1H, H-3), 7.69 (d, J = 8.3 Hz, 1H, H-5), 6.88 (d J = 8.1 Hz, 1H, H-6). **^{13}C NMR** (100.6 MHz, $CDCl_3$) δ (ppm): 161.5 (C-5'), 150.0 (C-4'), 147.6 (C-1), 141.9 (C-3), 138.0 (C-5), 119.8 (C-6), 116.6 (C-2), 89.9 (C-4). **FT-IR** (ATR) ν_{max} (cm^{-1}): 1690 (imine, C=N).

(*Z*)-(2-bromo-4-iodophenyl)carbonocyanidimidothioic acid / (2-bromo-4 iodophenyl)carbamothioyl cyanide (13)

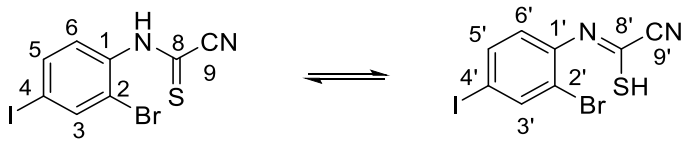

13: Thione **13': Thiol**

Method A: To a solution of 2-bromo-4-iodoaniline **11** (102.8 mg, 0.345 mmol) in DCM (10 ml) was added Appel's salt (82.3 mg, 0.395 mmol).The reaction mixture was allowed to stir for 15 min and then cooled to 0 °C. DBU (150.4 µL, 1.01 mmol) was added dropwise and the reaction was allowed to stir overnight. Thereafter, the reaction mixture was heated under reflux for 2 h at 40 °C. The crude mixture was washed with water and extracted with ethyl acetate. The organic layer was dried over anhydrous $MgSO_4$, filtered through celite and the solvent removed under reduced pressure. The title compound was purified by column chromatography eluting with ethyl acetate as a red solid (31.4 mg, 24.80 %).

Method B: Appel's salt (2.15 g, 10.3 mmol) was added to a solution of 2-bromo-4-iodoaniline **11** (3.00 g, 10.1 mmol) in DCM (20 mL) in a 100 mL round-bottom flask. The reaction mixture was allowed to stir for 1.5 hrs at room temperature under a nitrogen atmosphere. Anhydrous pyridine (1.6 mL, 20.2 mmol) was added slowly, and the resulting mixture was left to stir overnight. Thereafter, DCM and pyridine was removed under reduced pressure. Subsequently, 120 mg of the crude material in anhydrous DCM (2 mL) was cooled to below 0 °C. DBU (123.8 µL, 0.830 mmol) was added slowly and the reaction was left to stir for 1 hr under a nitrogen atmosphere. The solution was dissolved in ethyl acetate (2 mL), washed thrice with $NaHSO_4$ (1 mL), twice with water (1.5 mL) and once with brine (2 mL). The organic layer was dried over Na_2SO_4, filtered through celite and the solvent removed under reduced pressure. The crude product was purified via column chromatography to afford the cyanothioformamide **13** as a red solid (27.8 mg, 27%). **R_f = 0.20** (15% ethyl acetate / hexane). **^{1}H NMR** (300 MHz, $CDCl_3$): δ (ppm) 9.38 (s, 1H, SH/NH), 8.18 (d, *J* = 8.4 Hz, 1H, H-5), 8.04 (s, 1H, H-3), 7.72 (d, *J* = 8.4 Hz, 1H, H-6). **FT-IR** (ATR) ν_{max} (cm^{-1}): 2226 (nitrile, -CN).

2-Cyano-6-iodobenzo[d]thiazole (14)[3]

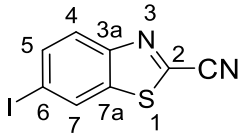

14

Method A: To a solution of crude imine **12** (505.1 mg, 1.17 mmol) in anhydrous pyridine (10.5 ml) was added copper iodide (221.6 mg, 1.16 mmol) followed by heating under microwave irradiation (400W) at 115 °C for 30 min at atmospheric pressure. Pyridine was removed under reduced pressure and the resulting dark residue was dissolved in ethyl acetate (40 mL) and washed with a saturated solution of sodium thioacetate (4 x 20 mL) and brine (1 x 20 mL). The organic layer was dried over sodium thiosulphate, filtered through celite and solvent removed under reduced pressure. The crude product was purified via column chromatography on silica gel to afford **14** as a pale yellow solid (25.8 mg, 59.17%).

Method B: A solution of purified imine **12** (478.9 mg, 1.10 mmol) and copper iodide (210.8 mg, 1.11 mmol) in sulfolane (11 mL) was heated under microwave irradiation (400W) whilst stirring at 115 °C for 30 min at atmospheric pressure.[4] The dark solution was dissolved in ethyl acetate (40 mL) and washed with a saturated solution of sodium thioacetate (4 x 20 mL) and brine (1 x 20 mL). The organic layer was dried over anhydrous magnesium sulphate, filtered through celite and solvent removed under reduced pressure. The crude product was purified via column chromatography on silica gel to afford **14** as a pale yellow solid (169.3 mg, 53.61%). **R_f = 0.42** (10% diethyl ether / petroleum ether). **^{1}H NMR** (300 MHz, $CDCl_3$): δ (ppm) 8.14 (s, 1H, H-7), 8.08 (d, J = 8.7 Hz, 1H, H-4), 7.76 (d, J = 8.7 Hz, 1H, H-5). **^{13}C NMR** (100.6 MHz, $CDCl_3$) δ (ppm):151.6 (C-2), 137.4 (C-7), 136.9 (C-3a), 131.9 (C-7a), 130.5 (C-4a), 124.5 (C-5), 112.6 (C≡N), 94.4 (C-6). **FT-IR** (ATR) ν_{max} (cm^{-1}): 2250 (nitrile, -CN). **MS (ESI+)**: *m/z* Calculated for C_8H_4NSI $[M+H]^+$ 286.91, found 286.91.

6-Iodobenzo[d]thiazole-2-carbothialdehyde (15)

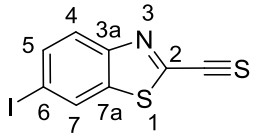

15

A mixture of 2-cyano-6-iodobenzothiazole **14** (38.5 mg, 0.135 mmol), CuI (2.5 mg, 0.0135 mmol), 1,10-phenanthroline (4.3 mg, 0.0269 mmol) and potassium thioacetate (50.3 mg, 0.440 mmol) in toluene (7 mL) was heated under reflux at 110 °C for 48 h under a nitrogen atmosphere. The reaction mixture was allowed to cool to room temperature and quenched with water. The organic material was extracted with diethyl ether (x2). The combined organic phase was dried over Na_2SO_4, filtered through celite and the solvent removed under reduced pressure. The title compound was purified via column chromatography on silica gel, eluting with 70% ethyl acetate/hexane to afford the product **15** as a dark solid (21.5 mg, 52.24%). **^{1}H NMR** (600 MHz, $CDCl_3$): δ (ppm) 7.54 (d, *J* = 8.6 Hz, 1H, H-4), 7.36 (t, *J* = 1.8 Hz, 1H, H-7), 7.13 (dd, *J* = 8.6, 2.5 Hz, 1H, H-5). **FT-IR** (ATR) ν_{max} (cm^{-1}): 1696 (C=N). **MS (ESI+)**: *m/z* Calculated for $C_8H_4NS_2I$ $[M+H]^+$ 304.88, found 304.9.

7.1.4 Pyridyl series

(*Z*)-4-chloro-*N*-(2,6-dichloropyridin-3-yl)-5*H*-1,2,3-dithiazol-5-imine (16)[5]

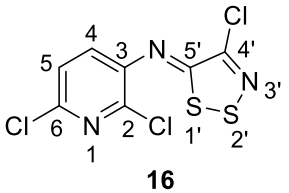

16

Appel's salt (882 mg, 3.18 mmol) was added to a solution of 3-amino-2,6-dichloropyridine (950 g, 3.18 mmol) in DCM (30 mL) in a 100 mL round-bottom flask. The reaction mixture was allowed to stir for 1 h at room temperature under a nitrogen atmosphere. Pyridine (0.5 mL, 6.36 mmol) was added slowly, and the resulting mixture was left to stir for 2 h. The solvent was removed under reduced pressure. The crude mixture was purified via column chromatography eluting with petroleum ether, to afford the dithiazole **16** as a yellow solid (411.8 mg, 62 %). **R_f = 0.70** (20% diethyl ether / pet ether). **^{1}H NMR** (300 MHz, $CDCl_3$): δ (ppm) 7.44 (d, *J* = 8.1 Hz, 1H, H-5), 7.35 (d, *J* = 8.1 Hz, 1H, H-4). **^{13}C NMR** (100.6 MHz,

$CDCl_3$) δ (ppm): 163.3 (C-5'), 147.6 (C-4'), 146.4 (C-6), 144.0 (C-2), 141.7 (C-3), 130.0 (C-4), 124.2 (C-5). **FT-IR** (ATR) ν_{max} (cm^{-1}): 1690 (imine, C=N).

5- chlorothiazolo[5,4-b]-pyridine-2-carbonitrile (17)[5]

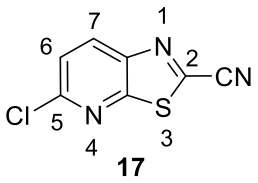

17

Method A: To a solution of 3-amino-2,6-dichloropyridine (50.6 mg, 0.310 mmol) in DCM (5 ml) was added Appel's salt (77.6 mg, 0.372 mmol). The reaction mixture was cooled to below 5 °C and DBU (45.8 µL, 0.306 mmol) was added. The reaction mixture was raised to room temperature and allowed to stir overnight. The solvent was then removed under reduced pressure. An additional two equivalents of DBU (91.6 µL, 0.612 mmol) was added and the reaction mixture was left to heat under reflux at 81 °C in DMSO overnight. The title compound **17** was purified by column chromatography, eluting with hexanes as a colourless solid (15 mg, 16.9 %).

Method B: A stirred solution of (*Z*)-4-chloro-*N*-(2,6-dichloropyridin-3-yl)-5*H*-1,2,3-dithiazol-5-imine **16** (10.8 mg, 0.0362 mmol) and copper iodide (6.1 mg, 0.0320 mmol) in anhydrous pyridine (10.5 mL) was heated at 115 °C for 30 min.[4] The dark solution was dissolved in ethyl acetate (3 mL) and washed with a saturated solution of sodium thioacetate (1.5 mL) and brine (1 mL). The organic layer was dried over sodium sulphate, filtered through celite and solvent removed under reduced pressure. The crude product was purified via column chromatography on silica gel to afford **17** as a colourless solid (1.73 mg, 24.4 %). $\mathbf{R_f}$ **= 0.70** (20% hexane / DCM). **^{1}H NMR** (300 MHz, $CDCl_3$): δ (ppm) 8.42 (d, *J* = 8.6 Hz, 1H, H-7), 7.62 (d, *J* = 8.6 Hz, 1H, H-6). **MS (ESI+)**: *m/z* Calculated for $C_7H_3N_3SCl$ $[M+H]^+$ 195.97, found 196.0.

7.1.5 Improved synthesis of thioether luciferins

(*Z*)-4-chloro-*N*-(4-(methylthio)phenyl)-5*H*-1,2,3-dithiazol-5-imine (18)

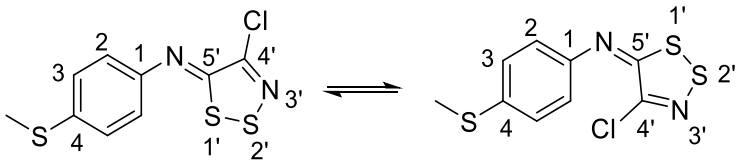

18

Appel's salt (157.6 mg, 0.756 mmol) and 4-(methylthio)aniline (105.0 mg, 0.754 mmol) were allowed to stir in DCM (10 mL) at rt for 1 hr. Thereafter, anhydrous pyridine (0.12 mL, 1.51 mmol, 2 eq) was added and left to stir for 2 h at rt under a nitrogen atmosphere. The crude material was subjected to column chromatography on silica gel with the desired product eluting with 20% diethyl ether / pet ether. The title compound **18** was isolated from the brown residue by column chromatography on silica gel (20% diethyl ether/pet ether) as a yellow solid (148.6 mg, 71.7 %). **R_f = 0.7** (20% diethyl ether/petroleum ether). **^{1}H NMR** (400 MHz, $CDCl_3$) δ (ppm) 7.33 (d, J = 8.7 Hz, 2H, H-3), 7.21 (d, J = 8.7 Hz, 2H, H-2), 2.52 (s, 3H, SMe).

6-(methylthio)benzo[d]thiazole-2-carbonitrile (19)[6]

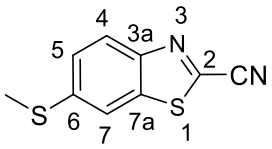

19

Appel's salt (6.55g, mmol) was added to a solution of 4-(methylthio)aniline (5.09 g, 24.7 mmol) in DCM (100 mL) in a 250 mL round-bottom flask. The reaction mixture was allowed to stir for 1 h at room temperature under a nitrogen atmosphere. Anhydrous pyridine (2.90 mL, 35.9 mmol) was added slowly, and the resulting mixture was left to stir for an additional 2 h. The solvent was removed under reduced pressure. Sulfolane (70 mL) was added and the resultant mixture was heated at 180 °C for 30 min. The crude mixture was dissolved in ethyl acetate and washed with a saturated solution of ammonium chloride and then water. The mixture was left to separate overnight. The organic layer was dried over Na_2SO_4, filtered through celite and solvent removed under reduced pressure. The brown residue was subjected to column chromatography to afford **19**, eluting with 20% diethyl ether / petroleum ether as an orange solid (5.94 mg, 78.8 %). **R_f = 0.50** (40% diethyl ether / petroleum ether). **^{1}H NMR**

(400 MHz, $CDCl_3$): δ (ppm): 8.06 (d, *J* = 8.8 Hz, 1H, H-4), 7.71 (d, *J* = 1.6 Hz, 1H, H-7), 7.49 (dd, *J* = 8.8, 1.6 Hz, 1H, H-5), 2.58 (s, 3H, SMe). **^{13}C NMR** (100.6 MHz, $CDCl_3$) δ (ppm): 149.9 (C-2), 141.7 (C-3a), 136.8 (C-6), 134.9 (C-7a), 126.9 (C-5), 125.0 (C-4), 116.9 (C-7), 113.2 (C-7), 15.8 (SMe). **FT-IR** (ATR) ν_{max} (cm^{-1}): 2226-(C≡N), 1579 (-C=N). **MS (ESI+)**: *m/z* Calculated for $C_9H_7N_2S_2$ $[M+H]^+$ 207.00, found 207.1. UV (ethanol) λ_{max} = 343 nm. Fluorescence (ethanol) λ_{ex} = 343 nm, λ_{em} = 450 nm.

(*S*)-2-(6-(methylthio)benzo[d]thiazol-2-yl)-4,5-dihydrothiazole-4-carboxylic acid (20)[6]

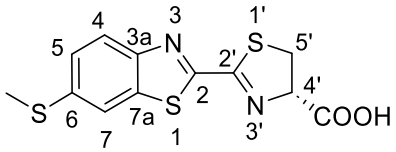

20

D-cysteine hydrochloride monohydrate (17.5 mg, 0.0996 mmol) and 6-(methylthio)benzo[d]thiazole-2-carbonitrile **19** (19.1 mg, 0.0926 mmol) were suspended in in 2:1 MeOH:H_2O (1 mL). K_2CO_3 (13.8 mg, 0.0998 mmol) was added and the yellow solution was allowed to stir under nitrogen overnight. Methanol was removed under reduced pressure and the remaining solution was acidified to pH 4 using 1 M HCl. The solution was then washed with water and the product extracted with ethyl acetate. The organic layer was dried over Na_2SO_4, filtered through celite and solvent removed under reduced pressure to afford **20** as a yellow solid (24.3 mg, 84.6%). **R_f = 0.01** (40% diethyl ether / petroleum ether). **^{1}H NMR** (400 MHz, $CDCl_3$): δ (ppm) 8.03 (d, *J* = 8.7 Hz, 1H, H-4), 7.73 (d, *J* = 1.4 Hz, 1H, H-7), 7.43 (dd, *J* = 8.7, 1.6 Hz, 1H, H-5) 5.44 (t, *J* = 9.7 Hz, 1H, H-4'), 3.81 (dd, *J* = 9.6, 1.7 Hz, 2H, H-5'), 2.58 (s, 3H, SMe). **^{13}C NMR** (100.6 MHz, $CDCl_3$) δ (ppm): 171.2 (COOH), 164.5 (C-2'), 159.2 (C-3a), 150.1 (C-2), 138.9 (C-7a), 136.7 (C-6), 125.7 (C-4), 123.9 (C-5), 118.2 (C-7), 78.1 (C-4'), 34.8 (C-5'), 14.8 (SMe). **FT-IR** (ATR) ν_{max} (cm^{-1}): 1727 (C=O). **MS (ESI+)**: *m/z* Calculated for $C_{12}H_{11}N_2O_2S_2$ $[M+H]^+$ 310.99, found 311.0. UV (H_2O) λ_{max} = 346 nm. Fluorescence (H_2O) λ_{ex} = 346 nm, λ_{em} = 500 nm.

6-(methylsulfinyl)benzo[d]thiazole-2-carbonitrile (21)[6]

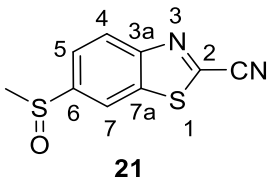

21

Method A: A solution of **19** (494.9 mg, 2.40 mmol) in 1:5 DCM:MeOH (3.5 mL) was cooled to 0 °C followed by the dropwise addition of a solution of $NaIO_4$ (515.7 mg, 2.41 mmol) in water (0.5 mL).[2] The reaction mixture was allowed to reach room temperature and allowed to stir for 12 h. Solvent was removed under reduced pressure. Water was added and the mixture was extracted twice with ethyl acetate. The organic layer was dried over anhydrous Na_2SO_4, filtered through celite and solvent removed under reduced pressure. The title compound was purified via column chromatography on silica gel (50% ethyl acetate/hexane) to afford **21** as an off-white solid (265.4 mg, 49.7 %).

Method B: To a solution of 6-(methylthio)benzo[d]thiazole-2-carbonitrile **19** (102.8 mg, 0.498 mmol) in DCM (4 mL) was added *m*-CPBA (84.4 mg, 0.491 mmol).[6] The resulting opaque solution was left to stir overnight. The solution was then diluted with ethyl acetate (20 mL) and washed with a saturated solution of sodium bicarbonate (2 x 10 mL). The organic layer was dried over Na_2SO_4, filtered through celite and solvent removed under reduced pressure. The title compound **21** was isolated from this yellow residue by column chromatography on silica gel (50% ethyl acetate/hexanes) as an off-white solid (83.4 mg, 75%). **R_f = 0.19** (40% ethyl acetate/hexanes). **^{1}H NMR** (400 MHz, $CDCl_3$) δ (ppm) 8.44 (d, J = 1.4 Hz, 1H, H-7), 8.35 (d, J = 8.5 Hz, 1H, H-4), 7.75 (dd, J = 8.5, 1.6 Hz, 1H, H-5), 2.82 (s, 3H, S(=O)Me). **^{13}C NMR** (100.6 MHz, $CDCl_3$) δ (ppm): 153.7 (C-6), 147.1 (C-2), 139.0 (C-3a), 136.4 (C-7a), 126.2 (C-4), 122.9 (C-5), 118.0 (C-7), 112.6 (C≡N), 44.3 (S(=O)Me). **FT-IR** (ATR) ν_{max} (cm^{-1}): 2228 (nitrile, -CN), 1056 (sulfoxide, -S=O). **MS (ESI+)**: *m/z* Calculated for $C_9H_7N_2OS_2$ $[M+H]^+$ 222.99, found 223.0. UV (ethanol) λ_{max} = 299 nm.

(*S*)-2-(6-((*S*)-methylsulfinyl)benzo[d]thiazol-2-yl)-4,5-dihydrothiazole-4-carboxylic acid (22)[6]

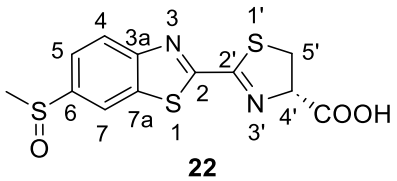

22

D-cysteine hydrochloride monohydrate (14.0 mg, 0.0797 mmol) and **21** (17.5 mg, 0.0787 mmol) were suspended in in 2:1 MeOH:H_2O (3 mL). K_2CO_3 (11.4 mg, 0.0825 mmol) was added and the solution was allowed to stir under nitrogen for 30 min. Methanol was removed under reduced pressure and the remaining solution was acidified to pH 4 using 1 M HCl. The solution was then washed with water and the product extracted with ethyl acetate. The organic layer was dried over anhydrous Na_2SO_4, filtered through celite and solvent removed under reduced pressure to afford **22** as a white solid (12.8 mg, 49.8%). **R_f = 0.01** (40% diethyl ether / petroleum ether). **^{1}H NMR** (400 MHz, 1:1 $CDCl_3$: CD_3OD): δ (ppm) 8.04 (s, 1H, H-7), 7.92 (d, *J* = 8.5 Hz, 1H, H-4), 7.43 (dd, *J* = 8.5 Hz, 1H, H-5) 5.08 (t, *J* = 9.6 Hz, 1H, H-4'), 3.47 (dd, *J* = 9.6, 4.3 Hz, 2H, H-5'a), 3.03 2.95 (m, 1H, 5-5'b), 2.52 (s, 3H, S(=O)Me). **^{13}C NMR** (100.6 MHz, 1:1 $CDCl_3$: CD_3OD) δ (ppm): 171.3 (COOH), 165.8 (C-2'), 163.1 (C-2), 154.3 (C-3a), 143.3 (C-6), 136.5 (C-7a), 124.8 (C-4), 121.4 (C-5), 117.9 (C-7), 77.9 (C-4'), 42.8 (C-5'), 34.7 (S(=O)Me). **FT-IR** (ATR) ν_{max} (cm^{-1}): 1727 (C=O). **MS (ESI+)**: *m/z* Calculated for $C_{12}H_{11}N_2O_3S_2$ [M+H] 326.99, found 327.0. UV (H_2O) λ_{max} = 308 nm.

7.2 General assay procedures

UV-vis Experiments (absorption spectra)

Absorption spectra for 6-(methylthio)benzo[d]thiazole and its derivatives were recorded with a Varian Cary 60 UV-Vis spectrophotometer, instrument version 2.00, using 1cm path length quartz cell cuvettes. Benzothiazole samples were prepared as a 0.1 mM ethanol solution and luciferin samples were prepared as a 0.1 mM H_2O solution unless otherwise stated. These samples were scanned from 200 nm to 800 nm. Data were analysed using Origin Software.

Fluorescence Spectrophotometry (excitation emission spectra)

Excitation and emission spectra were recorded on a TECAN infinite M200 fluorometer using a NanoQuant plate. Emission spectra were recorded at an excitation wavelength corresponding

to previously recorded absorption maxima. The compound 6-(methylthio)benzo[d]thiazole and its luciferin derivative were prepared as 0.01 mM ethanol and H_2O solutions respectively while 6-(methylsulfinyl)benzo[d]thiazole and its luciferin derivative were prepared as 0.1 mM ethanol and H_2O solutions respectively. These solutions were scanned from 280 nm to 850 nm (Ex. Slit/ Em. Slit 5 nm). Number of flashes = 25. Data were analysed using Origin Software.

Cell culture

HeLa (HPV 18-positive cervical cancer) cell lines were cultured in Dulbecco's modified Eagle's medium (DMEM, Gibco, Life Technologies/Thermo Fisher Scientific, USA) and the CaSki (HPV 16-positive cervical cancer) cell line was cultured in Roswell Park Memorial Institute medium (RPMI, Gibco, Life Technologies/Thermo Fisher Scientific, USA), with both media supplemented with 10% heat-inactivated fetal bovine serum (FBS, Gibco, USA), 100 U/ml penicillin and 100 µg/ml streptomycin (Gibco, USA). All cells were maintained in an incubator at 37 °C containing 5% carbon dioxide. Medium was replaced every 2 to 3 days and cells were routinely subjected to mycoplasma tests. Only mycoplasma free cells were used in experiments. Cell lines were purchased from the American Type Culture Collection (ATCC) and authenticated using short tandem repeat fingerprinting by Inqaba Biotechnical Industries (Pty) (Pretoria, South Africa).

Cell treatments

Making stock solutions

Compounds were prepared in 100% DMSO (Sigma Aldrich, Missouri, USA) to give a stock solution of 5 mM, using the following formula:

$$Volume\ (L) = \frac{\left(\frac{Mass\ (g)}{Molecular\ weight\ (g.mol^{-1})}\right)}{Concentration\ (10\ \text{x}\ 10^{-3}\ M)}$$

The stock solutions were stored at -20ºC and the stock solutions were subsequently diluted with working cell culture media to the desired final concentration and a vehicle control of the same DMSO concentration was also prepared.

MTT (3-(4,5-dimethylthiazol-2-yl)-2,5-diphenyltetrazolium bromide) assay

Cell viability was measured using the 3-(4,5-dimethylthiazol-2-yl)-2,5-diphenyl-trazolium bromide (MTT) assay which is based on the ability of metabolically active cells to metabolise the yellow tetrazolium salt, MTT, to purple formazan crystals by mitochondrial succinate dehydrogenase. An MTT kit (Roche, Switzerland) was used according to the manufacturer's instructions or MTT (M2128, Sigma Aldrich, Missouri, USA) and solubilising reagents were made up in the lab. Cells were seeded in 96-well plates and treated the next day at a confluency of 60%. Cells were treated with 10µM or 100µM of drug and 10µM or 100µM vehicle (DMSO). After treatment for 48 hours, images were taken using an EVOS M5000 Imaging System microscope (Thermo Fisher Scientific, USA). 48 hours later, 10µl of MTT reagent was added to each well and left to incubate for 4h followed by overnight incubation with 100µl solubilising reagent after which absorbance was measured at 585nm using a spectrophotometer (RT-2100C Microplate Reader, China). Wells with medium and drug only (no cells) were used as a blank. Mean cell viability for each treatment condition was calculated as a percentage of the mean vehicle control. At least three independent experiments in quadruplicate were performed.

Immunofluorescence

Cells were plated on glass coverslips and post treatment they were fixed with ice-cold 100% methanol at -20°C for 5min followed by 1XPBS washes and blocking and permeabilization with 0.2% Triton-X-100 (Sigma Aldrich, USA) and 5% BSA in 1XPBS for 30min at RT. Cells were imaged with an LSM 510, 710 or 880 confocal microscopes (Zeiss, Germany) using a Plan-Apochromat 63x/1.40 Oil DIC objective. In most cases, multiple z layers were acquired with 1µm step width, images were processed using ZEN 2012 imaging software (Zeiss, Germany) and maximum intensity projections were generated.

7.3 References

(1) Appel, R.; Janssen, H.; Siray, M.; Knoch, F. Synthese und Reaktionen des 4,5-Dichlor-1,2,3-dithiazolium-chlorids. *Chemische Berichte* **1985**, *118* (4), 1632-1643.

(2) Pirrung, M. C.; Carlson, A. D.; De Howitt, N.; Liao, J. Synthesis and bioluminescence of thioluciferin. *Bioorg Med Chem Lett* **2019**, *29* (19), 126591.

(3) Rylands, M. PhD thesis, unpublished. University of Cape Town, **2018**.

(4) Deau, E.; Dubouilh-Benard, C.; Levacher, V.; Besson, T. Microwave-assisted synthesis of novel N-(4-phenylthiazol-2-yl)-benzo[d]thiazole-, thiazolo[4,5-b]pyridine-, thiazolo[5,4-b]pyridine- and benzo[d]oxazole-2-carboximidamides inspired by marine topsentines and nortopsentines. *Tetrahedron* **2014**, *70* (35), 5532-5540.

(5) Koutentis, P. A.; Koyioni, M.; Michaelidou, S. S. The conversion of [(4-chloro-5H-1,2,3-dithiazol-5-ylidene)amino]azines into azine fused thiazole-2-carbonitriles. *Organic & Biomolecular Chemistry* **2013**, *11* (4), 621-629, 10.1039/C2OB26993G.

(6) Sharma, D. K.; Adams, S. T., Jr.; Liebmann, K. L.; Miller, S. C. Rapid Access to a Broad Range of 6'-Substituted Firefly Luciferin Analogues Reveals Surprising Emitters and Inhibitors. *Org Lett* **2017**, *19* (21), 5836-5839.

Synthesis and evaluation of bioluminescent probes as tools for anticancer drug discovery

Thesis presented for the degree of

Master of Science

by

Maryam Fredericks

Department of Chemistry

University of Cape Town

July 2025

Chapter 8 Supplementary materials

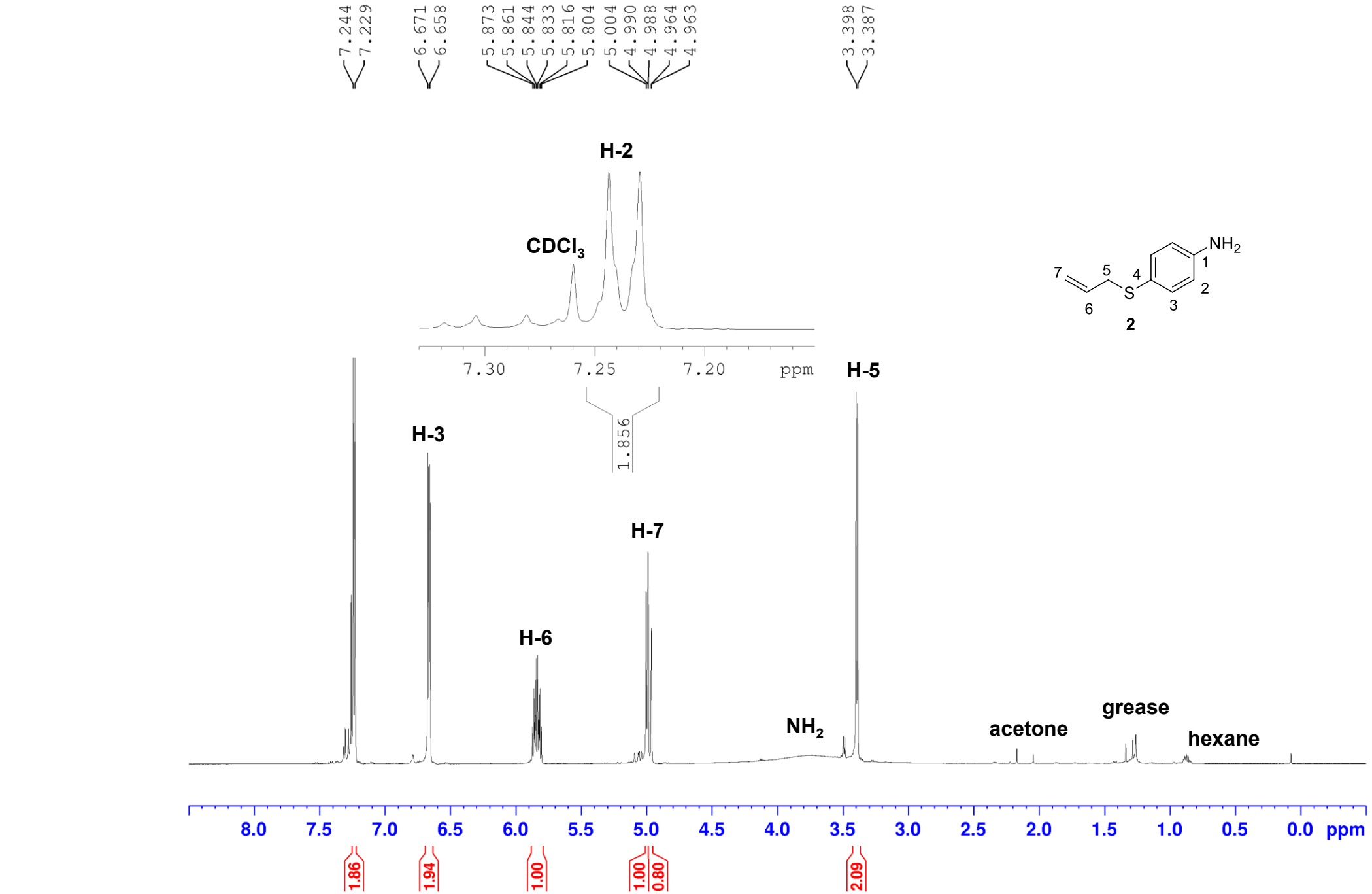
7.244
7.229
6.671
6.658
5.873
5.861
5.844
5.833
5.816
5.804
5.004
4.990
4.988
4.964
4.963
3.398
3.387
H-2
CDCl3
7.30
7.25
7.20
ppm
1.856
H-3
H-5
H-7
H-6
NH2
acetone
grease
hexane
NH2
1
2
3
4
5
6
7
S
2
8.0
7.5
7.0
6.5
6.0
5.5
5.0
4.5
4.0
3.5
3.0
2.5
2.0
1.5
1.0
0.5
0.0
ppm
1.86
1.94
1.00
1.00
0.80
2.09

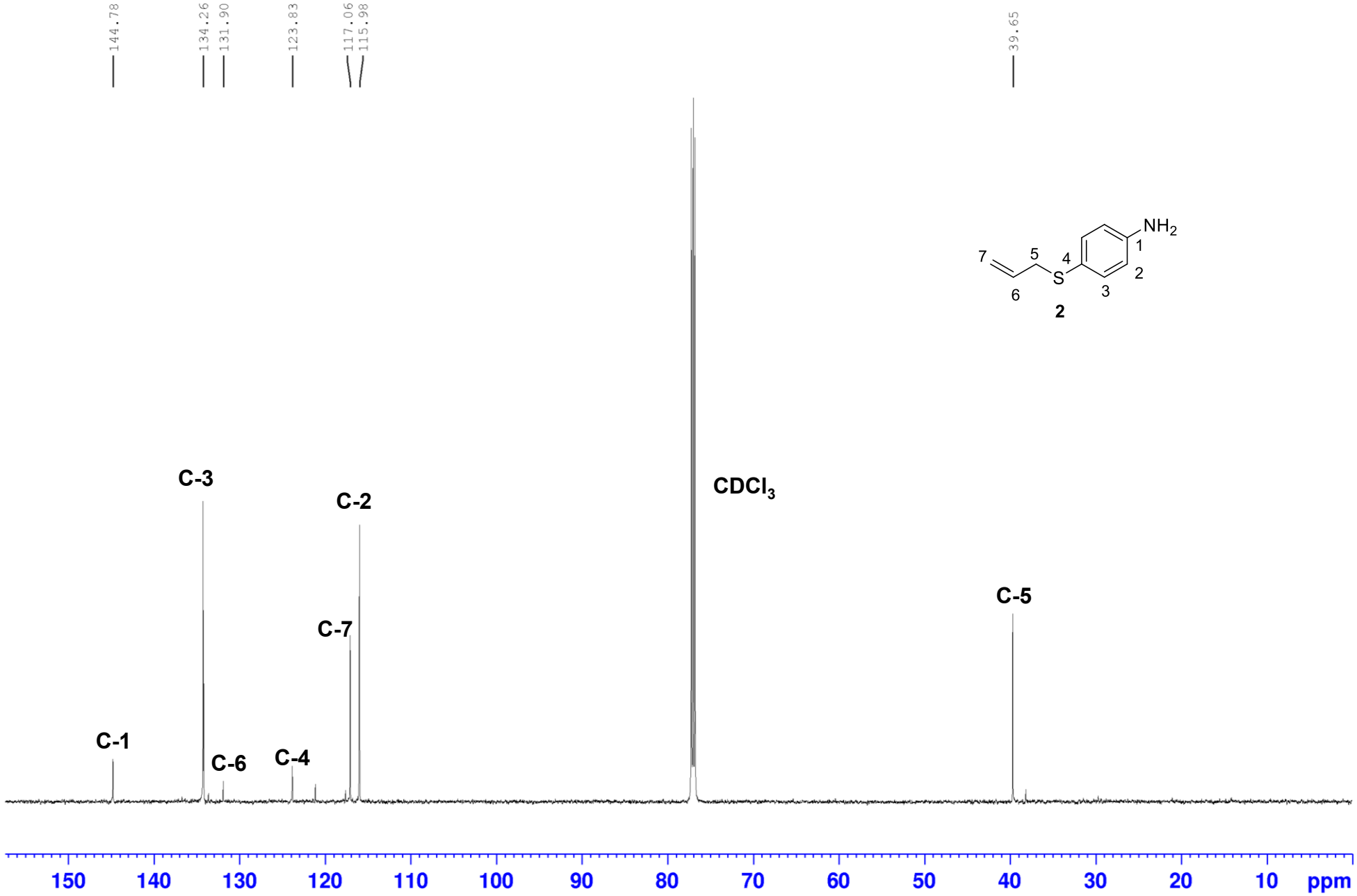
144.78
134.26
131.90
123.83
117.06
115.98
39.65
NH2
1
2
3
4
5
6
7
S
2
C-3
C-2
CDCl3
C-5
C-7
C-1
C-6
C-4
150
140
130
120
110
100
90
80
70
60
50
40
30
20
10
ppm

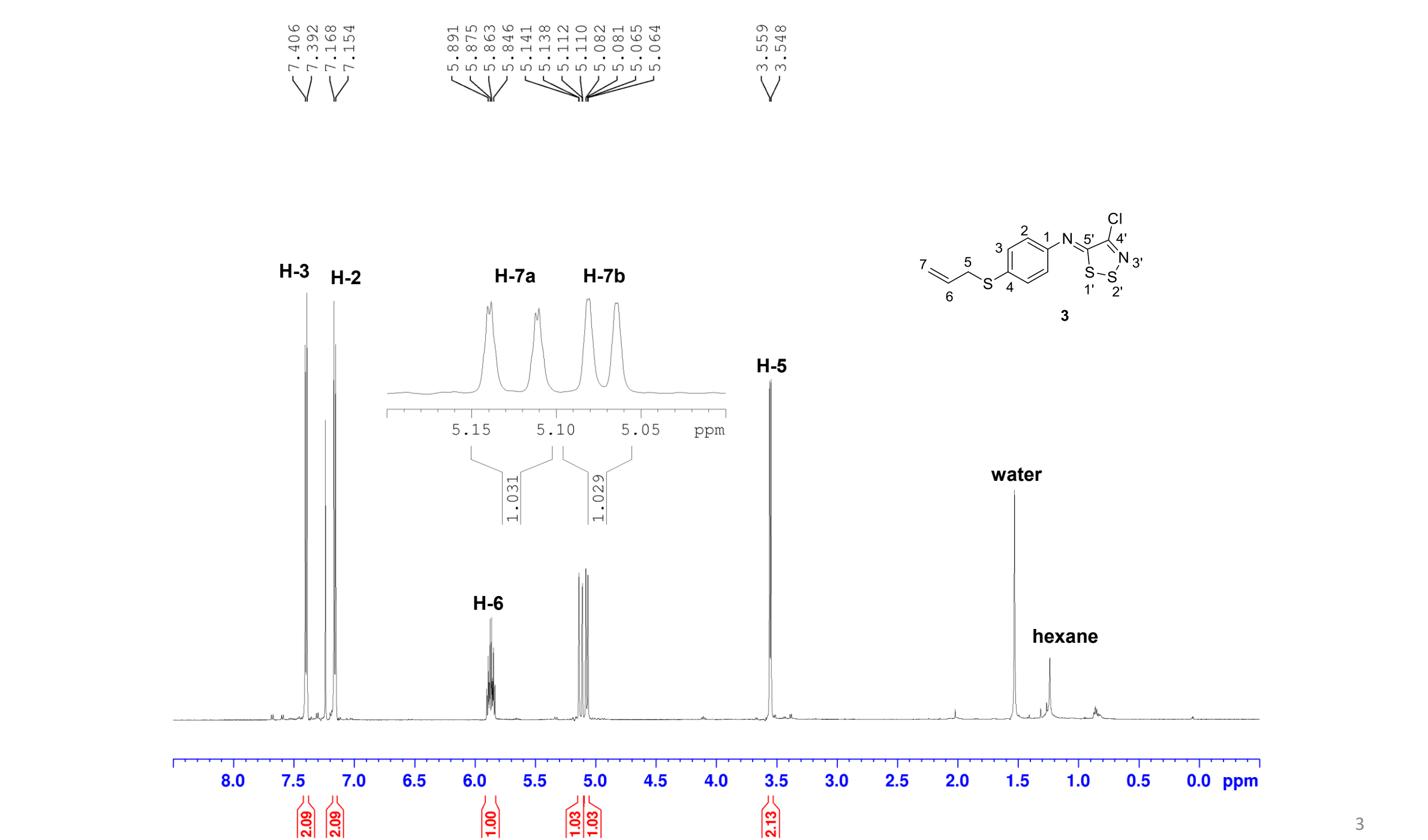
7.406
7.392
7.168
7.154
5.891
5.875
5.863
5.846
5.141
5.138
5.112
5.110
5.082
5.081
5.065
5.064
3.559
3.548
H-3
H-2
H-7a
H-7b
H-5
H-6
water
hexane
5.15
5.10
5.05
ppm
1.031
1.029
Cl
N
S
3
8.0
7.5
7.0
6.5
6.0
5.5
5.0
4.5
4.0
3.5
3.0
2.5
2.0
1.5
1.0
0.5
0.0
ppm
2.09
2.09
1.00
1.03
1.03
2.13

3

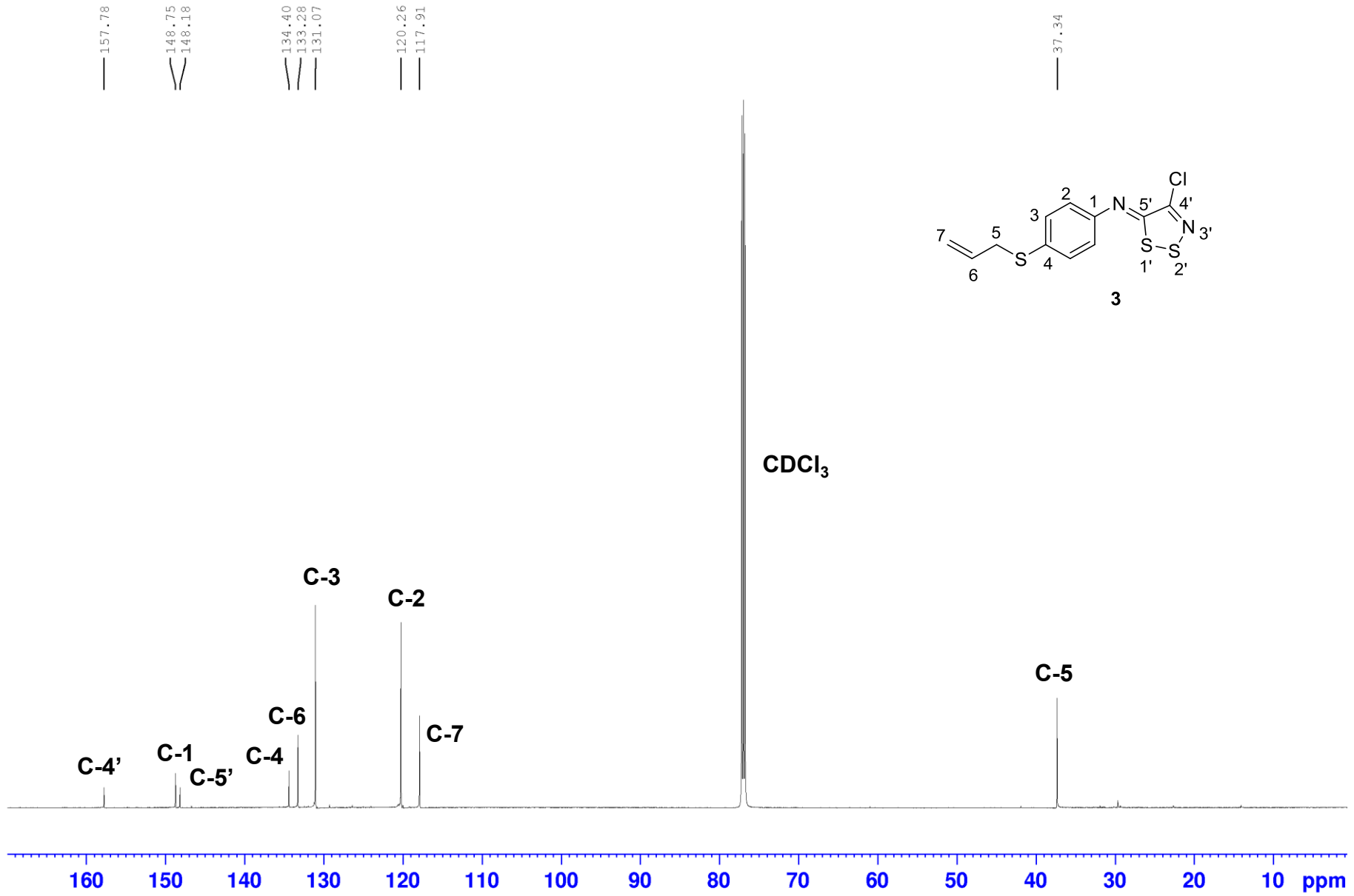
157.78
148.75
148.18
134.40
133.28
131.07
120.26
117.91
37.34
Cl
2
1
N
5'
4'
3
N
3'
7
5
S
S
S
6
4
1'
2'
3
CDCl3
C-3
C-2
C-5
C-6
C-7
C-1
C-4
C-4'
C-5'
160
150
140
130
120
110
100
90
80
70
60
50
40
30
20
10
ppm

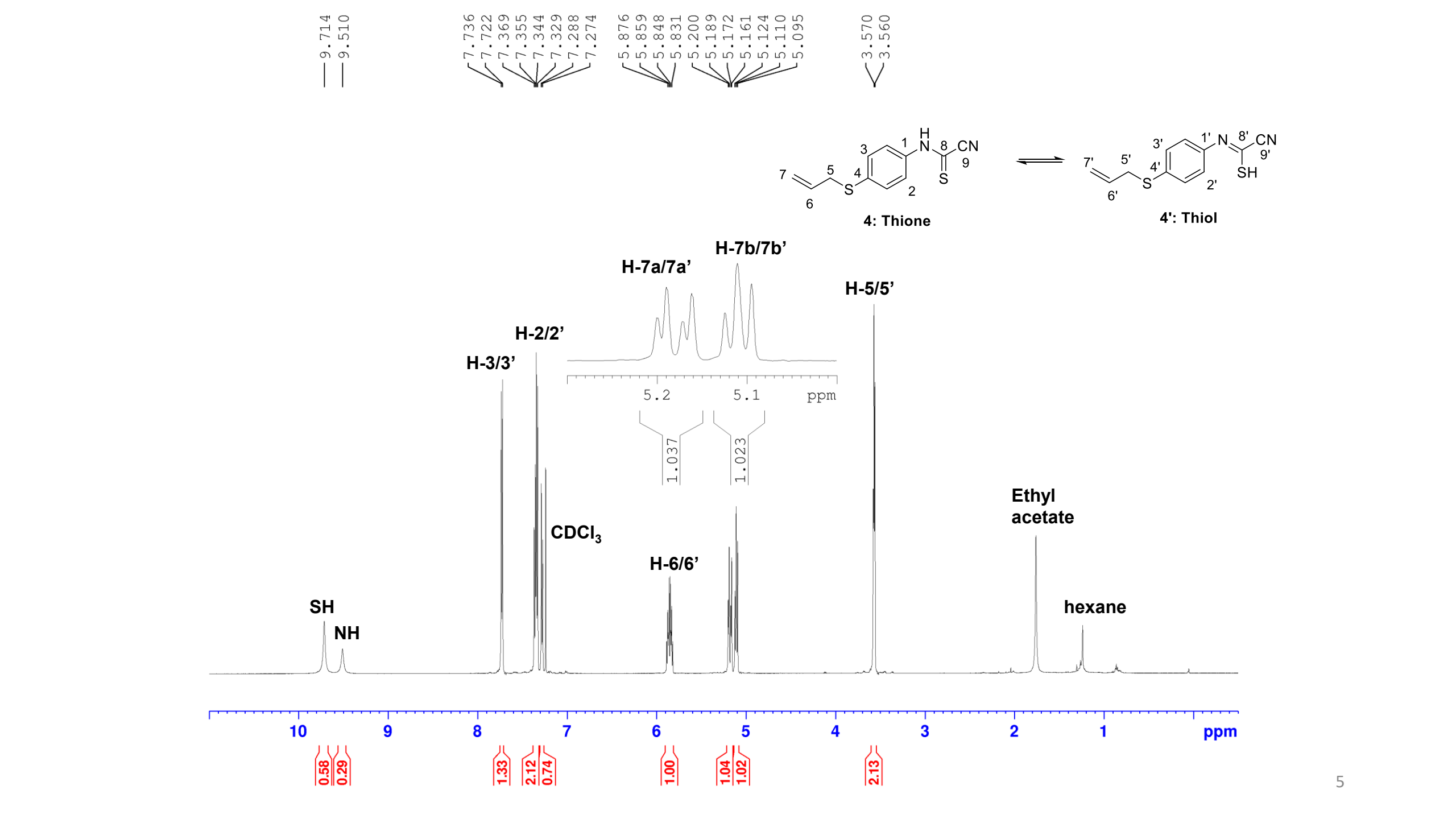
9.714
9.510
7.736
7.722
7.369
7.355
7.344
7.329
7.288
7.274
5.876
5.859
5.848
5.831
5.200
5.189
5.172
5.161
5.124
5.110
5.095
3.570
3.560
4: Thione
4': Thiol
H-7b/7b'
H-7a/7a'
H-5/5'
H-2/2'
H-3/3'
5.2
5.1
ppm
1.037
1.023
CDCl3
H-6/6'
Ethyl
acetate
SH
NH
hexane
10
9
8
7
6
5
4
3
2
1
ppm
0.58
0.29
1.33
2.12
0.74
1.00
1.04
1.02
2.13

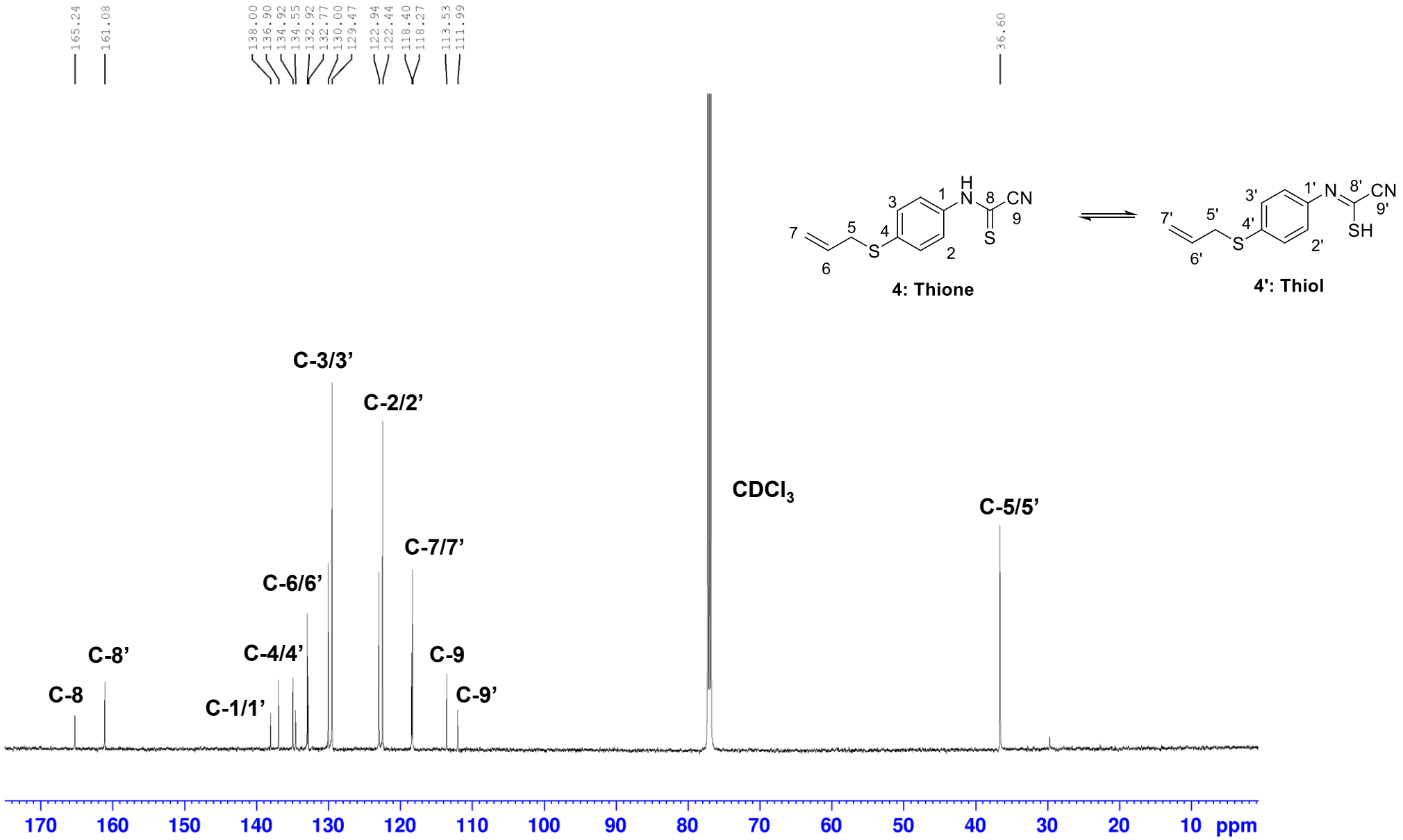
165.24
161.08
138.00
136.90
134.92
134.55
132.92
132.77
130.00
129.47
122.94
122.44
118.40
118.27
113.53
111.99
36.60
4: Thione
4': Thiol
C-3/3'
C-2/2'
C-7/7'
C-6/6'
C-4/4'
C-8'
C-8
C-1/1'
C-9
C-9'
CDCl3
C-5/5'
170
160
150
140
130
120
110
100
90
80
70
60
50
40
30
20
10
ppm

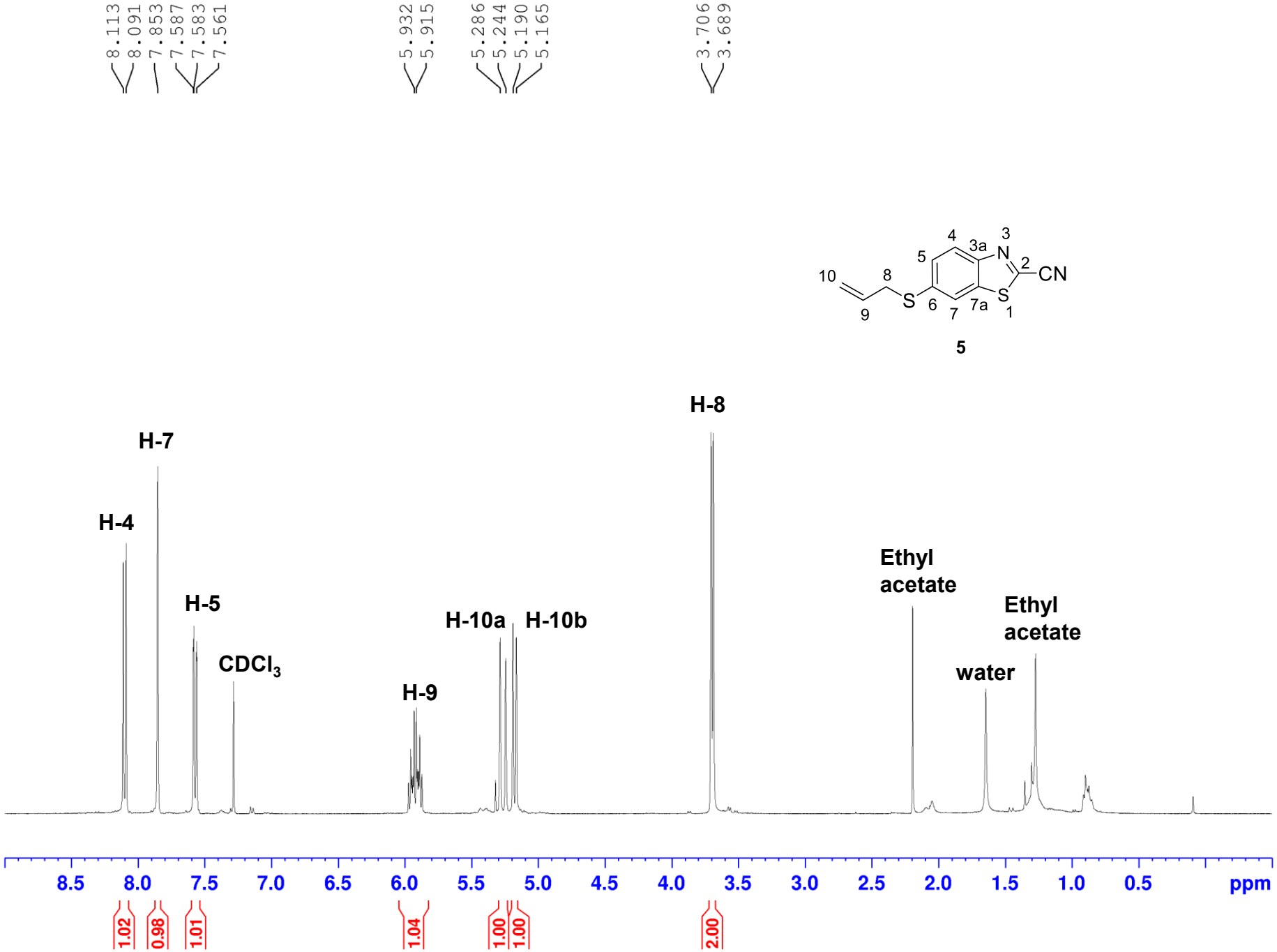
8.113
8.091
7.853
7.587
7.583
7.561
5.932
5.915
5.286
5.244
5.190
5.165
3.706
3.689
H-4
H-7
H-5
CDCl3
H-9
H-10a
H-10b
H-8
Ethyl acetate
water
Ethyl acetate
8.5
8.0
7.5
7.0
6.5
6.0
5.5
5.0
4.5
4.0
3.5
3.0
2.5
2.0
1.5
1.0
0.5
ppm
1.02
0.98
1.01
1.04
1.00
1.00
2.00

4
3a
3
N
2
CN
5
10
8
S
6
7
7a
S
1
9

5

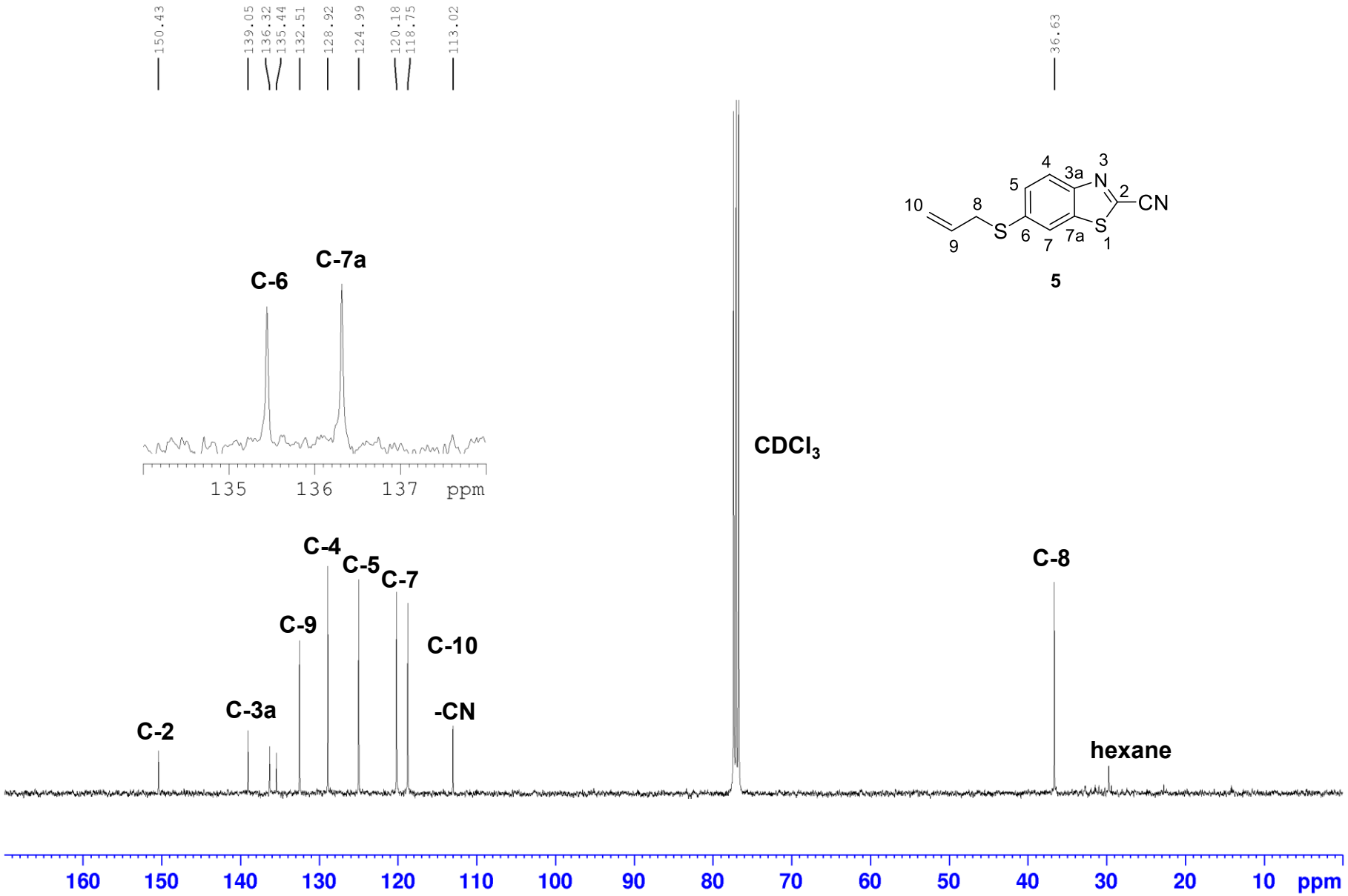
150.43
139.05
136.32
135.44
132.51
128.92
124.99
120.18
118.75
113.02
36.63
C-6
C-7a
135
136
137
ppm
CDCl3
C-4
C-5
C-7
C-9
C-10
C-3a
-CN
C-2
C-8
hexane
160
150
140
130
120
110
100
90
80
70
60
50
40
30
20
10
ppm

4
3a
3
N
5
2
CN
10
8
S
6
7
7a
S
1
9

5

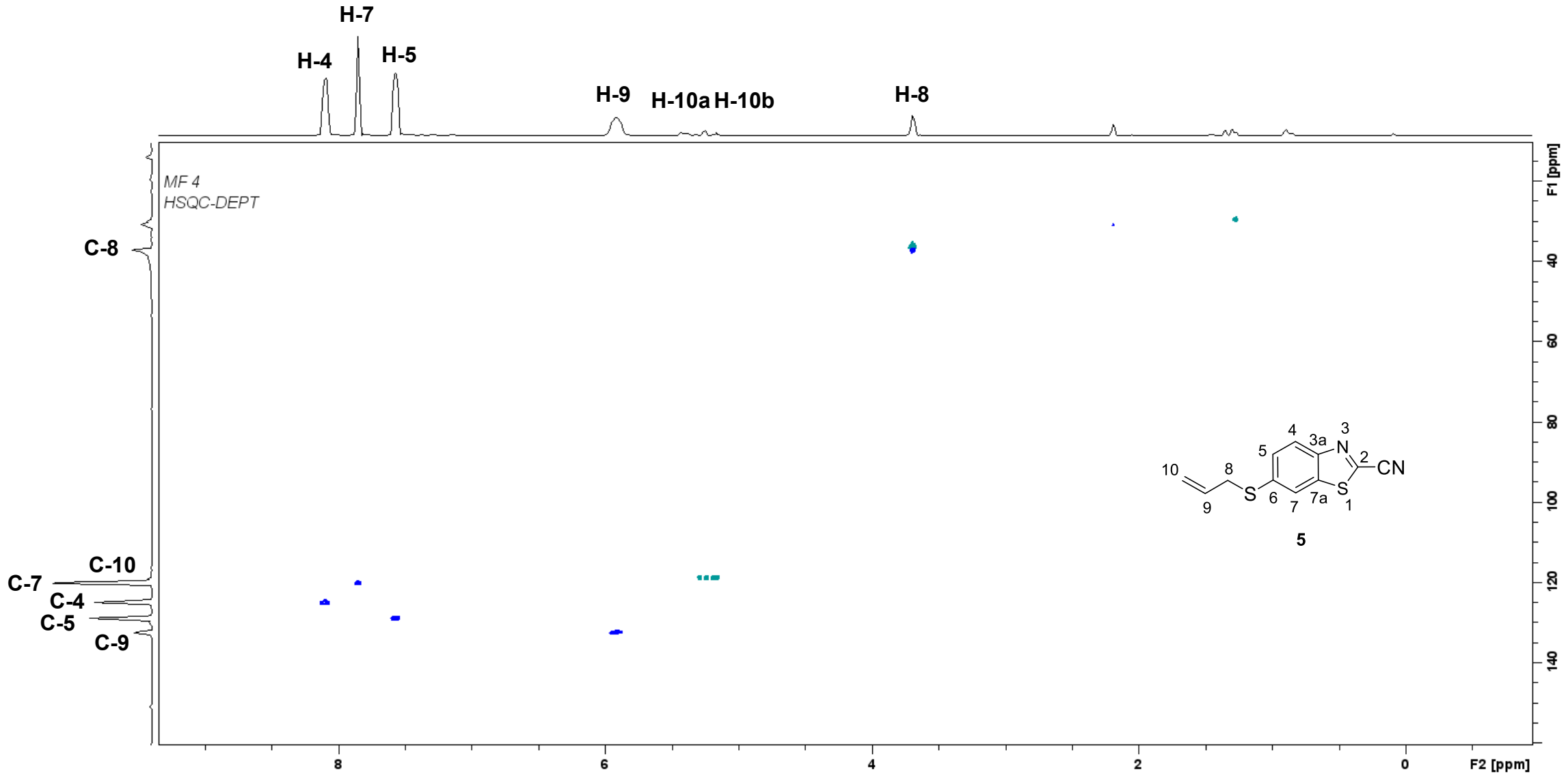
H-7
H-4
H-5
H-9
H-10a
H-10b
H-8
MF 4
HSQC-DEPT
C-8
C-10
C-7
C-4
C-5
C-9
F1 [ppm]
40
60
80
100
120
140
8
6
4
2
0
F2 [ppm]
4
3a
3
5
N
2
CN
10
8
S
6
7
7a
S
1
9
5

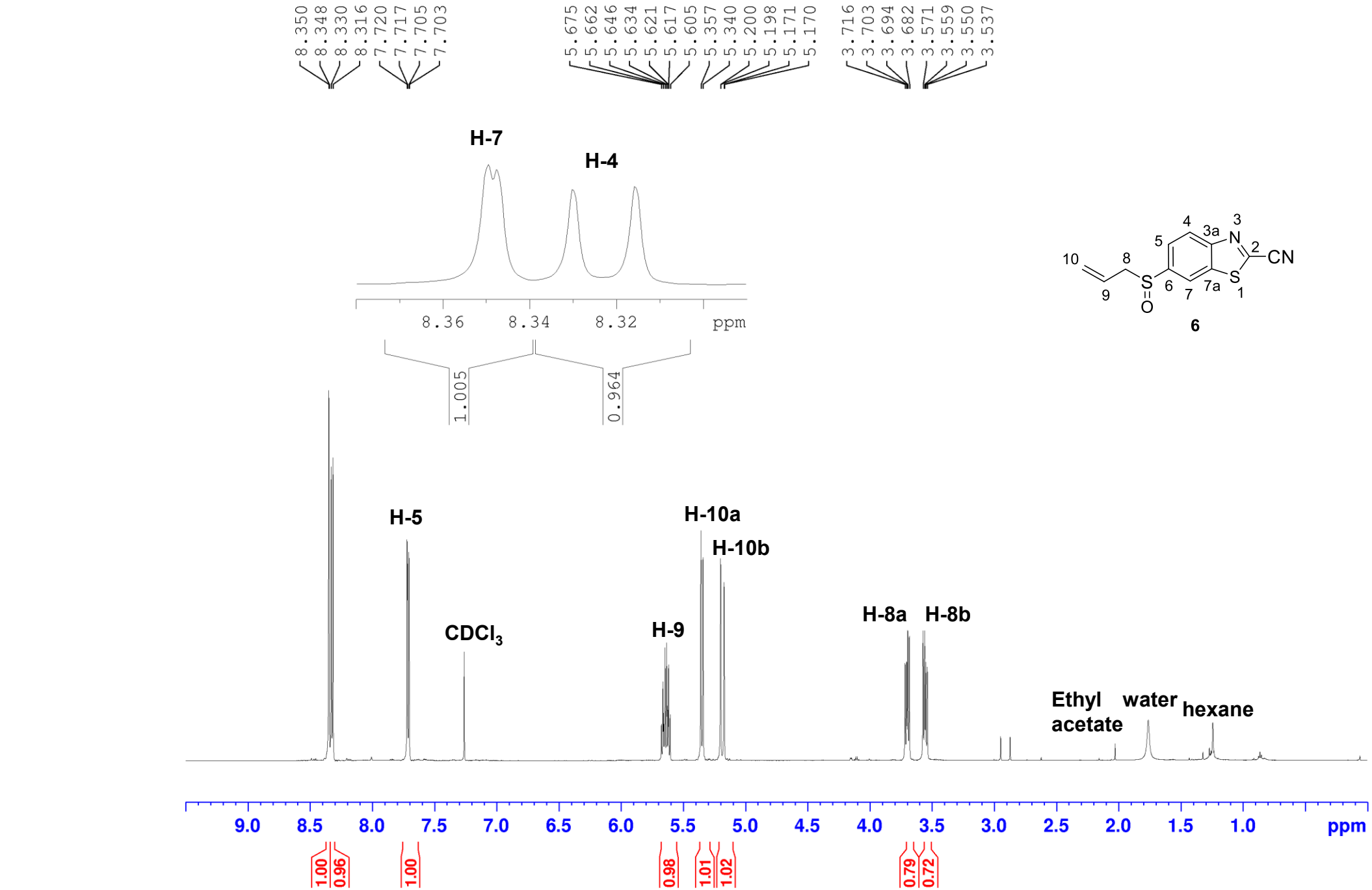
8.350
8.348
8.330
8.316
7.720
7.717
7.705
7.703
5.675
5.662
5.646
5.634
5.621
5.617
5.605
5.357
5.340
5.200
5.198
5.171
5.170
3.716
3.703
3.694
3.682
3.571
3.559
3.550
3.537
H-7
H-4
8.36
8.34
8.32
ppm
1.005
0.964
4
3a
3
N
2
CN
10
8
5
S
6
7
7a
S
1
9
O
6
H-5
H-10a
H-10b
CDCl3
H-9
H-8a
H-8b
Ethyl acetate
water
hexane
9.0
8.5
8.0
7.5
7.0
6.5
6.0
5.5
5.0
4.5
4.0
3.5
3.0
2.5
2.0
1.5
1.0
ppm
1.00
0.96
1.00
0.98
1.01
1.02
0.79
0.72

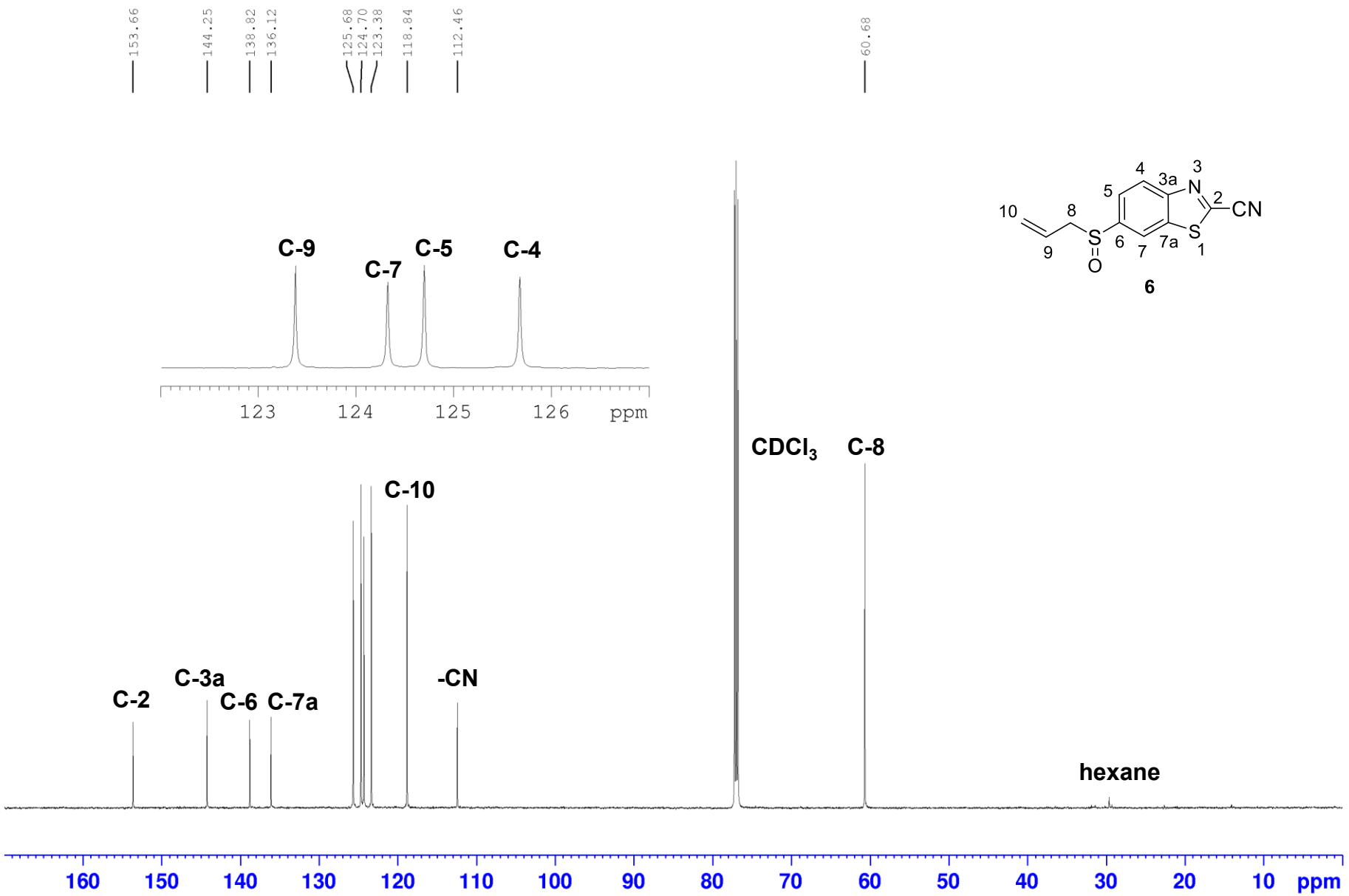
153.66
144.25
138.82
136.12
125.68
124.70
123.38
118.84
112.46
60.68
C-9
C-7
C-5
C-4
123
124
125
126
ppm
C-10
CDCl3
C-8
C-2
C-3a
C-6
C-7a
-CN
hexane
160
150
140
130
120
110
100
90
80
70
60
50
40
30
20
10
ppm
4
3a
3
N
2
CN
5
10
8
S
6
7a
S
1
9
O
7
6

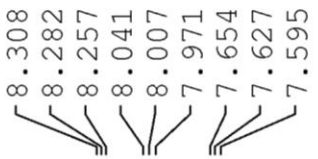
8.308
8.282
8.257
8.041
8.007
7.971
7.654
7.627
7.595

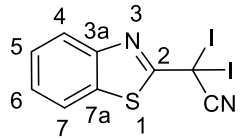
4
3a
3
N
2
I
I
CN
5
6
7
7a
S
1

9

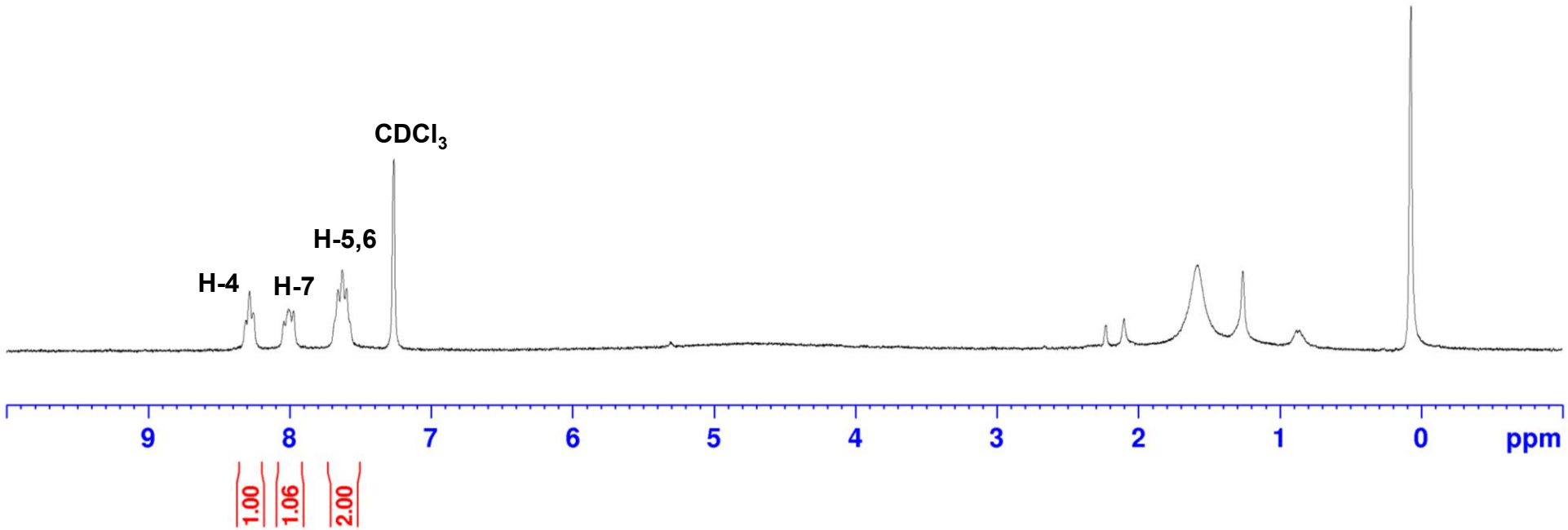
CDCl3
H-5,6
H-4
H-7
9
8
7
6
5
4
3
2
1
0
ppm
1.00
1.06
2.00

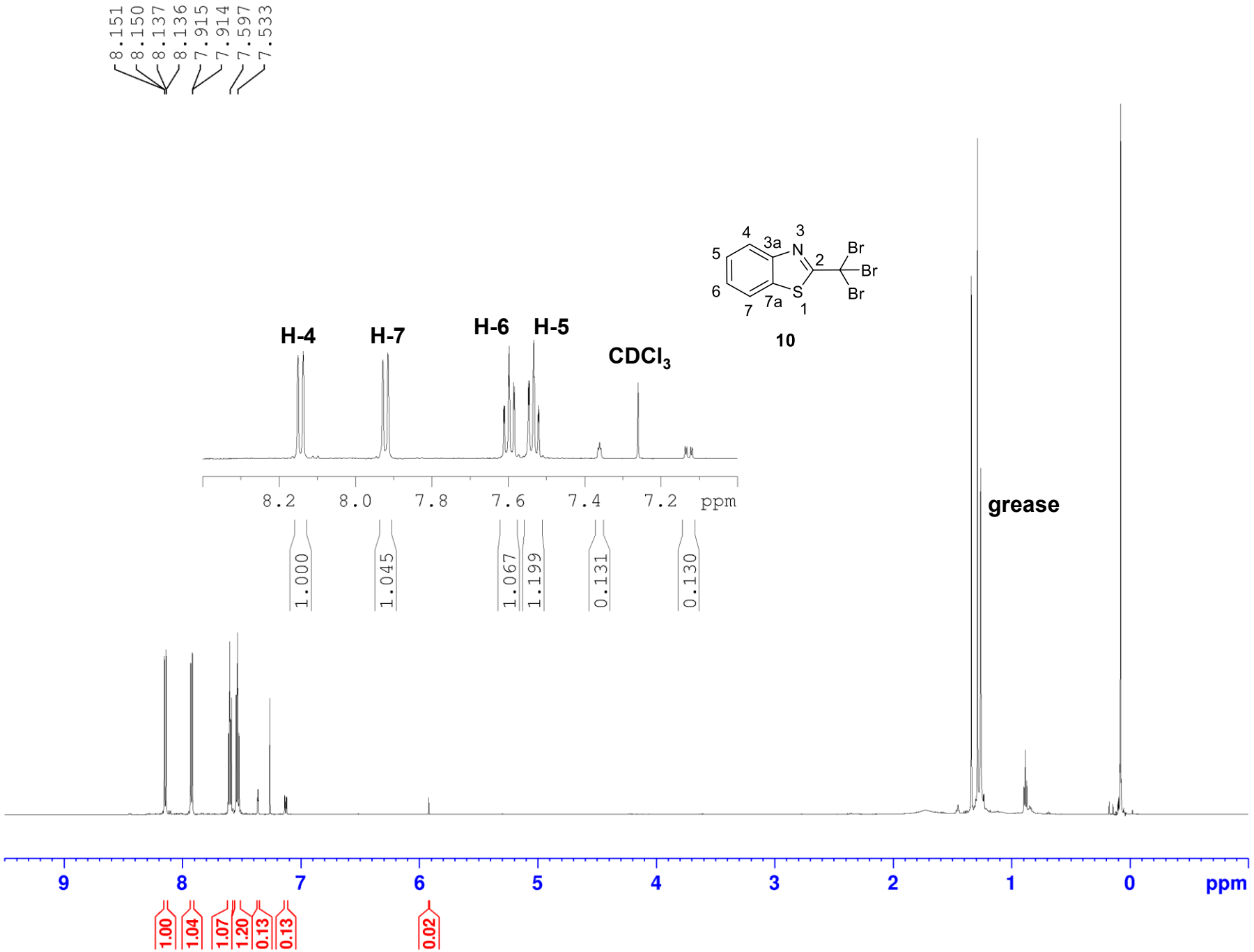
8.151
8.150
8.137
8.136
7.915
7.914
7.597
7.533
H-4
H-7
H-6
H-5
CDCl3
8.2
8.0
7.8
7.6
7.4
7.2
ppm
1.000
1.045
1.067
1.199
0.131
0.130
4
3a
3
5
N
2
Br
Br
Br
6
S
7
7a
1
10
grease
9
8
7
6
5
4
3
2
1
0
ppm
1.00
1.04
1.07
1.20
0.13
0.13
0.02

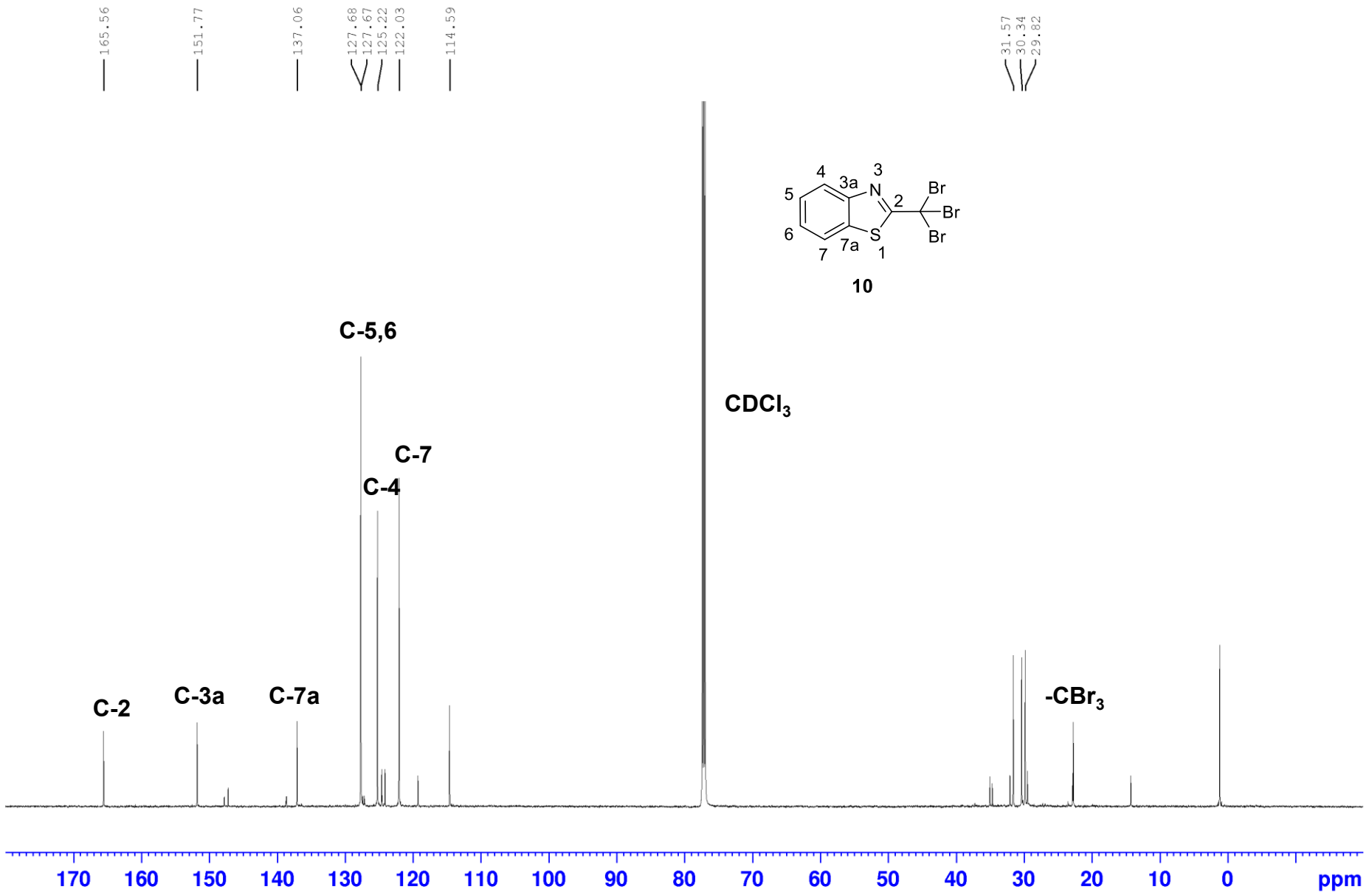
165.56
151.77
137.06
127.68
127.67
125.22
122.03
114.59
31.57
30.34
29.82
4
3a
3
N
2
Br
Br
Br
5
6
7
7a
S
1
10
C-5,6
CDCl3
C-7
C-4
C-2
C-3a
C-7a
-CBr3
170
160
150
140
130
120
110
100
90
80
70
60
50
40
30
20
10
0
ppm

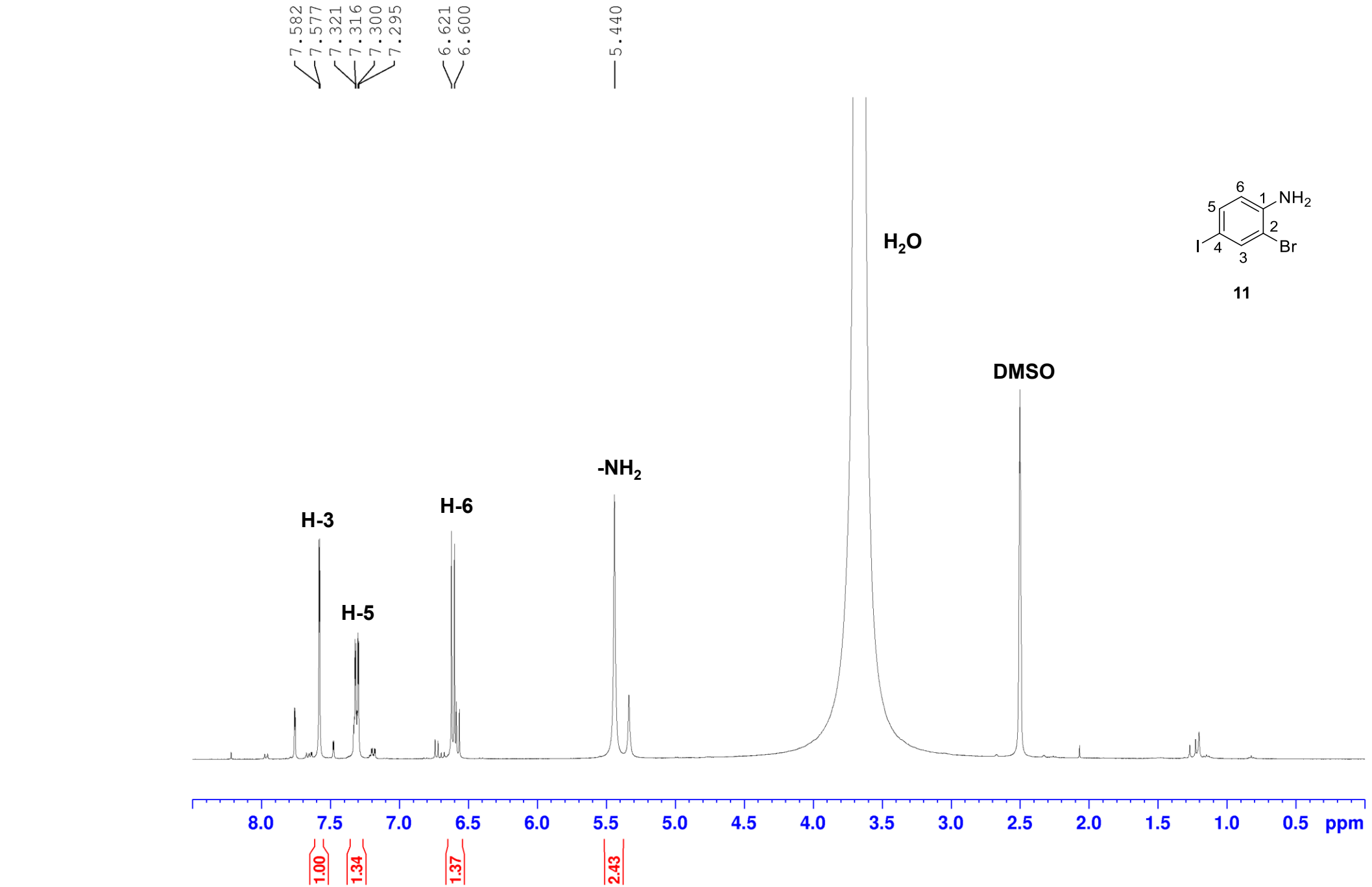
7.582
7.577
7.321
7.316
7.300
7.295
6.621
6.600
5.440
H-3
H-5
H-6
-NH2
H2O
DMSO
6
1
NH2
5
2
I
4
3
Br
11
8.0
7.5
7.0
6.5
6.0
5.5
5.0
4.5
4.0
3.5
3.0
2.5
2.0
1.5
1.0
0.5
ppm
1.00
1.34
1.37
2.43

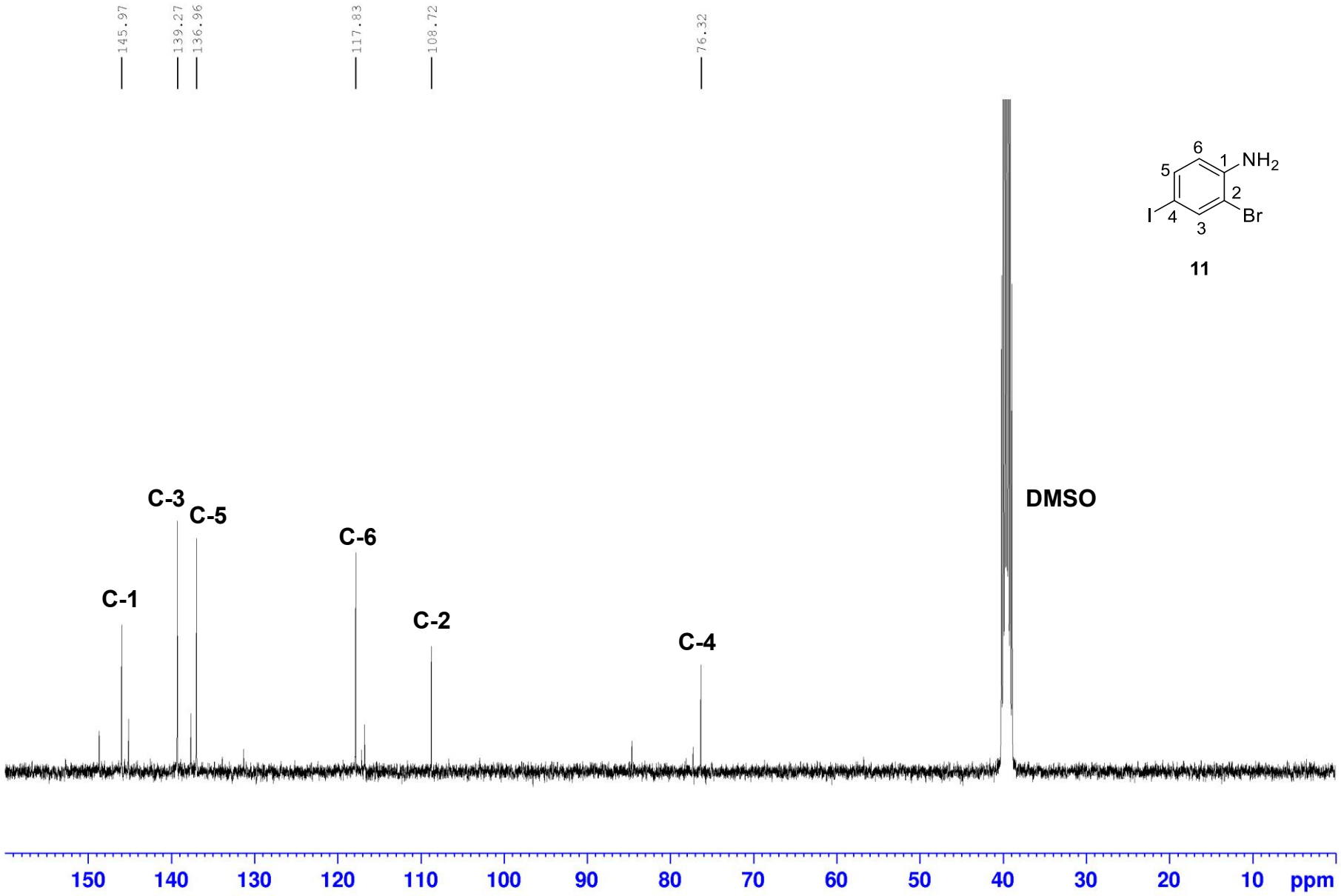
145.97
139.27
136.96
117.83
108.72
76.32
C-1
C-3
C-5
C-6
C-2
C-4
DMSO
150
140
130
120
110
100
90
80
70
60
50
40
30
20
10
ppm

6
1
NH2
5
2
I
4
3
Br

11

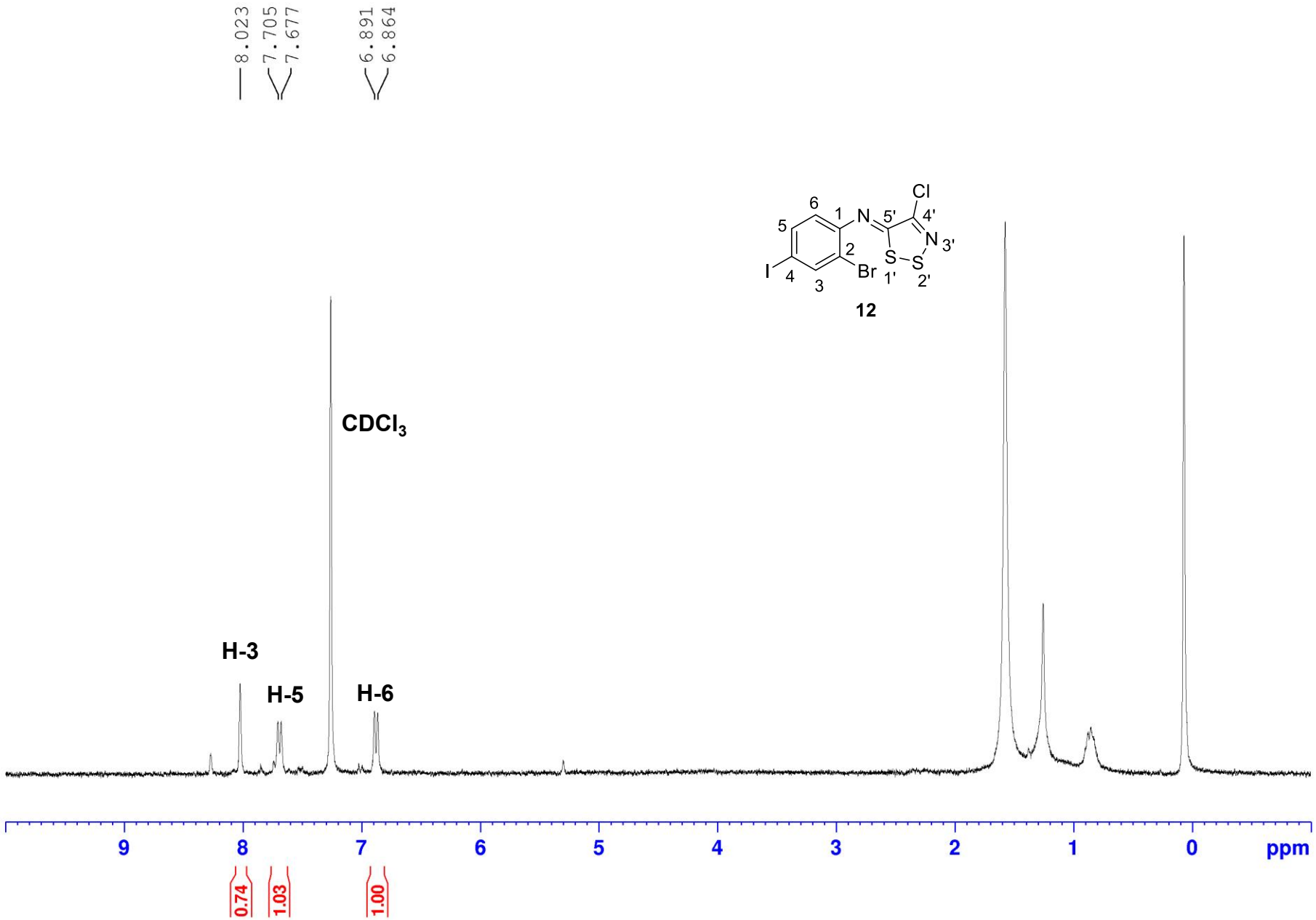
8.023
7.705
7.677
6.891
6.864
Cl
6
1
N
5'
4'
5
N
3'
2
S
S
I
4
Br
1'
2'
3
12
CDCl3
H-3
H-5
H-6
9
8
7
6
5
4
3
2
1
0
ppm
0.74
1.03
1.00

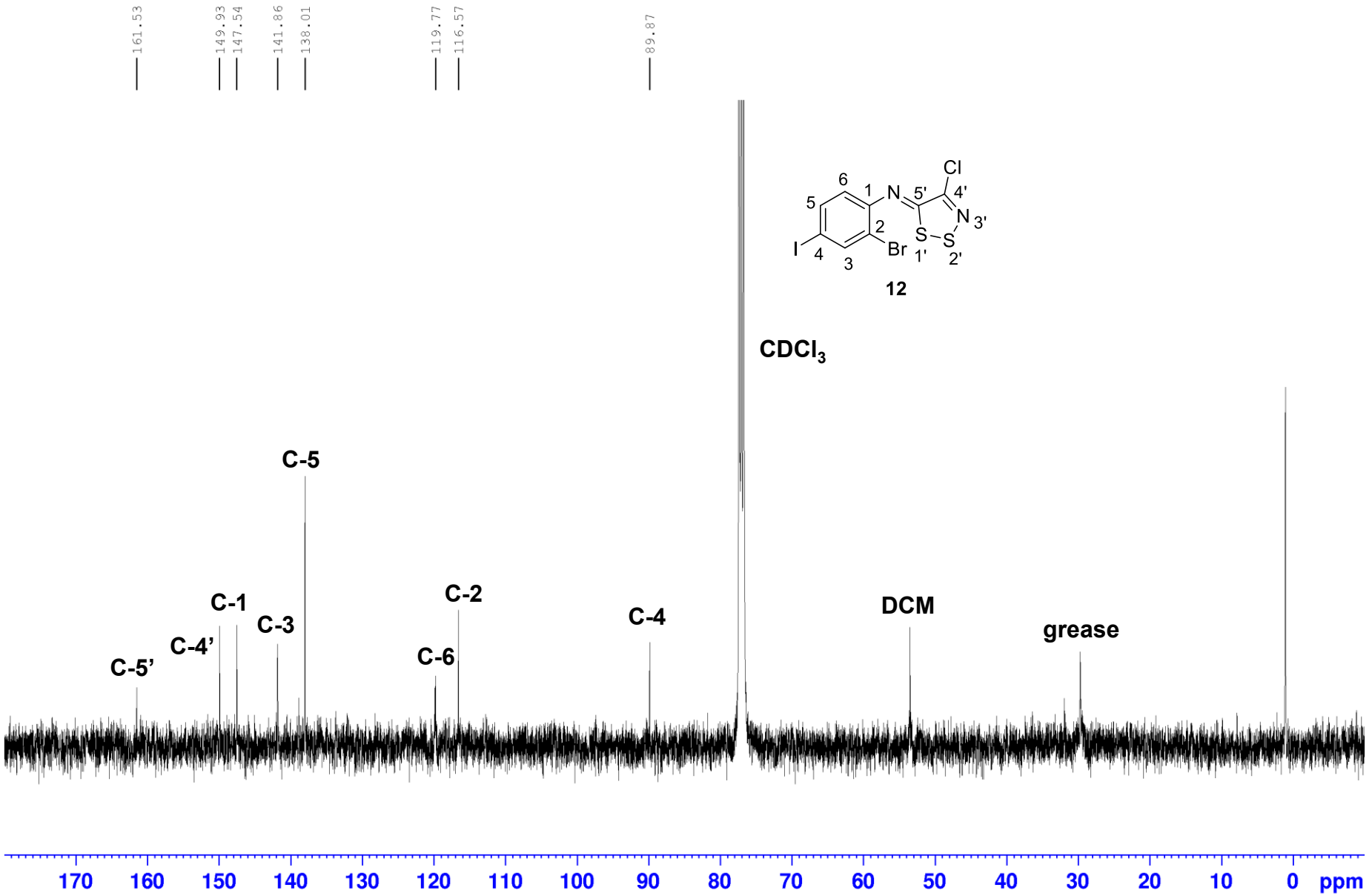
161.53
149.93
147.54
141.86
138.01
119.77
116.57
89.87
Cl
6
1
N
5'
4'
5
N
3'
2
S
S
I
4
Br
1'
2'
3
12
CDCl3
C-5
C-1
C-2
C-3
C-4'
C-5'
C-6
C-4
DCM
grease
170
160
150
140
130
120
110
100
90
80
70
60
50
40
30
20
10
0
ppm

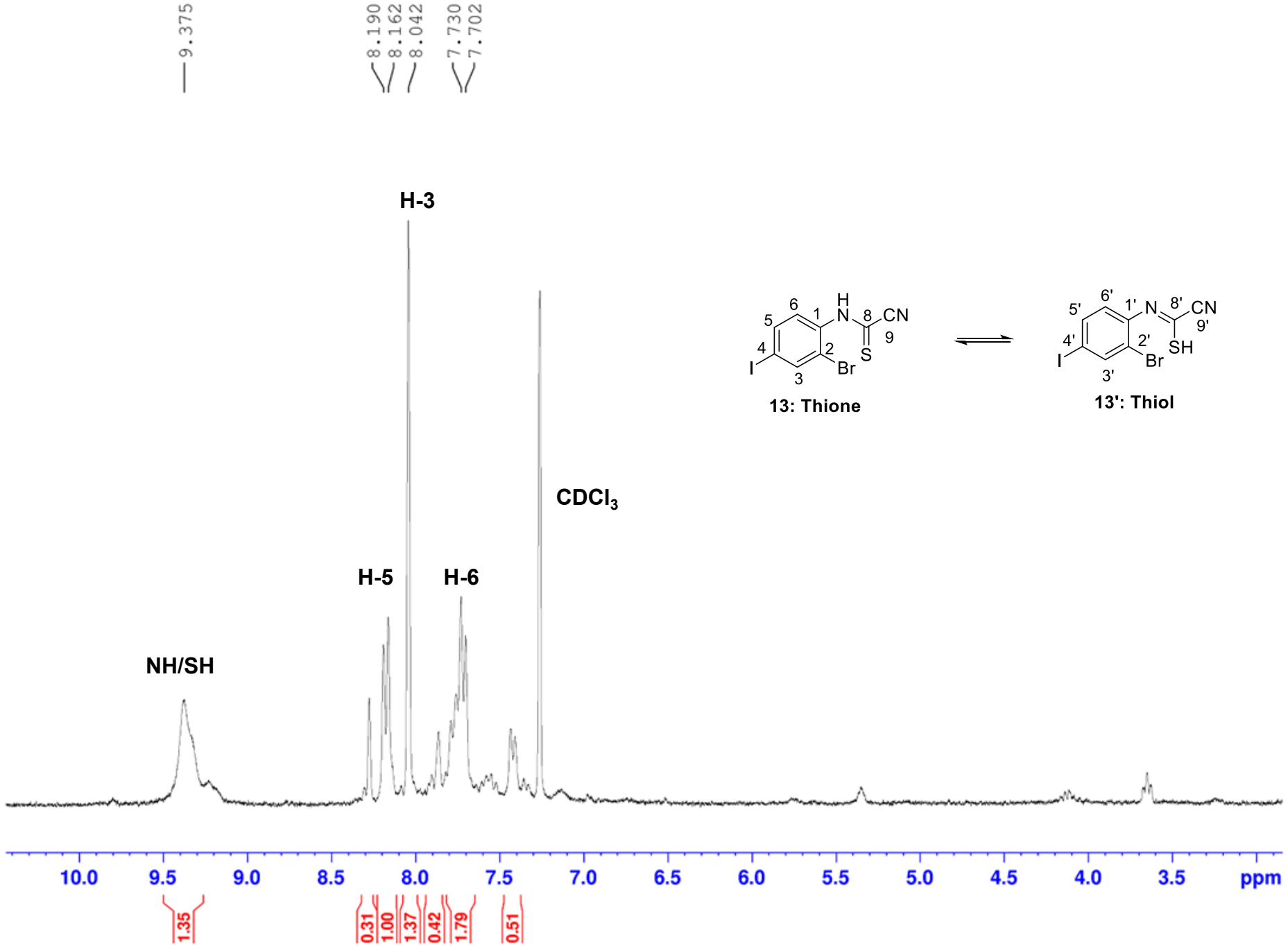
9.375
8.190
8.162
8.042
7.730
7.702
H-3
H-5
H-6
CDCl3
NH/SH
13: Thione
13': Thiol
10.0
9.5
9.0
8.5
8.0
7.5
7.0
6.5
6.0
5.5
5.0
4.5
4.0
3.5
ppm
1.35
0.31
1.00
1.37
0.42
1.79
0.51

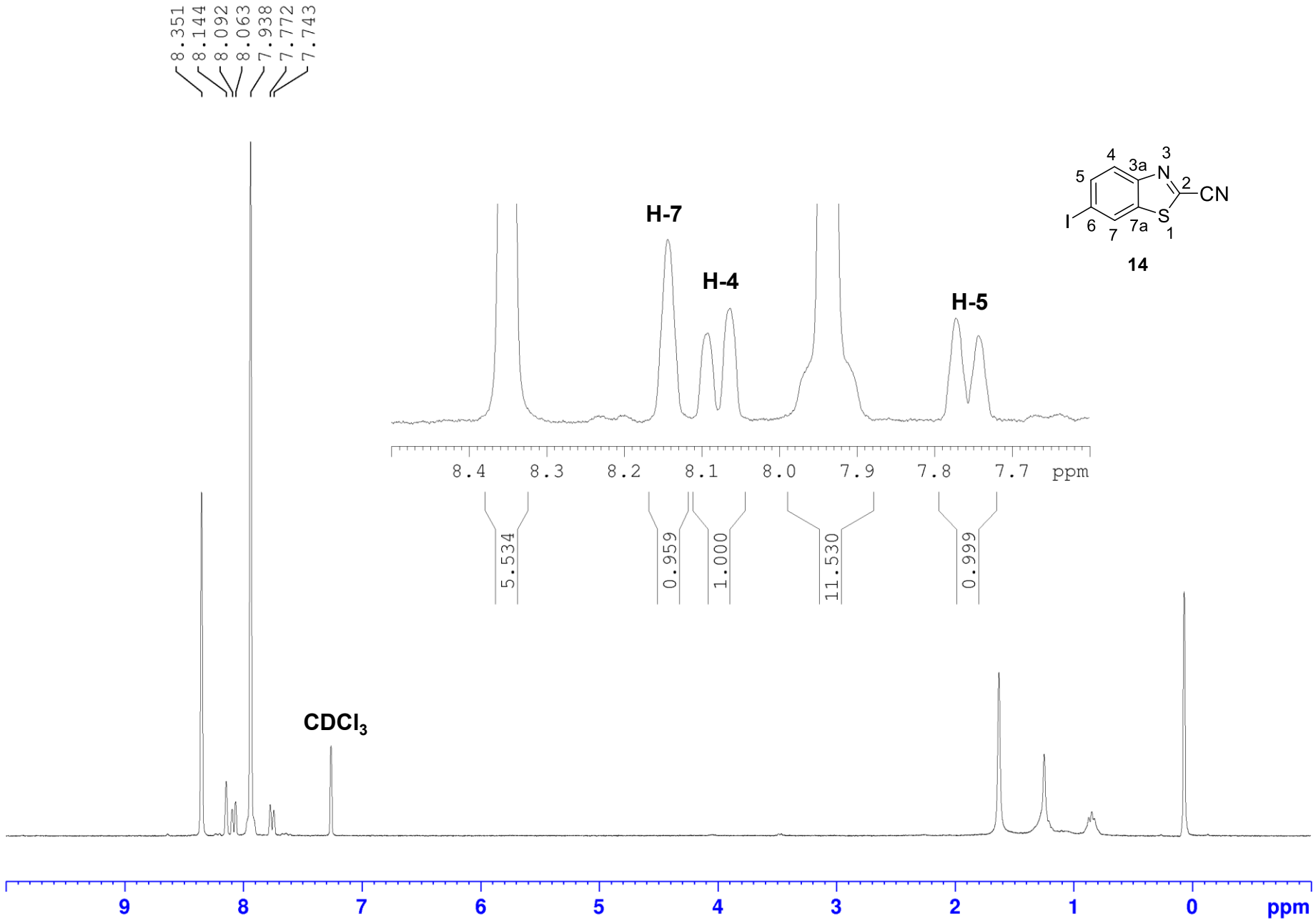
8.351
8.144
8.092
8.063
7.938
7.772
7.743
H-7
H-4
H-5
8.4
8.3
8.2
8.1
8.0
7.9
7.8
7.7
ppm
5.534
0.959
1.000
11.530
0.999
CDCl3
9
8
7
6
5
4
3
2
1
0
ppm
4
3a
3
N
2
CN
5
I
6
7
7a
S
1
14

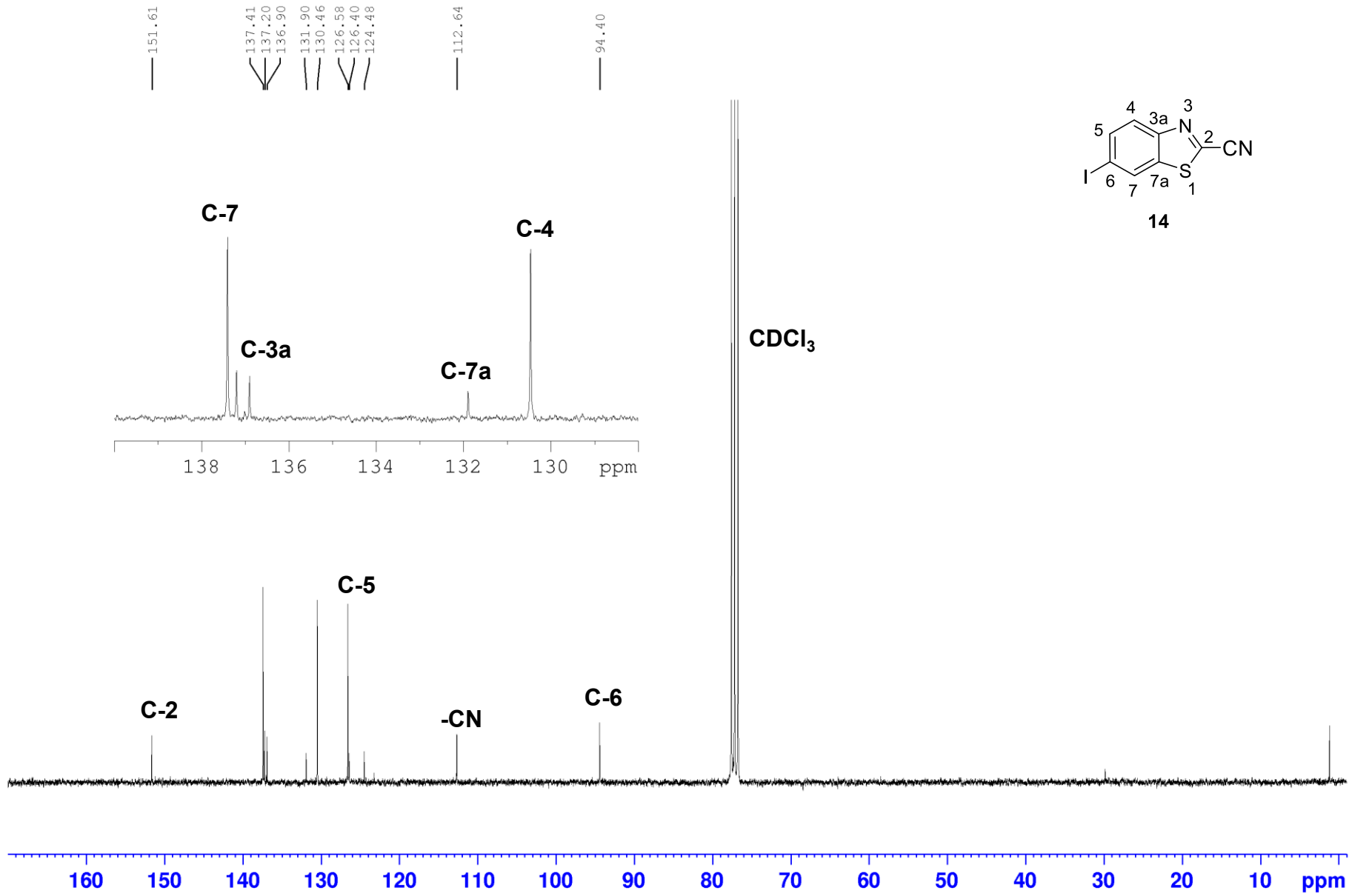
151.61
137.41
137.20
136.90
131.90
130.46
126.58
126.40
124.48
112.64
94.40
C-7
C-4
C-3a
C-7a
138
136
134
132
130
ppm
CDCl3
C-5
C-2
-CN
C-6
160
150
140
130
120
110
100
90
80
70
60
50
40
30
20
10
ppm

4
3a
3
N
2
CN
5
I
6
7
7a
S
1

14

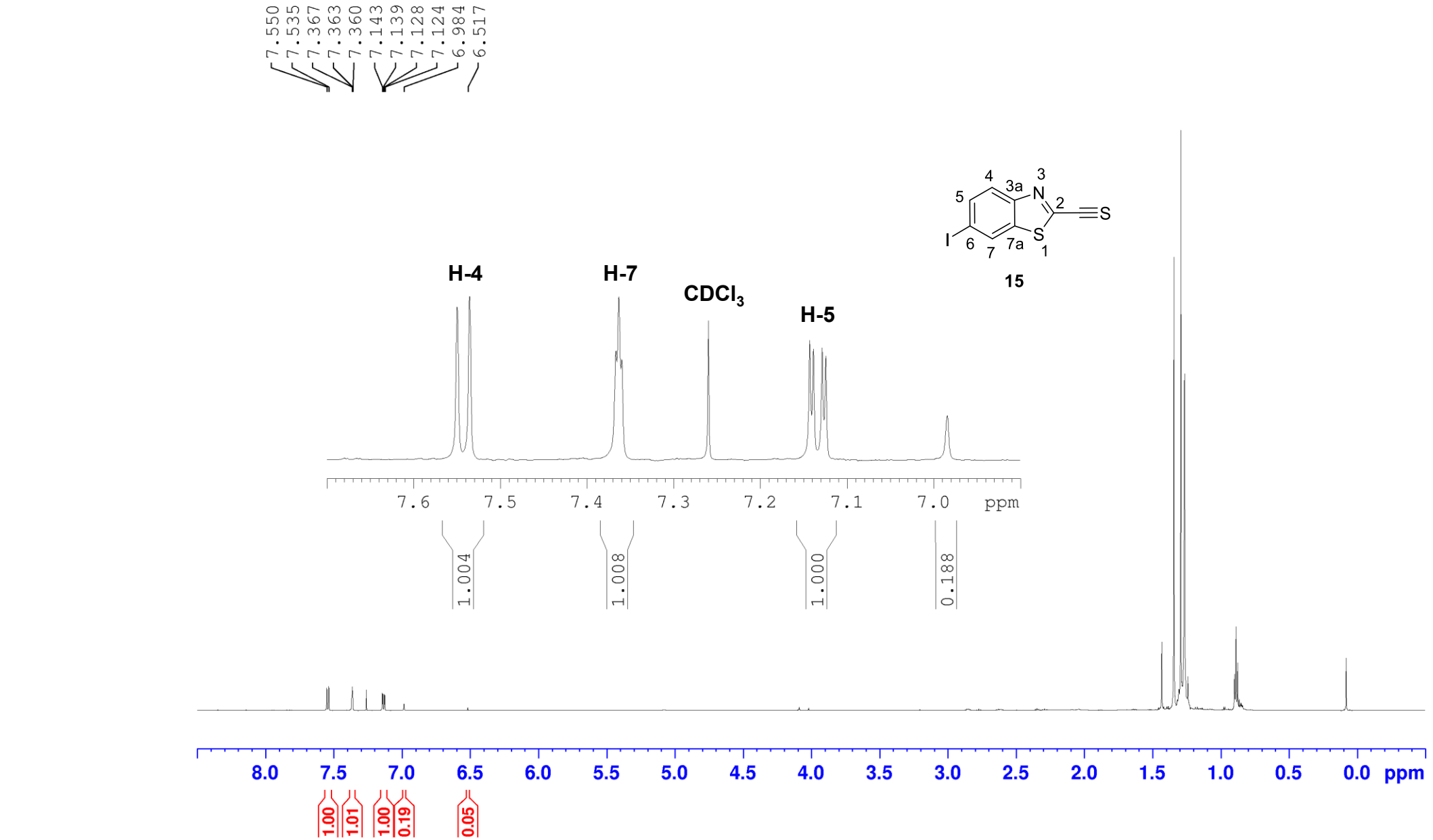
7.550
7.535
7.367
7.363
7.360
7.143
7.139
7.128
7.124
6.984
6.517
H-4
H-7
CDCl3
H-5
15
7.6
7.5
7.4
7.3
7.2
7.1
7.0
ppm
1.004
1.008
1.000
0.188
8.0
7.5
7.0
6.5
6.0
5.5
5.0
4.5
4.0
3.5
3.0
2.5
2.0
1.5
1.0
0.5
0.0
ppm
1.00
1.01
1.00
0.19
0.05

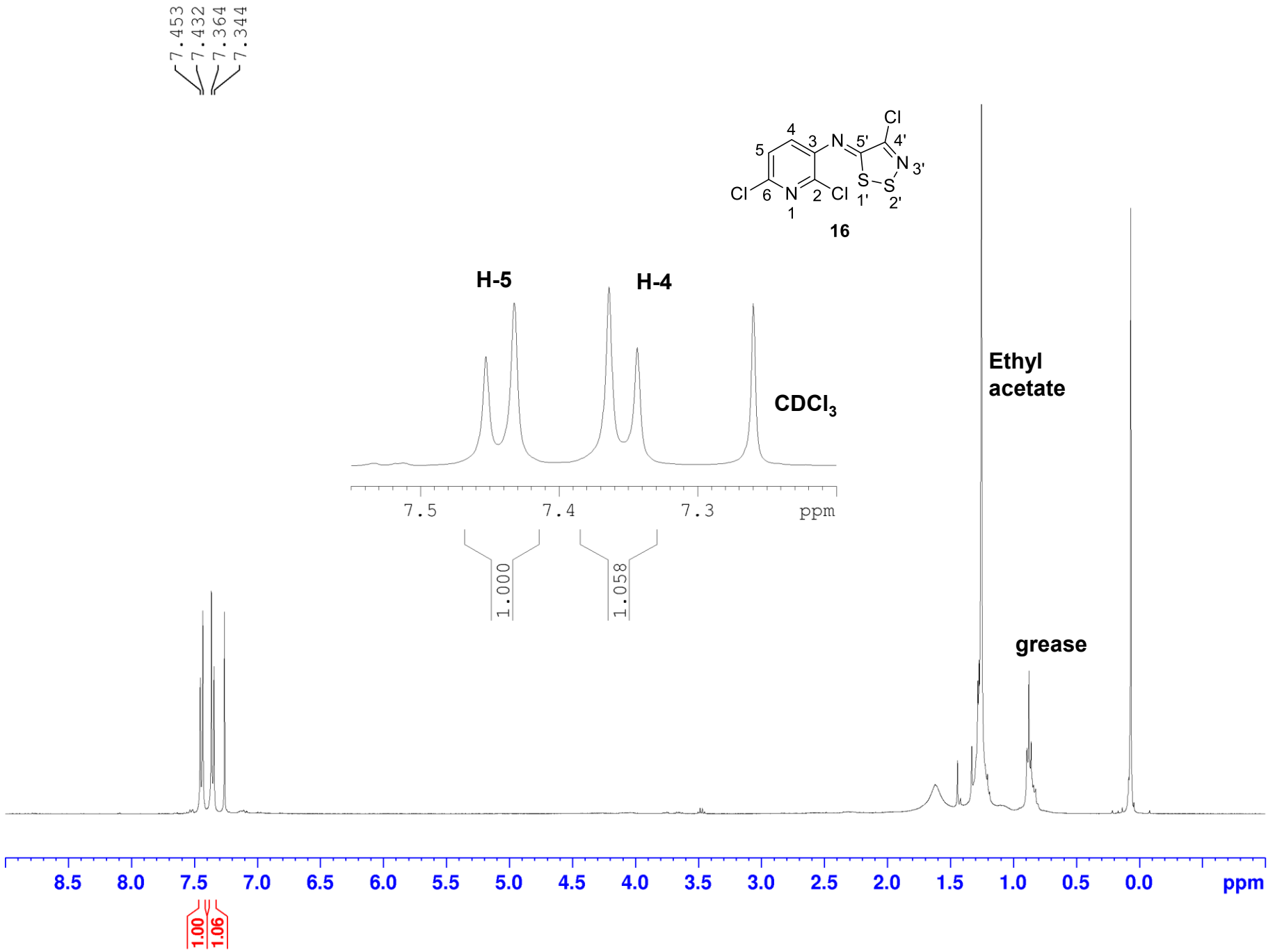
7.453
7.432
7.364
7.344
16
H-5
H-4
CDCl3
7.5
7.4
7.3
ppm
1.000
1.058
Ethyl acetate
grease
8.5
8.0
7.5
7.0
6.5
6.0
5.5
5.0
4.5
4.0
3.5
3.0
2.5
2.0
1.5
1.0
0.5
0.0
ppm
1.00
1.06

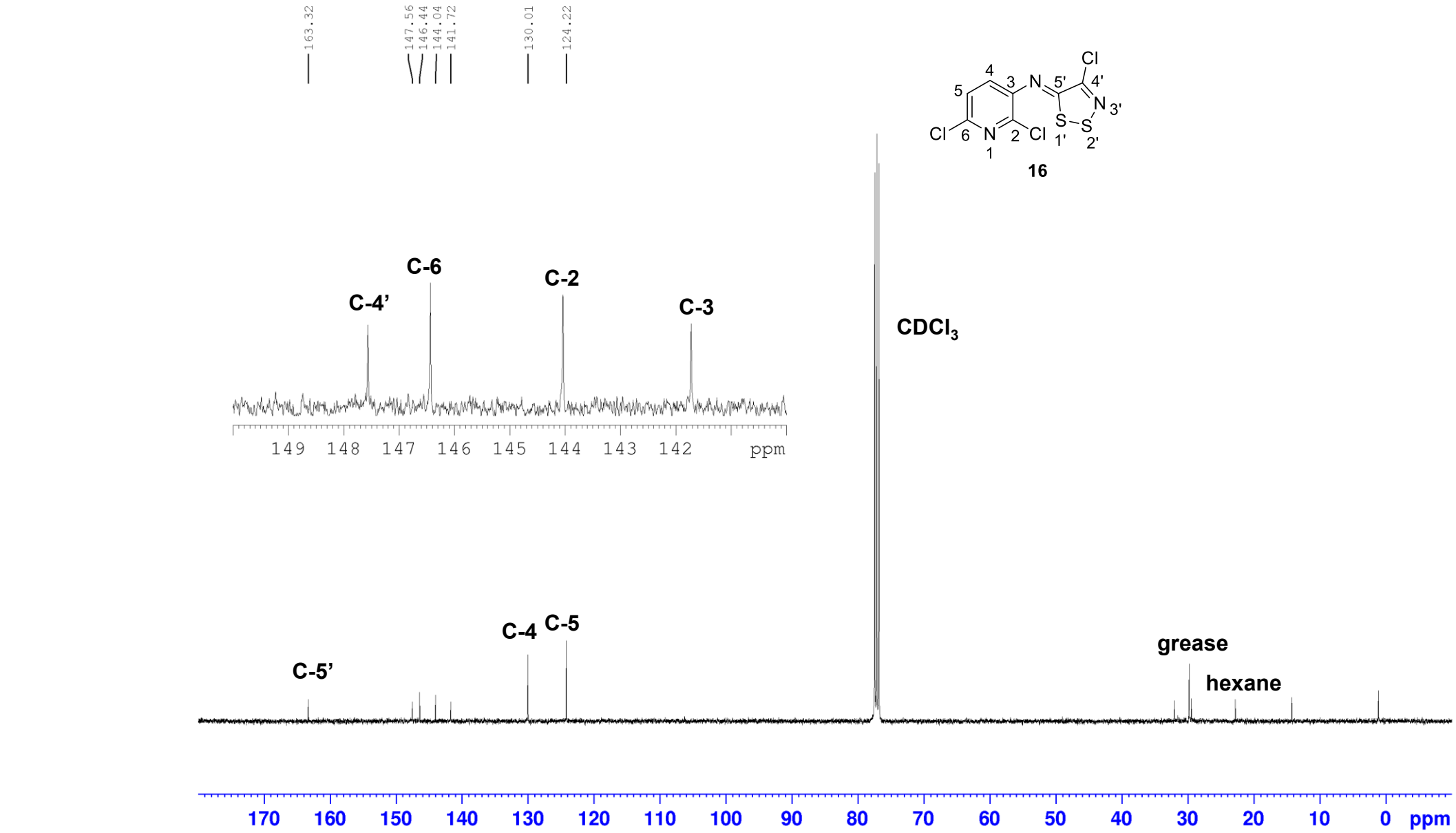
163.32
147.56
146.44
144.04
141.72
130.01
124.22
Cl
4
3
N
5'
4'
5
N
3'
S
S
Cl
6
N
2
Cl
1'
2'
1
16
C-6
C-4'
C-2
C-3
CDCl3
149 148 147 146 145 144 143 142 ppm
C-4
C-5
C-5'
grease
hexane
170 160 150 140 130 120 110 100 90 80 70 60 50 40 30 20 10 0 ppm

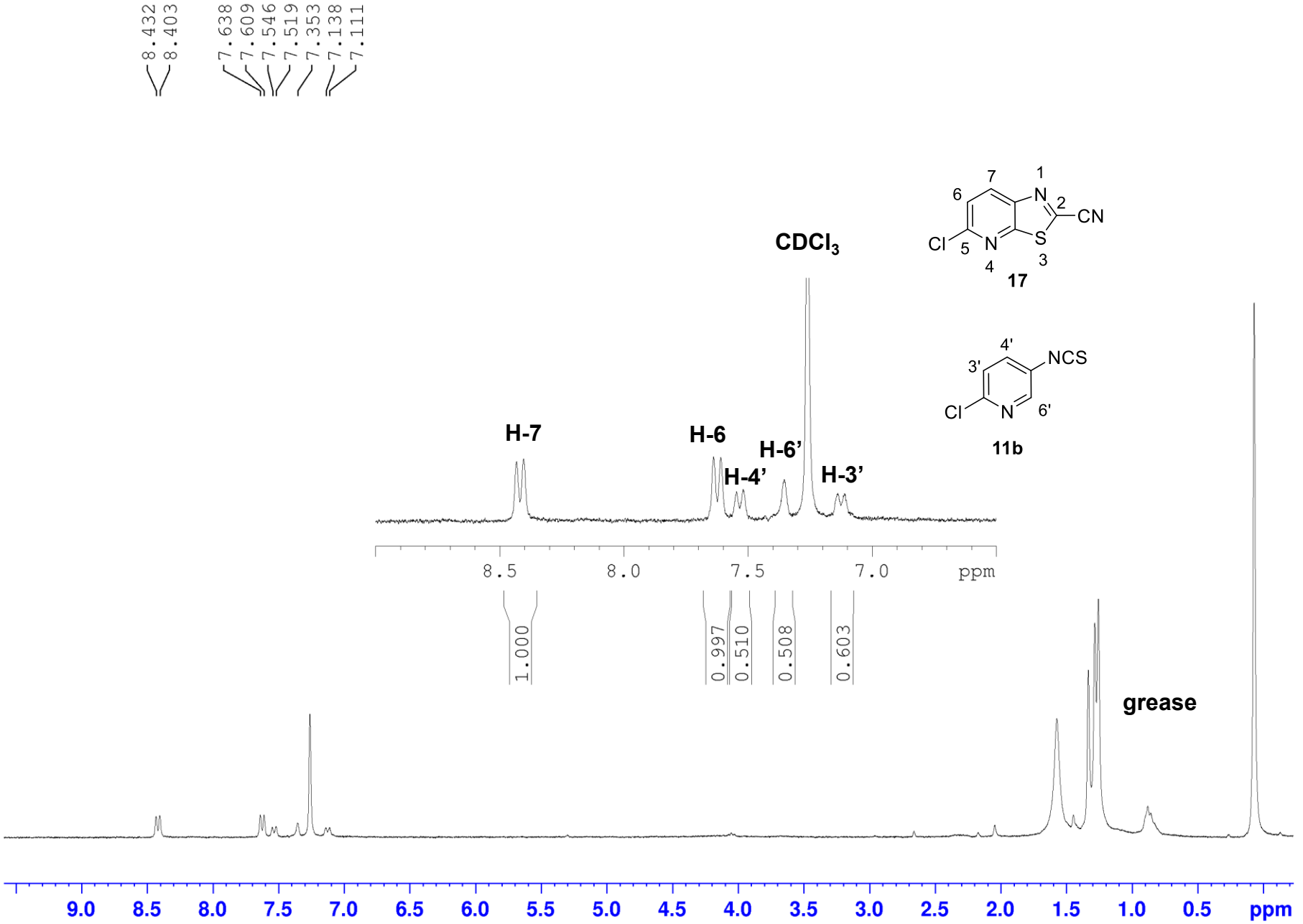
8.432
8.403
7.638
7.609
7.546
7.519
7.353
7.138
7.111
CDCl3
H-7
H-6
H-4'
H-6'
H-3'
8.5
8.0
7.5
7.0
ppm
1.000
0.997
0.510
0.508
0.603
grease
9.0
8.5
8.0
7.5
7.0
6.5
6.0
5.5
5.0
4.5
4.0
3.5
3.0
2.5
2.0
1.5
1.0
0.5
ppm
17
11b

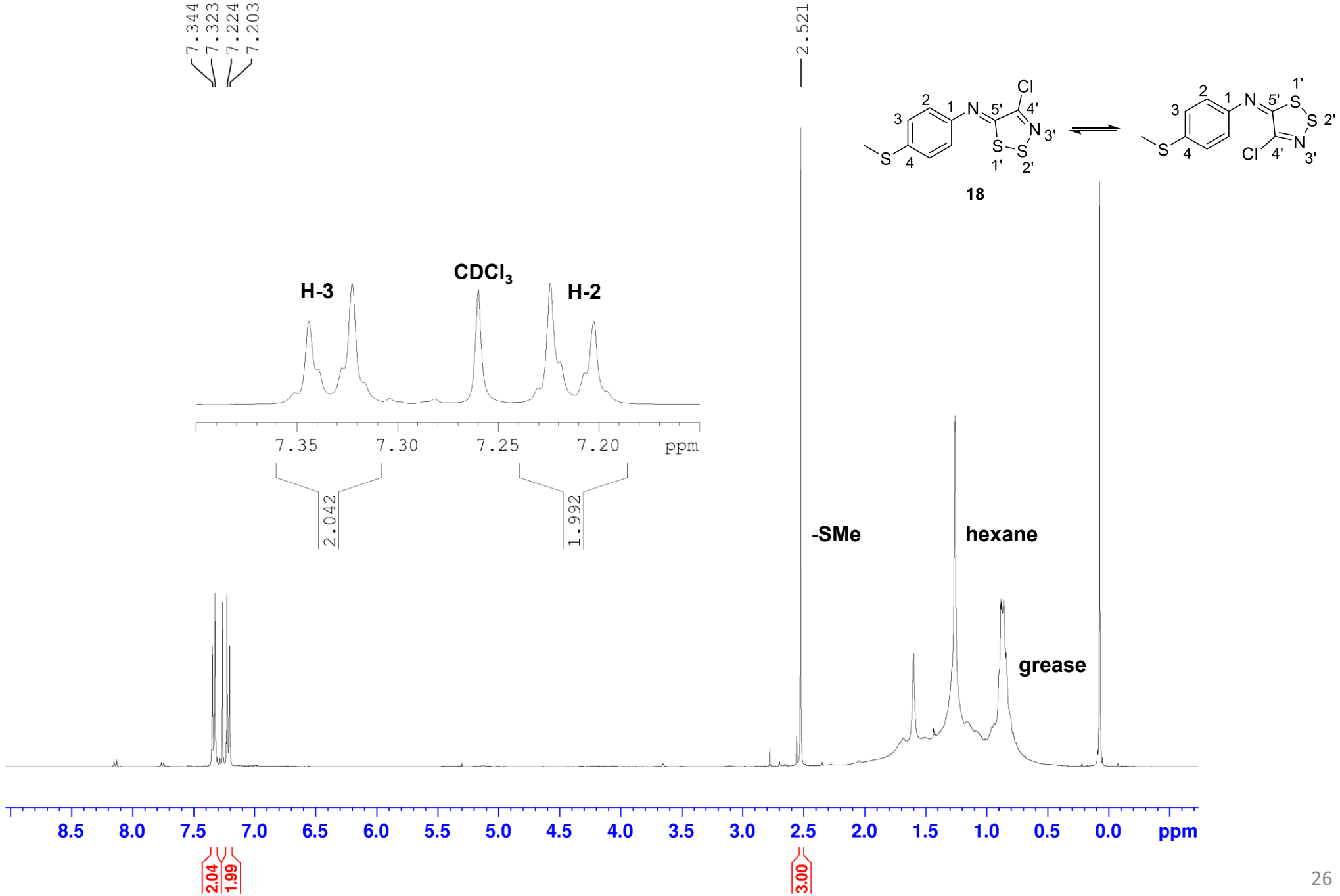
7.344
7.323
7.224
7.203
2.521
H-3
CDCl3
H-2
7.35
7.30
7.25
7.20
ppm
2.042
1.992
-SMe
hexane
grease
8.5
8.0
7.5
7.0
6.5
6.0
5.5
5.0
4.5
4.0
3.5
3.0
2.5
2.0
1.5
1.0
0.5
0.0
ppm
2.04
1.99
3.00

18

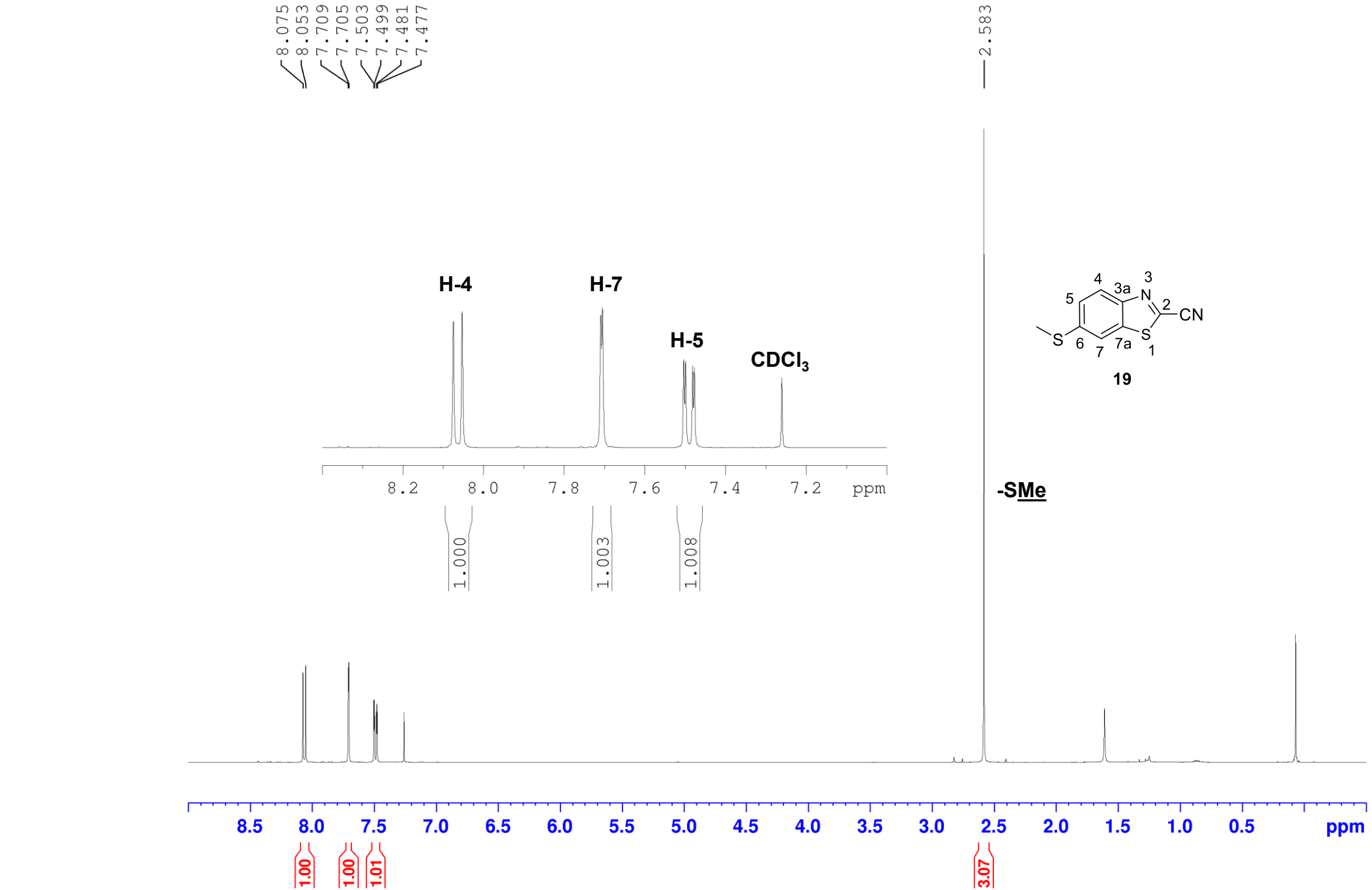
8.075
8.053
7.709
7.705
7.503
7.499
7.481
7.477
2.583
H-4
H-7
H-5
CDCl3
8.2
8.0
7.8
7.6
7.4
7.2
ppm
1.000
1.003
1.008
-SMe
19
8.5
8.0
7.5
7.0
6.5
6.0
5.5
5.0
4.5
4.0
3.5
3.0
2.5
2.0
1.5
1.0
0.5
ppm
1.00
1.00
1.01
3.07

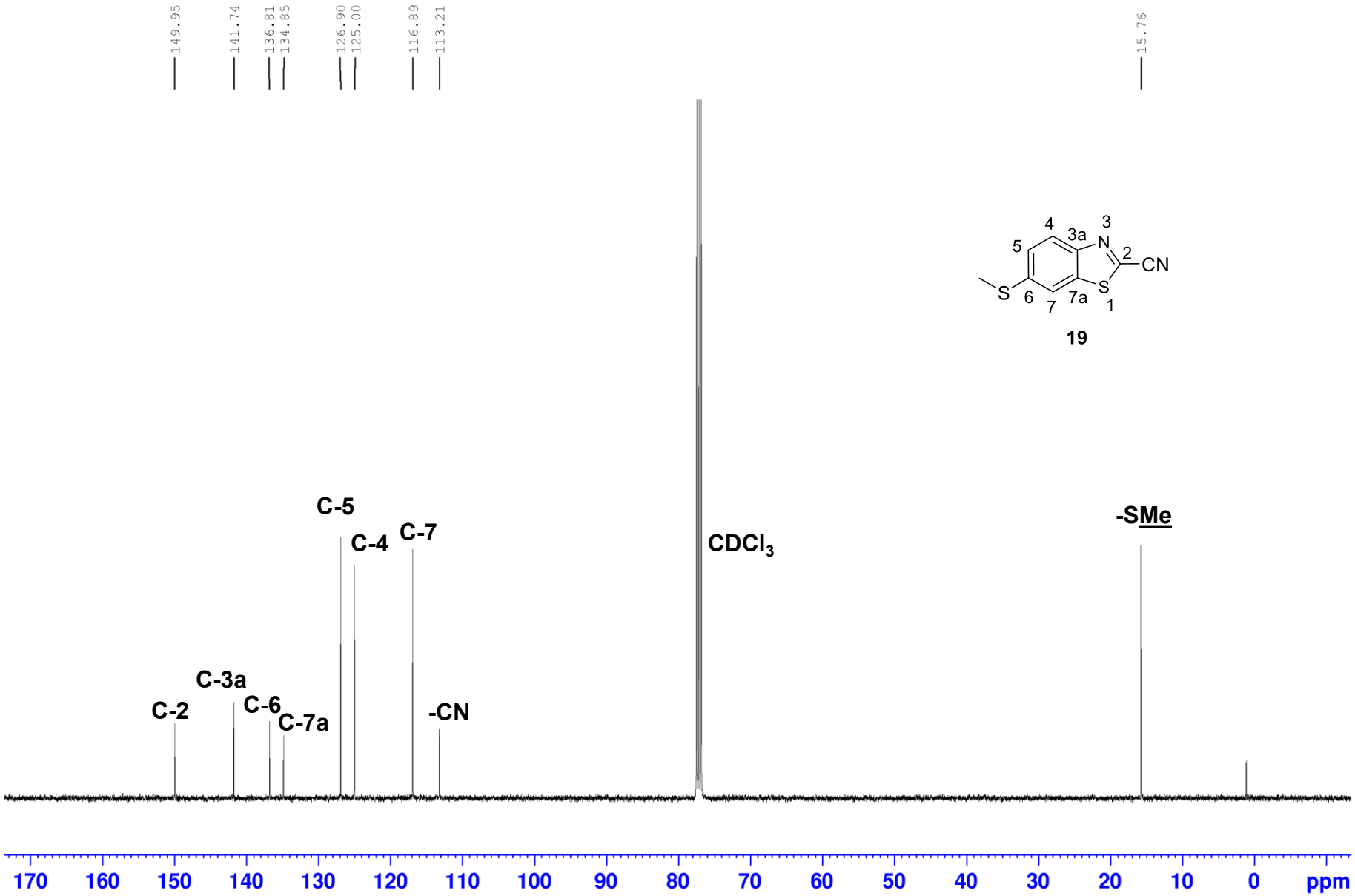
149.95
141.74
136.81
134.85
126.90
125.00
116.89
113.21
15.76
C-2
C-3a
C-6
C-7a
C-5
C-4
C-7
-CN
CDCl3
-SMe
170
160
150
140
130
120
110
100
90
80
70
60
50
40
30
20
10
0
ppm

4
3a
3
5
N
2
CN
S
6
7
7a
S
1

19

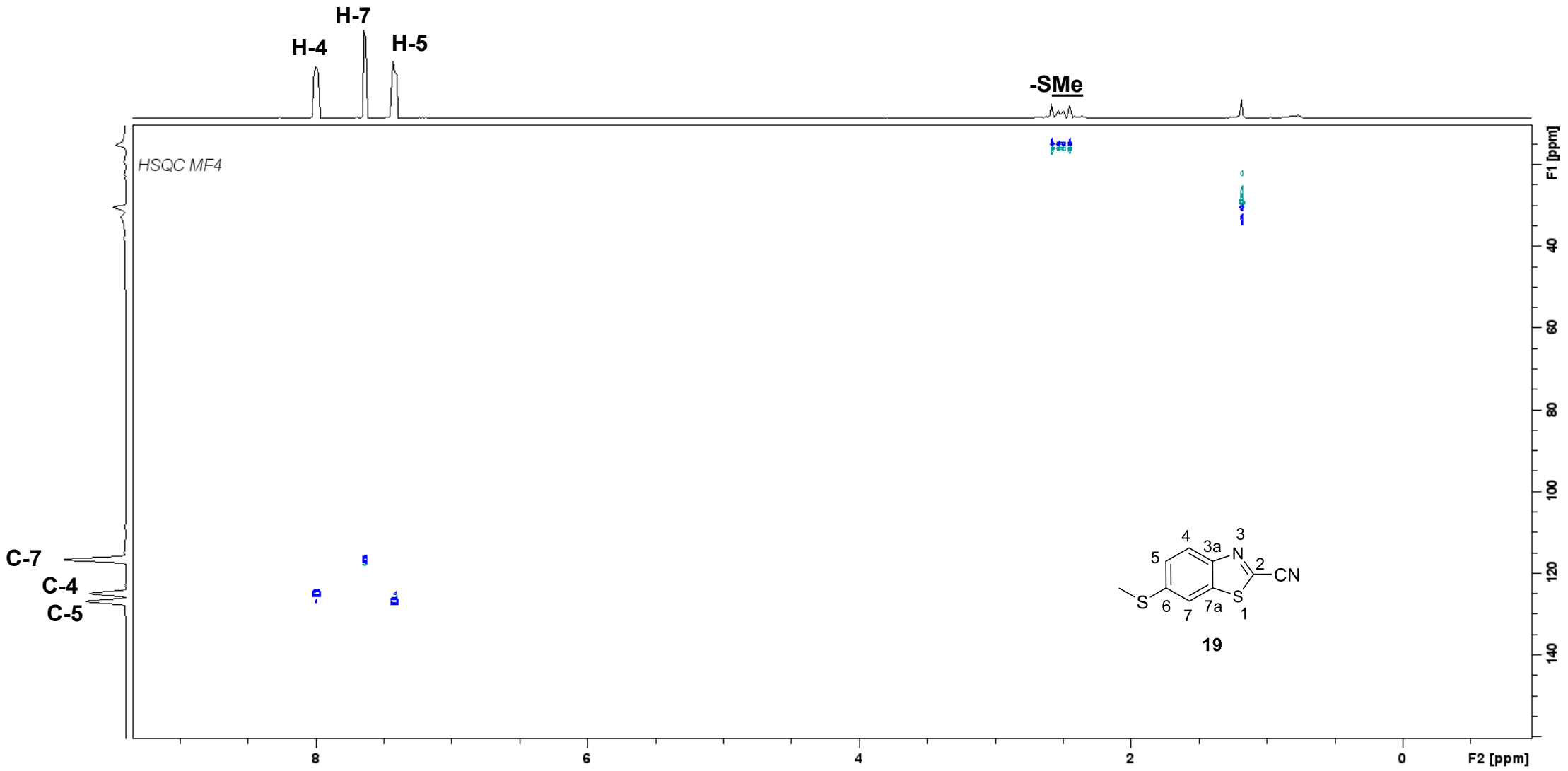
H-7
H-4
H-5
-SMe
HSQC MF4
C-7
C-4
C-5
F1 [ppm]
40
60
80
100
120
140
8
6
4
2
0
F2 [ppm]
4
3a
3
5
N
2
CN
S
6
7
7a
S
1
19

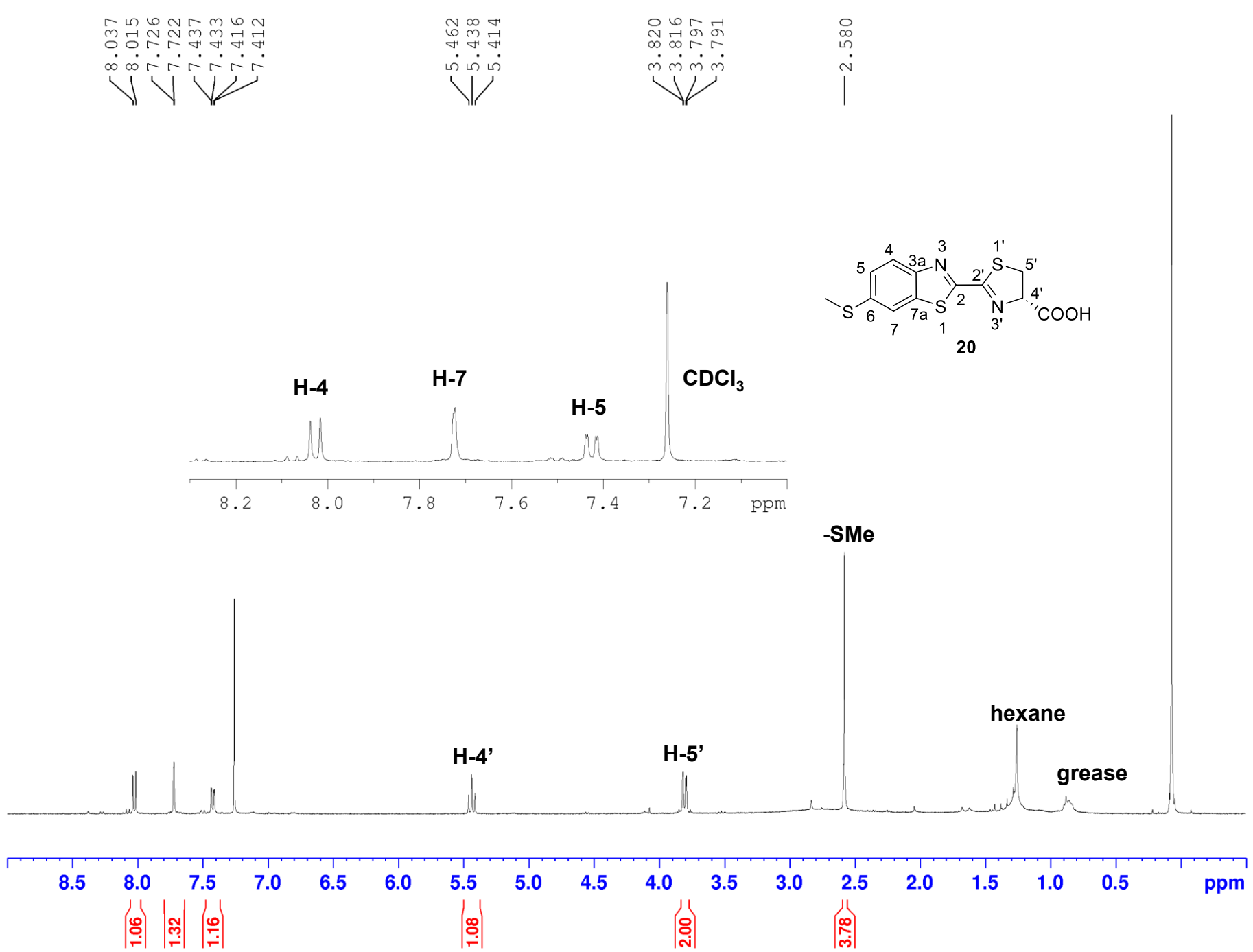
8.037
8.015
7.726
7.722
7.437
7.433
7.416
7.412
5.462
5.438
5.414
3.820
3.816
3.797
3.791
2.580
H-4
H-7
H-5
CDCl3
8.2
8.0
7.8
7.6
7.4
7.2
ppm
20
-SMe
hexane
grease
H-4'
H-5'
8.5
8.0
7.5
7.0
6.5
6.0
5.5
5.0
4.5
4.0
3.5
3.0
2.5
2.0
1.5
1.0
0.5
ppm
1.06
1.32
1.16
1.08
2.00
3.78

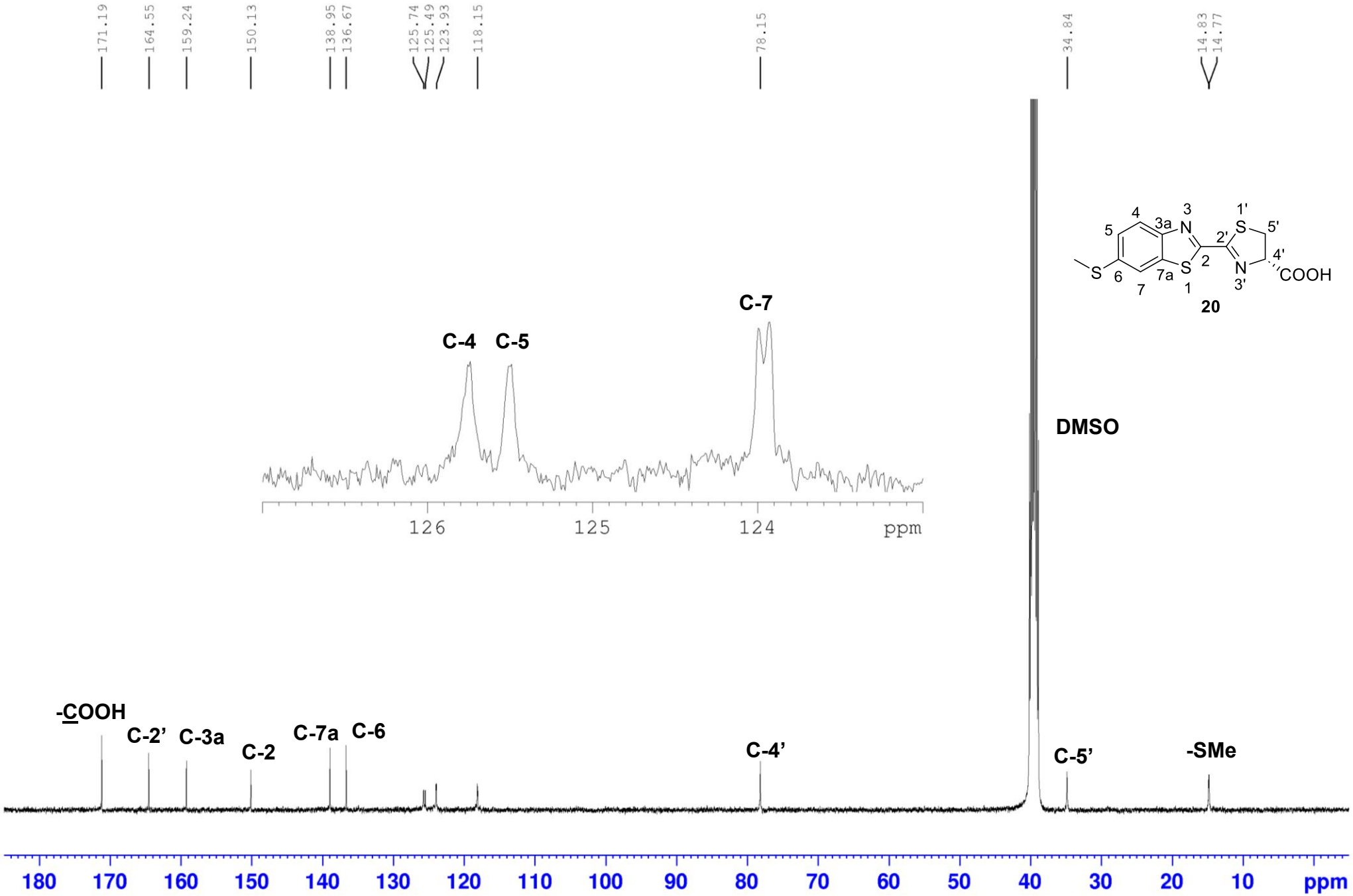
171.19
164.55
159.24
150.13
138.95
136.67
125.74
125.49
123.93
118.15
78.15
34.84
14.83
14.77
C-4
C-5
C-7
126
125
124
ppm
DMSO
-COOH
C-2'
C-3a
C-2
C-7a
C-6
C-4'
C-5'
-SMe
180
170
160
150
140
130
120
110
100
90
80
70
60
50
40
30
20
10
ppm

4
3a
3
N
1'
S
5'
5
2'
2
4'
S
6
7a
S
N
COOH
7
1
3'

20

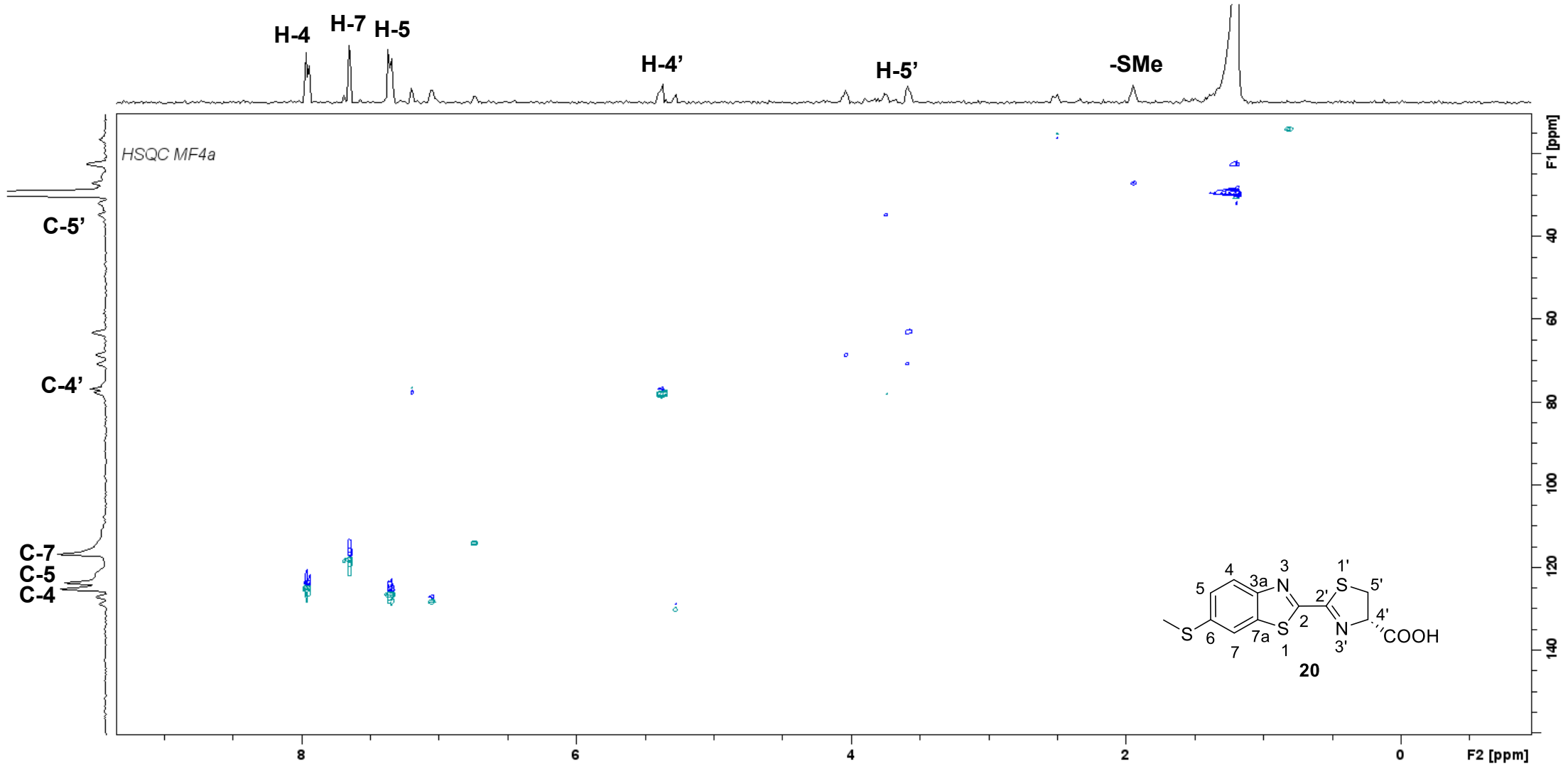
H-4
H-7
H-5
H-4'
H-5'
-SMe
HSQC MF4a
C-5'
C-4'
C-7
C-5
C-4
F1 [ppm]
F2 [ppm]
20

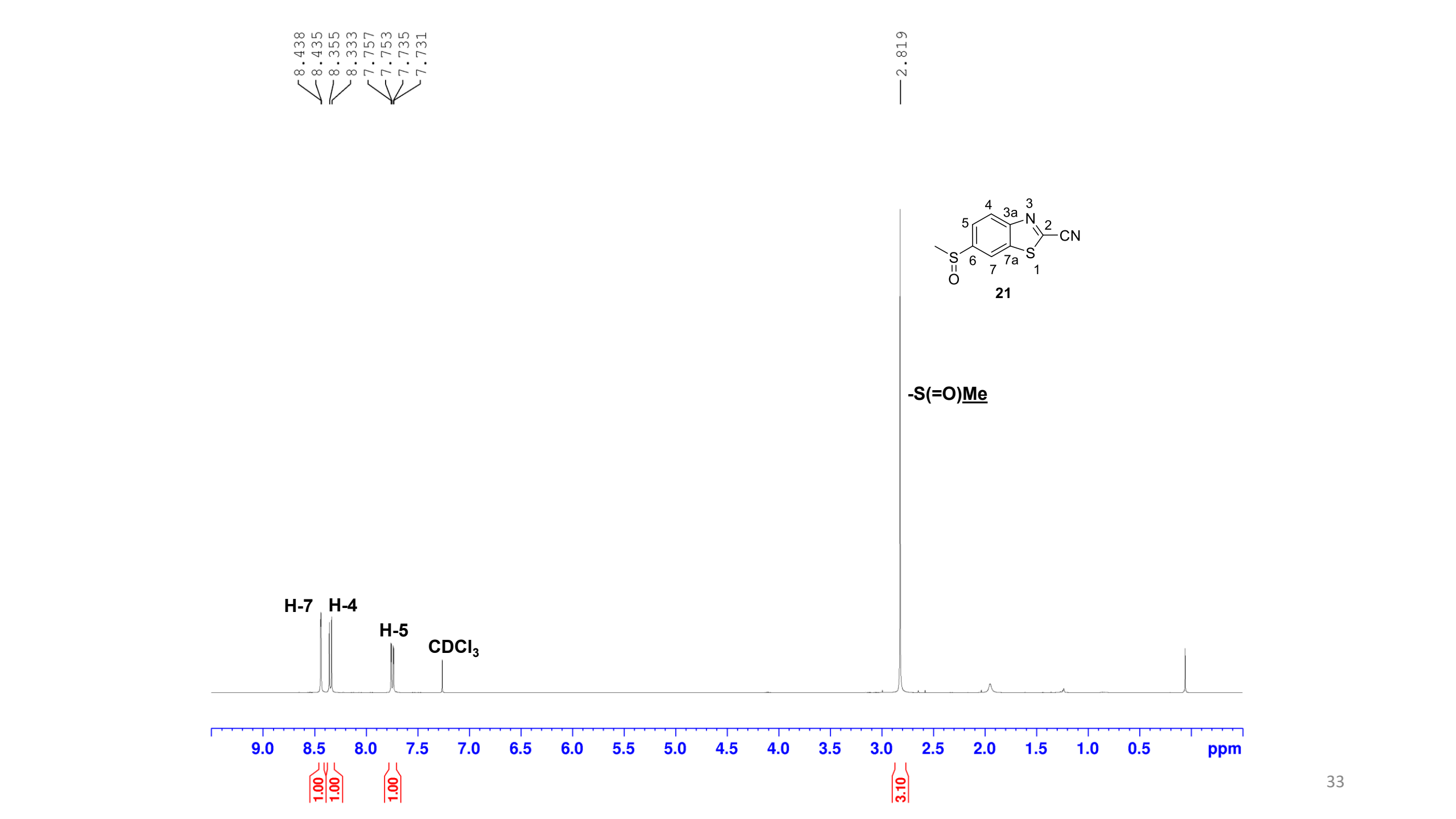
8.438
8.435
8.355
8.333
7.757
7.753
7.735
7.731
2.819
21
-S(=O)Me
H-7
H-4
H-5
CDCl3
9.0
8.5
8.0
7.5
7.0
6.5
6.0
5.5
5.0
4.5
4.0
3.5
3.0
2.5
2.0
1.5
1.0
0.5
ppm
1.00
1.00
1.00
3.10

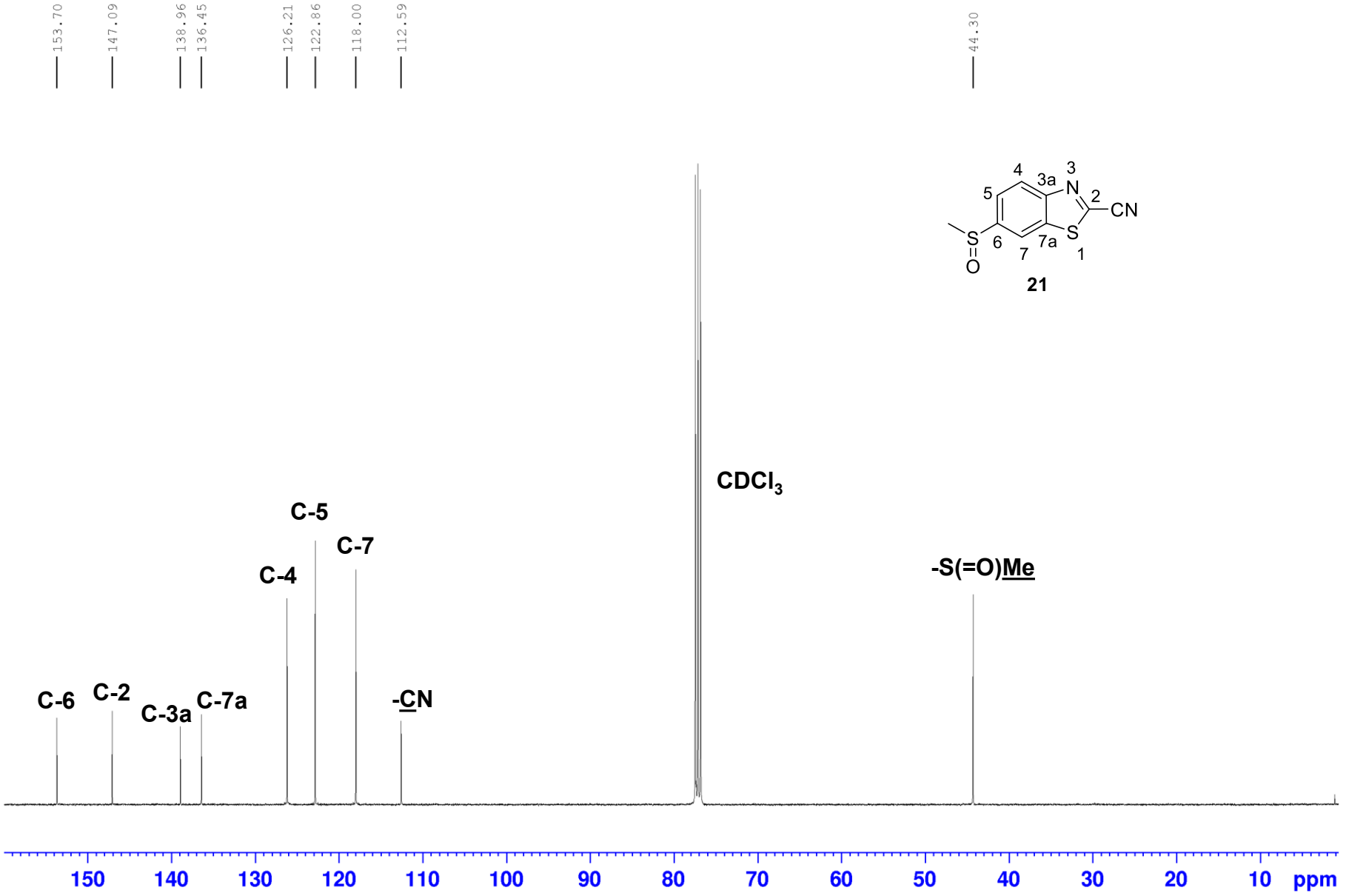
153.70
147.09
138.96
136.45
126.21
122.86
118.00
112.59
44.30
4
3a
3
N
2
CN
5
S
6
7
7a
S
1
O
21
CDCl3
C-5
C-7
C-4
-S(=O)Me
C-6
C-2
C-3a
C-7a
-CN
150
140
130
120
110
100
90
80
70
60
50
40
30
20
10
ppm

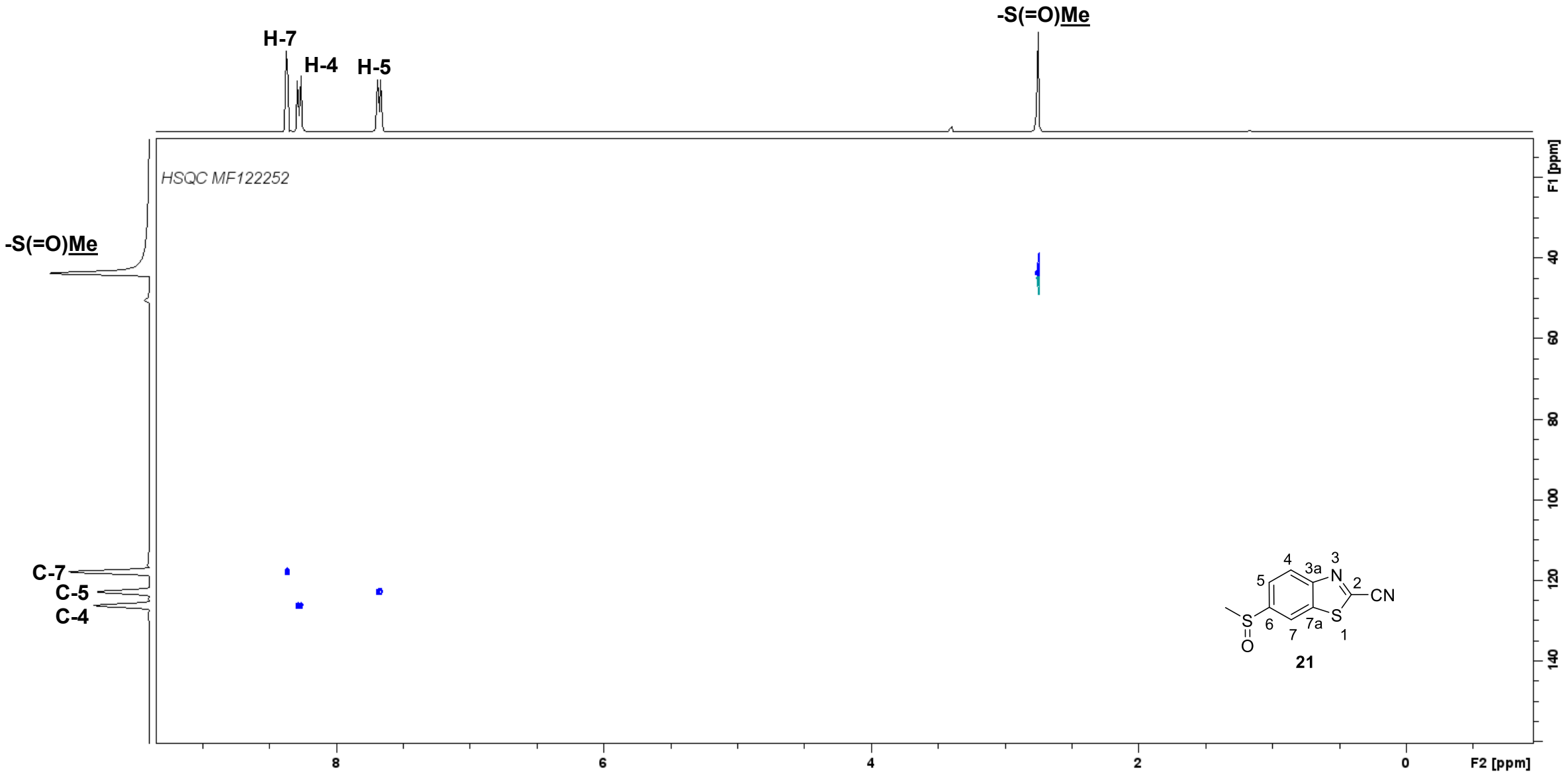
H-7
H-4
H-5
-S(=O)Me
HSQC MF122252
-S(=O)Me
C-7
C-5
C-4
F1 [ppm]
40
60
80
100
120
140
8
6
4
2
0
F2 [ppm]
4
3a
3
N
2
CN
5
S
6
7
7a
S
1
O
21

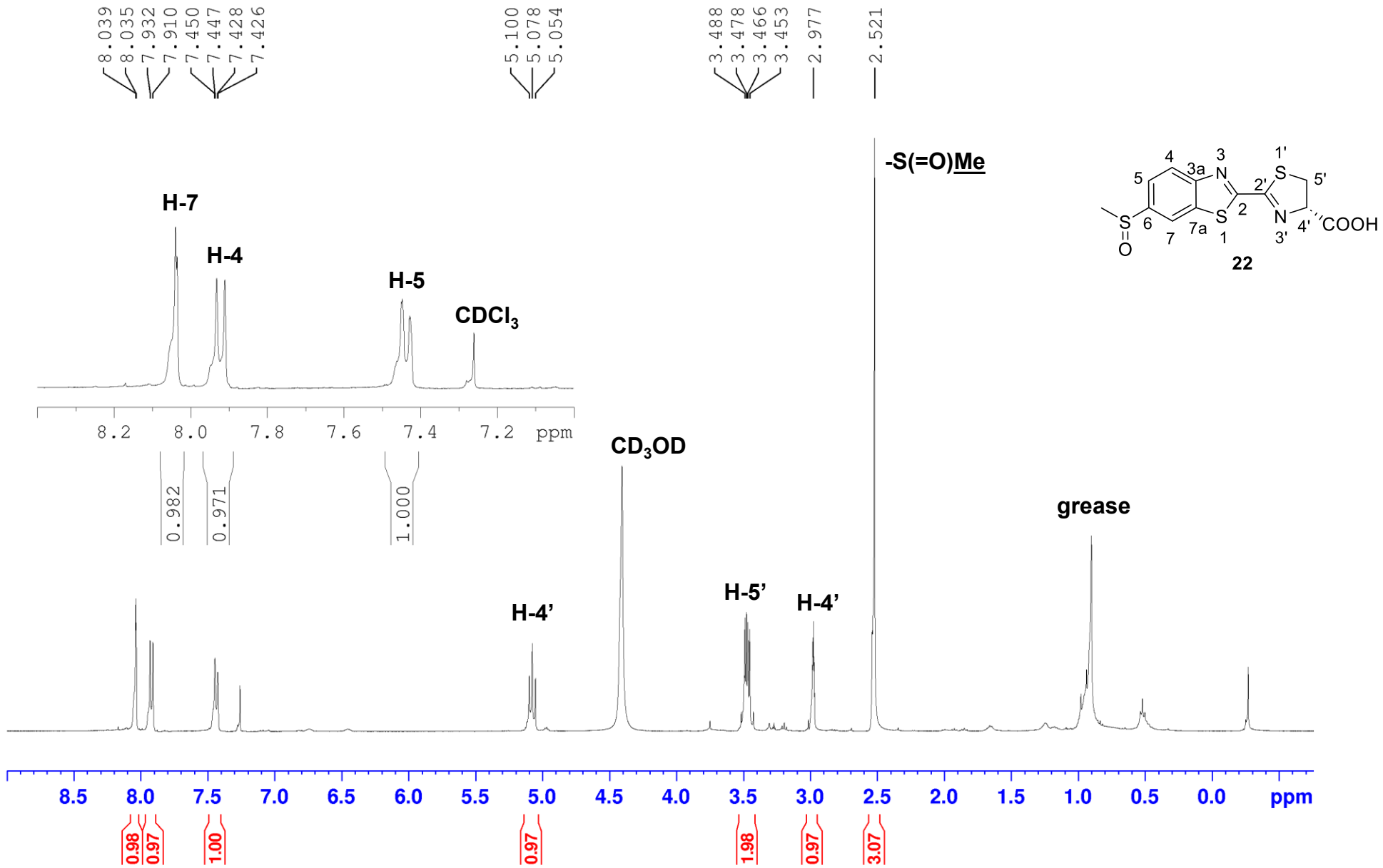
8.039
8.035
7.932
7.910
7.450
7.447
7.428
7.426
5.100
5.078
5.054
3.488
3.478
3.466
3.453
2.977
2.521
-S(=O)Me
H-7
H-4
H-5
CDCl3
CD3OD
H-4'
H-5'
H-4'
grease
0.982
0.971
1.000
8.2
8.0
7.8
7.6
7.4
7.2
ppm
8.5
8.0
7.5
7.0
6.5
6.0
5.5
5.0
4.5
4.0
3.5
3.0
2.5
2.0
1.5
1.0
0.5
0.0
ppm
0.98
0.97
1.00
0.97
1.98
0.97
3.07
COOH
22

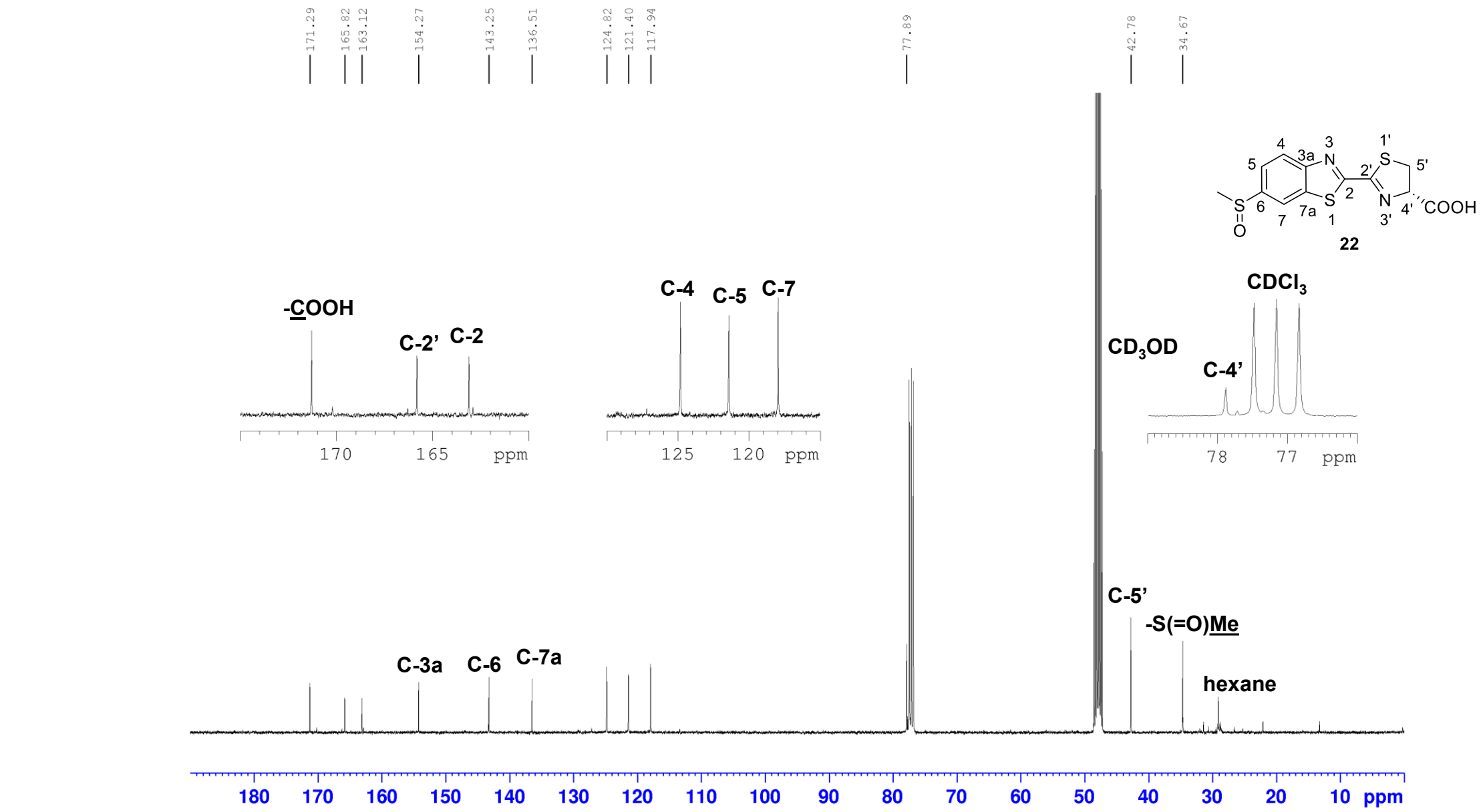
171.29
165.82
163.12
154.27
143.25
136.51
124.82
121.40
117.94
77.89
42.78
34.67
-COOH
C-2'
C-2
170
165
ppm
C-4
C-5
C-7
125
120
ppm
CDCl3
CD3OD
C-4'
78
77
ppm
22
C-5'
-S(=O)Me
hexane
C-3a
C-6
C-7a
180
170
160
150
140
130
120
110
100
90
80
70
60
50
40
30
20
10
ppm

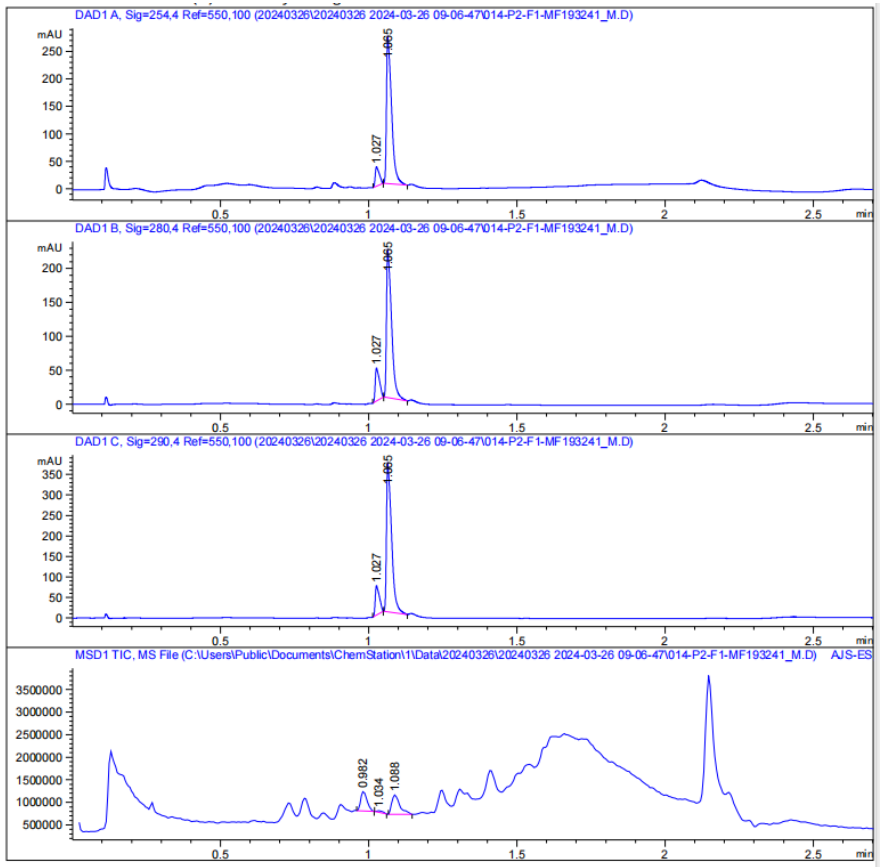

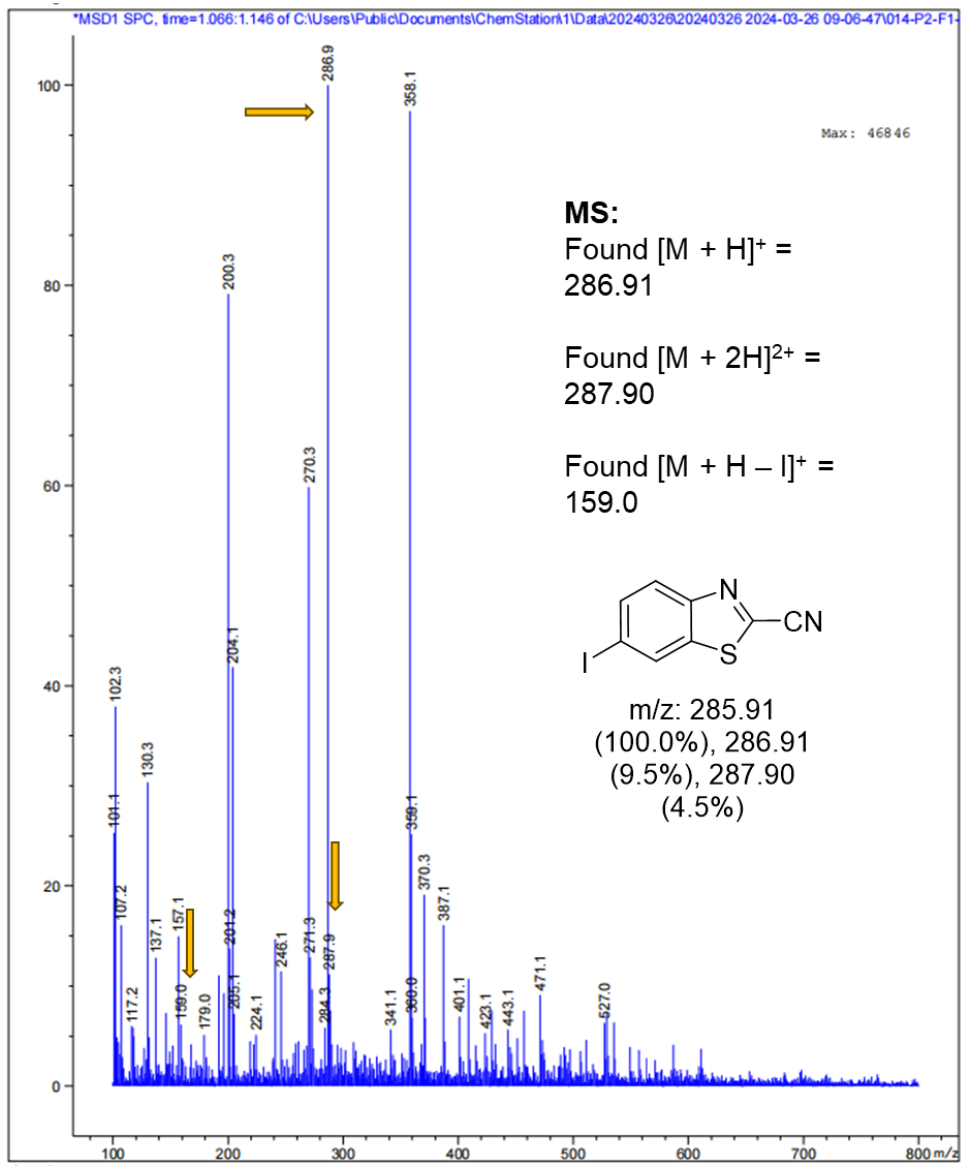

MS:

Found $[M + H]^+$ = 286.91

Found $[M + 2H]^{2+}$ = 287.90

Found $[M + H - I]^+$ = 159.0

m/z: 285.91 (100.0%), 286.91 (9.5%), 287.90 (4.5%)

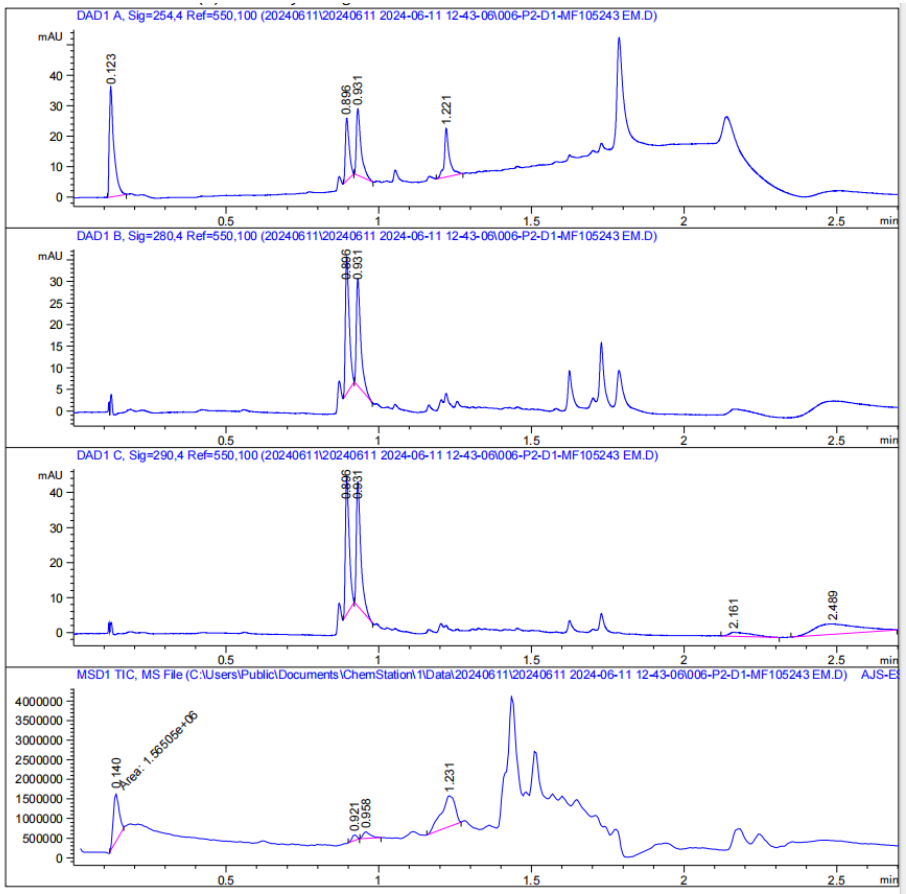

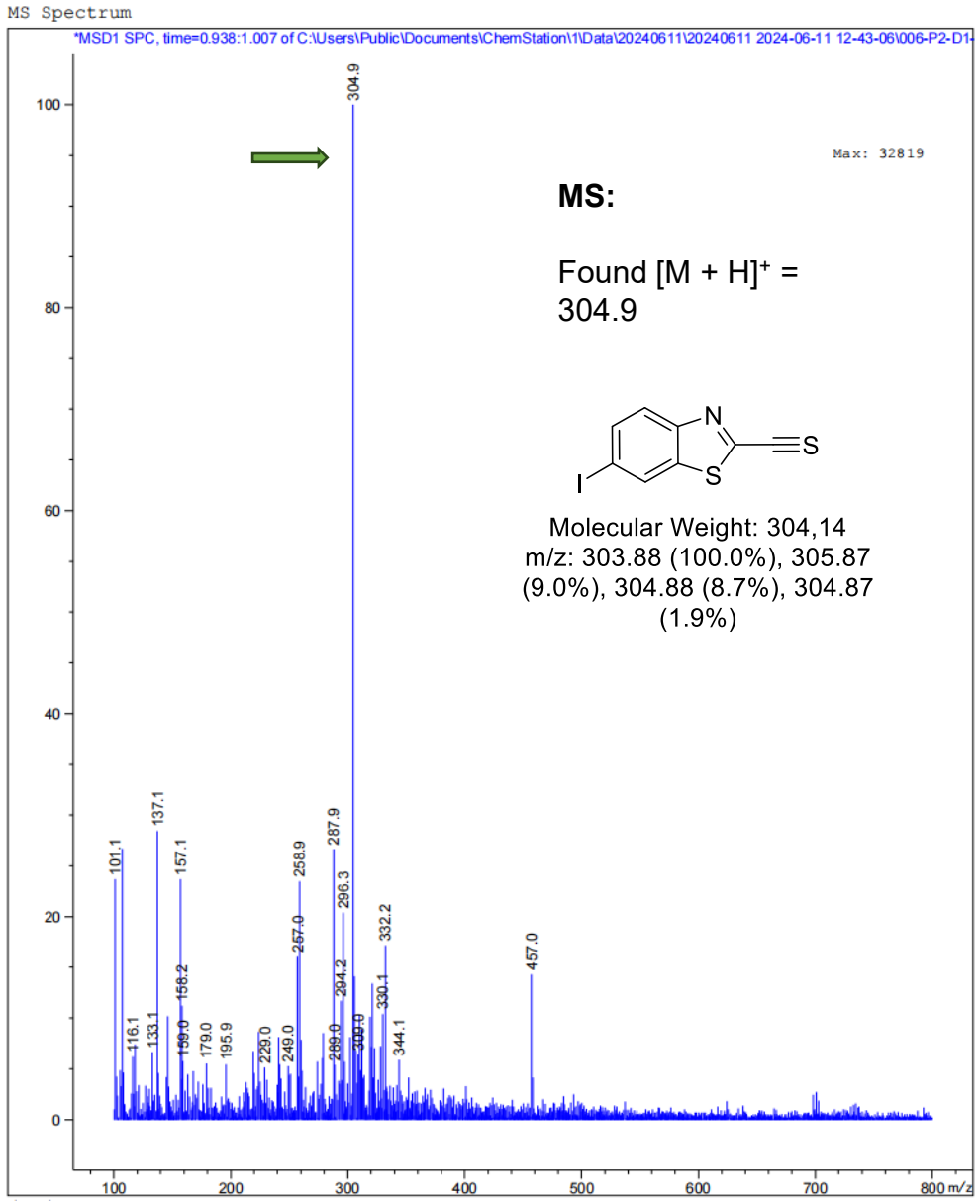

MS:

Found $[M + H]^+$ = 304.9

Molecular Weight: 304,14
m/z: 303.88 (100.0%), 305.87 (9.0%), 304.88 (8.7%), 304.87 (1.9%)